

# Molecular Design, Synthesis and Simulation of Histone Deacetylase Inhibitors

著者	Li Xiao Hui
year	2010-12
その他のタイトル	ヒストン脱アセチル化酵素阻害剤の分子設計、合成及び結合シミュレーション
学位授与年度	平成22年度
学位授与番号	17104乙生工第7号
URL	<a href="http://hdl.handle.net/10228/5474">http://hdl.handle.net/10228/5474</a>

**Kyushu Institute of Technology**

**The Dissertation for Degree of Doctor of Philosophy**

**Molecular Design, Synthesis and Simulation  
of Histone Deacetylase Inhibitors**

**Li Xiao Hui**

**December, 2010**

**Kyushu Institute of Technology**

**The Dissertation for Degree of Doctor of Philosophy**

**Molecular Design, Synthesis and Simulation  
of Histone Deacetylase Inhibitors**

**Li Xiao Hui**

**JSPS RONPAKU: CSC-10711**

**Graduate School of Life Science and Systems Engineering**

**Kyushu Institute of Technology, Japan**

**December, 2010**

# Content

Chapter 1 Histone Deacetylase and Histone Deacetylase Inhibitors.....	- 1 -
1.1 Histone deacetylase and histone acetyltransferase.....	- 1 -
1.2 Histone deacetylase family .....	- 2 -
1.3 The effect mechanism of HDAC inhibitors and HDAC .....	- 6 -
1.4 Structure class of HDAC inhibitors .....	- 8 -
1.4.1 Carboxylates .....	- 9 -
1.4.2 Hydroxamic acids .....	- 10 -
1.4.3 Benzamides.....	- 11 -
1.4.4 Electrophilic ketones .....	- 11 -
1.4.5 Cyclic peptide HDAC inhibitors .....	- 12 -
1.5 Molecular simulation of interactions between HDAC and HDAC inhibitors.....	- 30 -
1.6 Purpose of this study.....	- 32 -
1.7 References.....	- 35 -
Chapter 2 Molecular Simulation of Interactions between HDAC and Apicidin, Analogues .....	- 45 -
2.1 Introduction.....	- 45 -
2.2 Results and discussion .....	- 46 -
2.2.1 Sequence alignment and homology model validation .....	- 46 -
2.2.2 3D structure of the HDAC1 model.....	- 48 -
2.2.3 Interactions between HDAC1 and inhibitors.....	- 50 -
2.2.4 Selective inhibition of Apicidin on HDAC1 and HDAC8.....	- 55 -
2.3 Summary .....	- 57 -
2.4 Computational methodology.....	- 58 -
2.4.1 Model building and validation of HDAC1 .....	- 58 -
2.4.2 Docking calculation.....	- 59 -
2.4.3 Molecular dynamics simulation.....	- 59 -
2.5 References.....	- 60 -
Chapter 3 Synthesis of Non-natural Amino Acid.....	- 62 -
3.1 Introduction.....	- 62 -

3.2 Synthesis of H-Phe-OH derivatives .....	- 63 -
3.2.1 Synthesis of Boc-L-Phe(2-Me)-OH.....	- 64 -
3.2.2 Synthesis of Boc-L-Phe(3-Me)-OH.....	- 65 -
3.2.3 Synthesis of Boc-L-Phe(4-Me)-OH.....	- 65 -
3.2.4 Synthesis of Boc-L-Phe(3,5-2Me)-OH.....	- 66 -
3.3 Synthesis of <i>n</i> -methyl-amino-cyclohexane-carboxylic acid .....	- 66 -
3.3.1 Synthesis of H-(±)A2mc6c-OH.....	- 67 -
3.3.2 Synthesis of H-L-A3mc6c-OH.....	- 67 -
3.3.3 Synthesis of H-A4mc6c-OH.....	- 68 -
3.3.4 Synthesis of Z-Anmc6c-OH .....	- 69 -
3.4 Synthesis of amino acid containing chlorine .....	- 69 -
3.4.1 Synthesis of Boc-L-2-amino-5-chloropentanoic acid.....	- 69 -
3.4.2 Synthesis of Boc- L-2-amino-6-chlorohexanoic acid.....	- 70 -
3.6 References.....	- 71 -
Chapter 4 Molecular Design of Cyclic Tetrapeptide HDAC Inhibitors by Replacement of Aib in Chlamydocin Framework.....	- 73 -
4.1 Introduction.....	- 73 -
4.2 Results and discussion .....	- 75 -
4.2.1 Chemistry .....	- 75 -
4.2.2 Enzyme inhibition and biological activity .....	- 76 -
4.2.3 Cell growth inhibitory assay .....	- 77 -
4.2.4 Morphological reversion.....	- 78 -
4.2.5 Conformational studies by CD and NMR.....	- 79 -
4.2.6 Docking and molecular dynamics simulation for HDAC inhibitors towards HDACs .....	- 80 -
4.3 Summary.....	- 86 -
4.4 Experimental.....	- 86 -
4.4.1 Synthesis of <i>cyclo</i> (-L-Asu(NHOH)-(±)A2mc6c-L-Phe-D-Pro-).....	- 87 -
4.4.2 Synthesis of <i>cyclo</i> (-L-Asu(NHOH)-L-A3mc6c-L-Phe-D-Pro-).....	- 89 -
4.4.3 Synthesis of <i>cyclo</i> (-L-Asu(NHOH)-A4mc6c-L-Phe-D-Pro-).....	- 91 -
4.4.4 HDACs preparation and enzyme activity assay .....	- 94 -

4.4.5 The p21 promoter assay .....	- 95 -
4.4.6 Cell growth inhibition assay .....	- 96 -
4.4.7 Morphological reversion assay .....	- 97 -
4.4.8 Circular dichroism measurement .....	- 97 -
4.4.9 Molecular dynamics simulation.....	- 97 -
4.5 References.....	- 99 -
<b>Chapter 5 Molecular Design of Cyclic Tetrapeptide HDAC Inhibitors by Replacement of L-Phe in Chlamydocin Framework .....</b>	<b>- 101 -</b>
5.1 Introduction.....	- 101 -
5.2 Results and discussion .....	- 104 -
5.2.1 Chemistry .....	- 104 -
5.2.2 Cell growth inhibitory assay .....	- 105 -
5.2.3 Morphological reversion.....	- 107 -
5.2.4 Enzyme inhibition and biological activity .....	- 107 -
5.2.5 Conformation studies by CD and NMR .....	- 108 -
5.2.6 Docking and molecular simulation for the HDAC inhibitors towards HDAC8 .....	- 110 -
5.3 Summary .....	- 117 -
5.4 Experimental .....	- 117 -
5.4.1 Synthesis of <i>cyclo(-L-Am7(S2Py)-Aib-L-Phe-D-Pro-)</i> .....	- 118 -
5.4.2 Synthesis of <i>cyclo(-L-Am7(S2Py)-Aib-L-Phe(2-Me)-D-Pro-)</i> .....	- 121 -
5.4.3 Synthesis of <i>cyclo(-L-Am7(S2Py)-Aib-L-Phe(4-Me)-D-Pro-)</i> .....	- 123 -
5.4.4 Synthesis of <i>cyclo(-L-Am7(S2Py)-Aib-L-Phe(3,5-2Me)-D-Pro-)</i> .....	- 126 -
5.4.5 Synthesis of <i>cyclo(-L-Asu(NHOH)-Aib-L-Phe(4-Me)-D-Pro-)</i> .....	- 129 -
5.4.6 Circular dichroism measurement.....	- 130 -
5.4.7 Cell growth inhibition assay .....	- 130 -
5.4.8 Morphological reversion assay .....	- 131 -
5.4.9 Computational methodology for the HDAC inhibitors towards HDAC8.....	- 131 -
5.5 References.....	- 133 -
<b>Chapter 6 Molecular Design of Cyclic Tetrapeptide HDAC Inhibitors by Replacement of L-Phe in Chlamydocin Framework .....</b>	<b>- 136 -</b>

6.1 Introduction.....	- 136 -
6.2 Results and discussion .....	- 138 -
6.2.1 Chemistry .....	- 138 -
6.2.2 Enzyme inhibition and biological activity .....	- 139 -
6.2.3 Conformational study .....	- 140 -
6.2.4 Docking for HDAC inhibitors towards HDAC8 .....	- 142 -
6.3 Summary .....	- 144 -
6.4 Experimental .....	- 145 -
6.4.1 Synthesis of <i>cyclo(-L-Asu(NHOH)-Aib-L-Ac5-D-Pro-)</i> .....	- 145 -
6.4.2 Synthesis of <i>cyclo(-L-Asu(NHOH)-Aib-L-Pro-D-Pro-)</i> .....	- 148 -
6.4.3 Synthesis of <i>cyclo(-L-Asu(NHOH)-Aib-L-Ac6-D-Pro-)</i> .....	- 149 -
6.4.4 HDACs preparation and enzyme activity assay .....	- 152 -
6.4.5 The p21 promoter assay .....	- 152 -
6.4.6 Circular dichroism measurement .....	- 153 -
6.5 References.....	- 153 -
Chapter 7 Cyclic Tetrapeptide HDAC Inhibitors: a Potent Anticancer Prodrug.....	- 155 -
Acknowledgements .....	- 158 -
List of Publications .....	- 159 -
Presentations at Conferences.....	- 160 -

# Chapter 1

## Histone Deacetylase and Histone Deacetylase Inhibitors

### 1.1 Histone deacetylase and histone acetyltransferase

Recently, Cancer agent development has displaced from conventional cytotoxic chemotherapeutics to a more mechanism based targeted approach towards the common goal of tumour growth arrest. Histone deacetylase enzymes (HDACs) engaged attention as validated biological targets for the treatment of human cancer.<sup>[1,2]</sup>

In eukaryotic cells, nucleosome is the basic unit of chromatin (**Fig. 1.1**), and is composed of a fragment of DNA wrapped around a histone octamer formed by four histone partners (H3, H4 tetramer and two H2A, H2B dimers). DNA is maintained in a highly ordered and condensed form via its association with small histone. Histones are basic protein rich in lysine and arginine residues in N-terminal tail extending out of the nucleosome.<sup>[3]</sup> Histones take on extensive posttranslational modifications that affect gene expression. Reversible acetylation and deacetylation of  $\epsilon$ -amino group of lysine residus on histone tails by histone acetyl transferase (HAT) and HDAC enzymes play a crucial role in the epigenetic regulation of gene expression by changing the chromatin architecture and transcriptional activity.<sup>[4-7]</sup> Aberrant gene

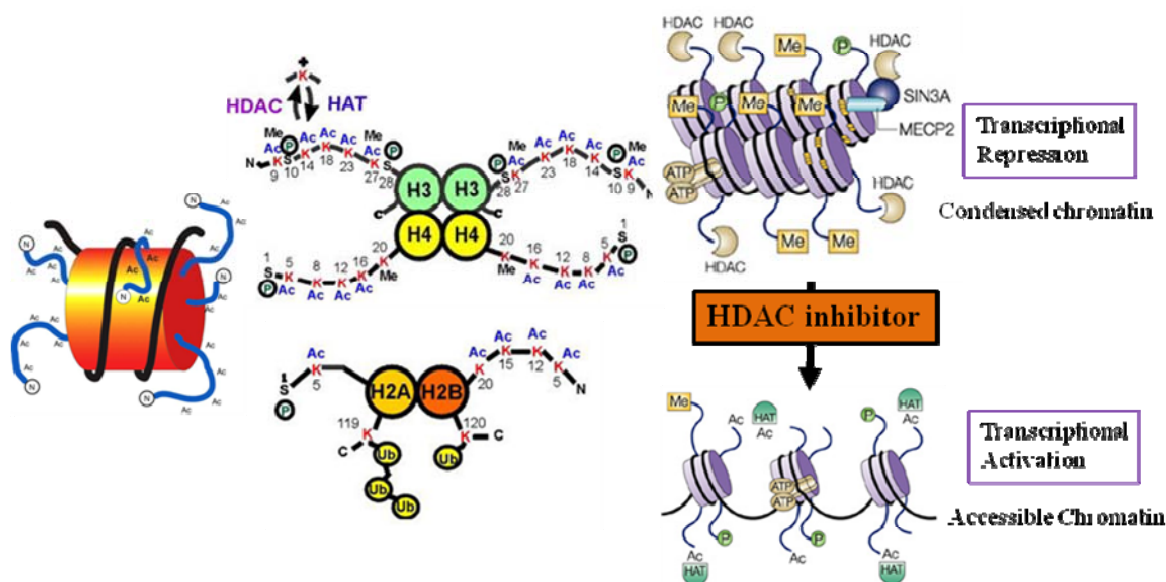


**Fig. 1.1** Organisation of the nucleosome and mechanism of action HDAC and HAT.



expression that results in functional inactivation of HAT or recruit of HDACs can induce tumor cell proliferation.<sup>[8]</sup> The level of histone acetylation and deacetylation controls the interaction of positively charged histones with the negatively charged DNA. Superdeacetylation of histone results in increasing positive charge density which will strengthen the interaction with the negatively charged DNA and thus inhibit the accessibility of regulators to DNA.<sup>[9]</sup> Therefore, in most case, histone acetylation enhances transcription while histone deacetylation represses transcription. Transcriptional deregulation of genes which caused by high histone deacetylation can lead to cancer developments which are involved in the control of cell cycle arrest, differentiation, and/or apoptosis.<sup>[10,11]</sup>

## 1.2 Histone deacetylase family

HDAC enzymes have emerged as validated biological targets for the treatment of human cancer.<sup>[12]</sup> HDAC enzymes family were found in animals, plants, fungi and bacterias. In 1996, HDAC1 was first identified using the HDAC inhibitor Trapoxin as an affinity from nuclear extract.<sup>[13]</sup> It was found that HDAC1 shares high sequence homology with yeast Rpd3, a global gene regulator and transcriptional co-repressor with histone deacetylase activity.<sup>[14]</sup> The human HDACs are classified into four different phylogenetic classes (class I, class II, class III and class IV, 18 subtype) according to their cellular localizations, structural, functional differences and on their sequence homology to their yeast orthologues Rpd3, HdaI and Sir2, respectively (**Fig. 1.2**)<sup>[15,16]</sup>. Class I includes HDAC1, 2, 3, and 8 that compounds are closely related to yeast

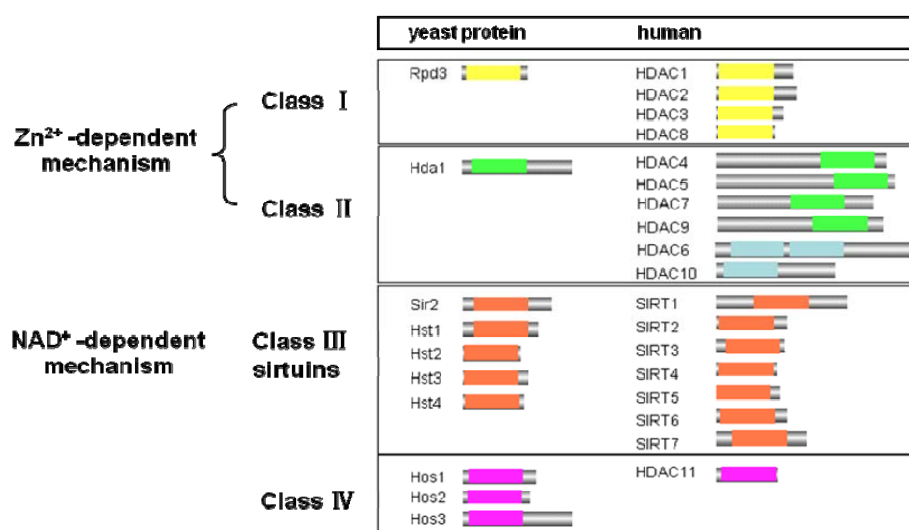


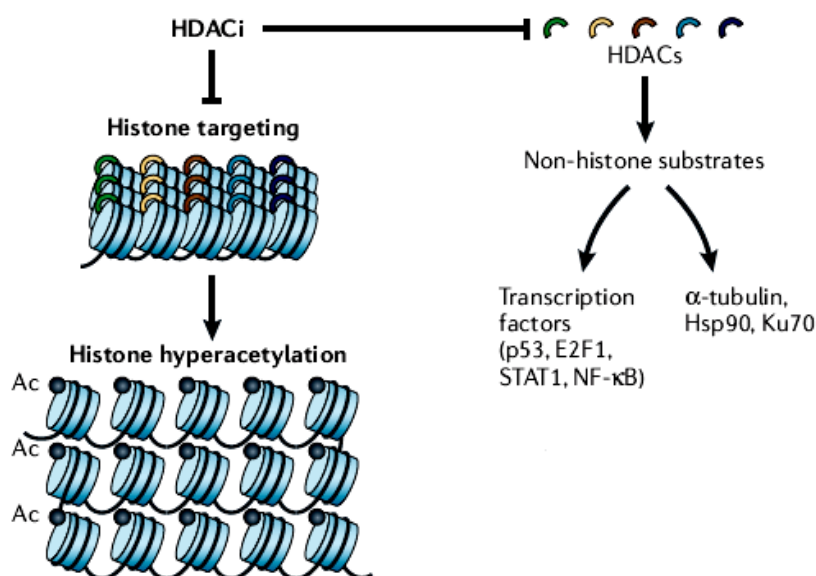
**Fig. 1.2** Classification of HDACs.

Rpd3 and shared homology in catalytic sites. Class II (HDAC4, 5, 6, 7, 9 and 10) shared domains yeast HDAC1. Class II HDAC is further subdivided into Class IIa and Class IIb. Class IIa (HDAC4, 5, 7, 9) have homology in two regions: the C-terminal catalytic domain and the N-terminal regulatory domain. Class IIa are defined by a large, functionally important N-terminal domain regulating nuclear-cytoplasmic shuttling and specific DNA-binding. Class IIb (HDAC6, 10) are found in the cytoplasm and contain two deacetylase domains in catalytic site and C-terminal zinc finger.<sup>[17]</sup> HDAC6 has emerged as a major deacetylase functioning of  $\alpha$ -tubulin deacetylase.<sup>[18]</sup> HDAC10 structurally relates to HDAC6, but contains one additional catalytically inactive domain. Its function is largely unknown.<sup>[19]</sup> Class IV, HDAC11 exhibits properties of class I and class II HDACs. HDACs class I and II are zinc-dependent enzymes that catalyze mechanism is similar for to remove the acetyl groups from the  $\epsilon$ -amino group of lysine residues of histone amino terminal tail. Class III is a series of the NAD<sup>+</sup>-dependent Sir2 family of enzymes.<sup>[20]</sup> It was demonstrated that different HDACs have distinct biological functions and are recruited to specific regions of the genome.<sup>[21,22]</sup> Overexpression of class I HDACs with concomitant down regulation and/or mutations of HATs are associated with a condensed chromatin structure preventing the access of transcription factors to DNA during gene expression causing cancer cells survival and progression. Selective inhibitors of class I HDACs has been shown to restore the acetylation of histones and the transcription of genes which induce cell cycle arrest and apoptosis of cancer cell lines.<sup>[23-25]</sup>

Class I HDACs contain 350-500 amino acid residues, while class II enzymes are usually about 1000 amino acid long. Due to the larger class II HDACs, they possess many additional structural features, including a lengthy N-terminal sequence. The class I and class II HDACs share a 320 amino acid residues region of homology, corresponding to the section of the enzyme that forms the catalytic pocket.<sup>[26]</sup> The highly conserved catalytic pocket presents challenges to development of selective HDAC inhibitors. However, some structural differences have been found and have been useful in generating class selective and isoform selective inhibitors.<sup>[27]</sup> Crystal structures of the HDAC enzymes and their homologues provide essential information for rational drug design of selective HDAC inhibitors. For a long time, structural information on zinc-dependent HDAC catalytic domains has been limited to a bacterial HDAC-like protein (HDLP).<sup>[30]</sup> HDLP resemble a class I enzyme catalytic site. Up to now, the crystal structures of a human class I enzyme (HDAC8)<sup>[28]</sup> and a bacterial class IIb HDAC-like amidohydrolase (HDAH)<sup>[31]</sup> have been reported. However, the structure of human class II HDAC7<sup>[29]</sup> and HDAC4<sup>[162]</sup> catalytic domain were reported.

Class I HDACs are highly expressed in gastric cancer, pancreatic cancer, colorectal cancer, prostate cancer, hepatocellular carcinoma and cervical carcinoma, and Class II HDACs are found mainly in breast cancer, colorectal cancer and oral squamous cell cancer.<sup>[32, 33]</sup> These isoforms HDACs have distinct cellular localizations and functions. Each HDAC gene occupies on a special chromosome site, and there are some differences in the genes of the amino acids on the surface of active pocket. The selectivity in binding to the amino acids at the rims of the pockets of different HDACs enabled the HDAC inhibitors to exhibit distinct inhibitory activities to different cancer cells, and even cytotoxicity. Design and synthesis of the isoform selective HDAC inhibitors with low adverse and toxic effects will be useful in special cancer therapy, and it will greatly influence the clinical treatment on cancers.

In addition to regulating the acetylation state of histones, HDACs can bind to, deacetylate and regulate the activity of a number of other proteins, including transcription factors (p53, E2F transcription factor 1 (E2F1) and nuclear factor- $\kappa$ B (NF- $\kappa$ B)) and proteins with diverse biological functions ( $\alpha$ -tubulin, Ku70 and heat-shock protein 90 (Hsp90)) (**Fig. 1.3**).<sup>[34]</sup> Therefore, HDAC inhibitors could have far reaching effects on multiple cellular processes. Two examples of non-histone acetylated proteins that might be affected by HDAC inhibition and involved in Huntington's disease and other polyglutamine repeat diseases are p53 and HSP90 (**Fig. 1.4 and Table 1.1**).<sup>[35]</sup> Thereby, a number of HDAC inhibitors are potent mediators of tumour cell death.



**Fi g. 1.3** Effects of HDACs inhibition on histone and non-histone proteins.

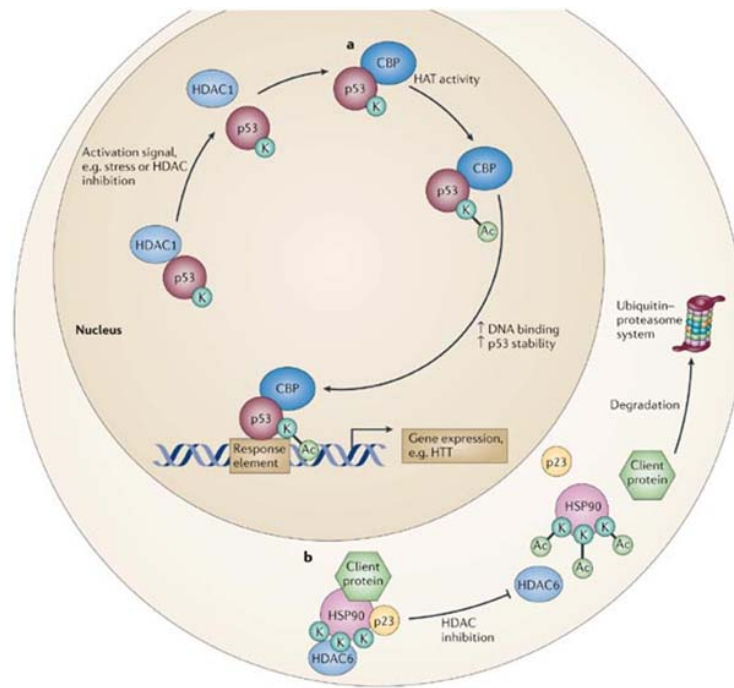


**Fig. 1.4** The function of HDAC and HAT for non-histone proteins.

**Table 1.1** Non-histone substrates of HDAC enzymes

Substrate	Function
$\alpha$ -Tubulin	Cytoskeletal
Importin- $\alpha$	Nuclear/cytoplasmic shuttling
$\beta$ catenin	Cell adhesion/transcription
TCF	DNA binding
p53	Tumour suppressor
E2F	Transcriptional cell cycle
pRb	Tumour suppressor
Hmg1(y)	Transcription
Hsp90	Molecular chaperone
YY1	Transcription
Bcl6	Transcription
UBF	Transcription
Cart-1	Structural organisation
P50; relA	Transcription/inflammation
HIV-1 Tat	Replication
Rb	Cell cycle

### 1.3 The effect mechanism of HDAC inhibitors and HDAC

In 1999, Finnin *et al.* first elucidated the interactions mechanism between Trichostatin A (TSA), suberoylanilide hydroxamic acid (SAHA) of the structural details of the class I/II HDAC inhibitors and histone deacetylase-like protein (HDLP).<sup>[30]</sup> The crystal structure of HDLP, which was isolated from a hyperthermophilic bacterium, *Aquifex aeolicus*; a homologue of mammalian class I/II HDAC with 35.2% sequence identity over 375 residues, was solved with the HDAC inhibitor TSA bound to the active site (**Fig. 1.5**). This structural information provided the first concrete evidence that this enzyme indeed contained an active site zinc-binding pocket, consistent with previous observations that HDAC activity was contingent upon the presence of a metal cofactor and strongly supported by the pronounced activity of certain hydroxamic acid-based inhibitors (TSA). The crystal structure shows that HDLP has a single-domain structure belonging to the open  $\alpha/\beta$  class of folds and the catalytic domain is very closely related to that of HDACs. The enzyme contains two Asp-His charge-relay systems, a structural feature which is conserved across the HDAC family. The prominent architectural feature of the ligand binding site shows the presence of a gently curved tubular pocket approximately 11Å deep whose walls are lined with hydrophobic and aromatic residues and 14Å cavity (Fig. 1.6). The cavity narrows to ~7.5Å near its center, constrained by the

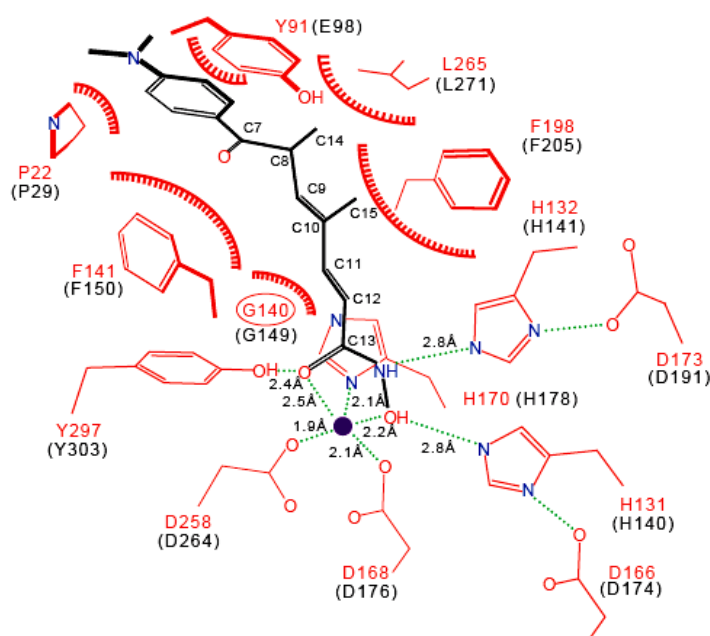


**Fig. 1.5** Crystal structure of TSA bound to the HDLP. HDLP residues are labelled in red with their counterparts in HDAC1 indicated in black.

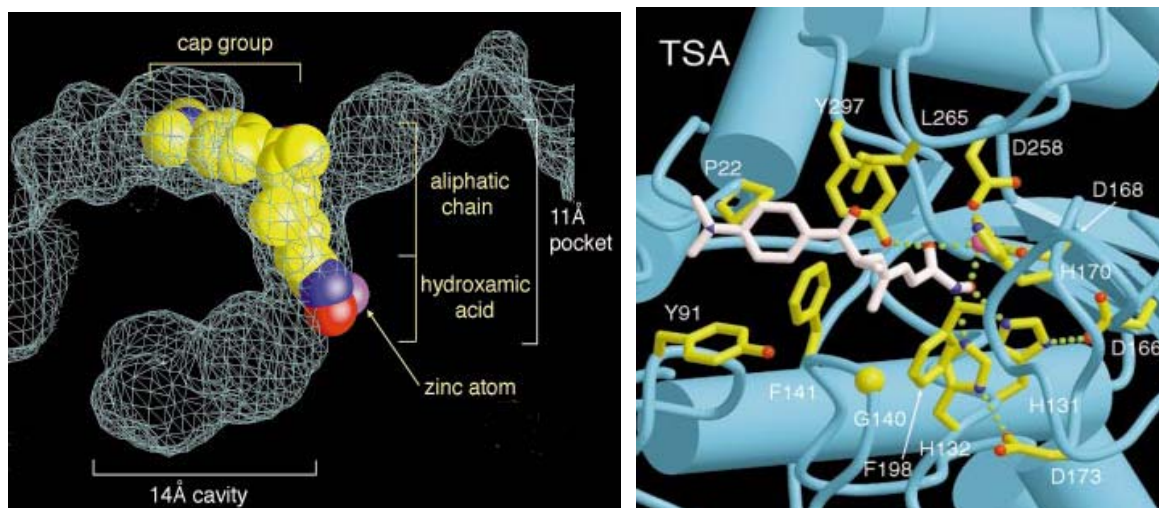


**Fig. 1.6** Surface representation of the channel and internal cavity of HDLP-TSA complex in the active site pocket.

parallel disposition of Phe 141 and Phe 198. In the crystal structure of the zinc-reconstituted enzyme, the zinc ion is positioned near the bottom of the pocket. It consists of His170, Asp258 and a water molecule. In the crystal structure of HDLP-TSA complex, TSA binds by inserting its long aliphatic chain into the HDAC pocket, making multiple contacts to the tube-like hydrophobic portion of the pocket. The hydroxamic acid group at one end of the aliphatic chain reaches the polar bottom of the pocket where it coordinates the zinc in a bidentate fashion and also contacts active site residues. The aromatic dimethylamino-phenyl group at the other end of the TSA chain makes contacts at the pocket entrance and in an adjacent surface groove, capping the pocket. The length of the aliphatic chain is optimal for spanning the length of the pocket and allowing contacts at the bottom and at the entrance of the pocket. In conclusion, the structure characteristics of HDAC inhibitors include three portions: the zinc binding group (ZBG), which interacts the zinc ion and engages in multiple hydrogen bonds with the amino acid residue at the active site of HDAC, the linker domain, which occupies the channel of HDAC, and the surface recognition domain, which interacts with amino acid residues on the rim of active pocket entrance. **Fig. 1.7** shows pharmacophore domains of SAHA and SAHA-HDLP hydrogen bond and chelation interactions in the active site.<sup>[36]</sup>

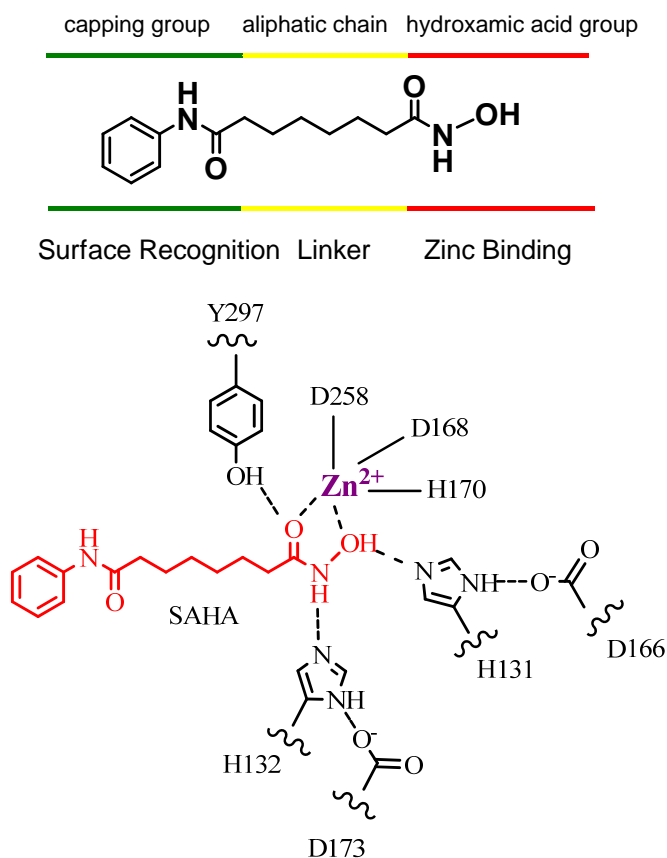


**Fig. 1.7** Pharmacophore domains of SAHA and SAHA-HDLP hydrogen bond and chelation interactions in the active site.

#### 1.4 Structure class of HDAC inhibitors

Abnormal activities of HATs and recruitment HDACs have been related to the pathogenesis of cancer. Inhibition HDACs activity can induce tumour cell growth arrest, differentiation and/or apoptosis *in vitro* and *in vivo* (**Fig. 1.8**),<sup>[37]</sup> and so HDAC inhibitors are evoking interest anticancer agents.<sup>[38,39]</sup>

In 1976, one of the first HDAC inhibitor TSA was isolated by Tsuji *et al.* from *Streptomyces hygroscopicus* as a fungistatic antibiotic active against *trichophyton*,<sup>[40]</sup> and the very potent HDAC activity of TSA was found by Yoshida *et al.* in 1990 in inducing friend leukemia cell differentiation and inhibiting cell cycle of normal fibroblasts in both the G1 and G2 phases, respectively.<sup>[41]</sup> Although the structures of HDAC inhibitors were different, inhibitors had similar three portions (the zinc binding group, linker and surface recognition). The zinc binding domain is analogous to the acetyl group of the N-acetylated Lys substrate, and it

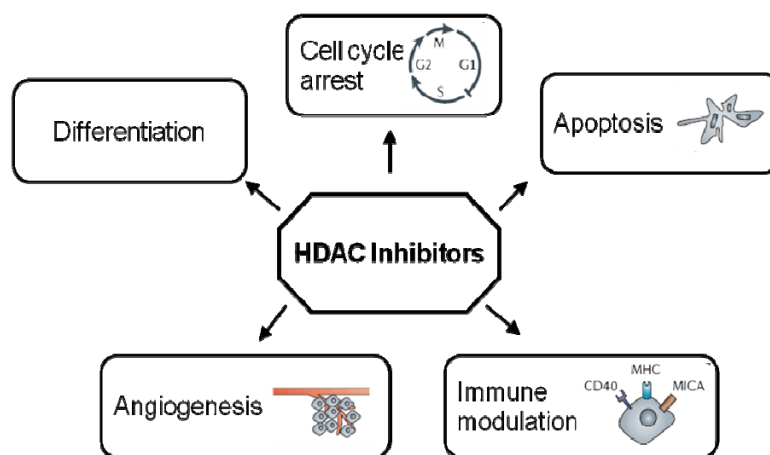


**Fig. 1.8** Biological effects of HDAC inhibitors.

interacts with  $Zn^{2+}$  ion and many of the same residues of HDAC. The zinc binding groups are typically a thiol, hydroxamic acid, carboxylic acid, ketone or substituted aniline. The inhibitory activity is determined by the length of the spacer and interactions of the spacer, hydrophobic surface binding scaffolds, and the strength of bonding between the functional group and the active site. According to chemical structure of inhibitors, in general, HDAC inhibitors are divided into six structure classes. There is a brief discussion of different HDAC inhibitors classes.

### 1.4.1 Carboxylates

In 1978, Boffa *et al.* identified the HDAC inhibitors such as butyric acid,<sup>[42]</sup> sodium phenylacetate with butyric acid derivatives, phenyl butyrate that one of the first HDAC inhibitors to be tested in proteins. In 2001, valproic acid of anticonvulsant was identified as HDAC inhibitor (**Fig. 1.9**).<sup>[43]</sup> The carboxylic acid, the zinc binding group is less active than the hydroxamic acid; may be due to weak coordination with  $Zn^{2+}$  ions. Despite being much less

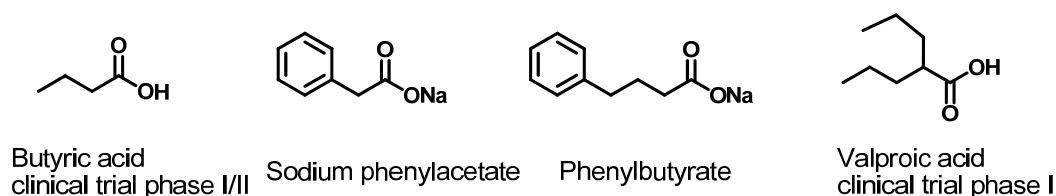


**Fig. 1.9** HDAC inhibitors of carboxylic acids class.



potent, these are currently among the best studied HDAC inhibitors. Valproic acid and phenyl butyrate have already been widely approved as an anti-epileptic treatment and some cancers, respectively, and valproic acid is a key regulator of many pathways in the cell.<sup>[44]</sup> Butanoic acid and valproic acid are undergoing clinical trials phase I/II and phase I, respectively.

### 1.4.2 Hydroxamic acids

The HDAC inhibitors of Hydroxamic acid constitute the broadest family of HDAC inhibitors; hydroxamic acid is one of the well-studied ligand for the active site  $Zn^{2+}$  of HDACs. The feature of inhibitors contains a hydroxamic acid functional group, such as natural products TSA and selected SAHA in synthesized hybrid.<sup>[45,46]</sup> The general structure of these substances consists of a hydrophobic linker that allows the hydroxamic acid moiety to chelate the  $Zn^{2+}$  ion at the bottom of HDAC active pocket, while the aromatic ring (bulky part of the molecule), which is the surface recognition domain, acts as a cap group. The linker domain consists of linear either saturated or unsaturated as 5- or 6-methylene hydrophobic spacer.<sup>[45]</sup> TSA and SAHA inhibit class I and class II HDACs, and are potent inhibitors of histone deacetylase, are active at nanomolar concentrations. SAHA has recently entered phase II clinical trials.<sup>[47,48]</sup> Based on the structure a large number of hydroxamate-derived HDAC inhibitors (TSA analogues and SAHA analogues) were designed and synthesized (**Fig. 1.10**).<sup>[49-64]</sup> These agents were evaluated as inhibitors of recombinant human HDAC, antiproliferative agents against a panel of human cell lines, and inducers of histone hyperacetylation and p21 expression. Structure activity relationship (SAR) study of these paradigmatic hydroxamate compounds were performed in a focused way by several research groups. Recently SAHA (Zolinza) approved by the FDA for the treatment of cutaneous T cell lymphoma (CTCL).<sup>[163,164]</sup>

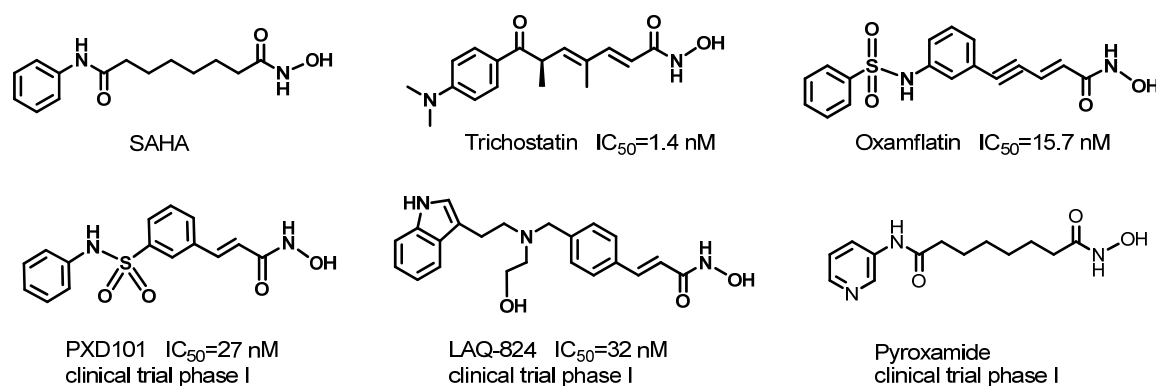


**Fig. 1.10** HDAC inhibitors of hydroxamic acid class.

### 1.4.3 Benzamides

The HDAC inhibitors of benzamide derivatives were synthesized by Suzuki *et al.* in 1999.<sup>[65,66]</sup> These HDAC inhibitors are the class of compounds which inhibit HDACs by ligating the active site  $Zn^{2+}$  ion with a benzamide moiety, no structural similarity with the previous HDAC inhibitors. These compounds are generally less potent than the corresponding hydroxamate compounds and cyclic tetrapeptide classes. The most potent compound of the series is named as MS-275 (**Fig. 1.11**), induces hyperacetylation of nuclear histone in some tumor cell lines and overexpression of p21. It has HDAC inhibitory activity of 5  $\mu$ M and shows significant anti-tumor activity in vivo. The evaluation of MS-275 demonstrated that it could inhibit partially purified human HDAC preparations and cause hyperacetylation of nuclear histones in various cell lines.<sup>[66,67]</sup> The MS-275 has entered clinical trials phase II. The other HDAC inhibitors of benzamide derivatives, such as CI-994 which is a 4-acetylamino-*N*-(2'-aminophenyl) benzamide as effective against mouse, rat and human tumor cells,<sup>[68]</sup> and is a potential drug for human acute myelocytic leukemia, colorectal cancer etc of a number of tumor diseases. The CI-994 is under clinical trials now.<sup>[69-71]</sup>

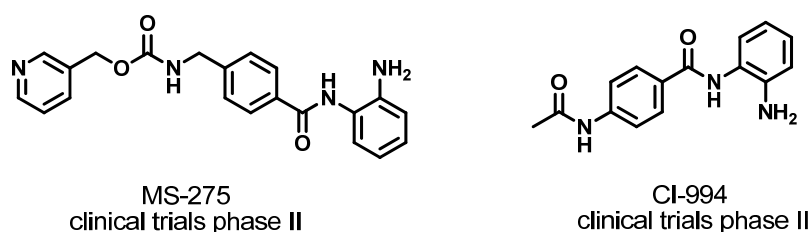


**Fig. 1.11** HDAC inhibitors of benzamides class.

### 1.4.4 Electrophilic ketones

Electrophilic ketones form a new class of HDAC inhibitors. The mechanism of these HDAC inhibitors might be hydrated form of the ketone acts as a transition-state to chelate the  $Zn^{2+}$  ion at the bottom of HDAC active pocket resemble carboxypeptidase A.<sup>[73,74]</sup> The series include various trifluoromethyl ketones and  $\alpha$ -ketoamide. In 2002, Frey *et al.* reported SAHA based straight chain trifluoromethyl ketones as HDAC inhibitors.<sup>[75]</sup> Wada synthesized  $\alpha$ -ketoesters and  $\alpha$ -ketoamides as HDAC inhibitors.<sup>[76]</sup> Several compounds in the series showed micromolar levels inhibitory activity, so they were developed by altering the aryl group, nanomolar

$\alpha$ -ketoamide HDAC inhibitors (**Fig. 1.12**). The inhibitors of electrophilic ketone class represent a relatively new group of HDACs substrate that has not yet been fully explored. We should develop farther structural variants so as to assess optimal design parameters and tolerances.

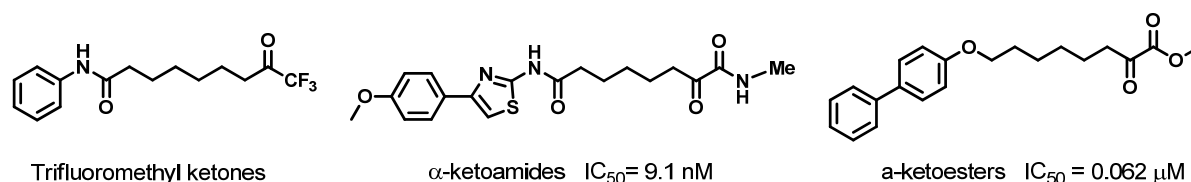


**Fig. 1.12** HDAC inhibitors of electrophilic ketones class.

### 1.4.5 Cyclic peptide HDAC inhibitors

Cyclic peptide-based HDAC inhibitor is a class of the most complicated compounds in HDAC inhibitors. The main structure of the HDAC inhibitors of cyclic peptide is composed of a macrocycle containing four amino acid residues (hydrophobic amino acids) in the surface recognition domain, an alkyl chain in the linker domain, and a functional group in the zinc ion binding domain (**Fig. 1.13**). Cyclic peptide-based HDAC inhibitors bind to the HDAC enzymes in a manner consistent with TSA. The aliphatic linker passes down the enzyme's channel, positioning the binding moiety in proximity to the active site zinc, while the macrocyclic portion interacts with the rim of the active site. The macrocycle in naturally occurring cyclic tetrapeptide inhibitors is arranged with a D-amino acid and an imino acid (Pro or Pip) flanking the amino acid bearing the linker moiety, which generates a constrained 12-membered cyclic structure with extensive internal hydrogen bonding. It is postulated that the D-configuration of the amino acid is necessary for tight association with the rim of the active site, thereby allowing

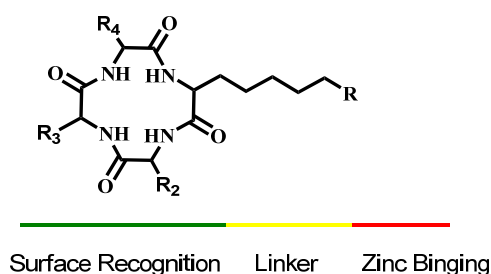


**Fig. 1.13** Pharmacophore domains of cyclic peptide HDAC inhibitors.

the linker to align and insert into the enzyme's channel.<sup>[77]</sup> According to the chemical structure of zinc ion binding domain of inhibitors, cyclic peptide HDAC inhibitors were divided into the following different structure classes.

### (1) Cyclic tetrapeptide containing epoxyketone

The class of cyclic tetrapeptide HDAC inhibitors contains a unique amino acid, (*S*)-2-amino-8-oxo-9,10-epoxydecanoic acid (Aoe) in zinc ion binding domain. The Aoe side chain is approximately isosteric with an acetylated lysine, suggesting that it functions as a mimic of an acetylated histone. Reduction or hydrolysis of the epoxide can result loss of biological activity of inhibitors. The Aoe residue induces irreversibly inactivate its receptor through covalent bond formation. This series compounds have two more structural features in common: at least one amino acid with (*R*) configuration and a proline or pipercolic acid residue. In 1974, Chlamydocin and dihydro-Chlamydocin were first isolated and characterized from *Diheterospora chlamydosporia* by Clossé *et al.* (**Fig.1.14**).<sup>[78]</sup> The structure of Chlamydocin contained an aromatic ring in its cyclic framework. Chlamydocin exhibited notable cytostatic activity *in vitro*. It is found to be a highly potent HDAC inhibitor, inhibiting HDAC activity *in vitro* with an IC<sub>50</sub> of 1.3 nM. Whereas Chlamydocin, with reduced its C8-carbonyl, was inert. The epoxyketone group of Chlamydocin was replaced by -OH, -CH<sub>2</sub>=CH<sub>2</sub>, -CH<sub>2</sub>CH<sub>3</sub> or -CH<sub>2</sub>CH<sub>2</sub>OH, the activity of HDAC inhibitors incoordinately reduced.<sup>[79]</sup> The prolyl-substituted Cyl-1 as well as its pipercolyl-variant Cyl-2 were produced by *Cylindrocladium scoparium*, were found as potent plant growth regulators.<sup>[80-82]</sup> The fungal metabolite

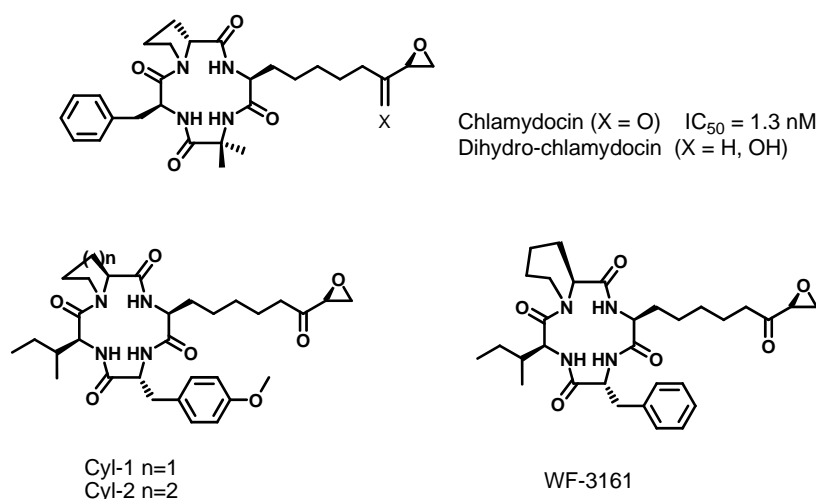


**Fig. 1.14** Several HDAC inhibitors of cyclic tetrapeptid containing epoxyketone.

WF-3161 that was obtained from *Petriella guttulata* also exhibited better antitumor activity *in vitro* and *in vivo*.<sup>[83]</sup>

HC-Toxin I that was isolated by *Helminthosporium carbonum*, was one of the first cyclic tetrapeptides in this structural class identified, and Liesch *et al.* characterized its chemical structure (**Fig.1.15**).<sup>[84]</sup> Later was revised structure by Knoche and co-workers.<sup>[85,86]</sup> HC-Toxins which are also cyclic tetrapeptide and have no aromatic ring in their cyclic framework are still inhibiting the HDACs. 9,10-2 hydroxy of HC-Toxin analogues is an inactivation.<sup>[87]</sup> Further investigations led to the identification of HC-Toxin III,<sup>[88]</sup> bearing a *trans*-3-hydroxyproline. Moreover, HC-Toxin II was also discovered, an analog in which one Ala residue was replaced by a Gly.<sup>[89]</sup> While HC-Toxin III was found to be comparable in potency to HC-Toxin, HC-Toxin II have low activity ( $EC_{50} = 7 \mu\text{g/mL}$  in a maize root inhibition assay) relative to HC-Toxin ( $EC_{50} = 0.2 \mu\text{g/mL}$ ). It is interesting to mention that this 35-fold decrease in efficacy originated from a relatively modest structural change.

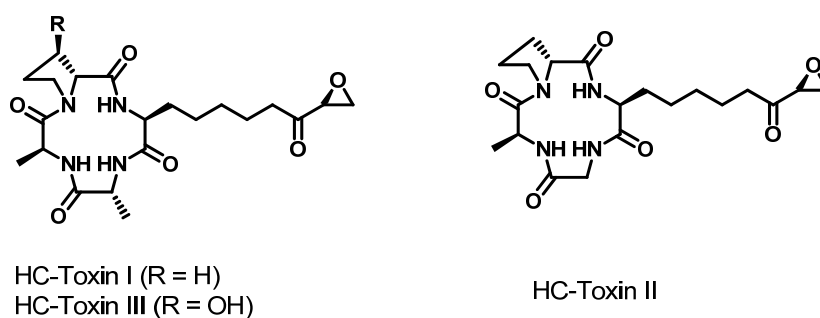


**Fig. 1.15** Several HDAC inhibitors of HC-Toxin analogues.

Trapoxins A and B which were produced in the fermentation broth of *Helicoma ambiens*,<sup>[90]</sup> can potentially inhibit cellular transformations. In their structure, they differ solely by the presence of either a cyclic imino acid D-Pip or D-Pro in the tetrapeptide scaffold (**Fig. 1.16**). Kijima *et al.* confirmed that inhibitory concentration of Trapoxin A was the same for *in vivo* and *in vitro* ( $<10 \text{ nM / L}$ ).<sup>[91]</sup> Taunton *et al.* synthesized Trapoxin B, [<sup>3</sup>H] Trapoxin B, I-trap and K-trap etc. These analogues have inhibition, toxicity and instability.<sup>[92]</sup>

HC-Toxin, Chlamydocin and Cyl-2 of three HDAC inhibitors were compared for phytotoxic efficacy to elucidate the relationship between cyclic tetrapeptide structure and biological activity.<sup>[93]</sup> The shifts in their respective biological activities correlated to overall cyclic peptide polarity. Consequently, it was postulated that these differences could be ascribed to a given

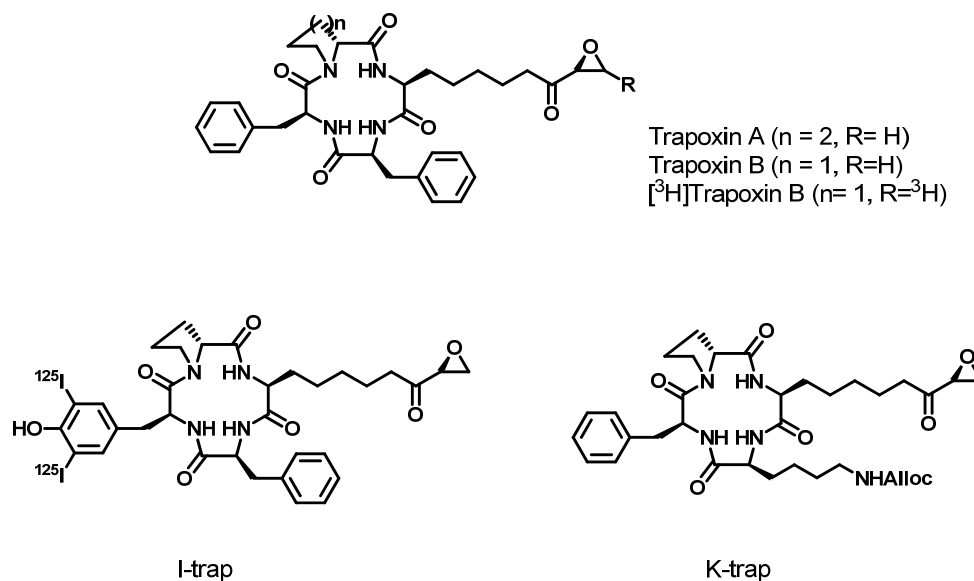


**Fig. 1.16** Several HDAC inhibitors of Trapoxin analogues.

analogues's potential ability to penetrate membranes, as increased hydrophobicity enhanced potency. HC-Toxin is 10-fold less potent than Chlamydocin against these sensitive maize hybrids.<sup>[94]</sup> This premise was further supported by the dramatically reduced efficacy of the more polar glycine variant of HC-Toxin, HC-Toxin II (approximately 3% as active as HC-Toxin). Chlamydocin, Cyl-1, Cyl-2, Trapoxins, HC-Toxin and WF-3161 have irreversible HDAC inhibitory activity for epoxyketone. On the basis of the irreversible inhibition of trapoxin B with HDAC enzyme, Schreiber isolated HDAC1 using affinity chromatography.<sup>[95, 96]</sup> Naturally occurring cyclic tetrapeptide based HDAC inhibitors containing epoxyketone functional group demonstrated the importance of the cyclic tetrapeptide moiety for the nanomolar inhibition of HDAC. Due to the irreversible nature of the epoxide based inhibitors; they did not receive much attention in the HDAC inhibitor research.

## (2) Cyclic tetrapeptide containing hydroxamic acids

The class HDAC inhibitors containing hydroxamic acids are all artificially synthesized as a series hybrid of TSA and cyclic tetrapeptide. These inhibitors contain a hydroxamic acid as the zinc binding group attached to a cyclic tetrapeptide scaffold (Cyl-1, Chlamydocin, Trapoxins, HC-Toxin etc.), and are reversible inhibitors of HDAC. The scaffold structure of cyclic hydroxamic-acid-containing peptide (CHAPs)<sup>[97]</sup> was constituted by varied changing the number of the amino acids, the pattern of amino acid chiral combinations, and the side chain

structure of each amino acid. The activity of cyclic tetrapeptide revealed importance of the cyclic tetrapeptide scaffold for high HDAC inhibitory activity. The structures of CHAP derivatives are represented as *cyclo(-Asu(NHOH)-AA2-AA3-Pro(Pip)-)*. CHAP 31 is one of the strongest the CHAPs with nanomolar activity ( $IC_{50} = 3.3$  nM), having the cyclic tetrapeptide part of natural cyclic peptide Cyl-1 (**Fig. 1.17**). CHAP31 shows antitumor activity in C57BL x DBA/2 F1 (BD2F1) mice bearing B16/BL6 tumor cells. CHAP31 inhibits the growth in four of five human tumor lines implanted into nude mice. These results suggest CHAP31 to be promising as a novel therapeutic agent for cancer treatment. Yoshida and coworkers synthesized and carried out a SAR study using several CHAPs containing cyclic tetrapeptide and cyclic octapeptide.<sup>[98]</sup> A comparative study of the activity of cyclic tetrapeptide and cyclic octapeptide revealed the importance of the cyclic tetrapeptide scaffold for high HDAC inhibitory activity.

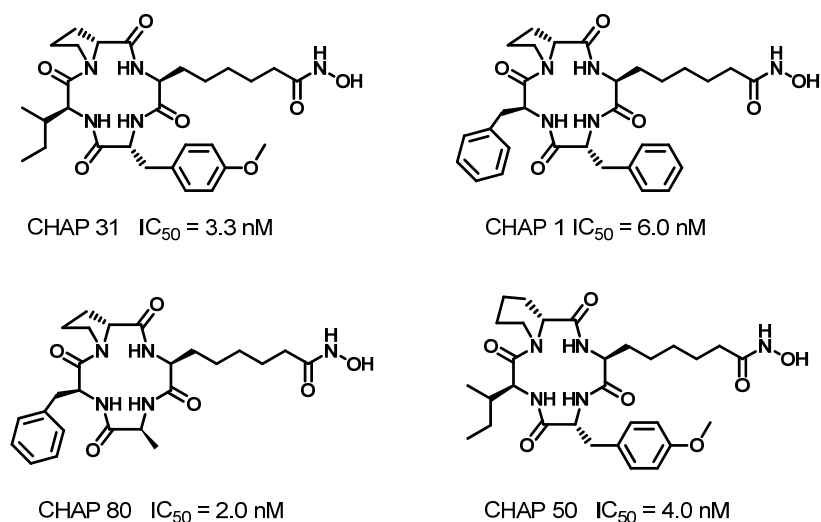


**Fig. 1.17** Several HDAC inhibitors of synthetic cyclic tetrapeptide hydroxamic acids peptide (CHAPs).

Recently, Binoy *et al.* designed and synthesized a cyclic hexapeptide hydroxamic acid inhibitor (*cyclo(-Ser-Asp-Asu(NHOH)-Thr-Ile-Gly-)*) for HDAC6 that  $\alpha$ -tubulin was the substrate (**Fig. 1.18**). But hexapeptide hydroxamic acid inhibitor showed very low HDAC inhibitory activity. To compare compounds conformation to the crystal structure of  $\alpha$ -tubulin showed the acetylated lysine of the cyclic hexapeptide substrate or the Asu(NHOH) of cyclic hexapeptide inhibitor was different from that around  $\alpha$ -tubulin's lysine-40.<sup>[99]</sup>

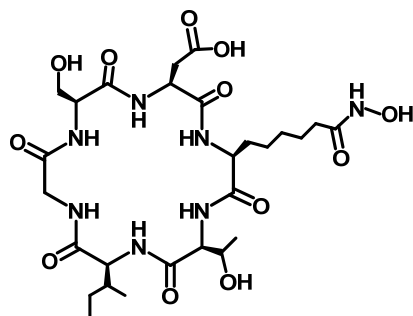


**Fig. 1.18** Cyclic hexapeptide hydroxamic acid inhibitor.

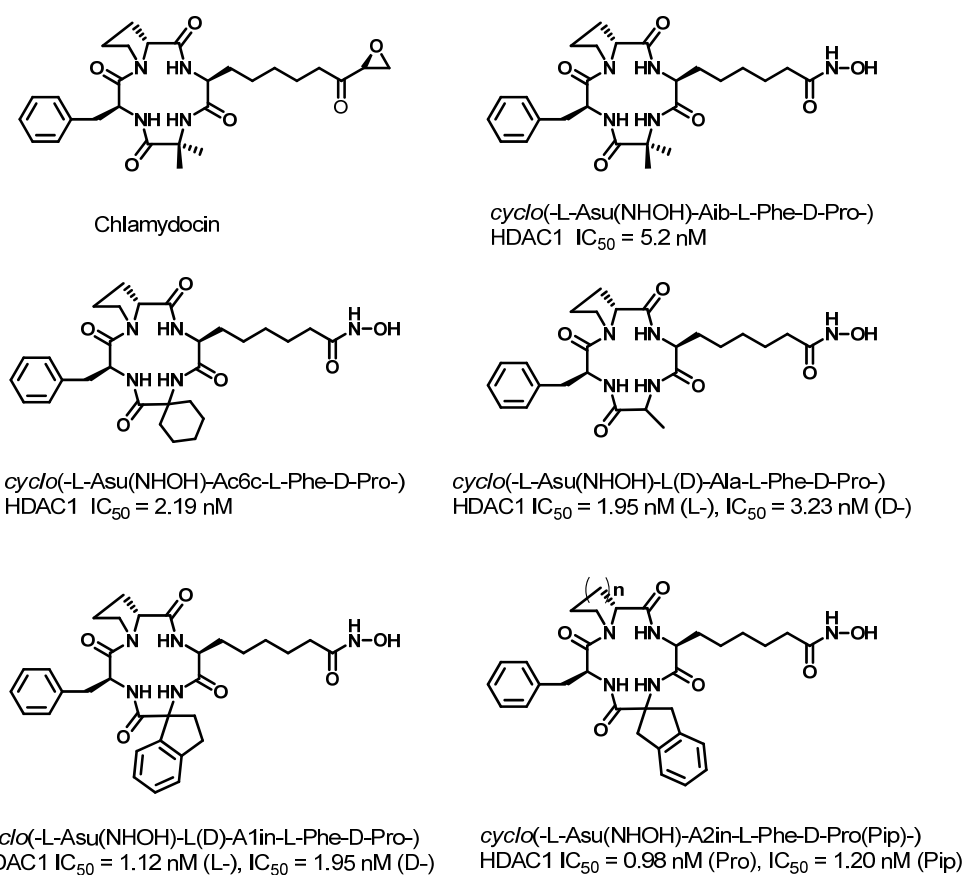


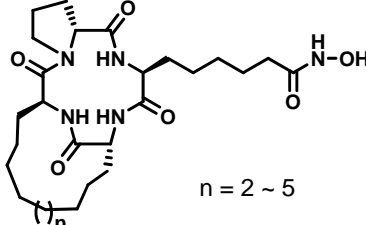
**Fig. 1.19** Several HDAC inhibitors of synthetic Chlamydocin hydroxamic acid analogues.

In 2004, Nishino *et al.* synthesized Chlamydocin hydroxamic acid analogues by replacing epoxy ketone moiety of Aoe by hydroxamic acid functional group (**Fig. 1.19**). In addition, they also have introduced several aromatic analogues in cyclic framework to study hydrophobic interaction of capping group, a number of amino-cycloalkanecarboxylic acids (Acc) were



introduced instead of the simple amino-isobutyric acid (Aib) for a variety of the series of Chlamydocin analogues. The compounds synthesized were tested for HDAC inhibitory activity and the results showed that many of them were potent HDAC inhibitors. The replacement of Aib residue of Chlamydocin with an aromatic amino acid enhanced the in vivo and in vitro inhibitory activity.<sup>[100]</sup>

In 2010, Nurul and coworkers synthesized a series of bicyclic tetrapeptide containing hydroxamic acids by changing the length of the aliphatic loop to explore the effect of the loop length on the activity of the inhibitors. The sequence and configuration of amino acids in CHAP31 are considered as the basis for designing the inhibitors. All the compounds as shown in **Fig. 1.20** are active in nanomolar range and specific toward HDAC4 compared with HDAC1 and HDAC6. They are about two times more active toward HDAC4 than HDAC1, and about 50 times more active than HDAC6.<sup>[101]</sup>



compounds	Loop size	IC <sub>50</sub> (nM)			EC <sub>1000</sub> (nM)
		HDAC1	HDAC4	HDAC6	P <sup>21</sup> promoter assay
TSA	-	23	44	65	20.0
2	-(CH <sub>2</sub> ) <sub>9</sub> -	9.1	5.4	330	92.0
3	-(CH <sub>2</sub> ) <sub>10</sub> -	9.1	5.5	410	7.2
4	-(CH <sub>2</sub> ) <sub>11</sub> -	11.0	4.5	280	2.6
5	-(CH <sub>2</sub> ) <sub>12</sub> -	13.0	5.0	240	2.0

**Fig. 1.20** HDAC inhibitors of bicyclic tetrapeptide hydroxamic acid.

In addition, there is a series of HDAC inhibitors with retrohydroxamate (N-formyl hydroxylamine) and N-acetyl hydroxylamine as zinc binding ligands. Based on the assumption, that retrohydroxamates can also act as good HDAC inhibitors, Nishino *et al.* synthesized and evaluated HDAC inhibitors of cyclic tetrapeptides with an optimum spacer length of five methylene units, as potent, long lived orally bioavailable matrix metalloproteinase's (MMPs) inhibitors, which are zinc proteases (**Fig. 1.21**).<sup>[102]</sup> Eventhough they have ten times lower

inhibitory activity than the corresponding hydroxamic acids, they are a novel class of inhibitors and have potential as anticancer agents.

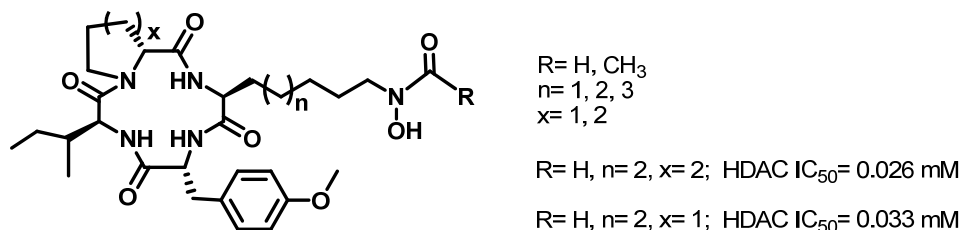
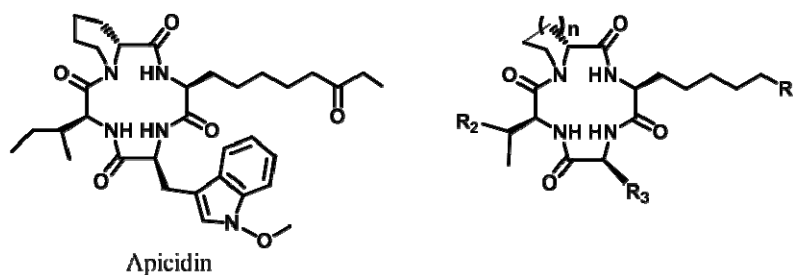


**Fig. 1.21** HDAC inhibitors containing retrohydroxamic acid.

### (3) Cyclic tetrapeptide containing ketone

Apicidin, is cyclopeptide HDACs inhibitor isolated from *Fusarium Pallodoroseum*, as a potent and broad spectrum antiprotozoal agent that exerts its biological activity by reversibly inhibiting HDAC activity.<sup>[103]</sup> A group of Merck research laboratory extensively studied the HDAC inhibitory activity of Apicidin and its synthetic analogues (**Fig. 1.22**).<sup>[104-110]</sup> Apicidin contains an ethyl ketone moiety in its side chain, and so it is different from other natural cyclic peptides like Trapoxin or HC-Toxin with epoxyketone side chain. The high potency of HDAC inhibitory activity of Apicidin further confirmed the importance of the cyclic tetrapeptide scaffold for the inhibitor design. The experimental IC<sub>50</sub> values of the HDACs inhibitors (Apicidin, Apicidin B, ApicidinC and analogue **d**) toward HDAC1 are 1, 10, 6 and 86 nM, respectively, while the IC<sub>50</sub> of Apicidin toward HDAC8 is above 1000 nM. The shift of keto group from position C-8 to C-9 decreases potency, confirming that the exact location of the C-8 keto group is critical for proper mimicking of acetylated histone lysine. On the other hand, if the ethyl ketone moiety is changed to hydroxamic acid, epoxyketone or methyl ester with a spacer of five methylene groups, the inhibitory activity is further enhanced.<sup>[111]</sup> Moreover, they found that the Trp residue of Apicidin was a key site and the replacement or modification of this moiety had great influence on the HDAC inhibitory activity which meant that the amino acid present in the cyclic tetrapeptide inhibitor had some interactions with the rim of the HDACs active site pocket.<sup>[112]</sup> The introduction of a basic group at the Trp's NH increased the HDAC activity and similar enhancement in activity was observed with the introduction of a bulky aryl substituent at the 2-position of Trp.



Compound	Name	n	R <sub>1</sub>	R <sub>2</sub>	R	HDAC (IC <sub>50</sub> nM)
1	Apicidin	n=2		CH <sub>2</sub> CH <sub>3</sub>		1.0
2	Apicidin B	n=1		CH <sub>2</sub> CH <sub>3</sub>		10.0
3	Apicidin C	n=2		CH <sub>3</sub>		6.0
4	Analogue d	n=2		CH <sub>2</sub> CH <sub>3</sub>		86.0
5	Apicidin A	n=2		CH <sub>2</sub> CH <sub>3</sub>		2.0
6						2.0
7						1.0
8						6.0
9						0.4
10	derivatives	n=2		CH <sub>2</sub> CH <sub>3</sub>		7.0
11						30.0
12						0.3
13						0.1
14						0.2

Fig. 1.22 Apicidin and analogues with changing side chain.

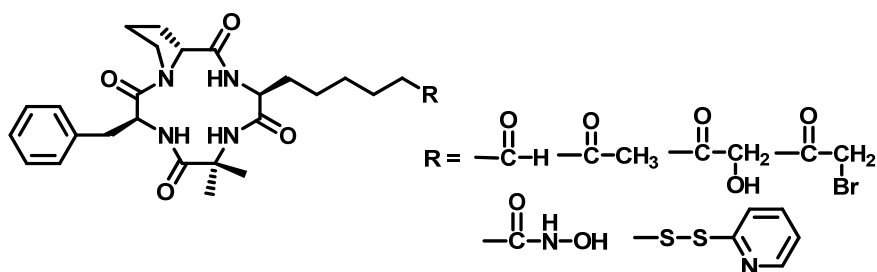
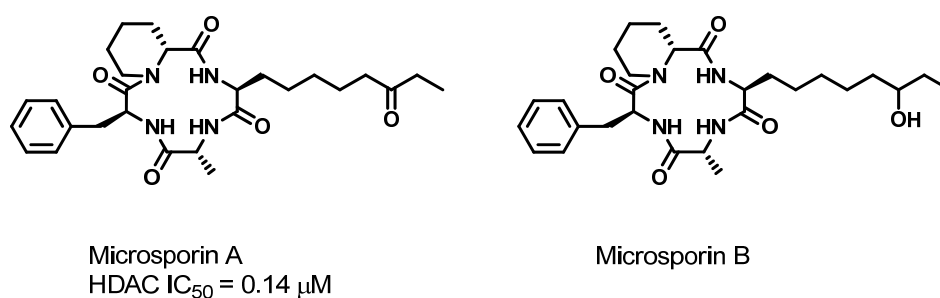


Fig. 1.23 HDAC inhibitory activity of Chlamydocin analogues bearing carbonyl as functional group.

Bhuiyan *et al.* have replaced the epoxy ketone moiety in Chlamydocin with several ketones and aldehyde to synthesize potent reversible and selective HDAC inhibitors.<sup>[113]</sup> They found most of them as potent inhibitors and some compounds have shown remarkable selectivity among HDAC subtypes (**Fig. 1.23**).

Two new cyclic peptides possess the unusual amino acid Aoda ((S)-2-amino-8-oxodecanoic acid) and its hydroxyl derivative ((2S)-2-amino-8-hydroxydecanoic acid), respectively. Microsporins A and B (**Fig. 1.24**), were isolated from culture extracts of the marine-derived fungus *Microsporium cf. gypseum* by Wenxin Gu *et al.* in 2007.<sup>[114]</sup> Microsporins A and B are potent inhibitors of histone deacetylase. Microsporin A showed in vitro cytotoxicity against human colon adenocarcinoma HCT-116 ( $IC_{50} = 0.6$  mg/mL) and a mean  $IC_{50}$  value of 2.7 mM in diverse 60-cell line panel. Microsporin B showed reduced in vitro cytotoxicity against HCT-116 ( $IC_{50} = 8.5$  mg/mL), which may indicate the importance of the Aoda ketone carbonyl group for biological activity.



**Fig. 1.24** Microsporins A and B as HDAC inhibitors.

In 2009, Ana and coworker designed and synthesized a series of  $\beta$ -amino acid-containing HDAC inhibitors inspired by cyclic tetrapeptide natural products (**Fig. 1.25**). To survey a diverse ensemble of pharmacophoric configurations, they systematically varied the position of the  $\beta$ -amino acid, amino acid chirality, functionalization of the  $Zn^{2+}$  coordinating amino acid side chain, and alkylation of the backbone amide nitrogen atoms around the macrocycle. The ethylketone-containing compounds that were most active against HeLa cell nuclear extract exhibited significant cell-specific cytotoxicity. The hydroxamic-acid-containing peptide inhibited the growth of all the test cell lines, consistent with its high potency against HDAC activity in HeLa nuclear extract. The compounds exhibited potent activities against a number of HDAC isoforms as well as effective antiproliferative and cytotoxic activities against human tumor cells.<sup>[115]</sup>

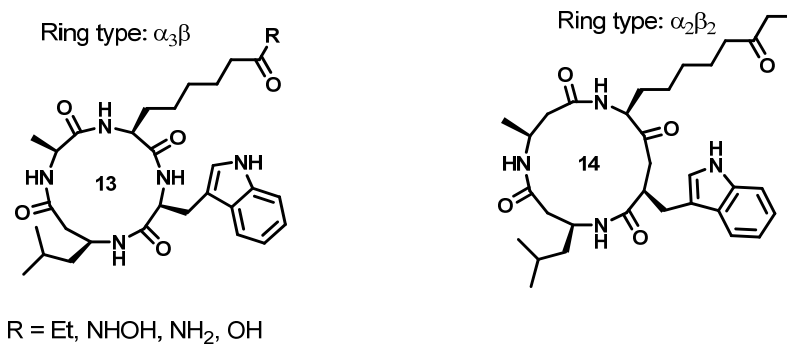


**Fig. 1.25** Cyclic tetrapeptide containing ketone and  $\beta$ -amino acid.

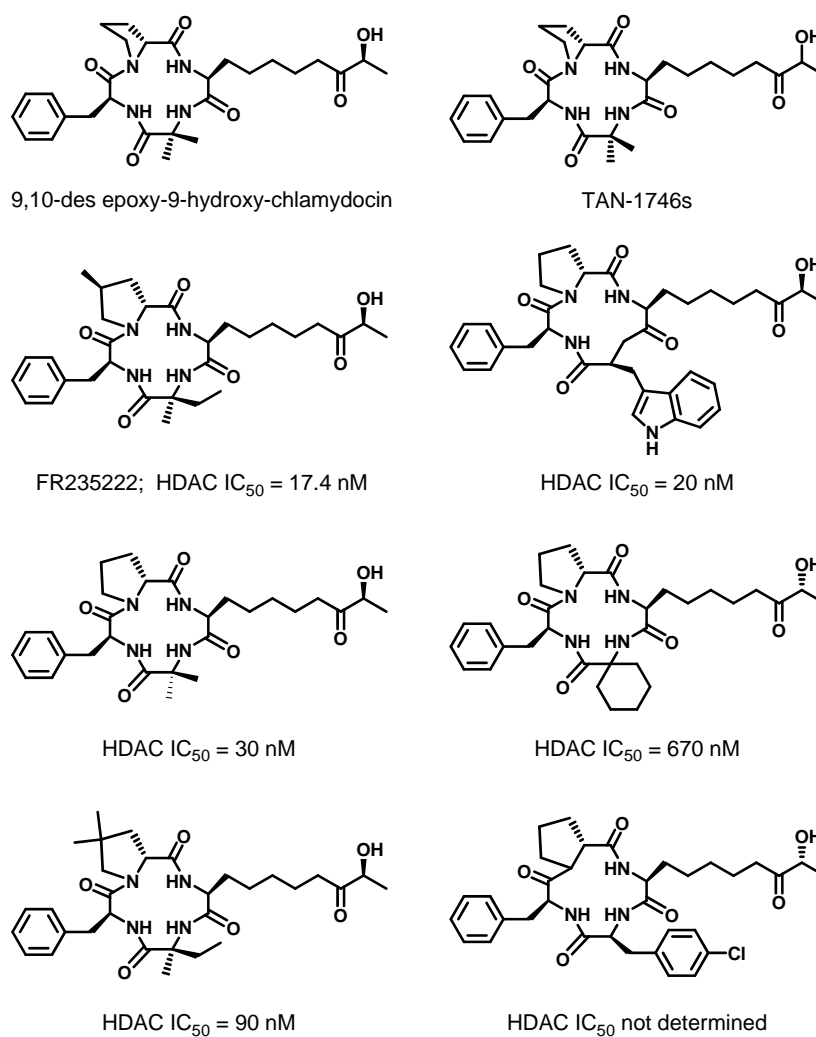


**Fig. 1.26.** HDAC inhibitors of cyclic tetrapeptides containing hydroxymethyl ketone.

#### (4) Cyclic tetrapeptide containing hydroxymethyl ketone

In 1994, a phytotoxic cyclotetrapeptide containing an unusual amino acid, 2-amino-8-oxo-9-hydroxydecanoic acid, was isolated from the fungus *Verticillium coccosporum*. Structurally, the peptide is closely related to the known peptide Chlamydocin<sup>[116]</sup> and the tumorigenic TAN-1746s (Fig. 1.26).<sup>[117]</sup> Both new analogs, as noted, lack the 9,10-epoxide and instead bear a 9-hydroxyl. A published patent has described a desepoxy-Trapoxin analog (FR-225497, compound not shown) which had good activity against human tumor cell lines in vitro ( $IC_{50}$  = 152 and 158 ng/mL against Jurkat and HT-29 cells, respectively).<sup>[118]</sup> A natural immunosuppressant FR235222, that potently inhibits mammalian HDACs has a Chlamydocin like cyclic tetrapeptide structure, inhibiting the HDACs ( $IC_{50}$  = 9.7 nM).<sup>[119]</sup> A number of synthetic FR235222 analogues that bearing a carboxylic or an hydroxamic acid functionality as Zn binding moiety replacement or modification of hydroxymethyl ketone moiety were reported (Fig. 1.26).<sup>[120]</sup>

#### (5) Cyclic tetrapeptide containing electrophilic ketones

Jose and coworker synthesized cyclotetrapeptides containing trifluoromethyl ketone and pentafluoroethyl ketone as the zinc binding functional group (Fig. 1.27).<sup>[121]</sup> HDAC inhibitory activity of these electrophilic ketones depends on the degree of hydration of the ketone, which can chelate with the zinc ion present in the deep pocket of HDAC binding site. Out of these compounds trifluoromethylketone are found to have excellent inhibitory activity. Changing from trifluoro to pentafluoro group did not increase the activity, probably because of the

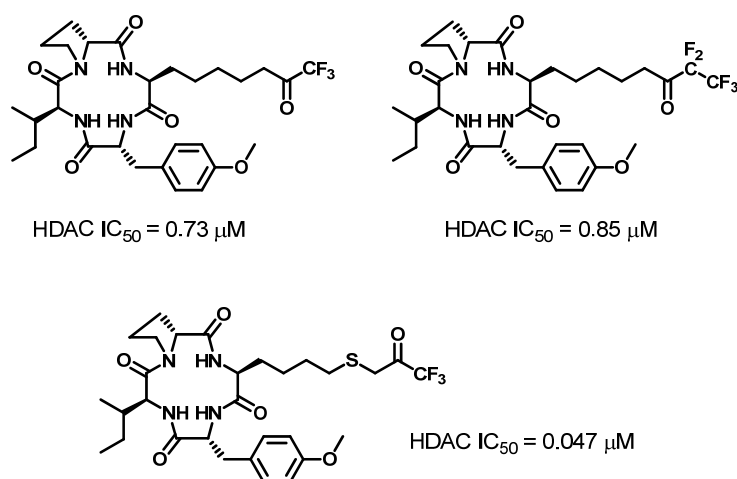
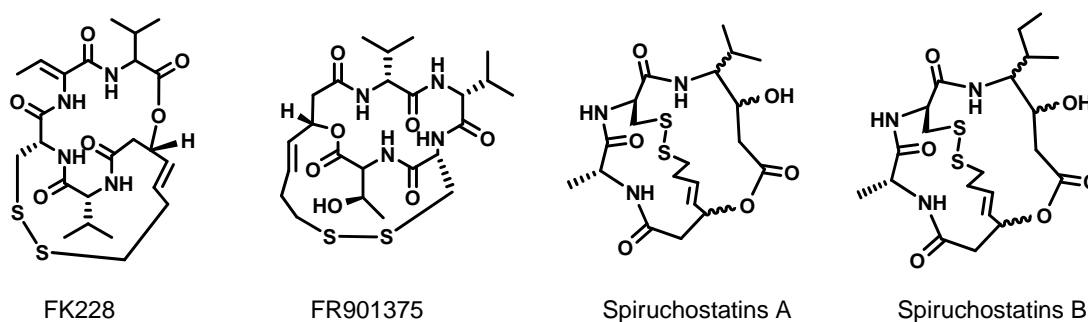


Fig. 1.27 Cyclic tetrapeptide containing electrophilic ketone.

balkiness of the pentafluoromethyl group. Incorporation of a sulfur atom to the carbonyl increased the activity that may provide different mode of ligation with  $Zn^{2+}$  ions, using longer spacer length.

#### (6) Cyclic peptides containing sulfur

FK228 (FR901228, depsipeptide) as a natural product was obtained from the fermentation broth of *Chromobacterium violaceum* by Fujisawa Pharmaceutical Co. Ltd. in 1991 along with the closely related depsipeptide, FR901375 (**Fig. 1. 28**).<sup>[122,123]</sup> FK228 includes a 16-membered cyclic depsipeptide bridged by a 15-membered macrocyclic disulfide ring, and is composed of L-Val, L-2-amino-2-butyleneic acid, D-Cys, D-Val and Hm7 (3S,4R-3-hydroxy-7-mercapto-4-heptenoic acid). There is no visible functional group in FK228 that interacts with the zinc ion in the HDAC active site. Furumai *et al.* demonstrated that the zinc-binding site of FK228 was the sulfhydryl functional group and converted to its active form by cellular reducing activity (**Fig. 1. 29**).<sup>[124]</sup>



**Fig. 1.28** HDAC inhibitors of sulfur-containing cyclic tetrapeptide.

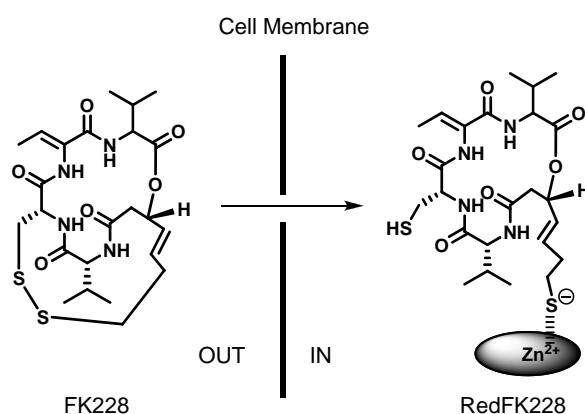


**Fig. 1.29** FK228 and RedFK228 (reduced form).

In 2001, Spiruchostatins A and B (**Fig. 1.28**) were isolated from *Pseudomonas* sp. as gene expression-enhancing substances. The structure consists of D-cysteine, D-alanine,  $\alpha$ -hydroxy acid and statine with potent HDAC inhibitory activity. They possess novel bicyclic depsipeptides involving 4-amino-3-hydroxy-5-methylhexanoic acid and 4-amino-3-hydroxy-5-methylheptanoic acid residues, respectively.<sup>[125]</sup> Recently, the total synthesis of Spiruchostatins was reported.<sup>[126,127]</sup>

In 2008, Luesch and co-workers isolated Largazole that is a densely functionalized macrocyclic depsipeptide from the cyanobacterium *Symploca* sp. (**Fig. 1.30**).<sup>[128-130]</sup> This natural product exhibits exceptionally potent and selective biological activity, with 2- to 10-fold differential growth inhibition in a number of transformed and non-transformed human- and murine-derived cell lines. The remarkable selectivity of this agent against cancer cells prompts particular interest in its mode of action and its value as a potential cancer chemotherapeutic. Albert *et al.* synthesized and assayed fourteen analogs of Largazole with six variants of the side-chain zinc-binding domain.<sup>[131]</sup>

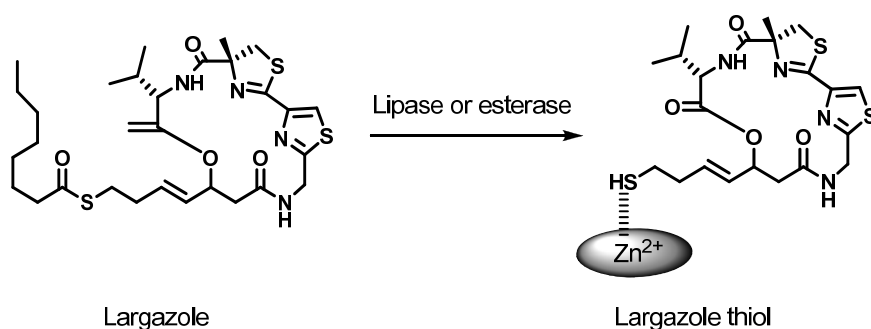


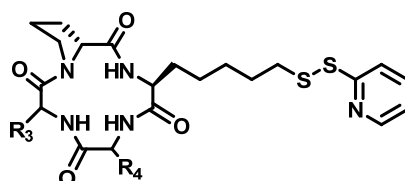
**Fig. 1.30** Largazole as HDAC inhibitors of Sulfur-containing cyclic tetrapeptides.

FK228 showed a potent *in vivo* antitumor activity and HDAC inhibitory activity.<sup>[132-140]</sup> FK228 was conducted in a phase I/II trial for patients with T-cell lymphoma, and these results suggested that inhibition of HDAC was a novel and potentially effective therapy.<sup>[141]</sup>

FK228 (Romidepsin INN, trade name Istodax) is an anticancer agent undergoing clinical trials as a treatment for cutaneous T-cell lymphoma (CTCL), peripheral T-cell lymphoma, and a variety of other cancers. Romidepsin is branded and owned by Gloucester Pharmaceuticals, now a part of Celgene. On November 5, 2009, it was approved by the U.S. Food and Drug Administration for the treatment of CTCL, after five years in the agency's fast track development program.<sup>[164,165]</sup>



In 1996, Khan *et al.* completed synthesis of FK228.<sup>[142]</sup> Recently, numerous improved synthesis methods were used for FK228 synthesis.<sup>[143-145]</sup> On the basis of this inhibitory activity of FK228, a series of HDAC inhibitors, sulfur-containing cyclic peptides (SCOPs), by replacing the L-Aoe[(2*S*,9*S*)-2-amino-8-oxo-9,10-epoxydecanoic acid] moiety of natural cyclic tetrapeptides with L-2-amino-7-mercaptoheptanoic acid (L-Am7) were synthesized by Nishino and coworkers.<sup>[146]</sup> These compounds were initially assayed for enzyme inhibition; they exhibited less activity in cell free condition. But in the p21 promoter assay most of the compounds showed good activity. Investigator considered that the disulfide bond was reduced in cell medium to give a sulfhydryl group, to regulate the activity of promoter gene by inhibiting HDAC enzymes. Accordingly, the cell free enzyme inhibition assays were carried out, in presence of 0.1 mM of DTT. The results of HDAC inhibitory activity and the p21 promoter assay of the compounds are shown in **Fig. 1. 31**.



Compound	IC <sub>50</sub> (nM)			HDAC1/ HDAC4 <sup>a</sup>	P <sup>21</sup> promoter assay EC <sub>1000</sub> (nM)
	HDAC1	HDAC4	HDAC6		
TSA	1.9	2.0	2.8	1.0	190
<i>cyclo</i> (-L-Am7(S2Py)-Aib-L-Phe-D-Pro-)	3.9	1.8	40	2.1	45
<i>cyclo</i> (-L-Am7(S2Py)-A2in-L-Ala-D-Pro-)	2.0	1.6	8.8	1.2	140
<i>cyclo</i> (-L-Am7(S2Py)-D-A1in-L-Ala-D-Pro-)	2.7	2.4	12	1.1	55
<i>cyclo</i> (-L-Am7(S2Py)-L-A1in-L-Ala-D-Pro-)	36	25	33	1.4	2000
<i>cyclo</i> (-L-Am7(S2Py)-D-2MePhe-L-Ala-D-Pro-)	170	70	71	2.4	25600
<i>cyclo</i> (-L-Am7(S2Py)-L-2MePhe-L-Ala-D-Pro-)	3.7	2.2	56	1.6	550
<i>cyclo</i> (-L-Am7(S2Py)-Aib-L-Ala-D-Tic-)	4.7	4.2	29	1.1	200
<i>cyclo</i> (-L-Am7(S2Py)-Aib-L-Phg-D-Pro-)	88	56	86	1.5	7400
<i>cyclo</i> (-L-Am7(S2Py)-Aib-L-Ph4-D-Pro-)	6.2	3.2	36	1.9	320
<i>cyclo</i> (-L-Am7(S2Py)-Aib-L-Ph5-D-Pro-)	5.3	2.7	43	1.9	110
<i>cyclo</i> (-L-Am7(S2Py)-Aib-L-Ser(Bzl)-D-Pro-)	3.2	1.6	24	2.0	72
<i>cyclo</i> (-L-Am7(S2Py)-Aib-L-Ser-D-Pro-)	6.4	4.0	26	1.6	580
<i>cyclo</i> (-L-Am7(S2Py)-Aib-L-Ala-D-Pro-)	9.4	5.2	43	1.8	750

<sup>a</sup> Selectivity of the enzymes

**Fig. 1.31** Comparative activity of SCOPs.

Nishino *et al.* also synthesized some stable disulfide dimers and hybrids with thiols (**Fig. 1.32**). These compounds showed potent inhibitory activity.<sup>[147]</sup> To know the interaction of aliphatic cap groups with HDACs, bicyclic peptide disulphide hybrid was also synthesized without aromatic ring in their macrocyclic framework.<sup>[148]</sup> The bicyclic peptide was found to be active in both cell free and cell based condition, and it had some selectivity among HDAC1 and HDAC6.

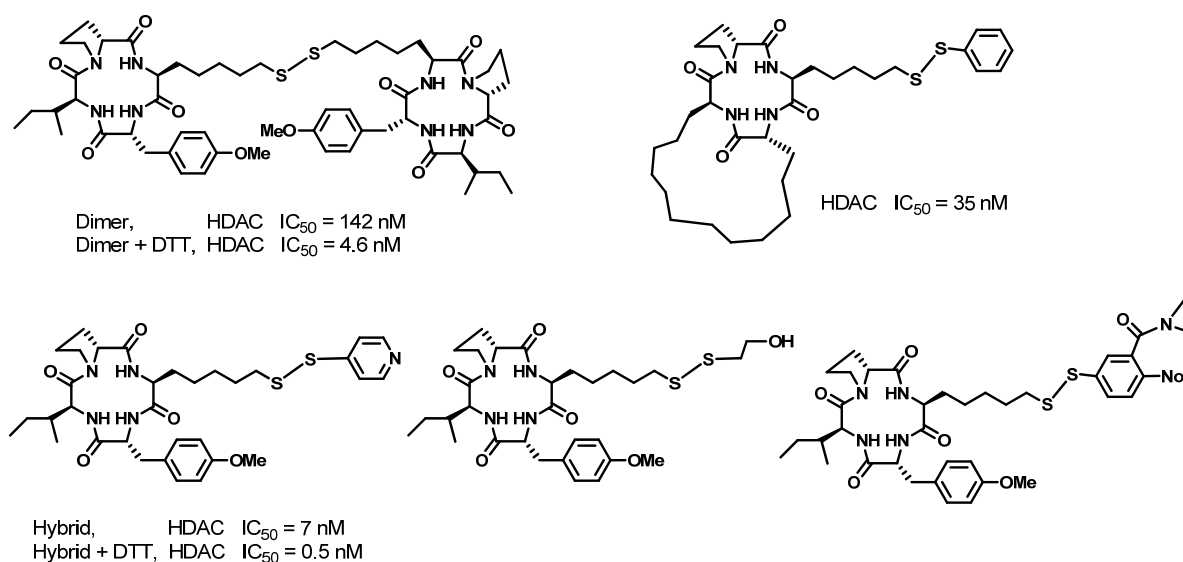


**Fig. 1.32** HDAC inhibitors of Sulfur-containing cyclic tetrapeptide.

#### (7) Cyclic tetrapeptide containing carboxylic or amide group

In 2006, Azumamide A-E were isolated from the marine sponge *Mycale izuensis* by Nakao *et al.* (**Fig. 1.33**),<sup>[149]</sup> and subsequently synthesized by Izzo *et al.*<sup>[150]</sup> Azumamides include three D- $\alpha$ -amino acids (D-Phe, D-Tyr, D-Ala, D-Val) and a unique  $\alpha$ -amino acid assigned as (*Z*, 2*S*, 3*R*)-3-amino-2-methyl-5-nonenedioic acid 9-amide (amnaa). The zinc-binding site of Azumamides is the carboxylic or amide functional group. To investigate the inhibitory activity of HDAC ligand, they performed Azumamides and the histone deacetylase-like protein (HDLP) model in the docking study.

In 2010, Bruno group synthesized a series of FR235222 analogues bearing a carboxylic functionality as Zn binding moiety (**Fig. 1.33**).<sup>[151]</sup> The compounds displayed submicromolar inhibitory activity on class I HDACs 1, 2, and 3. Its potency was similar to that measured on deacetylation reactions catalyzed by HDACs present in the nuclear extract (NE) from HeLa cells.

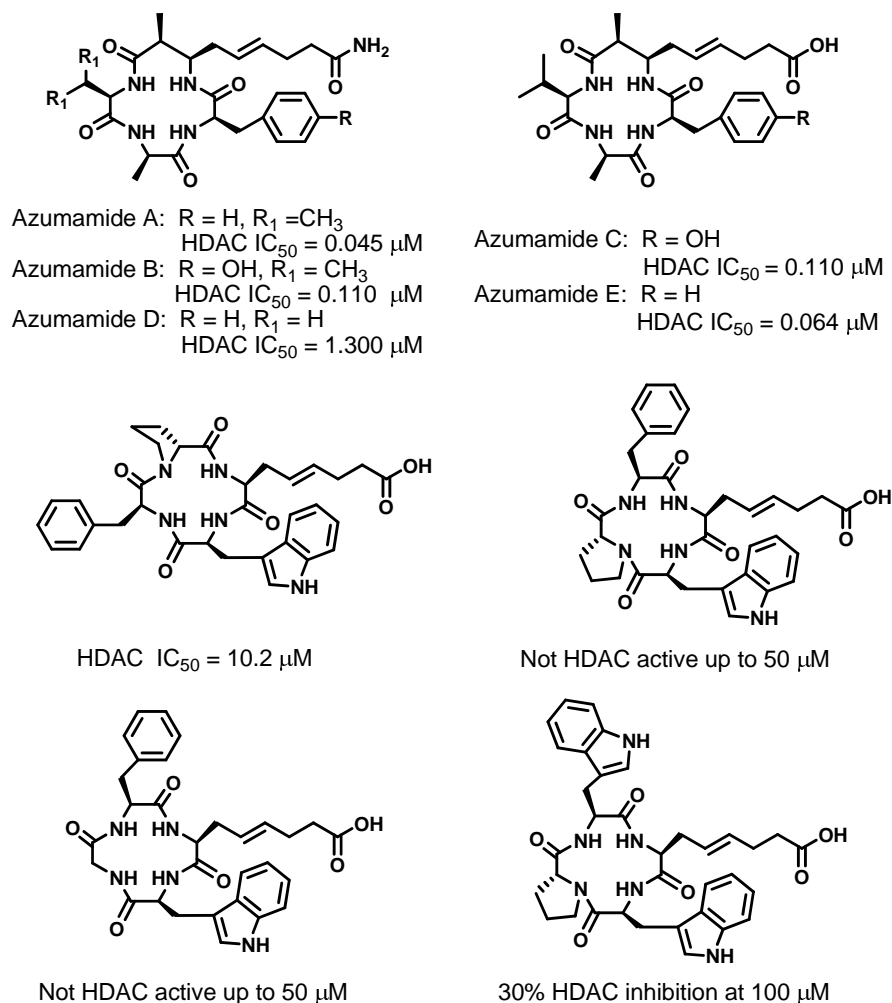


**Fig. 1.33** HDAC inhibitors of cyclic peptides containing carboxylic or amide group.

#### (8) Cyclic tetrapeptide containing guanidine

The derivatives based on HDAC inhibitor FR235222 were synthesized by Erinpritt and coworker in 2008 (**Fig. 1.34**).<sup>[152]</sup> They first reported utilizing guanidine group as relating to zinc ion of HDAC. These compounds exhibited both inhibition of HDAC activity and cytotoxicity against the pancreatic cancer cell line BxPC3.

#### (9) Miscellaneous of HDAC inhibitors of cyclic tetrapeptide

There are a number of HDAC inhibitors that can not be classified as a structural class. Meinke group synthesized HDAC inhibitors replacing the ketone side chain of Apicidins with

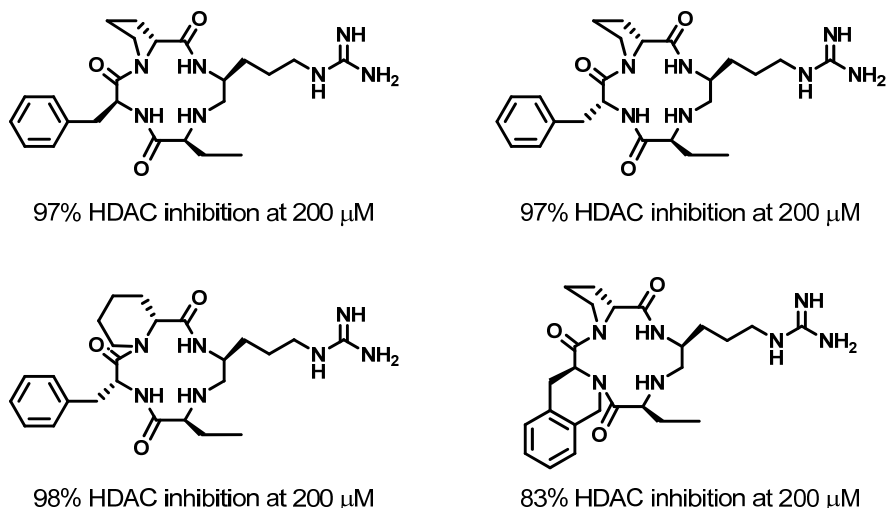


**Fig. 1.34** Cyclic tetrapeptide containing guanidine group.

phosphonate, showed very low HDAC inhibitory activity.<sup>[153]</sup> From all these phosphonate compounds studied for HDAC, it is clear that phosphonates are not good inhibitors for the HDAC inhibition, probably due to the highly acidic nature of phosphonate moiety, instead of the basic nature of the HDAC substrate. Jose *et al.* synthesized a phosphonate with a cap group of cyclic tetrapeptide and a spacer of five methylene units (**Fig. 1.35**).<sup>[154]</sup> The HDAC inhibitory activity study showed that the phosphonate cyclic tetrapeptide was a very weak inhibitor of HDAC.

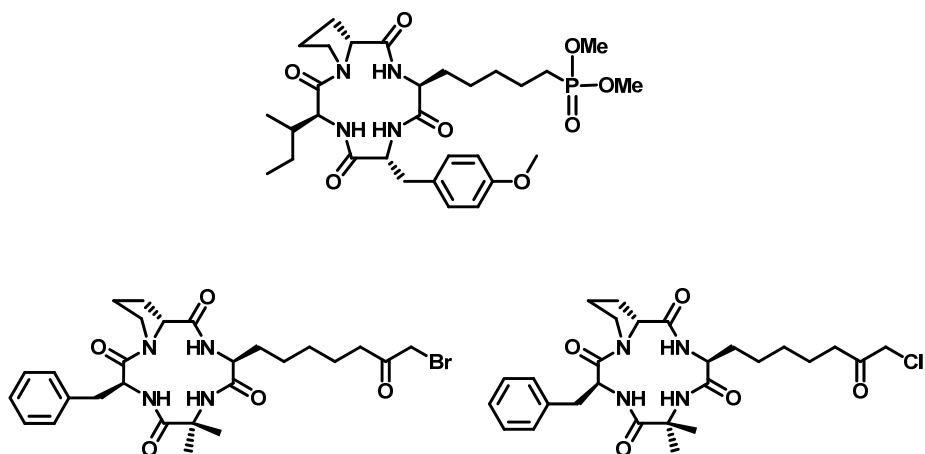


**Fig. 1.35** Miscellaneous HDAC inhibitors.

Rich *et al.* synthesized a cytostatic Chlamydocin derivative having  $\alpha$ -chloro ketone functional group as  $Zn^{2+}$  ligand of HDAC (**Fig. 1.35**). Though the new derivative exhibited somewhat decreased potencies in cell based antiproliferative assay (~3-4 fold) relative to the parent natural product, still it added a new variation to the zinc ligand library.<sup>[155]</sup> Bhuiyan *et al.* have replaced the epoxy ketone moiety in Chlamydocin with  $\alpha$ -bromo ketone functional group to synthesize HDAC inhibitors.<sup>[113]</sup>

### 1.5 Molecular simulation of interactions between HDAC and HDAC inhibitors

Recently, the study of protein simulation in computer science, medicinal chemistry, molecular biology and computational chemistry, have become a powerful tool for biology experiments and drug design. Crystal structures of the HDAC enzymes and their homologues provide essential information for rational drug design of selective HDAC inhibitors. The first structural information on zinc-dependent HDACs was derived from the crystal structure of histone deacetylase-like protein (HDLP), a bacterial enzyme sharing high homology to the HDACs around the binding pocket and containing a  $Zn^{2+}$  in its active site, bounded with TSA or SAHA.<sup>[30]</sup> Currently, crystal structure of HDAC8 has been reported, and its active site is similar to HDLP<sup>[30,156]</sup> and FB188 HDAH<sup>[31]</sup>. The structure of human class II HDAC7<sup>[29]</sup> and HDAC4<sup>[162]</sup> catalytic domain were reported.

Most of molecular simulation studies about the HDAC-inhibitor interactions are focused on small molecule inhibitors,<sup>[157,158]</sup> up to now only two contributions analyzing the binding contacts between HDLP and the tetracyclopeptide framework have been published: FR235222–HDLP<sup>[159,160]</sup> and Azumamide E-HDLP.<sup>[161]</sup> Cyclic peptides constitute the most structurally complex and diverse class of HDACs inhibitors.

Simone and coworker used the HDLP as target model in the docking calculations.<sup>[160]</sup> They performed on the *cis*- and *trans*-isomers of FR235222 analogues with the HDLP binding pocket, using AutoDock 3.0.5 software. The DMSO solution-state structures were obtained by 2D-NMR spectroscopy and were used as the initial conformations in the docking study. They analyzed the results obtained from docking to evaluate if one or both isomers interacted with the biological target (**Fig. 1.36 a**). It indicated that hydrophobic interactions contributed mostly to the stability of the complex. In particular, the indole ring (Trp) was able to interact efficiently with hydrophobic pockets located at the rim of zinc-containing tubular cavity. In addition, the change in C9 configuration caused a lowering in the binding affinities but didn't lead to a complete loss of HDAC inhibition activities.

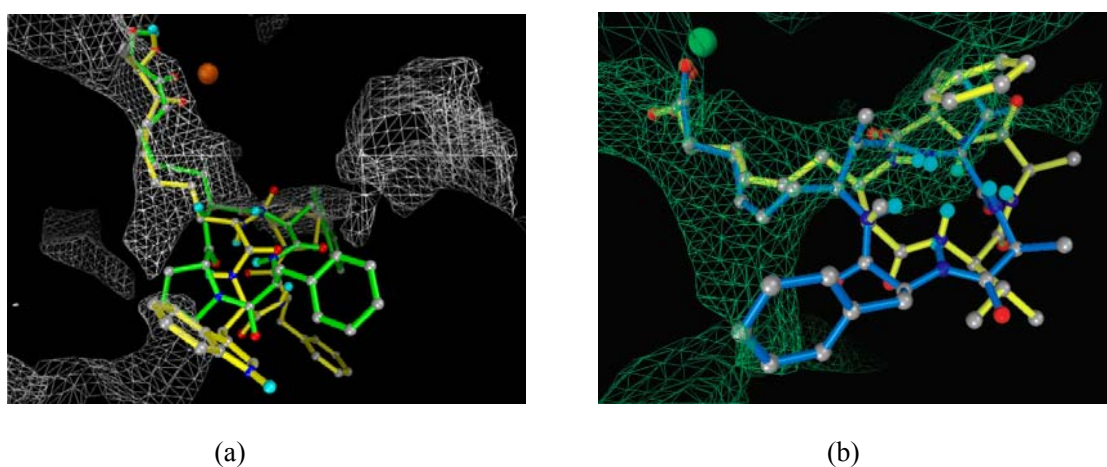
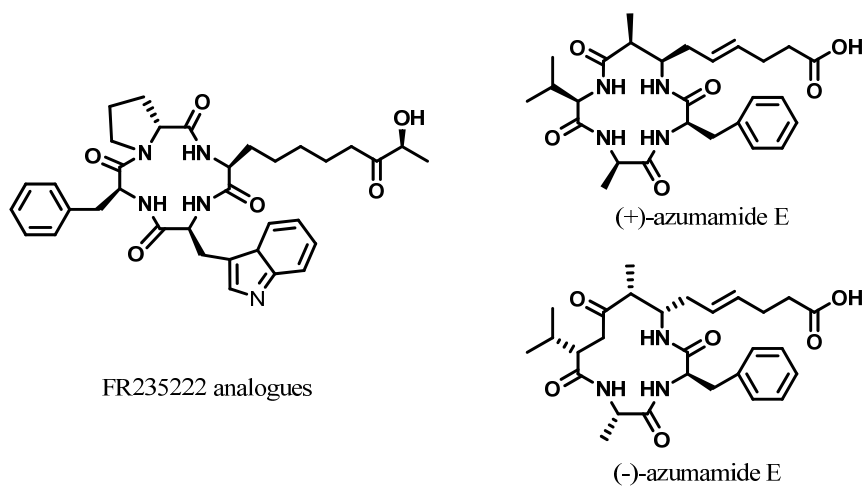


**Fig. 1.36** Cyclic peptide superimposition in the zinc-binding site. (a) *cis* and *trans* of FR235222 analogues. The  $Zn^{2+}$  is represented by a CPK sphere in dark orange. *trans* is depicted by sticks (yellow) and balls (by atom type: C, gray; polar H, sky blue; N, blue; O, red); *cis* is shown by sticks (green) and balls (by atom type: C, gray; polar H, sky blue; N, blue; O, red). (b) (+)-azumamide E and (-)-azumamide E. The  $Zn^{2+}$  is represented by a CPK sphere in dark green. (+)-azumamide E is depicted by sticks (yellow) and balls (by atom type: C, gray; polar H, sky blue; N, blue; O, red); (-)-azumamide E is shown by sticks (dark blue) and balls (by atom type: C, gray; polar H, sky blue; N, blue; O, red). The figure highlights the similar interactions with the 11 Å deep hydrophobic channel of the amnda side chains, whereas the phenyl groups of two compounds are located on opposite sides of the receptor surface hydrophobic pocket.

Nakia and coworker also performed on (+)-azumamide E and (-)-azumamide E, with the HDLP binding pocket (**Fig. 1.36 b**),<sup>[161]</sup> using the same AutoDock 3.0.5 software. The carboxylate moiety is of primary importance for its interactions network: it coordinates the zinc ion and establishes hydrogen bonds with Hε2 of H131 and H132, and OH of Y297. Moreover, the C3 linked esenoic chain makes stabilizing hydrophobic interactions with the zinc-containing

tubular pocket. The macrocyclic portion is accommodated in a shallow groove, establishing van der Waals interactions and hydrogen bonds with the receptor counterpart, and is formed by H170, Y196, A197, F198, and F200 residues. (+)-Azumamide E is a potent, selective inhibitor of class I HDACs 1-3.

In conclusion, HDACs inhibitors are well known as a unique and promising class of anticancer agents. They induce growth arrest, cell differentiation and apoptosis in tumor cells. However, these inhibitors, especial the hydroxamates, do not exhibit isozyme specificity in HDAC inhibition. It is obvious that the selective inhibition of specific HDACs is highly desirable and more likely to yield specific and nontoxic drugs.

After the X-ray structure determination of HDLP, the momentum of research on HDAC inhibitors increased and a large number of potent HDAC inhibitors are now available and most of them are in clinical trials. HDAC inhibitors which have been reported could provide information about the active site of HDACs. Cyclic peptides are of great help in finding the interactions of each HDAC in the rim region. The design of novel inhibitors based on the reported HDAC inhibitors and on the basis of the information on HDACs will lead to the synthesis of member selective inhibitors. HDAC research is currently focusing on the subtype selective inhibitors, which can be used as bioprobe to find the functions of each member of the HDAC family and also have potential as drugs for many specific diseases.

## **1.6 Purpose of this study**

Since Finnin *et al.* reported the crystal structure of HDLP and the interactions mechanism of HDLP-TSA complex, the structural information of HDAC inhibitors had been realized which is composed of three portions: the zinc binding group (ZBG), which interacts the zinc ion and engages in multiple hydrogen bonds with the amino acid residues at the active site of HDACs; The linker domain, which occupies the channel of HDACs; The surface recognition domain, which has cap group portion and interacts with amino acid residues on the rim of active pocket entrance. The rim of active pocket of HDACs have multiple grooves that can selectively interact with the cap group of inhibitors. These grooves of HDACs can be well interacted by proper cap group. Therefore, the cap group of inhibitors can be the promising target for improving potency and selectivity. These inhibitors contain aromatic ring in their surface recognition domain and it is proved that the aryl group portion may act as a cap to bind the rim of HDAC enzymes active pocket. The sequence diversity of surface recognition domain of HDAC inhibitors may choose to bind the amino acid residues on the rim of active pocket of

HDAC subtypes. The modification at cap group portion in inhibitor can provide better specificity. The surface recognition domain of the pharmacophore affects not only inhibitory potency but also selectivity. Specificity is a necessary condition for a useful inhibitor as a drug with high pharmacokinetic properties and oral bioavailability. The potent HDAC inhibitors of cyclic tetrapeptide bearing hydroxamic acid or epoxy ketone have very low selectivity to HDAC subtype. Considering the facts described above, author intended to develop HDAC inhibitors of cyclic tetrapeptide bearing different sequences of scaffold (diversity non-natural amino acid replace at four residues position) and different zinc chelating functional groups (disulfide hybrid and hydroxamic acid). Author carried out arrangement of aromatic rings and non-aromatic ring on these scaffolds to develop inhibitors towards HDAC and to know the interaction of cap group with HDACs surface binding region. Moreover, author also examined the SAR of selective HDAC inhibitors.

In Chapter 2 of this thesis, to explore the molecular details of the interactions between cyclic tetrapeptide and HDACs in the HDACs active site, author reported molecular dynamics (MD) study of Apicidin-HDAC1 and Apicidin-HDAC8. First, we constructed the 3D model of human HDAC1 structure using human HDAC8 as template and then validated using several evaluation programs. Subsequently docking studies were performed to analyze the binding modes between HDAC1 and Apicidin, its analogues. The selective inhibition of Apicidin was studied by comparing the binding modes of Apicidin and the two enzymes, followed by further molecular dynamics study of Apicidin-HDAC1 and Apicidin-HDAC8.

In Chapter 3 of this thesis, author reported the design and synthesis of non-natural amino acid for the use of synthesizing novel HDACs inhibitors of cyclic tetrapeptide. H-Phe-OH derivatives were synthesized for aromatic ring modification at 3-position of cyclic tetrapeptide scaffold. According to two different starting material (*tert*-butoxycarbonyl-amino-malonic acid diethyl ester and diethyl acetamidomalonate), Boc-L-Phe(*n*-Me)-OH was synthesized by two methods. *n*-methyl- amino-cyclohexane-carboxylic acid (Anmc6c) were synthesized by the Strecker reaction methods that is one of the most efficient and straightforward for the synthesis of  $\alpha$ -aminonitriles, which were very useful precursors for the synthesis of  $\alpha$ -amino acids and various nitrogen- containing heterocycles. These *n*-methyl-amino-cyclohexane-carboxylic acid (A2mc6c, A3mc6c and A4mc6c) were used for the synthesis of designed HDACs inhibitors of cyclic tetrapeptides at 2-position of scaffold to replace Aib residue. 2-amino-5-chloro-pentanoic acid (L-Ac5) and 2-amino-6-chloro-hexanoic acid (L-Ac6) were prepared for replacing aromatic ring at 3-position of cyclic tetrapeptide scaffold, because aromatic ring can



not be metabolize in liver, moreover, the side chain containing chlorine of L-Ac5 or L-Ac6 may be modified with oxygen or sulfur to chelating zinc ion of HDAC active pocket bottom.

In Chapter 4 of this thesis, author reported design and synthesis of HDACs inhibitors having Chlamydocin scaffold bearing hydroxamic acid as the zinc binding group, and *n*-methyl-amino-cyclohexane-carboxylic acid (Anmc6c) replaced Aib residue to explore inhibitors interaction with HDAC enzymes. The replacement of Aib residue of Chlamydocin with an aliphatic ring (Anmc6c) enhanced the *in vivo* and *in vitro* inhibitory activity. These compounds were tested for HDACs inhibitory activity and the results showed potent inhibition of HDAC. We also tested for antiproliferative *in vitro* by MTT assay against MCF-7 (human breast cancer), Hela (human cervix cancer), 7721 (human liver cancer) and K562 (human leukemia) cell lines. All compounds exhibited nanomolar concentration antitumor activities. We have carried out molecular docking studies on Chlamydocin–hydroxamic acid analogues and HDLP, HDAC8 and HDAH, respectively.

In Chapter 5 of this thesis, author reported design and synthesis of HDACs inhibitors having Chlamydocin scaffold bearing L-2-amino-7-(2-pyridyl)-disulphidyl heptanoyl (L-Am7(S2Py)), which equips thiol function group protected by disulfide hybrid. Chlamydocin is a naturally occurring cyclic tetrapeptide based HDAC inhibitor. Cyclic framework in Chlamydocin containing L-Phe is supposed to play an important role of cap group. To find out specific inhibitors for HDAC subtype, author focused on the benzene ring of L-Phe in Chlamydocin framework. Author here replaced the L-Phe residue of Chlamydocin with L-Phe(*n*-Me) to add exiguous hydrophobicity to study the role of aromatic ring in cap portion of cyclic tetrapeptide inhibitors. The synthesized compounds were tested for antiproliferative *in vitro* by MTT assay against MCF-7, Hela and 7721 cell lines, and then docked and molecular dynamics simulated towards HDAC8.

In Chapter 6 of this thesis, author reported design and synthesis of HDAC inhibitors of Phe replaced by aliphatic amino acid containing chlorine (L-Ac5 and L-Ac6) in Chlamydocin framework because the aromatic ring moiety of cyclic framework provide hydrophobic interaction with HDAC active pocket. but, HC-Toxins have no aromatic ring, which still inhibit the HDACs. In synthesis process, the L-Ac5 changed into L-Pro. Further investigation is needed to improve the activity. All compounds exhibited nanomolar concentration HDACs inhibitory activities.

In summary, author designed and synthesized different classes of HDAC inhibitors with diversity non-natural amino acid at different positions of cyclic tetrapeptide scaffold and with

different HDAC subtypes of ligands. This aim is to exploit cyclic tetrapeptide HDAC inhibitors, especially for the design of selective and potent cyclic tetrapeptide HDAC inhibitors.

## 1.7 References

- [1] Pennisi, E., *Science*, 1997, 275: 155-157.
- [2] Pazin, M. J.; Kadonaga, J. T., *Cell*, 1997, 89: 325-328.
- [3] Claude Monneret, *European Journal of Medicinal chemistry*, 2005, 40: 1-13.
- [4] Fiona McLaughlin; Nicholas B. La Thsngue, *Biochemical pharmacology*, 2004, 68: 1139-1144.
- [5] Hassig, C. A.; Schrieber, S. L., *Curr. Opin. Chem. Biol*, 1997, 1: 300–308.
- [6] Yoshida, M.; Matsuayama, A.; Komatsu, Y.; Nishino, N., *Curr. Med. Chem.*, 2003, 10: 2351–2358.
- [7] Grozinger, C. M.; Schrieber, S. L., *Chem. Biol.*, 2002, 9: 3–16.
- [8] Kouzarides, T., *Curr. Opin. Gen. Dev.*, 1999, 9: 40–48.
- [9] Luger K; Mader A W; Richmond R K; et al. *Nature*, 1997, 389(6648): 251 —260.
- [10] Marks P; Rifkind RA; Richon VM; Breslow R; Miller T, Kelly, *Nat Rev Cancer*, 2001, 1: 194-202.
- [11] A. Giannis et al., *Angew. Chem. Int. Ed.*, 2005, 44: 3186 – 3216.
- [12] Glozak, M.; Seto, E. *Oncogene*, 2007, 26: 5420-5431.
- [13] Tauton, J.; Hassig, C. A.; Schreiber, S. L.; *Science*, 1996, 272: 408-411.
- [14] Rundlett, S. E.; Carmen, A. A.; Kobayashi, R.; Bavikin, S.; Turner, B. M.; Grunstein, M. *Proc. Natl. Acad. Sci. USA*, 1996, 93: 14503-14508.
- [15] Ruijter, A. J.; van Gennip, A. H.; Caron, H. N.; Kemp, S.; van Kuilenburg, A. B. *Biochem. J.*, 2003, 370: 737-749.
- [16] Gregoretta, I. V.; Lee, Y. M.; Goodson, H. V.; *J. Mol. Biol.*, 2004, 338: 17-31.
- [17] Paul A Marks; Thomas Miller and Victoria M Richon, *current Opinion in Pharmacology*, 2003, 3: 344-351.
- [18] Hubbert, C.; Guardiola, A.; Shao, R.; Kawaguchi, Y.; Ito, A.; Nixon, A.; Yoshida, M.; Wang, X. F.; Yao, T. P. *Nature*, 2002, 417: 455-458.
- [19] Witt, O.; Hedgwig, E. D.; Milde, T.; Oehme, I. *Cancer Letters*, 2009, 277: 8-21.
- [20] Grozinger CM; Chao ED; Blackwell HE; Moazed D; Schreiber SL, *J Biol Chem*, 2001, 276: 38837-38843.

- [21] B.E. Bernstein, J.K. Tong and S.L. Schreiber, *Proc. Natl. Acad. Sci. USA*, 2000, 97: 13708–13713.
- [22] C. Foglietti, G. Filocamo, E. Cundari, E. De Rinaldis, A. Lahm, R. Cortese and C. Steinkuhler, *J. Biol. Chem.*, 2006, 281: 17968–17976.
- [23] Ten Holte, P.; Van Emelen, K.; Janicot, M.; Fong, P. C.; de Bono, J. S.; Arts, J. *Top. Med. Chem.*, 2007, 1: 293-331.
- [24] Paris, M.; Porcelloni, M.; Binaschi, M.; Fattori, D. J., *Med. Chem.*, 2008, 51: 1505-1514.
- [25] Moradei, O.; Vaisburg, A.; Martell, R. E., *Curr. Top. Med. Chem.*, 2008, 8: 841-850.
- [26] Hildmann, C.; Wegener, D.; Riester, D.; Hempel, R.; Schober, A.; Merana, J. *et al. J. Biotechnol.* 2006, 124: 258-270.
- [27] Wang D. F.; Helquist, P.; Wiech, N. L.; Wiest, O.; *J. Med. Chem.*, 2005, 48: 6936-6947.
- [28] Somoza, J. R.; Skene, R. J.; Katz, B. A.; Mol, C.; Ho, J. D.; Jennings, A. J.; *et al. Structure*, 2004, 12: 1325-1334.
- [29] Schuetz, A.; Min, J.; Allali-Hassani A.; Schapira, M.; Shuen, M.; Loppnau, P., *et al., J. Biol. Chem.*, 2008, 283: 11355-11363.
- [30] Finnin, M. S.; Donigian, J. R.; Cohen, A.; Richon, V. M.; Rifkind, R. A.; Marks, P. A.; Breslow, R.; Pavletich, N. P. *Nature*, 1999, 401: 188-193.
- [31] Nielsen, T. K.; Hildmann, C.; Dickmanns, A.; Schwienhorst, A.; Ficner, R. *J. Mol. Biol.* 2005, 354: 107-120.
- [32] Olaf Witt; Hedwig E.Deubzer; Till Milde; Ina Oehme, *Cancer Letters*, 2009, 277: 8-21.
- [33] Kyle V. Butler and Alan P. Kozikowski, *Current Pharmaceutical Design*, 2008, 14(6): 505-528.
- [34] Jessica E. Bolden; Melissa J. Peart and Ricky W. Johnstone. *Nature reviews drug discovery*, 2006, 5: 769-784.
- [35] Butler and Bates. *Nature Reviews Neuroscience*, 2006, 7: 784–796.
- [36] Thomas A. Miller, David J. Witter, sandro Belvedere. *J. Med. Chem.*, 2003, 46: 5097-5116.
- [37] Hildmann, C.; Wegener, D.; Riester, D.; Hempel, R.; Schober, A.; Merana, J. *et al. J. Biotechnol.* 2006, 124: 258-270.
- [38] Marks P, Rifkind RA, Richon VM, Breslow R, Miller T, Kelly WK.; *Nat.Rev cancer*, 2001, 1:194-202.
- [39] Kelly WK; O'Connor O; Marks PA, *Expert opin investig Drugs*, 2002, 11: 1695-1713.

- [40] Tsuji, N.; Kobayashi, M.; Nagashima, K.; Wakisaka, Y.; Koizumi, K., *J. Antibiot.* 1976, 29: 1-6.
- [41] Yoshida, M.; Kijima, M.; Akita, M.; Beppu, T., *J. Biol. Chem.* 1990, 265: 17174-17179.
- [42] Boffa, L. C.; Vidaldi, G.; Mann, R. S.; Allfrey, V. G., *J. Biol. Chem.*, 1978, 253: 3364-3366.
- [43] Phiel, C. J.; Zhang, F.; Huang, E. Y.; Guenther, M. G.; Lazer, A. M.; Klein, P. S. *J. Biol. Chem.*, 2001, 276: 36734-36741.
- [44] Blaheta RA, Nau H, Michaelis M, Cinatlt Jr J. *Curr Med Chem*, 2002, 9: 1417-33.
- [45] Breslow, R.; Belvedere, S.; Gershell, L. *Helv. Chim. Acta.* 2000, 83: 1685-1692.
- [46] Richon, V. M.; Webb, Y.; Merger, R.; Sheppard, T.; Jursic, B.; Ngo, L.; Civoli, F.; Richon, V. M.; et al. *Proc. Natl. Acad. Sci. USA.* 1998, 93: 5705-5708.
- [47] Richon, V. M.; et al. *Blood Cells, Mol. Dis.* 2001, 27: 260-264.
- [48] Marks, P. A.; et al. *J. Natl. Cancer Inst.* 2000, 92: 1210-1216.
- [49] Breslow, R.; Rifkind, R. A.; Marks, P. A. *Proc. Natl. Acad. Sci. USA.* 1996, 93: 5705-5708.
- [50] Jung, M.; Brosch, G.; Kölle, D.; Scherf, H.; Gerhäuser, C.; Loidl, P. *J. Med. Chem.*, 1999, 42: 4669-4679.
- [51] Wittich, S.; Scherf, H.; Xie, C.; Brosch, G.; Loidl, P.; Gerhäuser, C.; Jung, M. *J. Med. Chem.*, 2002, 45: 3296-3309.
- [52] Woo, S. H.; Frechette, S.; Khalil, E. A.; Bouchain, G.; Vaisburg, A.; Bernstein, N.; Moradei, O.; Leit, S.; Allan, M.; Fournel, M.; Trachy-Bourget, M-C.; Li, Z.; Besterman, J. M.; Delorme, D. *J. Med. Chem.*, 2002, 45: 2877-2885.
- [53] Glaser, K. B.; et al. *Mol. Cancer Ther.*, 2002, 1: 759-768.
- [54] Curtin, M. L.; Garland, R. B.; Heyman, R.; Frey, R. R.; Michaelides, M. R.; Li, J.; Pease, L. J.; Glaser, K. B.; Marcotte, P. A.; Davidson, S. K. *Bioorg. Med. Chem. Lett.*, 2002, 12: 2919-2923.
- [55] Kim, Y. B.; Lee, K-H.; Sugitha, K.; Yoshida, M.; Horinouchi, S. *Oncogene*, 1999, 18: 2461-2470.
- [56] Uesato, S.; Kitagawa, M.; Nagaoka, Y.; Maeda, T.; Kuwajima, H.; Yamori, T. *Bioorg. Med. Chem. Lett.* 2002, 12, 1347-1349.
- [57] Lu, Q.; Yang, Y-T.; Chen, C-S.; Davis, M.; Byrd, J. C.; Etherton, M. R.; Umar, A.; Chen, C-S. *J. Med. Chem.*, 2004, 47: 467-474.

- [58] Massa, S.; Mai, A.; Sbardella, G.; Esposito, M.; Ragno, R.; Loidl, P.; Brosch, G., *J. Med. Chem.*, 2001, 44: 2069-2072.
- [59] Mai, A.; Massa, S.; Ragno, R.; Esposito, M.; Sbardella, G.; Nocca, G.; Scatena, R.; Jesacher, F.; Loidl, P.; Brosch, G. *J. Med. Chem.*, 2002, 45: 1778-1784.
- [60] Mai, A.; Massa, S.; Ragno, R.; Cerbara, I.; Jesacher, F.; Loidl, P.; Brosch, G. *J. Med. Chem.*, 2003, 46: 512-524.
- [61] Sternson, S. M.; Wong, J. C.; Grozinger, C. M.; Schreiber, S. L. *Org. Lett.*, 2001, 3: 4239-4242.
- [62] Marson, C. L.; Savy, P.; Rioja, A. S.; Mahadevan, T.; Mikol, C.; Veerupillai, A.; Nsubuga, E.; Chahwan, A.; Joel, S. P. *J. Med. Chem.*, 2006, 49: 800-805.
- [63] Kahnberg, P.; Lucke, A. J.; Glenn, M. P.; Boyle, G. M.; Tyndall, J. D. A.; Parsons, P. G.; Fairlie, D. P. *J. Med. Chem.*, 2006, 49: 7611-7622.
- [64] Glen, M. P.; Kahnberg, P.; Boyle, G. M.; Hansford, K. A.; Hans, D.; Martyn, A. C.; Parsons, P. G.; Fairlie, D. P. *J. Med. Chem.*, 2004, 47: 2984-2994.
- [65] Suzuki, T.; Ando, T.; Tsuchiya, K.; Fukazawa, N. *J. Med. Chem.*, 1999, 42: 3001-3003.
- [66] Saito, A.; Yamashita, T.; Mariko, Y.; Nosaka, Y.; Tsuchiya, K.; Ando, T.; Suzuki, T.; Tsuruo, T.; Nakanishi, O. *Proc. Natl. Acad. Sci. USA.* 1999, 96: 4592-4597.
- [67] Jerry Jaboin, Jason Wild, Habib Hamidi, Chand Khanna, Chong Jai Kim, Robert Robey, Susan E. Bates, Carol J. Thiele, *Cancer Res.*, 2002, 62: 6108-6115.
- [68] P. Lelieveld, R.J.F. Middeldorp, L.M. Van Putten, *Cancer Chemother. Pharmacol.* 1985, 15: 88-91.
- [69] M.J. Graziano, T.A. Spoon, E.A. Cockrell, P.E. Rowse, A.J. Gonzales, *J. Biomed. Biotechnol.*, 2001, 1: 52-61.
- [70] H.M. El-Beltagi, A.C.M. Martens, P. Lelieveld, E.A. Haroun, A. Hagenbeek, *Cancer Res.*, 1993, 53: 3008-3014.
- [71] M.H. Seelig, M.R. Berger, *Eur. J. Cancer*, 1996, 32A: 1968-1976.
- [72] Claude Monneret, *European Journal of Medicinal Chemistry*, 2005, 40: 1-13.
- [73] Christianson, D. W.; Lipscomb, W. N. *J. Am. Chem. Soc.* 1986, 108: 4998-5003.
- [74] Walter, M. W.; Felici, A.; Galleni, M.; Soto, R. P.; Adlington, R. M.; *et al. Bioorg. Med. Chem. Lett.* 1996, 6: 2455-2458.
- [75] Frey, R. R.; Wada, C. K.; Garland, R. B.; Curtin, M. L.; Michaelides, M. R.; Li, J.; Pease, L. J.; Glaser, K. B.; Marcotte, P. A.; Bouska, J. J.; Murphy, S. S.; Davidson, S. K. *Bioorg. Med. Chem. Lett.* 2002, 12: 3443-3447.

- [76] Wada, C. K.; Frey, R. R.; Ji, Z.; Curtin, M. L.; Garland, R. B.; *et al. Bioorg. Med. Chem. Lett.* 2003, 13: 3331-3335.
- [77] Komatsu, Y.; Tomizaki, K.; Tsukamoto, M.; Kato, T.; Nishino, N.; Sato, S.; Yamori, T.; Tsuruo, T.; Furumai, R.; Yoshida, Y.; Horinouchi, S.; Hayashi, H. *Cancer Res.* 2001, 61: 4459-4466.
- [78] Closse, A.; Huguenin, R. *Helv. Chim. Acta.* 1974, 57: 553-545.
- [79] Furumai R, Komatsu Y, Nishino N, et al. *Proc. Natl. Acad. Sci., USA*, 2001, 98(1): 87-92.
- [80] Hirota, A.; Suzuki, A.; Suzuki, H.; Tamura, S. *Agr. Biol. Chem.* 1973, 37: 643-647.
- [81] Hirota, A.; Suzuki, A.; Aizawa, K.; Tamura, S. *Agr. Biol. Chem.* 1973, 37: 955-956.
- [82] Hirota, A.; Suzuki, A.; Tamura, S. *Agr. Biol. Chem.* 1973, 37: 1185-1189.
- [83] Umehara, K.; Nakahara, K.; Kiyoto, S.; Iwami, M.; Okamoto, M.; Tanaka, H.; Kohsaka, M.; Aoki, H.; Imanaka, H. *J. Antibiot.* 1983, 36: 478-483.
- [84] Liesch, J. M.; Sweeley, C. C.; Staffeld, G. D.; Anderson, M. S.; Weber, D. J.; Scheffer, R. P. *Tetrahedron* 1982, 38, 45-48.
- [85] Pope, M. R.; Ciuffetti, L. M.; Knoche, H. W.; McCrery, D.; Daly, J. M.; Dunkle, L. D. *Biochemistry*, 1983, 22: 3502-3506.
- [86] Gross, M. L.; McCrery, D.; Crow, F.; Tomer, K. B.; Pope, M. R.; Ciuffetti, L. M.; Knoche, H. W.; Daly, J. M.; Dunkle, L. D. *Tetrahedron Lett.* 1982, 23: 5381-5384.
- [87] Ciuffetti LM, Pope MR, Dunkle LD, et al. *Biochemistry*, 1983, 22(14): 3507-3510.
- [88] Tanis, S. P.; Horenstein, B. A.; Scheffer, R. P.; Rasmussen, J. B. *Heterocycles* 1986, 24: 3423-3431.
- [89] Kim, S-D.; Knoche, H. W.; Dunkle, L. D.; McCrery, D. A.; Tomer, K. B. *Tetrahedron Lett.* 1985, 26: 969-972.
- [90] Izakai, H.; Nagashima, K.; Sugita, K.; Yoshida, H.; et al., *Y. J. Antibiot.* 1990, 63: 1524-1532.
- [91] Kijima M, Yoshida M, Sugita K, et al. *Biol. Chem.*, 1993, 268(30): 22429-22435.
- [92] Taunton J, Collins JL, Schreiber SL. *J. Am. Chem. Soc.*, 1996, 118(43): 10412-10422.
- [93] Kim, S-D. *J. Biochem. Mol. Biol.* 1995, 28: 227-231.
- [94] Walton, J. D.; Earle, E. D.; Staehelin, H.; Grieder, A.; Hiroda, A.; Suzuki, A. *Experientia*, 1985, 41: 348-350.
- [95] Taunton, J.; Hassig, C. A.; Schreiber, S. L. *J. Am. Chem. Soc.* 1996, 118: 10412-10422.
- [96] Taunton, J.; Hassig, C. A.; Schreiber, S. L. *Science*, 1996, 272: 408-411.

- [97] Furumai, R.; Komatsu, Y.; Nishino, N.; Kochbin, S.; Yoshida, Y.; Horinouchi, S. *Proc. Natl. Acad. Sci. USA.*, 2001, 98: 87-92.
- [98] Yasuhiko Komatsu, Kin-ya Tomizaki, Makiko Tsukamoto, Tamaki Kato, *et al.*, *Cancer Research*, 2001, 61: 4459-4466.
- [99] Binoy Jose, Shinji Okamura, Tamaki Kato, Norikazu Nishino, Yuko Sumida and Minoru Yoshida, *Bioorganic & Medicinal Chemistry*, 2004, 12: 1351-1356.
- [100] Nishino, N.; Jose, B.; Shinta, R.; Kato, T.; Komatsu, Y.; Yoshida, M. *Bioorg. Med. Chem.* 2004, 12: 5777-5784.
- [101] Nurul M. Islam, Tamaki Kato, Norikazu Nishino *et al.*, *Bioorganic & Medicinal Chemistry Letters*, 2010, 20: 997-999.
- [102] Nishino, N.; Yoshikawa, D.; Watanabe, L. A.; Kato, T.; Jose, B.; Komatsu, Y.; Sumida, Y.; Yoshida, M. *Bioorg. Med. Chem. Lett.* 2004, 14: 2427-2431.
- [103] Singh, S. B.; Zink, D. L.; Polishook, J. D.; Dombrowski, A. W.; Darkin-Rattray, S. J.; Schmatz, D. M.; Goetz, M. A. *Tetrahedron Lett.* 1996, 37: 8077-8080.
- [104] Darkin-Rattray, S. J.; Gurnett, A. M.; Myers, R. W.; Dulski, P. M.; Crumley, T. M.; Allocco, J. J.; Cannova, C.; Meinke, P. T.; Colletti, S. L.; Bednarek, M. A.; Singh, S. B.; Goetz, M. A.; Dombrowski, A. W.; Polishook, J. D.; Schmatz, D. M. *Proc. Natl. Acad. Sci. USA.* 1996, 93: 13143-13147.
- [105] Singh, S. B.; Zink, D. L.; Liesch, J. M.; Dombrowski, A. W.; Darkin-Rattray, S. J.; Schmatz, D. M.; Goetz, M. A. *Org. Lett.* 2001, 3: 2815-2818.
- [106] Singh, S. B.; Zink, D. L.; Liesch, J. M.; Mosley, R. T.; Dombrowski, A. W.; Bills, G. F.; Darkin-Rattray, S. J.; Schmatz, D. M.; Goetz, M. A. *J. Org. Chem.* 2002, 67: 815-825.
- [107] Colletti, S. L.; Li, C.; Fisher, M. H.; Wyvratt, M. J.; Meinke, P. T., *Tetrahedron Lett.* 2000, 41: 7825-7829.
- [108] Meinke, P. T.; Colletti, S. L.; Ayer, M. B.; Darkin-Rattray, S. J.; Myers, R. W.; Schmatz, D. M.; Wyvratt, M. J.; Fisher, M. H. *Tetrahedron Lett.* 2000, 41: 7831-7835.
- [109] Colletti, S. L.; Myers, R. W.; Darkin-Rattray, S. J.; Schmatz, D. M.; Fisher, M.; Wyvratt, M. J.; H., Meinke, P. T. *Tetrahedron Lett.* 2000, 41: 7837-7841.
- [110] Meinke, P. T.; Liberator P. *Curr. Med. Chem.* 2001, 8: 211-235.
- [111] Colletti, S. L.; Myers, R. W.; Darkin-Rattray, S. J.; Gurnett, A. M.; Dulski, P. M.; Galuska, S.; Allocco, J. J.; Ayer, M. B.; Li, C.; Lim, J.; Crumley, T. M.; Cannova, C.; Schmatz, D. M.; Wyvratt, M. J.; Fisher, M. H.; Meinke, P. T. *Bioorg. Med. Chem. Lett.* 2001, 11: 107-111.

- [112] Colletti, S. L.; Myers, R. W.; Darkin-Rattray, S. J.; Gurnett, A. M.; Dulski, P. M.; Galuska, S.; Allocco, J. J.; Ayer, M. B.; Li, C.; Lim, J.; Crumley, T. M.; Cannova, C.; Schmatz, D. M.; Wyvratt, M. J.; Fisher, M. H.; Meinke, P. T. *Bioorg. Med. Chem. Lett.* 2001, 11: 113-117.
- [113] Bhuiyan, M. P. I.; Kato, T.; Okauchi, T.; Nishino, N.; Maeda, S.; Nishino, T. G.; Yoshida, M. *Bioorg. Med. Chem.* 2006, 14: 3438-3446.
- [114] Wenxin Gu, Mercedes Cueto, Paul R. Jensen, William Fenicalb, and Richard B. Silverman, *Tetrahedron*, 2007, 63: 6535–6541.
- [115] Ana Montero, John M. Beierle, Christian A. Olsen, and M. Reza Ghadiri, *J. Am. Chem. Soc.* 2009, 131: 3033–3041.
- [116] Gupta, S.; Peiser, G.; Nakajima, T.; Hwang, Y-S. *Tetrahedron Lett.* 1994, 35: 6009-6012.
- [117] Yoshimura, K.; Tsubotani, S.; Okazaki, K. *JP 7196686*, 1995.
- [118] Mori, H.; Abe, F.; Yoshimura, S.; Takase, S.; Hino, M. WO200008048-A2, 2000.
- [119] Xie, W.; Zou, B.; Pei, D.; Ma, D. *Org. Lett.* 2005, 7: 2775-2777.
- [120] Simone Di Micco, Stefania Terracciano, Ines Bruno, Manuela Rodriquez, Raffaele Riccio, Maurizio Taddei, Giuseppe Bifulco, *Bioorganic & Medicinal Chemistry*, 2008, 16: 8635–8642.
- [121] Binoy Jose, Yusuke Oniki, Tamaki Kato, Norikazu Nishino, Yuko Sumidaa and Minoru Yoshida, *Bioorganic & Medicinal Chemistry Letters*, 2004, 14: 5343–5346.
- [122] Fujisawa Pharmaceutical Co., Ltd. Jpn. Kokai Tokkyo Koho, JP,03141296, 1991.
- [123] (a) Ueda, H.; Nakajima, H.; Hori, Y.; Fujita, T.; Nishimura, M.; Goto, T.; Okuhara, M. *J. Antibiot. (Tokyo)* 1994, 47: 301–10. (b) Shigematsu, N.; Ueda, H.; Takase, S.; Tanaka, H.; Yamamoto, K.; Tada, T. *J. Antibiot. (Tokyo)* 1994, 47: 311–314. (c) Ueda, H.; Manda, T.; Matsumoto, S.; Mukumoto, S.; Nishigaki, F.; Kawamura, I.; Shimomura, K. *J. Antibiot. (Tokyo)* 1994, 47: 315–323.
- [124] Furumai, R.; Matsuyama, A.; Kobashi, M.; Lee, K-H.; Nishiyama, M.; Nakajima, H.; Tanaka, A.; Komatsu, Y.; Nishino, N.; Yoshida, M.; Horinouchi S. *Cancer Res.* 2002, 62: 4916-4921.
- [125] Shin-ya, K.; Masuoka, Y.; Ngai, A.; Furihata, K.; Nagai, K.; Suzuki, K.; Hayakawa, Y.; Seto, Y. *Tetrahedron Lett.* 2001, 42: 41-44.
- [126] Alexander Yurek-George, Fay Habens, Matthew Brimmell, Graham Packham, and A. Ganesan, *J. Am. Chem. Soc.* 2004, 126: 1030-1031.



- [127] Nicole A. Calandra, Yim Ling Cheng, Kimberly A. Kocak, Justin S. Miller, *Org. Lett.*, 2009, 11(9): 1971-1974.
- [128] Taori, K.; Paul, V. J.; Luesch, H. *J. Am. Chem. Soc.* 2008, 130: 1806–1807.
- [129] Ying, Y.; Taori, K.; Kim, H.; Hong, J.; Luesch, H. *J. Am. Chem. Soc.* 2008, 130: 8455–8459.
- [130] Bowers, A.; West, N.; Taunton, J.; Schreiber, S. L.; Bradner, J. E.; Williams, R. M. *J. Am. Chem. Soc.* 2008, 130: 11219–11222.
- [131] Albert A. Bowers, Nathan West, Tenaya L. Newkirk, Annie E. Troutman-Youngman, Stuart L. Schreiber, Olaf Wiest, James E. Bradner, Robert M. Williams, *Org. Lett.*, 2009, 11(6): 1301-1304.
- [132] Nakajima, H.; Kim, Y. B.; Terano, H.; Yoshida, M.; Horinouchi, S. *Exp. Cell. Res.* 1998, 241: 126-133.
- [133] Kojiro Taura, Yuza Yamamoto<sup>1</sup>, Akio Nakajima, Koichiro Hata, Hiroshi Uchinami, Kei Yonezawa, Etsuro Hatano, Norikazu Nishino, Yoshio Yamaoka, *J Gene Med.*, 2004; 6: 526–536.
- [134] Piekarz RL, Robey R, Sandor V, *et al. Blood*, 2001, 98(9): 2865-2868.
- [135] Sawa H, Murakami H, Kumagai M, *et al. Acta Neuropathol*, 2004, 107(6): 523–531.
- [136] Taura K, Yamamoto Y, Nakajima A, *et al. J Gene Med.*, 2004, 6(5): 526–536.
- [137] Shizukuda Y, Piekarz RL, Bates SE, *et al. Cardiovascular Drugs and Therapy*, 2005, 19(1): 89–90.
- [138] You Mie Lee, Se-Hee Kim, Hae-Sun Kim, Myung Jin Son, Hidenori Nakajima, Ho Jeong Kwon and Kyu-Won Kim, *Biochemical and Biophysical Research Communications*, 2003, 300: 241–246.
- [139] Yuka Sasakawa, Yoshinori Naoe, Takashi Inoe *et al.*, *Biochemical pharmacology*, 2002, 64: 1079-1090.
- [140] Yuka Sasakawa, Yoshinori Naoe, Takeshi Inoue, Tatsuya Sasakawa, Masahiko Matsuo, Toshitaka Manda, Seitaro Mutoh, *Cancer Letters*, 2003, 195: 161–168.
- [141] Richard L. Piekarz, Rob Robey, Victor Sandor, Susan Bakke, Wyndham H. Wilson, Laila Dahmouh, Douglas M. Kingma, Maria L. Turner, Rosemary Altemus, and Susan E. Bates, *Blood*. 2001, 98: 2865-2868.
- [142] Khan W. Li, Jerry Wu, Wenning Xing, and Julian A. Simon, *J. Am. Chem. Soc.* 1996, 118: 7237-7238.

- [143] Albert A. Bowers, Thomas J. Greshock, Nathan West, Guillermina Estiu, Stuart L. Schreiber, Olaf Wiest, Robert M. Williams, James E. Bradner, *J. Am. Chem. Soc.* 2009, 131: 2900–2905.
- [144] Shijun Wen, Graham Packham, A. Ganesan, *J. Org. Chem.*, 2008, 73: 9353–9361.
- [145] Thomas J. Greshock, Deidre M. Johns, Yasuo Noguchi, Robert M. Williams, *Org. Lett.*, 2008, 10(4): 613-616.
- [146] Gururaj M. Shivashimpi, Satoshi Amagai, Tamaki Kato, Norikazu Nishino, *Bioorg. Med. Chem.*, 2007, 15: 7830-7839.
- [147] Nishino, N.; Jose, B.; Okamura, S.; Ebisusaki, S.; Kato, T.; Sumida, Y.; Yoshida, M. *Org. Lett.*, 2003, 5: 5079-5082.
- [148] Nishino, N.; Shivashimpi, G. M.; Soni, P. B.; Bhuiyan, M. P. I.; Kato, T.; Maeda, S.; Tomonori G. Nishino; Yoshida, M. *Bioorg. Med. Chem.* 2008, 16: 437-445.
- [149] Nakao, Y.; Yoshida, S.; Matsunaga, S.; Shindoh, N.; Terada, Y.; Nagai, K.; Yamashita, J. K.; Ganesan, A.; van Soest, R. W. M.; Fusetani, N. *Angew. Chem., Int. Ed.* 2006, 45: 7553-7557.
- [150] Izzo, I.; Maulucci, N.; Bifulco, G.; De Riccardis, F. *Angew. Chem., Int. Ed.* 2006, 45: 7557-7560.
- [151] Stefania Terracciano, Simone Di Micco, Giuseppe Bifulco, Paola Gallinari, Raffaele Riccio, Ines Bruno, *Bioor Med chem*, 2010,18: 3252-3260.
- [152] Erinprit K. Singh, Suchitr Ravula, Chung-Mao Pan, Po-Shen Pan, Rober C. Vasko, Stephanie A. Iapera, Sujith V. W. weerasinghe, Mary Kay H. Pflum, Shelli R. McAlpine, *Bioorganic & Medicinal Chemistry Letters*, 2008, 18: 2549-2554.
- [153] Colletti, S. L.; Myers, R. W.; Darkin-Rattray, S. J.; Gurnett, A. M.; Dulski, P. M.; Galuska, S.; Allocco, J. J.; Ayer, M. B.; Li, C.; Lim, J.; Crumley, T. M.; Cannova, C.; Schmatz, D. M.; Wyvratt, M. J.; Fisher, M. H.; Meinke, P. T. *Bioorg. Med. Chem. Lett.* 2001, 11: 113-117.
- [154] Jose, B.; Kato, T.; Sumida, Y.; Yoshida, M.; Nishino, N. *American peptide symposium*, 2003.
- [155] Shute, R. E.; Dunlap, B.; Rich, D. H. *J. Med. Chem.* 1986, 30: 71-78.
- [156] Vannini A, Volpari C, Filocamo G, *et al. Proceeding of the National Academy of Sciences of the United States of America*, 2004, 101(42): 15064-15069.
- [157] D.F. Wang, O.G. Wiest, P. Helquist, H.Y. Lan-Hargest and N.L. Wiech, *J. Med. Chem.*, 2004, 47: 3409–3417.

- [158] D.F. Wang, P. Helquist, N.L. Wiech and O. Wiest, *J. Med. Chem.*, 2005, 48: 6936–6947.
- [159] Simone Di Micco, Stefania Terracciano, Ines Bruno, Manuela Rodriguez, Raffaele Riccio, Maurizio Taddei, Giuseppe Bifulco, *Bioorganic & Medicinal Chemistry*, 2008, 16: 8635–8642.
- [160] M. Rodriguez, S. Terracciano, E. Cini, G. Settembrini, I. Bruno, G. Bifulco, M. Taddei and L. Gomez-Paloma, *Angew. Chem. Int. Ed.* 2006, 118: 437–441.
- [161] Nakia Maulucci, Maria Giovanna Chini, Simone Di Micco, Irene Izzo, Emiddio Cafaro, Adele Russo, Paola Gallinari, Chantal Paolini, Maria Chiara Nardi, Agostino Casapullo, Raffaele Riccio, Giuseppe Bifulco, and Francesco De Riccardis, *J. Am. Chem. Soc.* 2007, 129: 3007-3012.
- [162] Matthew J. Bottomley<sup>1</sup>, Paola Lo Surdo<sup>1</sup>, Paolo Di Giovine, Agostino Cirillo, Rita Scarpelli, Federica Ferrigno, Philip Jones, Petra Neddermann, Raffaele De Francesco, Christian Steinkühler, Paola Gallinari, and Andrea Carfi', *The Journal of Biological Chemistry*, 2008, 283(39): 26694–26704.
- [163] Mann, B. S.; Johnson, J. R.; Cohen, M. H.; Justice, R.; Pazdur, R. *Oncologist*, 2007, 12: 1247–1252.
- [164] Erinpriti K. Singh, Lidia A. Nazarova, Stephanie A. Lopera, Leslie D. Alexander, Shelli R. McAlpine, *Tetrahedron Letters*, 2010, 51: 4357–4360.
- [165] Jinhai Fan, Jennifer Stanfield, Yi Guo, Jose A. Karam, Eugene Frenkel, Xiankai Sun, and Jer-Tsong Hsieh, *Clin Cancer Res.*, 2008, 14(4): 1200-1207.

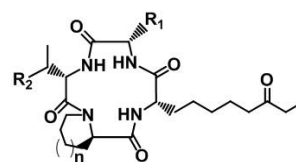
## Chapter 2

# Molecular Simulation of Interactions between HDAC and Apicidin, Analogues

### 2.1 Introduction

Modulation of the acetylation state of lysine residues found in the accessible N-terminal of core histones plays a pivotal role in the regulation of gene expression.<sup>[1,2]</sup> Acetylation and deacetylation of histones are controlled by two corresponding enzymes, HDACs and HAT.<sup>[3]</sup> The HDACs strongly influence gene silencing as they are inappropriately recruited to key locations in nucleosomes through their interactions with transcription complexes.<sup>[4]</sup> Inhibition of HDACs represents a new strategy in human cancer therapy and the inhibitors are potent inducers of growth arrest, differentiation and apoptosis of tumor cells. A wide variety of HDAC inhibitors of both small molecule (Trichostatin A, TSA<sup>[5]</sup>) and cyclopeptides (Azumamide,<sup>[6]</sup> FR235222<sup>[7]</sup> and FK-228<sup>[8]</sup>) have been reported. Among them, Apicidin (*cyclo*(L-Trp(OMe)-L-Ile-D-Pip-L-Aode), **Fig. 2.1**), isolated from *Fusarium pallidoroseum*, is a potent and broad-spectrum antiprotozoal agent which exerts its biological activity by reversibly inhibiting HDACs.<sup>[9,10]</sup>

The first structural information on zinc-dependent HDACs was derived from the crystal structure of histone deacetylase-like protein (HDLP), a bacterial enzyme sharing high homology to the HDACs around the binding pocket and contains a Zn<sup>2+</sup> in its active site, bounded with Trichostatin (TSA) or suberanilohydroxamic acid (SAHA).<sup>[11]</sup> Recently, the crystal structure of human HDAC8 was described by two independent groups, proposing a catalytic mechanism which is similar to the mechanism proposed from HDLP.<sup>[12,13]</sup> The crystallographic structure of human HDAC1 is not available yet. An alignment shows 41%



Compounds	Name	n	R <sub>1</sub>	R <sub>2</sub>
1	Apicidin	n=2		CH <sub>2</sub> CH <sub>3</sub>
2	Apicidin B	n=1		CH <sub>2</sub> CH <sub>3</sub>
3	Apicidin C	n=2		CH <sub>3</sub>
4	Analogue 4	n=2		CH <sub>2</sub> CH <sub>3</sub>

**Fig. 2.1** The structure of Apicidin and analogues.

sequence identity of human HDAC8 and HDAC1. The residues around the  $Zn^{2+}$  binding site of HDAC8 are completely conserved in all human class I HDACs.

Most of molecular simulation studies about the HDAC-inhibitor interactions are focused on small molecule inhibitors,<sup>[14,15]</sup> up to now only two contributions analyzing the binding contacts between HDLP and the tetracyclopeptide framework have been published: FR235222-HDLP and Azumamide E-HDLP.<sup>[16,17]</sup> Cyclic peptides constitute the most structurally complex and diverse class of HDACs inhibitors. There is strong evidence that the three-dimensional appendage orientations of tetracyclopeptides Apicidin and its analogues significantly influence the inhibitor-enzyme recognition pattern.<sup>[18,19]</sup> However, the details of recognition between tetracyclopeptides and HDACs are only partly known. The scarce information on the role played by the cyclic tetrapeptide cap group in the HDACs recognition process prompted us to explore the molecular details of the interactions between HDACs and Apicidin and its analogues. Here, the 3D model of human HDAC1 structure was constructed using human HDAC8 as template and then validated by several evaluation programs. Subsequently docking studies were performed to analyze the binding modes between HDAC1 and the tetracyclopeptides. The selective inhibition of Apicidin was studied by comparing the binding modes of Apicidin and the two enzymes, followed by further molecular dynamics study of Apicidin-HDAC1 and Apicidin-HDAC8.

## 2.2 Results and discussion

### 2.2.1 Sequence alignment and homology model validation

The sequence alignment of HDAC1 and HDAC8 is shown in **Fig. 2.2**, indicating 41% sequence identity between the two enzymes. It shows that the residues making up the active site and contacting the inhibitors were conserved these two HDACs, which was in agreement with the study of Somoza *et al.*<sup>[12]</sup> However, comparing with HDAC8, HDAC1 has an additional segment in its C-terminal domain that is about 110 amino acids. Since the function of these residues was proposed to recruit the enzyme to large protein complexes that may modulate its enzymatic activity and localization,<sup>[20]</sup> they were omitted in further studies considering no similar sequences founded.

The quality of the human HDAC1 model was then evaluated with three different validation tests. The  $\phi/\psi$  distributions listed in **Table. 2.1** showed that there were 91.4% of the residues in the HDAC1 model and 90.1% of HDAC8 template appeared in core regions, respectively. And

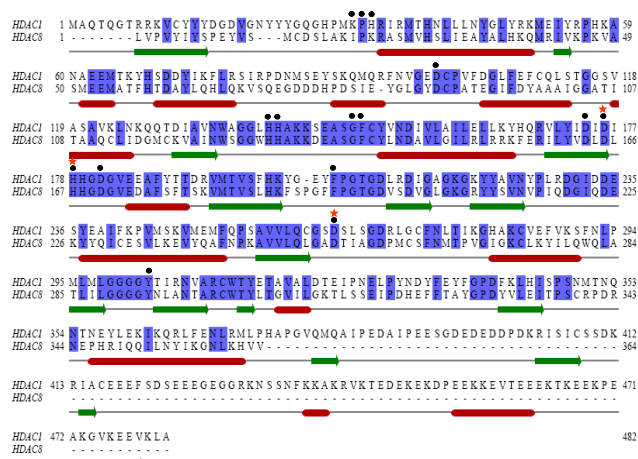


**Fig. 2.2** Sequence alignment between human HDAC 1 and HDAC8. The secondary structure assignment was derived from the HDAC8 structure. The residues forming active pocket are demarcated by red asterisk and those binding to zinc are demarcated by black dots.

**Table 2.1** The  $\phi/\psi$  dihedral angle distribution of HDAC1 and HDAC8

Value calculated	Percentages of residues	
	HDAC1 model	HDAC8 template
Core	91.4%	90.1%
Allowed	7.6%	9.3%
Generously allowed	0.9%	0.3%
Disallowed	0	0.3%

\*The Phi, Psi region percentages were calculated by PROCHECK.

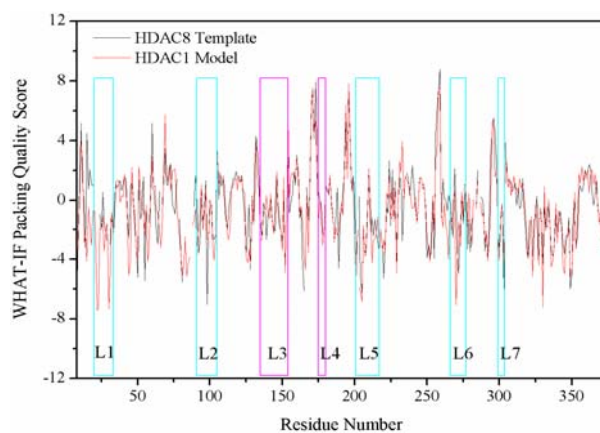


**Fig. 2.3** The WHATIF packing quality scores calculated for the template HDAC8 and the homology model HDAC1.

none of the model residues was found in disallowed regions, while one template residue was found there. Summarizing the results of the PROCHECK analysis, the stereochemical quality of the model was better than that of the template. Packing quality of the model was analyzed by the WHAT-IF Coarse Packing Quality Control test and depicted in **Fig. 2.3**. The key loops (L1: 20-33, L2: 91-105, L3: 134-154, L4: 175-180, L5: 201-216, L6: 265-277 and L7: 299-304) which formed a part of the binding site were marked by frames. For a reliable structure, the WHATIF packing scores should be above -5.0. In general, the HDAC1 model had similar packing scores compared with the template X-ray structure. A few residues were poorly packed based upon scores lower than -5.0. However, these values were also similar to the ones in the HDAC8 template. When checking with ERRAT, the score for the model was 73.15, suggesting that the backbone conformation and non-bonded interactions of the model were all reasonable within a normal range. The results of three validation tests showed that the HDAC1 model was reliable for performing further docking studies.

### 2.2.2 3D structure of the HDAC1 model

In general, the overall structure of human HDAC1 model was similar to the X-ray structure of HDAC8. The structure comprises of a centrally located 8  $\beta$ -sheets enclosed by 16  $\alpha$ -helices. There were seven key loops L1-L7 forming the walls of the binding site (**Fig. 2.4**). The L3 and L4 located at the bottom of the active pocket nearing  $\text{Zn}^{2+}$  and house the catalytic machinery of the enzyme. L1, L2 and L6 formed rim of enzyme surface entrance. L5 and L7 located at channel. The superimposition of the HDAC1 homology model and the HDAC8 X-ray structure with the co-crystallized inhibitor TSA is shown in **Fig. 2.4a**, with RMSD 2.38 Å of the backbone atoms. The binding site was demarcated by the presence of TSA and  $\text{Zn}^{2+}$ . The active pocket walls of HDAC1 model consisted of residues Phe150, Phe205, Asp181, Gly149, Leu271 and Tyr303. These residues were identical with that of HDAC8, with the exception of Leu271, which was a methionine in HDAC8.<sup>[12,13]</sup> The HDAC1 model gave a reasonable geometry of the zinc binding part (**Fig. 2.4b**). The distances of  $\text{Zn}^{2+}$ -Asp176(O $\delta$ 1),  $\text{Zn}^{2+}$ -Asp264(O $\delta$ 1) and  $\text{Zn}^{2+}$ -His178(N $\delta$ 1) were 2.60, 2.59 and 2.67 Å in HDAC1 model while the counterparts in HDAC8 were 1.97, 1.94 and 2.15 Å. There were also two charge-relay systems formed by His140-Asp174 and His141-Asp181, respectively.

At the entrance portion of the active pocket, there was a Glu98 (**Fig. 2.5(1)a**) in HDAC1 instead of Tyr100 comparing with HDAC8 (**Fig. 2.5(1)b**). This change made the pocket entrance more open in HDAC1, indicating that the inhibitors with large cap groups can bind to

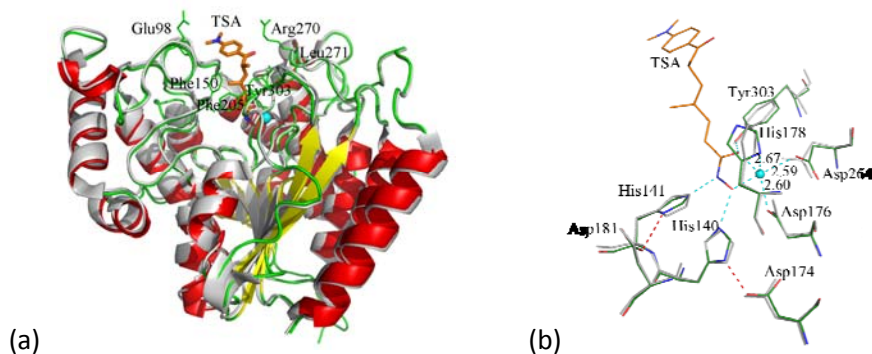


**Fig. 2.4** (a) Superimposition of HDAC1 model (red: helices, yellow: sheets, green: loops) and HDAC8 X-ray structure (grey: cartoon) with the co-crystallized inhibitor TSA (orange sticks). (b) The zinc geometry at the active site of HDAC1 (green) with HDAC8 counterpart (grey). (The cyan dashed lines represent hydrogen bonds while the red ones represent the two Asp-His charge delay systems in HDAC1).

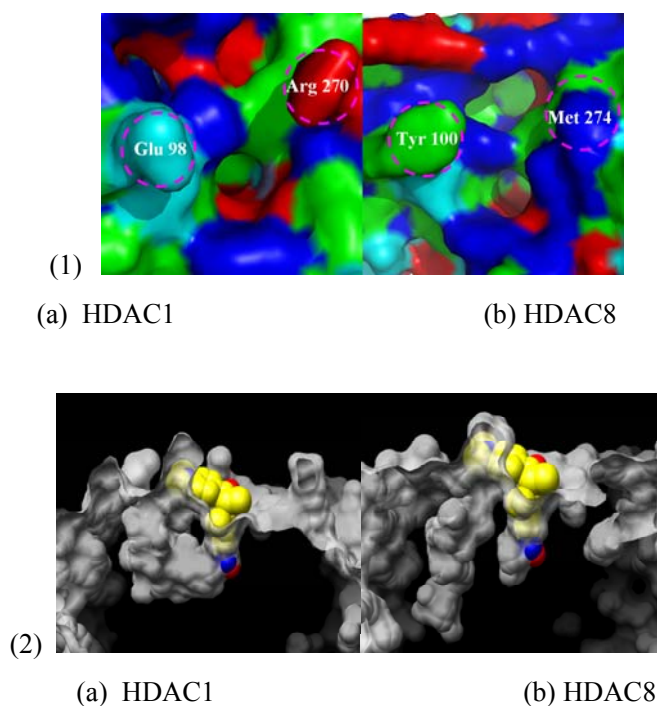


**Fig. 2.5** (1) The surface representation of the active pocket of HDAC1 model and the HDAC8 template. The surface residues are color coded based on their nature: electropositive (red), electronegative (cyan), polar (green) and nonpolar (blue). The magenta circles demarcate the location of two residues, which are not conserved between human HDAC1 and HDAC8. (2) Surface representation of the internal cavity nearing the active pocket of HDAC1 (a) and HDAC8 (b) The TSA (yellow) is locating in the active pocket.



the active site in a more favorable manner. Another unconserved residue around the active pocket was Arg270, which was Met274 in HDAC8 (**Fig. 2.5(1)b**). These portions were different in electrostatic and hydrophobic properties between HDAC1 and HDAC8, which may influence the binding of inhibitors with large cap groups. There was an internal cavity near the active pocket in HDAC8 structure with accommodating acetic acid and two water molecules from deacetylation. Compared to HDAC8, the one end of the internal cavity of HDAC1 connected to the active pocket (similar to HDAC8) and the other end swerved and formed an entrance which moved the acetic acid and water out. So, it is likely to inhibit deacetylation for design molecules that interact with the entrance of the internal cavity (**Fig. 2.5 (2)**).

### 2.2.3 Interactions between HDAC1 and inhibitors

In order to validate the computation accuracy of AutoDock 4.0, HDLP-TSA and HDAC8-TSA crystal complexes were employed to perform redocking studies and the redocking results were compared with the original crystal structures. When redocking TSA to HDLP, two major poses appeared with two opposite orientations of the N, N-dimethylaminobenzyl group of TSA. In one case, the dimethylaminobenzyl group positions in the groove formed by Pro22, Tyr91 and Phe141. This kind of conformation took 18% of all with RMSD < 2.0 Å (compared with crystal TSA conformation). While in the other case, about 23% of all conformations interacted with the opposite groove formed by His170, Phe200, Leu265 and Ser266 with their dimethylaminobenzyl groups. The two grooves can be favorable binding positions for inhibitors with large caps, like cyclotetrapeptides. Interestingly, when redocking TSA to HDLP with several crystal waters remained, the percentage of the first conformation was dramatically increased to 63%, indicating that redocking studies with crystal waters involved were more accurate, as mentioned in former studies.<sup>[21]</sup> Similar results were obtained for HDAC8-TSA, indicating that AutoDock 4.0 program is capable of performing further docking studies.

Four tetracyclopeptides, Apicidin (**1**), Apicidin B (**2**), Apicidin C (**3**) and Apicidin analogue 4 (**4**), have been reported as HDACs inhibitors with IC<sub>50</sub> values of 1, 10, 6 and 86 nM, respectively.<sup>[18]</sup> To understand how these inhibitors bind to the enzyme, docking studies were performed following the procedure described in the methodology section. As a result, the zinc-chelated conformation of Apicidin is rightly the lowest binding energy conformation ( $\Delta G_{\text{binding}} = -9.67$  kcal/mol), and the binding mode is shown in **Fig. 2.6**. The keto-carbonyl moiety was of primary importance in coordinating with Zn<sup>2+</sup> in a distance of 1.78 Å and establishing hydrogen bonds with the O(H) of Tyr303. This hydrogen bond was very important

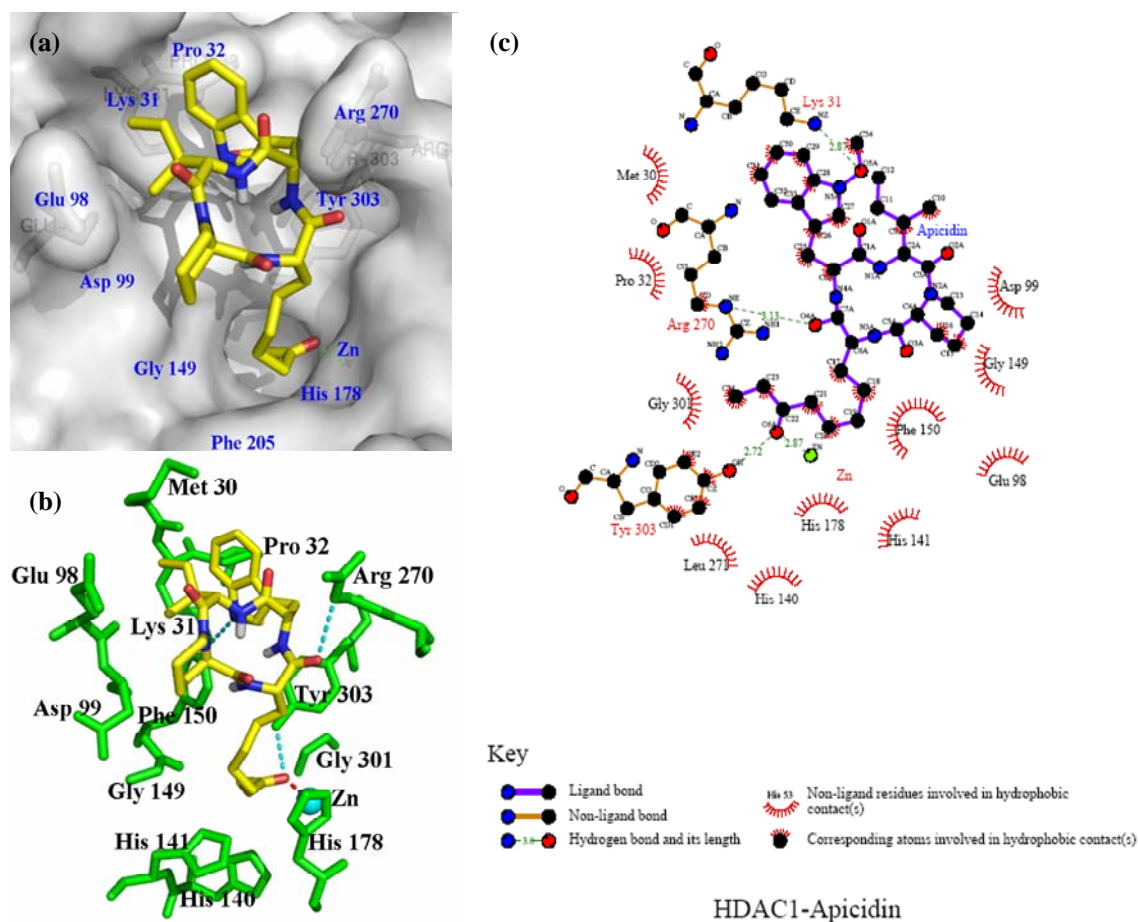


**Fig. 2.6** 3D model of the interactions between apicidin and the HDAC1 model binding site. Apicidin is shown as sticks with the carbon atoms colored yellow. (a) surface representation of the lowest binding energy conformation (top view); (b) important residues in close contact (green) with the inhibitor, cyan dashed lines represent hydrogen bonds (side view); (c) 2D representation of Apicidin and HDAC1 showing hydrophobic contacts and hydrogen bonds.

for stabilizing the binding of ligands to the enzyme.<sup>[22]</sup> Moreover, the long 8-oxo-decanoyl side chain made stabilizing hydrophobic interactions with the zinc-containing tubular pocket containing Tyr303, Gly301, Leu271, His178, Phe150, Gly149 and His141. The macrolactam portion was accommodated in a shallow groove at the rim of the active pocket formed by Glu98, Lys31, Tyr303 and Arg270, establishing van der Waals interactions and a hydrogen bond. The tetrapeptide core extended its hydrophobic interactions thanks to the N-O-methyl-Trp side chain, which interacted with the receptor counterpart involving Tyr303, Arg270, Phe150, Met30 and Pro32. The piperidinyl side chain purely established hydrophobic interactions with Asp99 and it is mostly exposed to the environment. The isoleucyl side chain made hydrophobic

interactions barely with Glu98 and Phe150. Three hydrogen bonds were formed between Apicidin and HDAC1, shown in both **Fig. 2.6c** and **Table 2.2**.

**Table 2.2** The hydrogen bonds obtained from the docking results of the four tetracyclopeptides and HDAC1 model.

Inhibitors	Hydrogen Bonds		
	Donor	Acceptor	Distance(Å)
<b>1</b>	Tyr303 : OH	<b>1</b> : O6	2.72
	Arg270 : NE	<b>1</b> : O4	3.13
	Lys31 : NZ	<b>1</b> : O5	2.87
<b>2</b>	Arg270 : NE	<b>2</b> : O3	3.32
	Lys31 : NZ	<b>2</b> : O5	3.27
<b>3</b>	Arg270 : NE	<b>3</b> : O2	3.36
<b>4</b>	No hydrogen bond founded		

The lowest binding energy conformation of Apicidin B ( $\Delta G_{\text{binding}} = -8.94$  kcal/mol) coordinates zinc ion in a similar manner of Apicidin, but no hydrogen bond was formed between its keto-carbonyl and Tyr303 (**Fig. 2.7a** and **b**). The long 8-oxo-decanoyl side chain made hydrophobic interactions with fewer residues involved in the tubular pocket than Apicidin, which may decrease the biological activities of the inhibitor. The cyclic backbone of Apicidin B was accommodated in the same position at the rim of the pocket, while it took a different orientation. Since the side chains of Ile and Pro pointed to the outside environment, no hydrophobic contact was established by them, which could be another reason for less biological activities. In contrast, the N-O-methyl-Trp side chain formed favorable  $\pi$ - $\pi$  interaction with the Tyr303 side chain besides hydrophobic interactions mentioned above, which may slightly increase the biological activities.

The binding mode of Apicidin C ( $\Delta G_{\text{binding}} = -9.05$  kcal/mol) was almost the same with Apicidin B, except the Val side chain (**Fig. 2.7c** and **d**). Although there were Val and piperidinyl instead of Ile and Pro, their side chains still pointed outside environment. The piperidinyl side chain formed no interaction, while the Val side chain established hydrophobic interactions with residues Glu98 and Phe150.

The analogue **4** differed with Apicidin on the side chain, with the N-O-methyl-Trp side chain replaced by the group drawn in **Fig. 2.1**. Comparing with Apicidin, the zinc-chelated conformation of **4** ( $\Delta G_{\text{binding}} = -8.54$  kcal/mol) was not the lowest binding energy conformation,

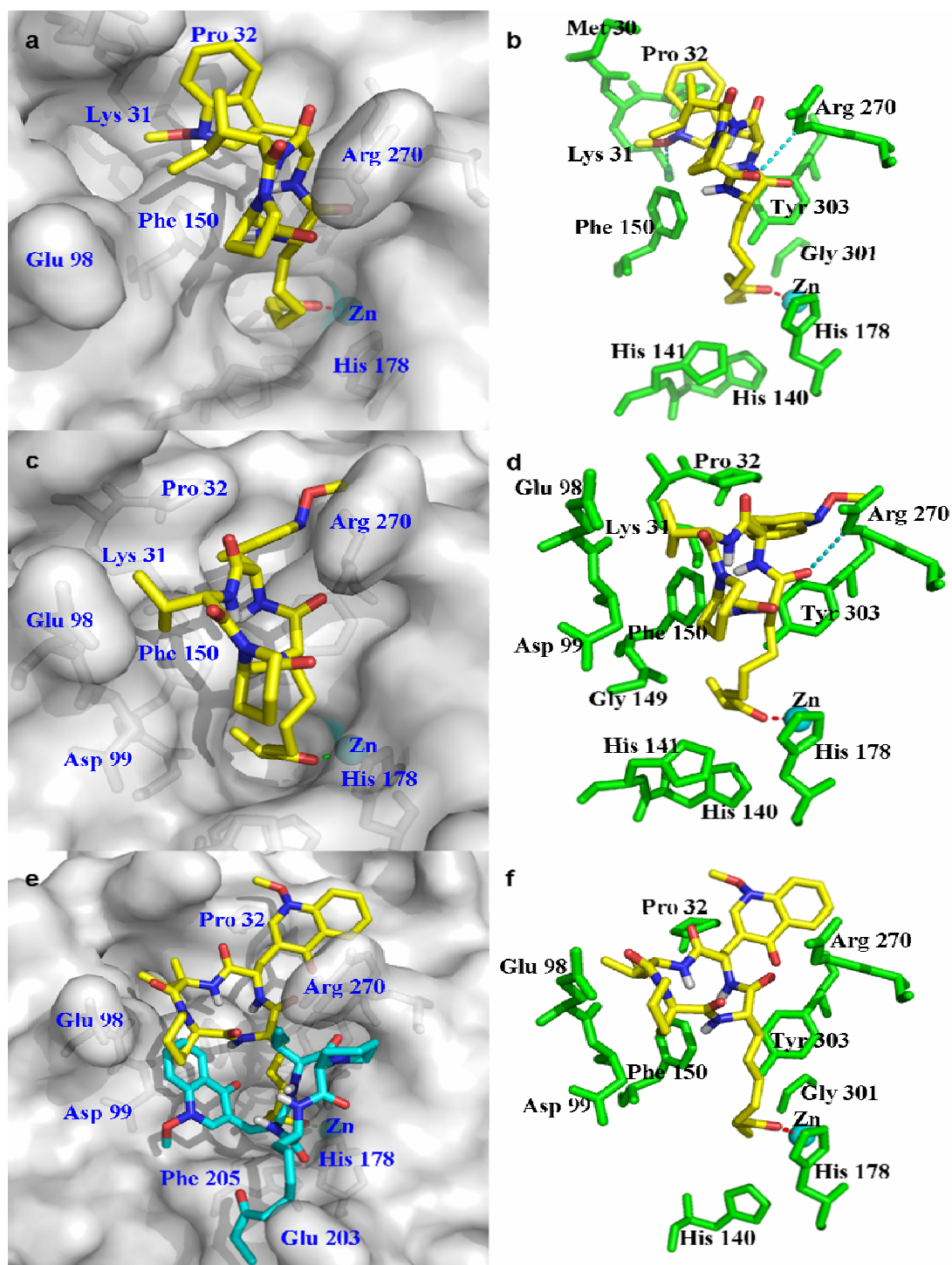


**Fig. 2.7** 3D model of the interactions between Apicidin analogues (yellow sticks) and the HDAC1 model binding site. Surface representation of the zinc-chelated conformation of Apicidin B (a), Apicidin C (c) and analogue **4** (e); Important residues in close contact (green) with Apicidin B (b), Apicidin C (d) and analogue **4** (f). The cyan sticks in (e) are the lowest binding energy conformation of **4**. Cyan dashed lines represent hydrogen bonds.

suggesting decrease of binding activity (**Fig. 2.7e**). The cyclic backbone of the lowest binding energy conformation blocked the entrance of the active pocket with the 8-oxo-decanoyl side chain pointing outside ( $\Delta G_{\text{binding}} = -9.19$  kcal/mol). The cyclic frame of the zinc-chelated conformation was quite the same with Apicidin, making similar interactions with the receptor counterparts (**Fig. 2.7f**). The only difference between the chemical structures of **1** and **4** was the side chain groups of the Trp-like residue. And a significant different orientation occurred in this portion according to the docking results (**Fig. 2.7e**). The modified side chain of **4** established less hydrophobic interactions with HDAC1 and formed  $\pi$ - $\pi$  interaction with the Tyr303 side chain. It can be concluded from the structure-energy analysis of **2** and **4** that, the  $\pi$ - $\pi$  interactions between tetracyclopeptides and Tyr303 were positive but not leading factors for biological activities.

The atoms of the zinc-chelated conformations which form hydrogen bonds with HDAC1 are summarized in **Table 2.2**. The calculated binding energy of the enzyme-inhibitor complexes were higher than the experimental data. Such an inconsistency in the docking results can happen in AutoDock docking studies, as few interactions between the inhibitors and enzyme may be missing since the side chains of the protein residues were not allowed to move during the docking process. But the semiempirical free energy functions<sup>[29]</sup> in AutoDock 4 enabled a reasonable good linear relationship between calculated binding energy from docking and experimental values, as shown in **Fig. 2.8**.

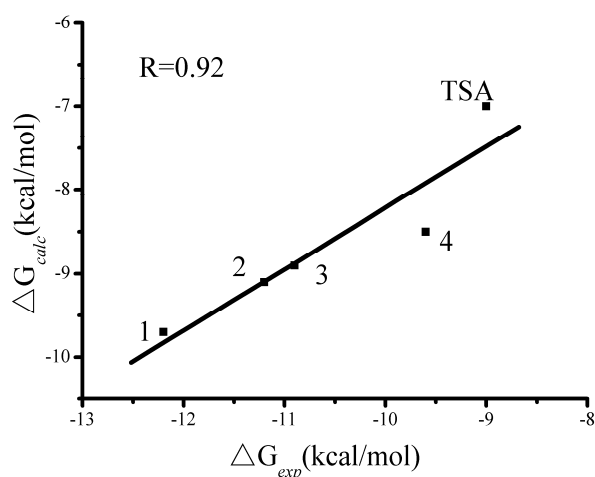


**Fig. 2.8** Correlation between the predicted binding energies ( $\Delta G_{\text{calc}}$ ) and the experimental values ( $\Delta G_{\text{exp}}$ ).

## 2.2.4 Selective inhibition of Apicidin on HDAC1 and HDAC8

Apicidin is known as isoform selective inhibitor for class I HDACs, with  $IC_{50}$  value of 1 nM for HDAC1 while  $IC_{50} > 1000$  nM for HDAC8.<sup>[13]</sup> In the present study, Apicidin was also docked to HDAC8, gaining two main binding poses (**Fig. 2.9**). The lowest binding energy conformation was zinc-chelated, like the HDAC1-Apicidin achieved above, with its cyclic backbone accommodating in an opposite groove formed by Phe208, His180, Gly97 and

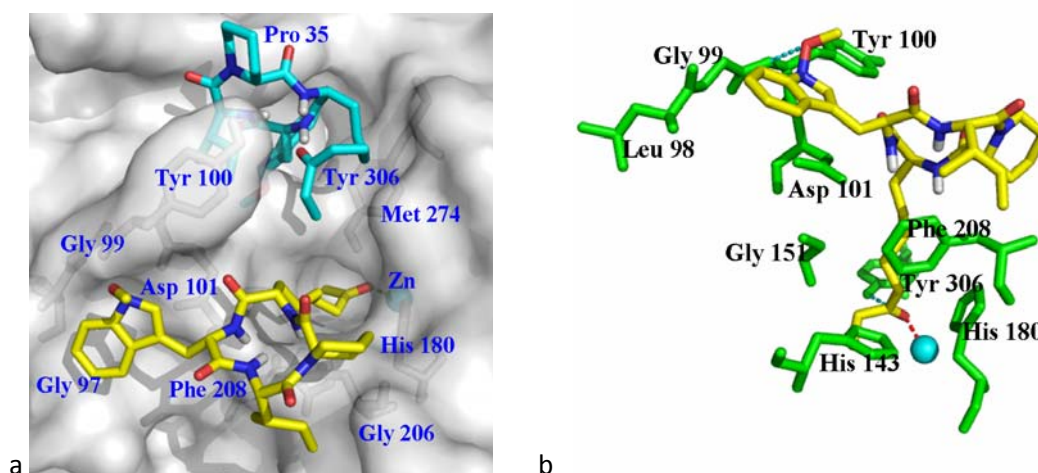


**Fig. 2.9** 3D model of the interactions between Apicidin and HDAC8 binding site. (a) surface representation of the zinc-chelated conformation (shown as sticks with the carbon atoms colored yellow) and the lowest binding energy conformation (cyan), top view; (b) important residues in close contacts (green) with the inhibitor, side view. Cyan dashed lines represent hydrogen bonds.

Asp101. So the N-O-methyl-Trp side chain was far away from Tyr306 and it was impossible for forming any hydrophobic interactions or  $\pi$ - $\pi$  interaction with this residue. Comparing with Apicidin-HDAC1 (**Fig. 2.6b**), there were less residues forming hydrophobic interactions and less hydrogen bonds in Apicidin-HDAC8 (**Fig. 2.9b**), which mean less stabilities and lower inhibitory activity. An important difference between the docking results of HDAC1-Apicidin and HDAC8-Apicidin was that, several clusters of conformations following the lowest binding energy conformation (ranked by binding energy scores) block the cavity adjacent to the HDAC8 active site with their cyclic backbones instead of coordinating  $Zn^{2+}$ . While in the docking of Apicidin to HDAC1 model, the lowest binding energy conformation and several followings were all zinc-chelated structures. And the second binding mode mentioned above makes less hydrophobic interactions because of decreased contact area. It was mentioned in a

previous study that, large amount of non-zinc-chelated conformations in one docking related to less biological activity of the cyclopeptide inhibitor.<sup>[17]</sup>

The comparison of the two enzyme structures showed that, the Tyr100 and Met274 in HDAC8 were replaced by the Glu98 and Arg270 in HDAC1 (**Fig. 2.5**) at the entrance portion of the active pocket. These changes made the pocket entrance more open in HDAC1, so the cyclic tetrapeptides can bind to the active site in a more favorable manner. Since the entrance of HDAC8 is less open and a second cavity adjacent the active pocket exists, inhibitors with large cap groups were apt to bind in the second cavity instead of coordinating  $Zn^{2+}$ . The surrounding environment near the active pocket including the unconserved residues and the second cavity may be responsible for the selective inhibition of Apicidin between HDAC1 and HDAC8.

To better understand the selective inhibition of Apicidin, a 3000 ps MD simulations were successfully performed on the complexes of Apicidin binding to HDAC1 and HDAC8. The root-mean-squared-fluctuation (RMSF) and potential energy remained stable after approximately the first 2200 ps of the simulation for the two systems studied (**Fig.2.10**). The RMSF value of residues at the active site of Apicidin-HDAC1 is smaller to Apicidin-HDAC8,

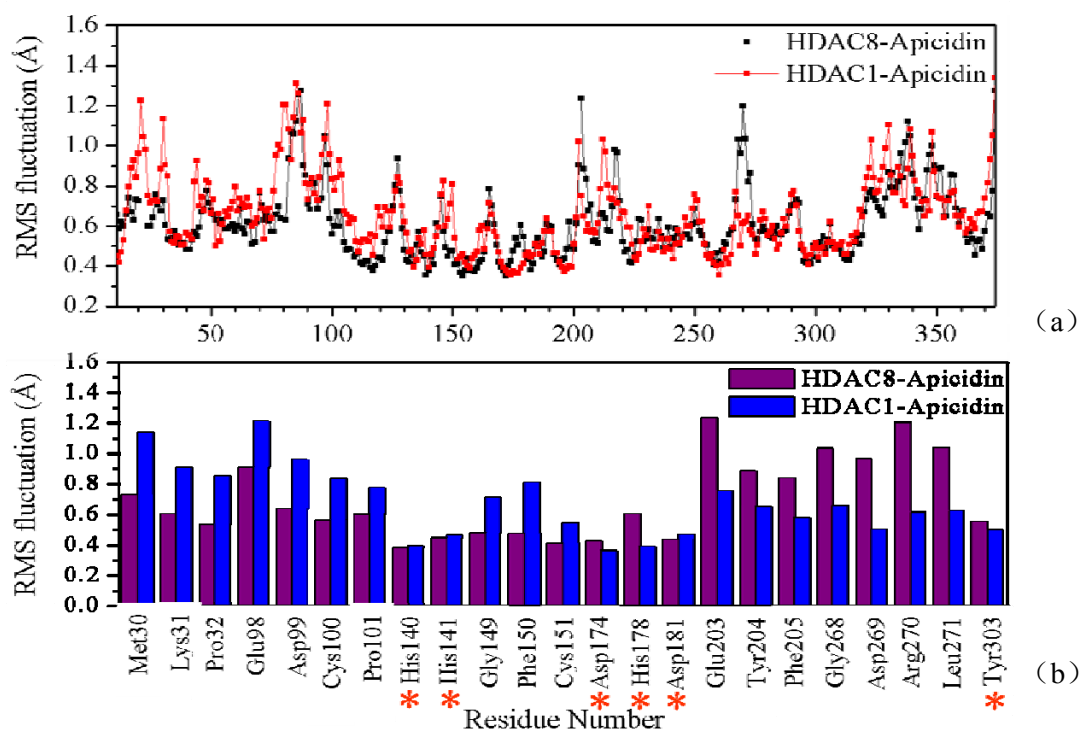


**Fig. 2.10** The average RMSF for amino acid residues of complexes during the last 800ps. (a) all residues; (b) residues in the active pocket (around  $Zn^{2+}$  demarcated by asterisk).

that means Apicidin-HDAC1 complex structure is stable. The Glu98 and Arg270 residues locate at the entrance of HDAC1 active pocket, The Arg plays an important role in forming stable interactions with Apicidin. The hydrogen bonds between Apicidin and HDACs were examined on the basis of the trajectories of the MD simulation (**Fig. 2.11**). The hydrogen bond existence maps showed that, Apicidin mainly created two hydrogen bonds with Tyr303 (Donor: Tyr303 OH, hydrogen: Tyr303 HH, acceptor: Aode O=C8; Index 0) and with His178 (Donor: His178 NE2, hydrogen: His178 HE2, acceptor: Aode O=C; Index 11). In contrast, no hydrogen bond lasted through the simulation between Apicidin and HDAC8. This prominent difference in hydrogen existence maps gave another reason for the selective inhibitory activity of Apicidin.

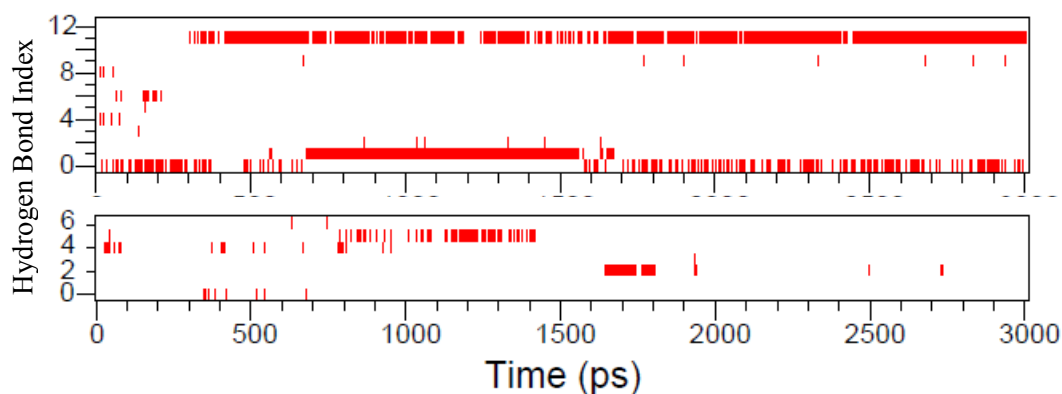


**Fig. 2.11** Hydrogen bond existence maps during the 3000 ps on molecular dynamics simulation of Apicidin-HDAC1 (a) and Apicidin-HDAC8 (b). Shadow zone represents that the location of donor, receptor and hydrogen atom is suitable for the hydrogen bond while white zone represents unsuitable.

## 2.3 Summary

The 3D model of HDAC1 has been constructed based on the X-ray structure of human HDAC8. And it was proved to be qualified for further studies by three independent validation tests. The interactions between the tetracyclopeptide inhibitors and the enzyme were described in details after docking. The keto-carbonyl moiety of tetracyclopeptides chelating with zinc ion is the basis of low binding energy. The tetracyclopeptide **4** contacted less residues of HDAC1 than Apicidin does, consistent with its lower inhibitory activity ( $\Delta G_{\text{binding}} = -8.54$  kcal/mol) than Apicidin ( $\Delta G_{\text{binding}} = -9.67$  kcal/mol). The Tyr100 and Met274 in HDAC8 were replaced by the Glu98 and Arg270 in HDAC1 at the entrance portion of the active pocket. These changes made



the pocket entrance more open in HDAC1, so that tetracyclopeptides bound to the active site in a more favorable manner. The docking of Apicidin to HDAC8 showed that, inhibitors with large cap groups were apt to bind in the second cavity near the active pocket instead of coordinating with  $Zn^{2+}$ . The Apicidin binding to the second cavity decreased its inhibitory activity toward HDAC8. The fact that there were two hydrogen bonds retaining through the MD simulation in Apicidin-HDAC1 while none in Apicidin-HDAC8, it was another reason for the selective inhibition of Apicidin. This study will be helpful for the optimization of cyclic tetrapeptide HDAC inhibitors, especially for the design of selective HDACs inhibitors.

## **2.4 Computational methodology**

### **2.4.1 Model building and validation of HDAC1**

The amino acid sequence of Human HDAC1 was obtained from the National Center for Biotechnology Information (NCBI) protein sequence database, Genbank Accession Number Q13547. The sequence extracted from one chain of human HDAC8 obtained from the Protein Data Bank (PDB ID: 1T64), was employed as template. Automated sequence alignment was carried out by ClustalW2 program<sup>[23]</sup> on the freely available automated web server of EBI (European Bioinformatics Institute; <http://www.ebi.ac.uk>).

The homology modeling program MODELLER 9v4<sup>[24]</sup> was employed to build the human HDAC1 model using the crystal structure of human HDAC8 as template. Twenty models were built using the alignment file generated above. And geometry optimizations and molecular dynamics simulations were performed during the building processes. The methods involved in geometry optimizations and molecular dynamics simulations were Conjugative Descent and Simulated Annealing, respectively. Among the 20 models, those with the lowest conditional probability density functions values (molpdf) or Discrete Optimized Protein Energy (DOPE) scores<sup>[25]</sup> were selected for further validation.

The quality of the final HDAC1 model was checked by three independent tests, PROCHECK<sup>[26]</sup>, WHATIF<sup>[27]</sup> and ERRAT<sup>[28]</sup>. The PROCHECK program was used to analyze the stereochemical quality of the model. The packing quality of the model was evaluated by another validation test, WHATIF Coarse Packing Quality Control value. The ERRAT program checked overall quality of the structure for non-bonded atomic interactions, and higher scores mean higher quality. The normally accepted range is >50 for a high quality model. All of the above

assessments were implemented on both HDAC1 model and HDAC8 crystal structure for comparison.

### **2.4.2 Docking calculation**

To understand the binding modes between HDACs and the cyclic tetrapeptides, docking studies were conducted with AutoDock 4.0 program<sup>[29,30]</sup> using a Lamarckian genetic algorithm. We chose the AutoDock docking protocol and scoring function on the basis of the successful application in the interpretation of the inhibitory activity of several HDAC ligands<sup>[14,17]</sup>. The active site of HDAC protein was covered by a grid box size of 56×72×76 points with a spacing of 0.375 Å between the grid points. For TSA and the tetracyclopeptides Apicidin analogues, all the single bonds except the amide bonds and cyclic bonds were treated as active torsional bonds. For each inhibitor, two hundred independent dockings, i.e. 200 runs, were performed using genetic algorithm searches. A maximum number of 250 000 000 energy evaluations and a maximum number of 10 000 generations were implemented during each genetic algorithm run. The default nonbonded zinc parameters in Autodock 4.0<sup>[29]</sup> were employed after being validated by the redocking studies of two crystal enzyme-inhibitor complexes, HDLP-TSA (resolution 2.0 Å) and HDAC8-TSA (resolution 1.9 Å). The crystallographic structure of Apicidin was obtained from Cambridge Crystallographic Data Centre, and the deposition number is CCDC 274844.<sup>[31]</sup> The other Apicidin analogues were constructed manually based on Apicidin and minimized for further docking studies. The LigPlot program<sup>[32]</sup> was also employed to analyze the docking results focusing on hydrogen bonds and hydrophobic interactions.

### **2.4.3 Molecular dynamics simulation**

MD simulations were performed using GROMACS program (version 3.3.3) with the GROMOS96 force field.<sup>[33]</sup> The starting geometries for the simulation were prepared from the docked conformation of Apicidin-HDAC1 and Apicidin-HDAC8 complexes. Before the simulation, the energy of the complexes was minimized using 5000 steps of a combined steepest-descent/conjugate gradient algorithms protocol. Each system was solvated by a layer of water molecules of 10 Å length in all directions. After a 50 ps position-restrained dynamics, each simulation preceded 3000 ps under periodic boundary conditions with NPT ensemble by using Berendsen's coupling algorithm at 300 K. Simulation trajectory analyses were done by analysis tools in GROMACS.

## 2.5 References

- [1] K. Luger, A.W. Mader, R.K. Richmond, D.F. Sargent and T.J. Richmond, *Nature*, 1997, 389: 251–260.
- [2] E. Pennisi, *Science*, 1997, 275: 155–157.
- [3] S.K. Kurdistani and M. Grunstein, *Nat. Rev. Mol. Cell. Biol.* 2003, 4: 276–284 .
- [4] H.H. Ng and A. Bird, *Trends. Biochem. Sci.* 2000, 25: 121–126.
- [5] M. Yoshida, M. Kijima, M. Akita and T. Beppu, *J. Biol. Chem.* 1990, 265:17174–17179.
- [6] Y. Nakao, S. Yoshida, S. Matsunaga, N. Shindoh, Y. Terada, K. Nagai, J.K. Yamashita, A. Ganesan, R.W.M. Soest van and N. Fusetani, *Angew. Chem. Int. Ed.* 2006, 45: 7553–7557.
- [7] H. Mori, Y. Urano, F. Abe, S. Furukawa, S. Furukawa, Y. Tsurumi, K. Sakamoto, M. Hashimoto, S. Takase, M. Hino and T. Fujii, *J. Antibiot.* 2003, 56: 72–79.
- [8] H. Ueda, H. Nakajima, Y. Hori, T. Goto and M. Okuhara, FR901228, *J. Antibiot.* 1994, 47: 301–310.
- [9] S.B. Singh, D.L. Zink, J.D. Polishook, A.W. Dombrowski, S.J. Darkin-Rattray, D.M. Schmatz and M.A. Goetz, *Tetrahedron. Lett.* 1996, 37: 8077–8080.
- [10] S.J. Darkin-Rattray, A.M. Gurnett, R.W. Myers, P.M. Dulski, T.M. Crumley, J.J. Allocco, C. Cannova, P.T. Meinke, S.L. Colletti, M.A. Bednarek, S.B. Singh, M.A. Goetz, A.W. Dombrowski, J.D. Polishook and D.M. Schmatz, *Proc. Natl. Acad. Sci. USA* 1996, 93: 13143–13147.
- [11] M.S. Finnin, J.R. Donigian, A. Cohen, V.M. Richon, R.A. Rifkind, P.A. Marks, R. Breslow and N.P. Pavletich, *Nature*, 1999, 401: 188–193.
- [12] J.R. Somoza, R.J. Skene, B.A. Katz, C. Mol, J.D. Ho, A.J. Jennings, C. Luong, A. Arvai, J.J. Buggy, E. Chi, J. Tang, B.C. Sang, E. Verner, R. Wynands, E.M. Leahy, D.R. Dougan, G. Snell, M. Navre, M.W. Knuth, D.E. McRee and L.W. Tari, *Structure*, 2004, 12: 1325–1334.
- [13] A. Vannini, C. Volpari, G. Filocamo, E. Caroli Casavola, M. Brunetti, D. Renzoni, P. Chakravarty, C. Paolini, R. De Francesco, P. Gallinari, C. Steinkuhler and S. Di Marco, *Proc. Natl. Acad. Sci. USA* 2004, 101: 15064–15069.
- [14] D.F. Wang, O.G. Wiest, P. Helquist, H.Y. Lan-Hargest and N.L. Wiech, *J. Med. Chem.* 2004, 47: 3409–3417.
- [15] D.F. Wang, P. Helquist, N.L. Wiech and O. Wiest, *J. Med. Chem.* 2005, 48: 6936–6947.
- [16] M. Rodriguez, S. Terracciano, E. Cini, G. Settembrini, I. Bruno, G. Bifulco, M. Taddei and L. Gomez-Paloma, *Angew. Chem. Int. Ed.* 2006, 118: 437–441.
- [17] N. Maulucci, M.G. Chini, S.D. Micco, I. Izzo, E. Cafaro, A. Russo, P. Gallinari, C. Paolini, M.C. Nardi, A. Casapullo, R. Riccio, G. Bifulco and F.D. Riccardis, *J. Am. Chem. Soc.* 2007, 129: 3007–3012.
- [18] S.L. Colletti, R.W. Myers, S.J. Darkin-Rattray, A.M. Gurnett, P.M. Dulski, S. Galuska, J.J. Allocco, M.B. Ayer, C. Li, J. Lim, T.M. Crumley, C. Cannova, D.M. Schmatz, M.J. Wyvratt, M.H. Fisher and P.T. Meinke, *Bioorg. Med. Chem. Lett.* 2001, 11: 113–117.
- [19] R. Furumai, Y. Komatsu, N. Nishino, S. Khochbin, M. Yoshida and S. Horinouchi, *Proc. Natl. Acad. Sci. USA*, 2001, 98: 87–92.
- [20] B.E. Bernstein, J.K. Tong and S.L. Schreiber, *Proc. Natl. Acad. Sci. USA* 2000, 97: 13708–13713.

- [21] B.C. Roberts and R.L. Mancera, *J. Chem. Inf. Model.* 2008, 48: 397–408.
- [22] C.L. Yan, Z.L. Xiu, X.H. Li, S.M. Li, C. Hao and H. Teng, *Proteins*, 2008, 73: 134–149.
- [23] J.D. Thompson, D.G. Higgins and T.J. Gibson, *Nucleic. Acids. Res.* 1994, 22: 4673–4680.
- [24] A. Fiser and A. Sali, *Methods. Enzymol.* 2003, 374: 461–491.
- [25] M.Y. Shen and A. Sali, *Protein. Sci.* 2006, 15: 2507–2524.
- [26] R.A. Laskowski, D.S. Moss and J.M. Thornton, *J. Mol. Biol.* 1993, 231: 1049–1067.
- [27] G. Vriend and C. Sander, *J. Appl. Cryst.* 1993, 26: 47–60.
- [28] C. Colovos and T.O. Yeates, *Protein. Sci.* 1993, 2: 1511–1519.
- [29] R. Huey, G.M. Morris, A.J. Olson and D.S. Goodsell, *J. Comput. Chem.* 2007, 28: 1145–1152.
- [30] G.M. Morris, D.S. Goodsell, R.S. Halliday, R. Huey, W.E. Hart, R.K. Belew and A.J. Olson, *J. Comput. Chem.*, 1998, 19: 1639–1662.
- [31] M. Kranz, P.J. Murray, S. Taylor, R.J. Upton, W. Clegg and M.R. Elsegood, *J. Peptide. Sci.* 2006, 12: 383–388.
- [32] A.C. Wallace, R.A. Laskowski and J.M. Thornton, *Protein. Eng.* 1995, 8: 127–134.
- [33] D. van der Spoel, E. Lindahl, B. Hess, G. Groenhof, A. E. Mark and H. J. C. Berendsen, *J. Comp. Chem.* 2005, 26: 1701–1719.

## Chapter 3

### Synthesis of Non-Natural Amino Acid

#### 3.1 Introduction

Reversible  $\epsilon$ -amino groups of lysine residues acetylation and deacetylation on histone tails by HAT and HDAC enzymes play an important role in the epigenetic regulation of gene expression via altering the chromatin architecture and controlling the accessibility of DNA and histones to transcriptional regulators.<sup>[1-2]</sup> More recently, HDACs have also been shown to deacetylate nonhistone proteins, predominantly transcription factors.<sup>[3-6]</sup> HDAC inhibitors are a promising series of anticancer agents that affect gene regulation. The sequence diversity of surface recognition domain of HDAC inhibitors may choose to bind the amino acid residues on the rim of active pocket of HDAC subtype.<sup>[7-9]</sup> The modification at cap group portion of inhibitor can provide better specificity. The surface recognition domain of the pharmacophore affects not only inhibitory potency but also selectivity. To find out specific inhibitors, author focused on the four amino acid residues in framework. Our aim was to synthesize potent and selective cyclic tetrapeptide HDAC inhibitors. A number of modifications are carried out to the cyclic tetrapeptide framework for replacing amino acid at four positions, respectively. Accordingly, we designed and synthesized several non-natural amino acids to replaced amino acid residues of Chlamydocin framework (**Fig. 3.1**). At first, we designed methyl

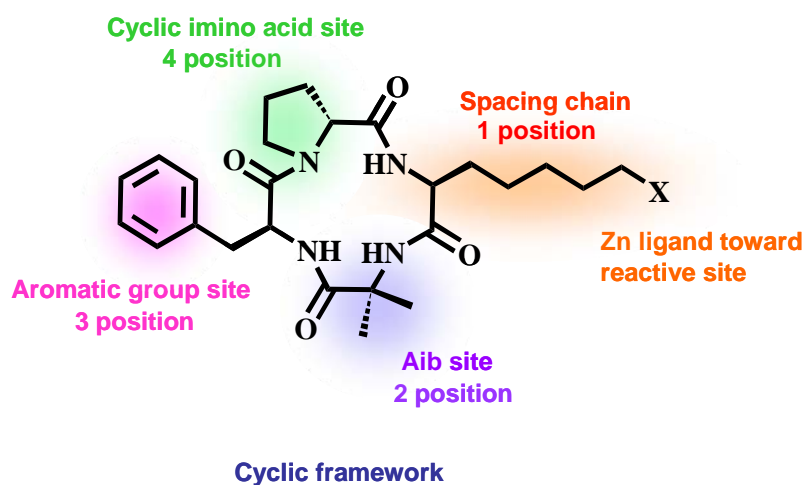
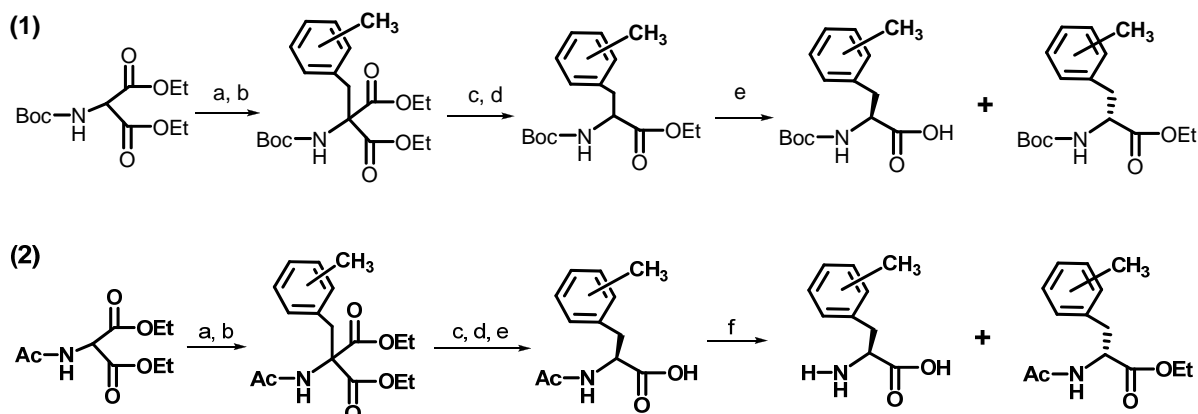


**Fig. 3.1** Design the site of non-natural amino acids in HDAC inhibitors framework.

phenylalanine (L-Phe(2-Me), L-Phe(4-Me) and L-Phe(3,5-2Me)) to replace phenylalanine at 3-position of cyclic framework to investigate interaction between surface recognition domain of HDAC inhibitors and HDACs, moreover, at 3-position of cyclic framework, we also designed two amino acids containing chlorine (Ac5 and Ac6) to discuss whether the aromatic ring of the HDAC inhibitors affects the potency of HDAC inhibitors or not. In addition, for chelating zinc ion of HDAC active site, the side chain containing chlorine of Ac5 or Ac6 can be modified by oxygen or sulfur. Author designed and synthesized three kinds of *n*-methyl-amino-cyclohexane-carboxylic acid (*Anmc6c*) (*n*=2; 3; 4) using the Strecker reaction method for replacing Aib at 2-position of scaffold to know the interaction of aliphatic cap group with the surface of HDAC enzymes.

### 3.2 Synthesis of H-Phe-OH derivatives

The non-natural amino acids of H-Phe-OH derivatives were designed and synthesized for aromatic ring modification at 3-position of cyclic tetrapeptide HDAC inhibitors. This has resulted in the development of vast number of methods for the synthesis of non-natural amino acids. They include at least 100 derivatives of phenylalanine, in which the phenyl group was widely modified, while aliphatic amino acids have been paid less attention. We are interested in the synthesis of optically pure non-natural aromatic amino acids containing methyl. According to different starting materials (diethyl (Boc-amino) malonate and diethyl acetamidomalonate),



**Scheme 3.1** Synthesis of methyl-phenylalanine (H-Phe(*n*-Me)-OH).

Reagents and conditions (1): (a) Na, anhyd EtOH, reflux, 30 min; (b) BrCH<sub>2</sub>C<sub>6</sub>H<sub>4</sub>CH<sub>3</sub>, reflux, 6 h; (c) NaOH aq., EtOH, 4 h; (d) toluene, reflux, 3 h; (e) subtilisin Carlsberg, DMF/H<sub>2</sub>O (1/3), 4 h. (2): (a) Na, anhydrous EtOH, reflux, 30 min; (b) BrCH<sub>2</sub>C<sub>6</sub>H<sub>4</sub>CH<sub>3</sub>, reflux, 6 h; (c) NaOH aq., EtOH, 4 h; (d) toluene, reflux, 3 h; (e) NaOH aq., EtOH, 4 h; (f) acylase CoCl<sub>3</sub> 6H<sub>2</sub>O, H<sub>2</sub>O, pH 8, 24 h.

Methyl Boc-L-Phe-OH derivatives were synthesized by the reported procedure<sup>[10]</sup> as illustrated in **Scheme 3.1**. L-Phe(*n*-Me) (*n* = 2; 4; 3,5) were used for the synthesis of designed cyclic tetrapeptides in Chapter 5. *N*-methylbenzyl bromides were separately coupled with diethyl Boc-amino- malonate by using NaOEt in ethanol. One of the ethyl ester groups of adduct was hydrolyzed by two equivalent of 2 M NaOH at room temperature. The oily monoacid monoester after work-up was then subjected to the decarboxylation by refluxing in toluene. Finally, Boc-DL-Phe(*n*-Me)-OEt was subjected to the action of subtilisin Carlsberg from *Bacillus licheniformis* (Sigma) in a mixture of DMF and water (1:3, v/v). Boc-L-Phe(*n*-Me)-OH was isolated as colorless oil with excellent purity in quantitative yield.

### 3.2.1 Synthesis of Boc-L-Phe(2-Me)-OH

#### 3.2.1.1 Synthesis of Boc-L-Phe(2-Me)-OH from diethyl (Boc-amino) malonate (MW = 279.33):

Metallic sodium (1.24 g, 54 mmol) was dissolved in anhydrous EtOH (54 mL) and diethyl (Boc-amino) malonate (17.84 g, 64.8mmol) was added to the solution. After refluxing for 30 minutes, the mixture was cooled to room temperature and then 2-methylbenzyl bromide (10 g, 54 mmol) was added and refluxed for 5 hours. The reaction mixture was carried out by the addition of 2N NaOH aq (5 mL) for Hydrolysis. After 5 hours, ethanol was evaporated and the unreacted 2-methylbenzyl bromide was removed by extraction with ether. Then the aqueous solution was extracted with ethyl acetate at pH 2~3 by citric acid and washed with brine. After drying over MgSO<sub>4</sub> and concentrating, the resulting Boc-DL-Phe(2-Me)-OEt(OH) was obtained(90%). The residue was dissolved in toluene (100 mL) and refluxed for 5 hours and toluene was evaporated and then was purified by silica gel chromatography to obtain Boc-DL-Phe(2-Me)-OEt (81%). Finally Boc-DL-Phe(2-Me)-OEt was subjected to the action of subtilisin Carlsberg from *Bacillus licheniformis* (Sigma) in a mixture of DMF and H<sub>2</sub>O (1:3, v/v) at 37 °C. The aqueous solution was extracted with ethyl acetate at pH 3 to obtained Boc-L-Phe(2-Me)-OH was isolated as colorless oil (85%). Characterization data for: HPLC: r.t. 6.853 min, 100%.  $[\alpha]_D^{26} = +11.18^\circ$  (C, 2.3, CH<sub>3</sub>OH); ESI-MS:  $[M-H]^+$  278.0,  $[M+Cl]^-$  314.0 for C<sub>15</sub>H<sub>21</sub>NO<sub>4</sub> (calcd 279.33). IR(Neat): 3333(NH), 3023, 2980(CH), 1707 (C=O,COOH), 1659(C=O, -CONH), 1591, 1494(C=C, Ar), 1169, 1049(CN). <sup>1</sup>H-NMR (400 MHz, DMSO):  $\delta$  1.33(s, 9H), 2.26(s, 3H), 3.18(m, 1H), 3.60(s, 1H), 4.12 (s, 1H), 7.04(m, 4H).

### 3.2.1.2 Synthesis of Boc-L-Phe(2-Me)-OH from diethyl acetamidomalonate

Metallic sodium (1.24 g, 54 mmol) was dissolved in anhydrous EtOH (54 mL) and diethyl acetamidomalonate (14.08 g, 64.8mmol) was added to the solution. After refluxing for 30 minutes, the mixture was cooled to room temperature and then 2-methylbenzyl bromide (10 g, 54 mmol) was added and refluxed for 5 hours. The reaction mixture was carried out by the addition of 3N NaOH aq ( 20 mL) for Hydrolysis. Ethanol was evaporated and the unreacted 2-methylbenzyl bromide was removed by extraction with ether. Then the aqueous solution was extracted with ethyl acetate at pH 2~3 by HCl and washed with brine. After drying over MgSO<sub>4</sub> and concentrating, the resulting Ac-DL-Phe(2-Me)-OEt(OH) was obtained (60–80%). The residue was dissolved in toluene (100 mL) and refluxed for 5 hours and toluene was evaporated and then was purified by silica gel chromatography to obtain Ac-DL-Phe(2-Me)-OEt (9.58 g, 43.3 mmol, 80%). The residue was dissolved in ethanol (50 mL) and hydrolysis and work up was carried out as described above to get Ac-DL-Phe(2-Me)-OH (75%). The Ac-DL-Phe(2-Me)-OH (43.3 mol) was dissolved in water (170 mL) at pH 7 by the addition of 1N NaOH aq.(43 mL, 43 mmol). Then CoCl<sub>2</sub>·6H<sub>2</sub>O (51.5 mg, 1 mM) and acylase (2.2 g) were added and incubated at 38<sup>0</sup>C for 24 hours. H-L-Phe(2-Me)-OH (2.1 g, 11.7 mmol) was solidified from the aqueous solution and was filtered after cooling the reaction mixture and washed with water and ethanol. The aqueous solution was extracted with ethyl acetate at pH 3 to recover Ac-D-Phe(2-Me)-OH(59%). The Boc protection of H-L-Phe(2-Me)-OH yielded Boc-L-Phe(2-Me)-OH as colourless oil in quantitative yield (95%).

### 3.2.2 Synthesis of Boc-L-Phe(3-Me)-OH

Boc-L-Phe(3-Me)-OH was synthesized in the same manner as 3.2.1.1 described reaction to obtain as white foam (43%). Characterization data for: HPLC: r.t. 6.987 min.  $[\alpha]_D^{26} = +11.33^\circ$ (C, 2.6, CH<sub>3</sub>OH); ESI-MS:  $[M-H]^+$  278.0,  $[M+Cl]^-$  314.0 for C<sub>15</sub>H<sub>21</sub>NO<sub>4</sub> (calcd 279.33). IR(Neat): 3342(NH), 2978, 2934(CH), 1716(C=O, COOH), 1610(NH, -CONH), 1591, 1506(C=C, Ar), 1166, 1057(CN); <sup>1</sup>H-NMR (400 MHz, DMSO):  $\delta$  1.31(s, 9H), 2.29(s, 3H), 2.89(m, 1H), 3.36(s, 1H), 4.09 (s, 1H), 7.15(m, 4H).

### 3.2.3 Synthesis of Boc-L-Phe(4-Me)-OH

Boc-L-Phe(4-Me)-OH was synthesized in the same manner as 3.2.1.1 described reaction to obtain as white foam (48%). Characterization data for: HPLC: r.t. 7.024 min.  $[\alpha]_D^{30} =$



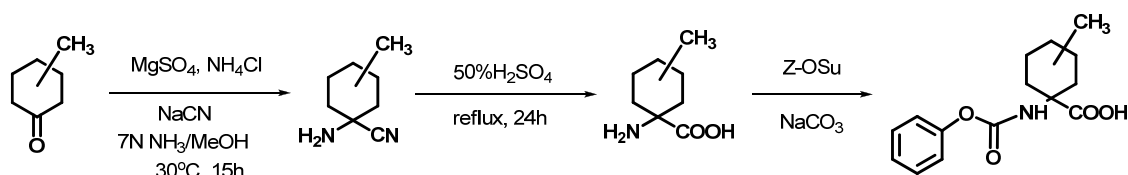
+12.39°(C, 1.7, CH<sub>3</sub>OH); ESI-MS: [M-H]<sup>+</sup> 278.0, [M+Cl]<sup>-</sup> 314.0 for C<sub>15</sub>H<sub>21</sub>NO<sub>4</sub> (calcd 279.33). IR(Neat): 3331(NH), 2978, 2930(CH), 1716(C=O,COOH), 1515, 1484 (C=C, Ar), 1166, 1056(CN); <sup>1</sup>H-NMR (400 MHz, DMSO): δ 1.27(s, 9H), 2.20(s, 3H), 2.78 (s, 1H), 3.52(m, 1H), 4.02 (m, 1H), 7.06(m, 4H).

### 3.2.4 Synthesis of Boc-L-Phe(3,5-2Me)-OH

Boc-L-Phe(3,5-2Me)-OH was synthesized in the same manner as 3.2.1.1 described reaction to obtain as white foam (2.06 g, 7.8 mmol, 33%). HPLC: r.t. 7.136 min. ESI-MS: [M-H]<sup>+</sup> 292.0, [M+Cl]<sup>-</sup> 328.0 for C<sub>16</sub>H<sub>23</sub>NO<sub>4</sub> (calcd 293.36).

### 3.3 Synthesis of *n*-methyl-amino-cyclohexane-carboxylic acid

In the field of organic chemistry for the synthesis of  $\alpha$ -aminonitriles, the Strecker reaction is one of the most efficient and straightforward method,<sup>[10]</sup> which is very useful precursors for the synthesis of  $\alpha$ -amino acids or various nitrogen-containing heterocycles.<sup>[11,12]</sup>  $\alpha$ -Amino acids are also of great biological and economical importance due to their significance in chemistry and biology. Herein, author designed and synthesized three kinds of *n*-methyl-amino-cyclohexane-carboxylic acids: ( $\pm$ )-2-methyl-amino-cyclohexane-carboxylic acid (A2mc6c), 3-methyl-amino-cyclohexane-carboxylic acid (A3mc6c) and 4-methyl-amino-cyclohexane-carboxylic acid (A4mc6c) based on the reported procedure as illustrated in **Scheme 3.2**. These amino acids were used for the synthesis of designed HDAC inhibitors of cyclic tetrapeptides in Chapter 4. This reaction conditions was crucial for using NaCN for conversion the starting material methylcyclohexanone to methylcyclohexane amino nitrile. The use of an excess of ketone ensured that complete consumption of NaCN occurred. The optimal conditions involved concentration of nearly all the NH<sub>3</sub>/MeOH from the reaction mixture under reduced pressure and temperature, dilution with MTBE, and filtration of the inorganic solids.<sup>[13]</sup> Hydrolysis of methylcyclohexane amino nitrile in 50% H<sub>2</sub>SO<sub>4</sub> was refluxed for 24 hours to provide a crude



**Scheme 3.2** Synthesis of *n*-methyl-amino-cyclohexane-carboxylic acids (H-Anmc6c-OH).

aqueous solution of *n*-methyl-amino-cyclohexane-carboxylic acids followed by adjusting the pH to 5 ~ 6 by the addition of 10 N NaOH to separate out products.

### **3.3.1 Synthesis of H-(±)A2mc6c-OH**

#### **3.3.1.1 Preparation of (±)2-methyl-cyclohexane amino nitrile (MW=138.21):**

MgSO<sub>4</sub> (6.14 g, 51.0 mmol), NH<sub>4</sub>Cl (2.73 g, 51.0 mmol), NaCN (4.75 g, 96.9 mmol) was dissolved into 7 M NH<sub>3</sub> in MeOH (58 mL) in a round-bottom flask. The solution was stirred and cooled to -5 °C to -10 °C. The internal temperature of the slurry was -5 °C and rose to 8 °C after stirring for 10 minutes as some of the solids dissolved. To the solution was added (±)2-methylcyclohexanone (13 mL, 102.0 mmol). The internal temperature slowly rose from 8 °C to 35 °C over the course of 1 hour, at which point it slowly decreased to 30 °C and was held at this temperature for 15 hours. The reaction was monitored by TLC. The solvent was then removed under reduced pressure (~30 mmHg) while maintaining the internal temperature < 30 °C until nearly all of the MeOH and ammonia were removed. The resulting slurry of inorganic salts and the product was diluted with 66 mL of MTBE, stirred at room temperature for 30 min, and filtered. The inorganic wet cake was washed with MTBE (10 mL). The solvent was concentrated under reduced pressure (~30 mmHg) while maintaining the internal temperature < 20 °C. The amino nitrile as oily compound was obtained (14.1 g, 102.0 mmol). TLC: R<sub>f</sub> 0.8 (CHCl<sub>3</sub>/MeOH/CH<sub>3</sub>COOH = 90/10/2).

#### **3.3.1.2 Synthesis of (±)2-methyl-amino-cyclohexane-carboxylic acid (MW= 157.1103):**

To the oily compound was added 64 mL (6 eq) of 50% v/v of H<sub>2</sub>SO<sub>4</sub>, and subjected to the carboxylation by refluxing. The reaction mixture was then heated to 100 °C for 24 hours. The reaction mixture was allowed to cool to room temperature, and the pH was adjusted to 5 ~ 6 by the portion addition of 10 N NaOH. The amino acid was separated out and filtered. The wet cake was washed with water and dried under air-dry for 24 hours to give 6.1 g (38.8 mmol, 39%) of H-(±)A2mc6c-OH as an analytically pure colorless solid. HR-FAB-MS: [M+H]<sup>+</sup> 158.1196, for C<sub>8</sub>H<sub>16</sub>NO<sub>2</sub> (calcd 157.1103).

### **3.3.2 Synthesis of H-A3mc6c-OH**

#### **3.3.2.1 Preparation of 3- methyl-cyclohexane amino nitrile (MW=138.21):**

NH<sub>4</sub>Cl (11.50 g, 214 mmol), NaCN (10.04 g, 210 mmol) was dissolved into NH<sub>3</sub>(aq. conc.) (37

mL) and H<sub>2</sub>O (53 mL). To the solution was added 3-methylcyclohexanone (25 mL, 200 mmol) in ether (17 mL). After stirring for 68 hours at room temperature. The reaction was monitored by TLC. The solution was dissolved in ether, and then washed with water. The superfluous NaCN was removed by water layer. After concentrating ether, the resulting oily substance was obtained 3-methylcyclohexanone amino nitrile (27.65 g, 200 mmol, 100%). TLC: R<sub>f</sub> 0.65 (CHCl<sub>3</sub>/MeOH/ CH<sub>3</sub>COOH = 90/10/2).

### **3.3.2.2 Synthesis of 3-methyl-amino-cyclohexane-carboxylic acid (MW= 157.1103):**

To the oily compound was added 6 N HCl (58 mL), CH<sub>3</sub>COOH (58 mL) and subjected to the carboxylation by refluxing. The reaction mixture was then heated to 100 °C for 96 hours. The reaction mixture was allowed to cool to room temperature, and the pH was adjusted to 5 ~ 6 by the portionwise addition of 10 N NaOH. The amino acid was separated out and filtered. The wet cake was washed with water and dried under air-dry for 24 hours to give 1.2 g (7.8 mmol, 3.9%) of 3-methyl-cyclohexane amino acid as white foam. HR-FAB-MS: [M+H]<sup>+</sup> 158.1121, for C<sub>8</sub>H<sub>16</sub>NO<sub>2</sub> (calcd 157.1103).

### **3.3.3 Synthesis of H-A4mc6c-OH**

#### **3.3.3.1 Preparation of 4-methyl-cyclohexane amino nitrile (MW=138.21):**

NH<sub>4</sub>Cl (8.94 g, 167 mmol), NaCN (7.79 g, 159 mmol) was dissolved into NH<sub>3</sub> (aq. conc.) (28 mL) and H<sub>2</sub>O (40 mL). To the solution was added 4-methylcyclohexanone (17 mL, 152 mmol) in ether (17 mL). After stirring for 68 hours at room temperature. The reaction was monitored by TLC. The solution was dissolved in ether, and then washed with water. The superfluous NaCN was removed by water layer. After concentrating ether, the resulting oily substance was obtained 4-methylcyclohexanone amino nitrile (22.00 g, 152 mmol, 100%). TLC: R<sub>f</sub> 0.65 (CHCl<sub>3</sub>/MeOH/ CH<sub>3</sub>COOH = 90/10/2).

#### **3.3.3.2 Synthesis of 4-methyl-amino-cyclohexane-carboxylic acid (MW= 157.1103):**

To the oily compound was added 6 N HCl (58 mL), CH<sub>3</sub>COOH(58 mL) and subjected to the carboxylation by refluxing. The reaction mixture was then heated to 100 °C for 96 hours. The reaction mixture was allowed to cool to room temperature, and the pH was adjusted to 5 ~ 6 by the portionwise addition of 10 N NaOH. The amino acid was separated out and filtered. The wet cake was washed with water and dried under air-dry for 24 hours to give 0.16 g (0.76 mmol,

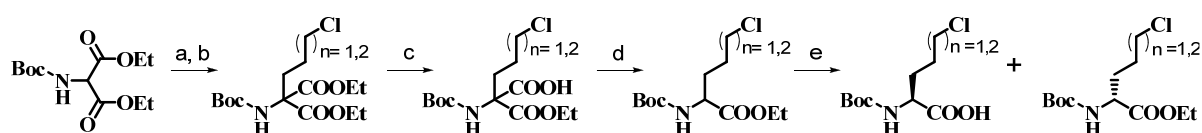
0.5%) of H-A4mc6c-OH as white foam. HR-FAB-MS:  $[M+H]^+$  158.1152, for  $C_8H_{16}NO_2$  (calcd 157.1103).

### 3.3.4 Synthesis of Z-Anmc6c-OH

To a suspension of *n*-methyl-amino-cyclohexane-carboxylic acid (5 mmol) in acetone (5 mL) and water (5 mL) were added Z-Osu (5 mmol) and triethyl amine (15 mmol). After stirring for overnight, acetone was removed by evaporation; residue was extracted by ether, the water layer was added ethyl acetate, and then washed with an aqueous 10% citric acid solution and brine. After drying over  $MgSO_4$  and concentrating, the resulting crude product was purified by crystallization in diethyl ether/petroleum ether (1:9 v/v) to yield (85-90%).

### 3.4 Synthesis of amino acid containing chlorine

Boc-2-amino-chloro-pentanoic acid (Boc-L-Ac5-OH) and Boc-2-amino-chloro-hexanoic acid (Boc-L-Ac6-OH) were synthesized using the same manner as 3.2.1 described reaction to obtain (**Scheme 3.3**). The two amino acid were used for the synthesis of designed HDAC inhibitors of cyclic tetrapeptides in Chapter 6. The two reason of synthesis (Ac5) and (Ac6): hydrophobic L-Ac5 and L-Ac6 replaced L-Phe at 3-position of cyclic tetrapeptide scaffold, to compare their inhibit HDAC activity with reported HDAC inhibitors and probe deeply into essential of aromatic ring in cyclic framework; the side chain containing chlorine of L-Ac5 or L-Ac6 may be modified with oxygen or sulfur to chelate zinc ion of HDAC active pocket bottom.



**Scheme 3.3** Synthesis of amino acid containing chlorine.

Reagents and conditions: (a) Na, anhyd EtOH, reflux, 30 min; (b)  $Br(CH_2)_3$  or  $4Cl$ , reflux, 6 h; (c) NaOH aq., EtOH, 4 h; (d) toluene, reflux, 3 h; (e) subtilisin Carlsberg, DMF/ $H_2O$  (1/3), 4 h.

### 3.4.1 Synthesis of Boc-L-2-amino-5-chloropentanoic acid

#### 3.4.1.1 Synthesis of Boc-DL-Ac5-OEt(OH) (MW=323.77):

Metallic sodium (2.3 g, 100 mmol) was dissolved in anhydrous EtOH (100 mL) and diethyl (Boc-amino)malonate (27.5 g, 140 mmol) was added to the solution. After refluxing for 30 minutes, the mixture was cooled to room temperature and then 1-bromo-3-chloro-propane (17.3 g, 110 mmol) was added and refluxed for 5 hours. Ethanol was evaporated, and then the aqueous solution was extracted with ethyl acetate and washed with water and brine. After drying over MgSO<sub>4</sub> and concentrating, the resulting 2-*tert*-butoxycarbonylamino-2-(3-chloro-propyl)-malonic acid diethyl ester (Boc-DL-Ac5-OEt(OEt)) was obtained (32.1 g, 91.2 mmol, 91%). The reaction mixture was carried out by the addition of one equivalent of 1 M NaOH (150 mL) at low temperature (0<sup>0</sup>C) for hydrolysis in three aliquots with 30 minutes time interval. The reaction product was checked by TLC (R<sub>f</sub> 0.20, CHCl<sub>3</sub>/MeOH=9/1). After 4 hours, ethanol was evaporated and the unreacted 1-bromo-3-chloro-propane was removed by extraction with 4% NaHCO<sub>3</sub> and ether. Then the aqueous solution was extracted with ethyl acetate at pH 2~3 by citric acid and washed with brine. After drying over MgSO<sub>4</sub> and concentrating, the resulting 2-*tert*-butoxycarbonylamino-2-(3-chloro-propyl)-malonic acid monoethyl ester (Boc-DL-Ac5-OEt(OH)) was obtained (20.1 g, 62.1 mmol, 68%).

#### **3.4.1.2 Synthesis of Boc-L-Ac5-OH (MW=251.71):**

The residue was dissolved in toluene (100 mL) and refluxed for 5 hours and checked by TLC (R<sub>f</sub> 0.8, CHCl<sub>3</sub>/MeOH=9/1) and toluene was evaporated and then was purified by silica gel chromatography (φ5.0 x 20 cm, 1% methanol/chloroform) to obtain 2-*tert*-butoxycarbonyl-5-chloro pentanoic acid ethyl ester (11.0 g, 39.3 mmol, 63%, HPLC: r.t. 5:30 min, B: 0-100%). Finally Boc-DL-Ac5-OEt (11.0 g, 39.2 mmol) was subjected to the action of subtilisin (40 mg) Carlsberg from *Bacillus licheniformis* (Sigma) in a mixture of DMF (40 mL) and H<sub>2</sub>O (120 mL) at pH 7, 37<sup>0</sup>C for 4 hours. The aqueous solution was extracted with ethyl acetate at pH 3 to obtain 2-*tert*-butoxycarbonyl-5-chloro-pentanoic acid (Boc-L-Ac5-OH) was isolated as colorless oil (4.9 g, 19.4 mmol, 50%, HPLC: r.t. 5.36 min, B: 0-100%).

#### **3.4.2 Synthesis of Boc- L-2-amino-6-chlorohexanoic acid**

##### **3.4.2.1 Synthesis of Boc-DL-Ac6-OEt(OH) (MW=337.80):**

Metallic sodium (2.3 g, 100 mmol) was dissolved in anhydrous EtOH (100 mL) and diethyl (Boc-amino) malonate (27.5 g, 140 mmol) was added to the solution. After refluxing for 30 minutes, the mixture was cooled to room temperature and then 1-bromo-4-chloro-butane (18.9

g, 110 mmol) was added and refluxed for 5 hours. Ethanol was evaporated, and then the aqueous solution was extracted with ethyl acetate and washed with water and brine. After drying over MgSO<sub>4</sub> and concentrating, the resulting 2-*tert*-butoxycarbonylamino-2-(4-chloro-butyl)-malonic acid diethyl ester (Boc-DL-Ac6-OEt(OEt)) was obtained (32.1 g, 87.7 mmol, 88%). The reaction mixture was carried out by the addition of one equivalent of 1 M NaOH (150 mL) at low temperature (0°C) for hydrolysis in three aliquots with 30 minutes time interval. The reaction product was checked by TLC (R<sub>f</sub> 0.30, CHCl<sub>3</sub>/MeOH=9/1). After 4 hours, ethanol was evaporated and the unreacted 1-bromo-3-chloro-propane was removed by extraction with 4% NaHCO<sub>3</sub> and ether. Then the aqueous solution was extracted with ethyl acetate at pH 2~3 by citric acid and washed with brine. After drying over MgSO<sub>4</sub> and concentrating, the resulting 2-*tert*-butoxycarbonylamino-2-(4-chloro-butyl)-malonic acid monoethyl ester (Boc-DL-Ac6-OEt (OH)) was obtained (20.1 g, 59.5 mmol, 68%).

#### 3.4.2.2 Synthesis of Boc-L-Ac6-OH (MW=293.79):

The residue was dissolved in toluene (100 mL) and refluxed for 5 hours and checked by TLC (R<sub>f</sub> 0.8, CHCl<sub>3</sub>/MeOH=9/1) and toluene was evaporated and then was purified by silica gel chromatography(φ5.0 x 20 cm, 1% methanol/chloroform) to obtain 2-*tert*-butoxycarbonyl-6-chloro-hexanoic acid ethyl ester (15.6 g, 53.1 mmol, 89%, HPLC: r.t. 5:30 min, B: 0-100%). Finally Boc-DL-Ac6-OEt (15.6 g, 53.1 mmol) was subjected to the action of subtilisin (40 mg) Carlsberg from *Bacillus licheniformis* (Sigma) in a mixture of DMF (40 mL) and H<sub>2</sub>O (100 mL) at pH 7, 37 °C for 4 hours. The aqueous solution was extracted with ethyl acetate at pH 3 to obtained 2-*tert*-butoxycarbonyl-6-chloro-hexanoic acid (Boc-L-Ac6-OH) was isolated as colorless oil (10.8 g, 40.6 mmol, 76%, HPLC: r.t. 5.97 min, B: 0-100%).

### 3.6 References

- [1] Kao, H. Y., Downes, M., Ordentlich, P., and Evans, R. M., *Genes Dev.* 2002, 14: 55-66.
- [2] Yoshida, M.; Matsuayama, A.; Komatsu, Y.; Nishino, N. *Curr. Med. Chem.* 2003, 10: 2351–2358.
- [3] Chen, L., Fischle, W., Verdin, E., and Greene, W. C. *Science*, 2001, 293: 1653–1657.
- [4] Yuan, Z. L., Guan, Y. J., Chatterjee, D., and Chin, Y. E. *Science*, 2005, 307: 269–273.
- [5] Ito, A., Kawaguchi, Y., Lai, C. H., Kovacs, J. J., Higashimoto, Y., Appella, E., and Yao, T. P. *EMBO J.* 2002, 21: 6236–6245.
- [6] Glozak, M. A., Sengupta, N., Zhang, X., and Seto, E. *Gene (Amst.)*, 2005, 363: 15–23.
- [7] Michael S. Finnin, Jill R. Donigian, Alona Cohen, Victoria M. Richon, Richard A. Rifkind, Paul A. Marks, Ronald Breslow Nikola P. Pavletich, *Nature*, 1999, 401(9): 188-193.

- [8] Matthew J. Bottomley<sup>1</sup>, Paola Lo Surdo<sup>1</sup>, Paolo Di Giovine, Agostino Cirillo, Rita Scarpelli, Federica Ferrigno, Philip Jones, Petra Neddermann, Raffaele De Francesco, Christian Steinkühler, Paola Gallinari, and Andrea Carfi<sup>1</sup>, *The Journal of Biological Chemistry*, 2008, 283(39): 26694–26704.
- [9] Anja Schuetz, Jinrong Min, Abdellah Allali-Hassani, Matthieu Schapira, Michael Shuen, Peter Loppnau, Ralph Mazitschek, Nick P. Kwiatkowski, Timothy A. Lewis, Rebecca L. Maglathin, Thomas H. McLean, Alexey Bochkarev, Alexander N. Plotnikov, Masoud Vedadi, and Cheryl H. Arrowsmith, *The Journal of Biological Chemistry*, 2008, 283(17): 11355–11363.
- [10] Strecker, A. *Ann. Chem. Pharm.* 1850, 75: 27.
- [11] Haruro Ishitani, Susumu Komiyama, Yoshiki Hasegawa, and Shuji Kobayashi, *J. Am. Chem. Soc.* 2000, 122: 762-766.
- [12] Shuji Masumoto, Hiroyuki Usuda, Masato Suzuki, Motomu Kanai, and Masakatsu Shibasaki, *J. Am. Chem. Soc.* 2003, 125: 5634-5635.
- [13] Jeffrey T. Kuethe, Donald R. Gauthier, Jr., Gregory L. Beutner, and Nobuyoshi Yasuda, *J. Org. Chem.* 2007, 72: 7469-7472.

## Chapter 4

# Molecular Design of Cyclic Tetrapeptide HDAC Inhibitors by Replacement of Aib in Chlamydocin Framework

### 4.1 Introduction

Deregulation of HAT and HDAC has been implicated in the formation and development of certain human cancers by changing the expression pattern of various genes. It is therefore proposed that HDACs are a potential target for the development of anticancer agent. As a result, design and synthesis of novel HDAC inhibitors is a promising field for research. The search for compounds with antitumor activities to develop novel HDAC inhibitors with potency and safety has been still going on. Recently, scientists have been reported HDAC inhibitors as naturally occurring HDAC inhibitors, Trichostatin A (TSA),<sup>[1]</sup> depsipeptide FK228,<sup>[2-4]</sup> Chlamydocin,<sup>[5]</sup> Trapoxin,<sup>[6]</sup> Cyl-1,<sup>[7]</sup> Cyl-2,<sup>[8]</sup> HC-toxins,<sup>[9]</sup> Apicidin.<sup>[10,11]</sup> Synthetic TSA-related, SAHA-related,<sup>[12-14]</sup> CHAPs,<sup>[15,16]</sup> SCOPs,<sup>[17]</sup> and Chlamydocin analogs with various binding functional groups<sup>[18,19]</sup> inhibitors have been also reported. All these inhibitors exhibit the inhibitory activity for zinc-dependent HDAC classes I and II. Several of these HDAC inhibitors inhibit tumor growth and many of them are under clinical trials. Base on X-ray crystallography, inhibition model of HDLP is proposed and it consists of three domains: a zinc binding site; a surface recognition with capping group; a linker connecting the zinc binding and surface recognition.<sup>[20]</sup> It is plausible that the active site and linker unit are essential but only bind to the pocket in enzyme, a capping site covering the rim surrounding binding pocket determine the selectivity of HDAC inhibitors. As the rim of the opening to the binding pocket has less homology between HDAC isoforms at the active site, the modification of cap group allows having a significant impact upon isoform selectivity.<sup>[21]</sup> The surface of the HDAC enzymes that surrounds the binding pocket has multiple grooves,<sup>[22]</sup> which could be exploited by inhibitors with appropriate cap groups to improve potency and selectivity of inhibitors. Modification of the cap group of HDAC inhibitors can lead to increase significantly the selectivity aim at HDAC isoforms.<sup>[23]</sup>

In this Chapter of thesis, based on naturally occurring HDAC inhibitors, trichostatin A (TSA) and Chlamydocin, we designed and synthesized a series of HDAC inhibitors bearing surface



recognition of Chlamydocin framework and zinc binding site of TSA. Chlamydocin is a cyclic tetrapeptide containing an epoxyketone moiety in the side chain so that it is an irreversible inhibitor of HDAC. Author replaced the epoxyketone moiety of Chlamydocin with hydroxamic acid to design potent and reversible inhibitors of HDAC. In addition, a series of methyl-amino-cyclohexane-carboxylic acids (*A<sub>n</sub>mc6c*) were introduced instead of the amino-isobutyric acid (Aib) for a variety of Chlamydocin analogues (**Fig. 4.1**). The replacement of Aib residue of Chlamydocin with an aliphatic ring (*A<sub>n</sub>mc6c*) enhanced the *in vivo* and *in vitro* inhibitory activity. These compounds were tested for HDAC inhibitory activity and the results showed that they were potent inhibitors of HDACs. We also tested for antiproliferative *in vitro* by MTT assay against MCF-7 (human breast cancer), Hela (human cervix cancer), K-562 (human leukemia) and 7721 (human liver cancer) cell lines. All compounds exhibited nanomolar

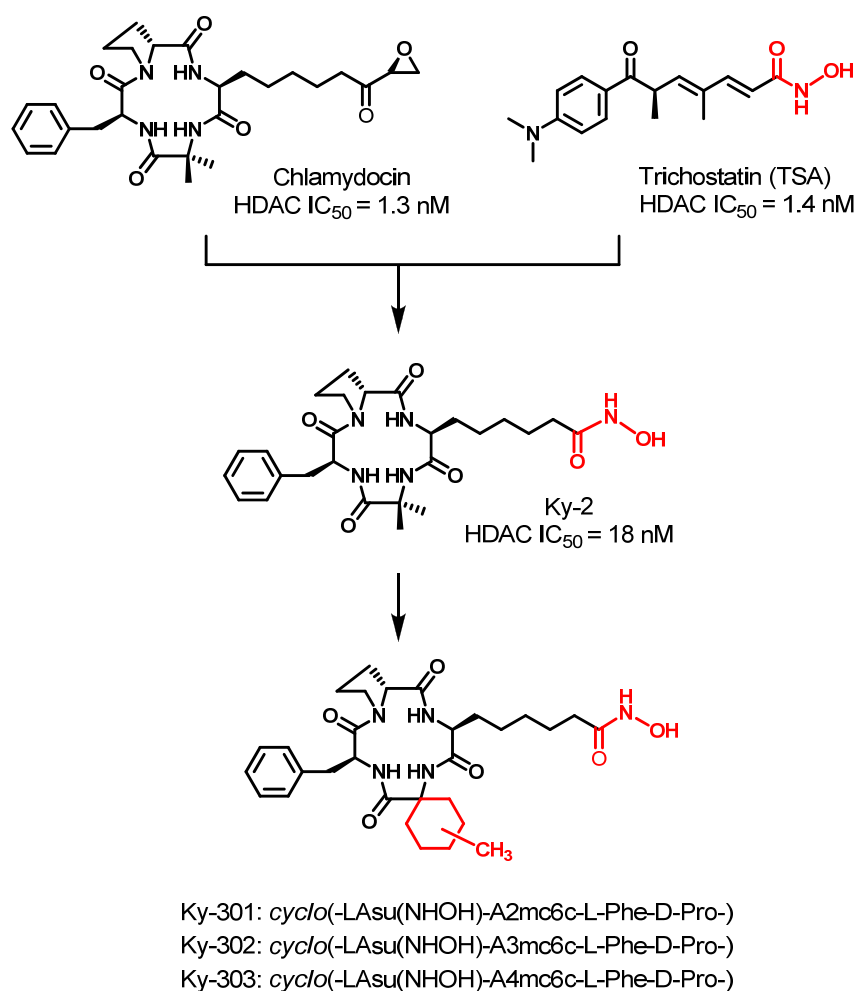


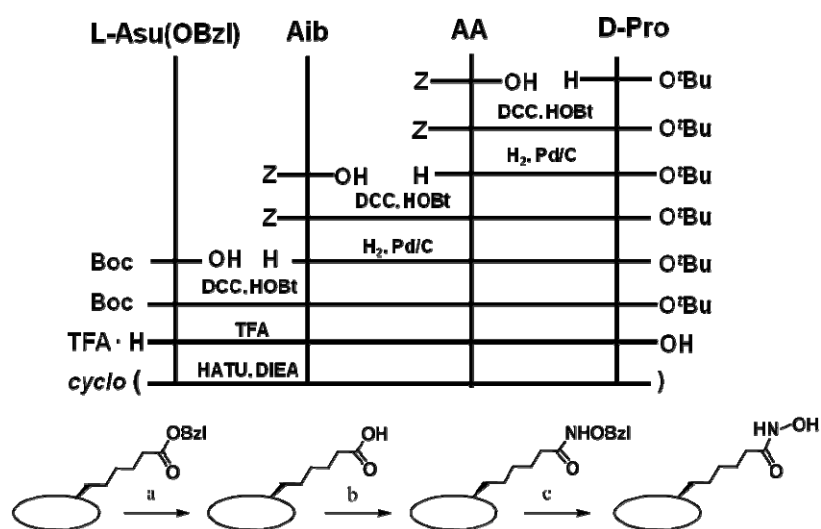
**Fig. 4.1** Design and synthesis Chlamydocin–hydroxamic acid analogues.

concentration antitumor activities. We have carried out circular dichroism and molecular docking studies on Chlamydocin–hydroxamic acid analogue and HDLP, HDAC8 and HDAH, respectively.

## 4.2 Results and discussion

### 4.2.1 Chemistry

Herein we synthesized potent HDAC inhibitors based on the natural product Chlamydocin and TSA. Author proposed to synthesize Chlamydocin–hydroxamic acid analogue for replacing the epoxyketone moiety of Chlamydocin by hydroxamic acid of TSA as the zinc binding group, Ky-2 was synthesized. we prepared non-natural amino acids (methyl-amino-cyclohexane-carboxylic acids (*A<sub>n</sub>mc6c*)) described in 3.3 of Chapter 3 to replace Aib residue at 2-position of Ky-2. For this, we initially synthesized Chlamydocin–hydroxamic acid analogue using solution-phase peptide coupling method as show in **Scheme 4.1**. *tert*-Butyl protected D-Pro was coupled with Z-L-Phe to give the dipeptide Z-L-Phe-D-Pro-O<sup>t</sup>Bu. The Z group of dipeptide was deprotected by catalytic hydrogenation and coupled with Z-Aib using DCC/HOBt orderly. The Z group of the resulted tripeptide Z-*A<sub>n</sub>mc6c*-L-Phe-D-Pro-O<sup>t</sup>Bu was deprotected by catalytic hydrogenation. It was then coupled with Boc protected amino suberic acid benzyl ester (Boc-L-Asu(OBzl)) to give linear tetrapeptide Boc-L-Asu(OBzl)-*A<sub>n</sub>mc6c*-L-Phe-D-Pro-O<sup>t</sup>Bu.



**Scheme 4.1** Synthetic strategy of Chlamydocin–hydroxamic acid analogue.

Reagents: (a) H<sub>2</sub>, Pd/C, MeOH; (b) HCl·NH<sub>2</sub>-OBzl, DCC/HOBt, DMF; (c) Pd-BaSO<sub>4</sub>, CH<sub>3</sub>COOH. AA: A<sub>2</sub>mc6c, A<sub>3</sub>mc6c, A<sub>4</sub>mc6c.

The C-terminal and N-terminal protections of the tetrapeptide were removed by treatment with trifluoroacetic acid (TFA) and the resulted linear peptide was cyclized in DMF under high dilution condition using HATU as a coupling reagent to give *cyclo(-L-Asu(OBzl)-Anmc6c-L-Phe-D-Pro-)* in 60~70% yield. The OBzl of side chain of cyclic peptide was deprotected by catalytic hydrogenation and then coupled with hydroxylamine hydrochloride and the resulted product was deprotected by catalytic hydrogenation to yield the desired compounds and finally purified using gel filtration. We replaced Aib residue with non-natural amino acids to study the effect on the HDACs inhibitory activity. All the synthesized compounds were characterized by <sup>1</sup>H NMR and high resolution FAB-MS (HR-FAB-MS). The purity of the compounds was determined by HPLC analysis and all the synthesized cyclic tetrapeptides showed purity above 97%.

#### 4.2.2 Enzyme inhibition and biological activity

We assayed these synthesized compounds for HDACs inhibitory activity using HDAC1, HDAC4 and HDAC6 enzymes prepared by 293T cells. In addition, to know the inhibitory activity of these compounds in cell based condition, we carried out p21 promoter assay. The results of HDAC inhibitory activity and the p21 promoter assay of compounds are shown in **Table 4.1**.

Inhibitory activity of Trichostatin A and Ky-2 are also shown in **Table 4.1** for comparison with synthesized compounds. These compounds showed good activity in both cell free and cell based conditions in nanomolar range. Further, these compounds were poorly inhibited by

**Table 4.1** HDAC inhibitory activity and p21 promoter assay data

No.	Compounds	HDAC inhibitory activities IC <sub>50</sub> (nM)			p21 promoter activity EC <sub>1000</sub> (nM)
		HDAC1	HDAC4	HDAC6	
	Trichostatin A	23	34	65	20.0
Ky-2	<i>cyclo(-L-Asu(NHOH)-Aib-L-Phe-D-Pro-)</i>	18	17	230	18.0
Ky-301	<i>cyclo(-L-Asu(NHOH)-A2mc6c-L-Phe-D-Pro-)</i>	10	6.4	130	8.0
Ky-302	<i>cyclo(-L-Asu(NHOH)-A3mc6c-L-Phe-D-Pro-)</i>	15	14	160	2.9
Ky-303	<i>cyclo(-L-Asu(NHOH)-A4mc6c-L-Phe-D-Pro-)</i>	11	12	170	4.3

HDAC6 compared to HDAC1 and HDAC4 and their selectivity was 10 times better (HDAC6/HDAC1 = 10). In the cellular activity, compound Ky-302 showed the best activity than Ky-301 and Ky-303, which 6-fold increased than Ky-2 and Trichostatin A. All of the cyclic tetrapeptides were excellent in p21 promoter-inducing activity. This was probably because of the presence of an aliphatic ring (Ac6c) of hydrophobicity which increased interacts with the rim of HDACs active pocket. Also cell permeability was enhanced in this case, which was reflected in their p21 activity data. The variation of HPLC retention time, which can be used as a parameter for hydrophobicity, could be correlated with p21 promoter-inducing activity.

#### 4.2.3 Cell growth inhibitory assay

The compounds were tested for antiproliferative *in vitro* by MTT assay against MCF-7 (human breast cancer), HeLa (human cervix cancer), 7721 (human liver cancer) and K-562 (human leukemia) cell lines. Three HDAC inhibitors were added to culture medium at the concentrations of 20, 40, 60, 80, 100 nM. The IC<sub>50</sub> was shown in **Table 4.2**. All compounds showed good antitumor activities, which inhibited cell proliferation at nanomolar concentration. All these three compounds had selectivity for the four human cancer cell lines, further, showed better sensitivity on MCF-7 than the other cell lines. The compound Ky-302 showed a stronger activity than the other two for HeLa and K-562 cell lines. The result coincided with the data from p21 promoter assay activity experiment.

**Table 4.2** Cell growth inhibitory assay data

Compounds	IC <sub>50</sub> (μM)			
	HeLa	MCF-7	7721	K-562
Ky-301	0.295	0.030	0.213	> 3.5
Ky-302	0.048	0.026	0.297	0.044
Ky-303	0.232	0.043	0.262	> 3.5

#### 4.2.4 Morphological reversion

The inhibitors were found to induce dramatic changes in cellular shape under light microscopy. After the MCF-7 cell and 7721 cell were treated by the synthesized compounds with concentration of 100 nM for 24 hours, which were supposed to be changed into flattened, rounded and spindle shapes, and the cellular borders became obviously bigger and gaps among cells (Fig. 4.2).

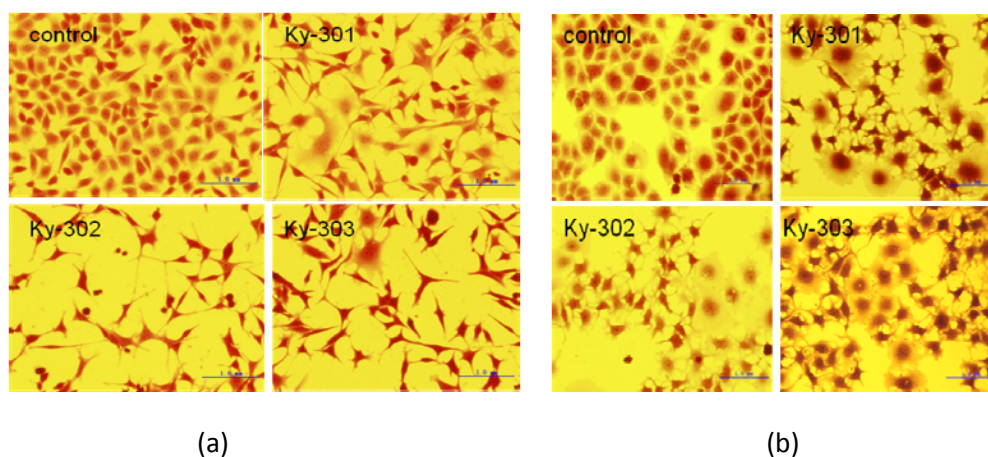


Fig. 4.2 Morphological reversion of (a) MCF-7 and (b)7721 cell lines ( $\times 400$ ).

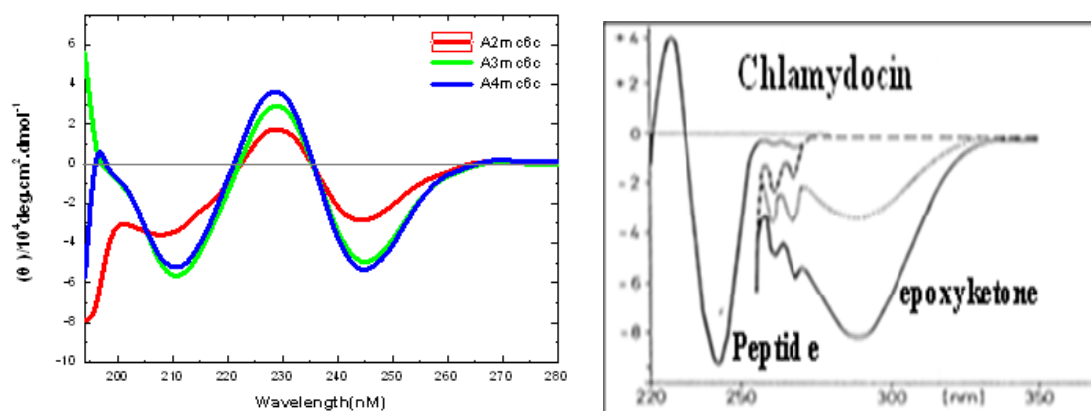
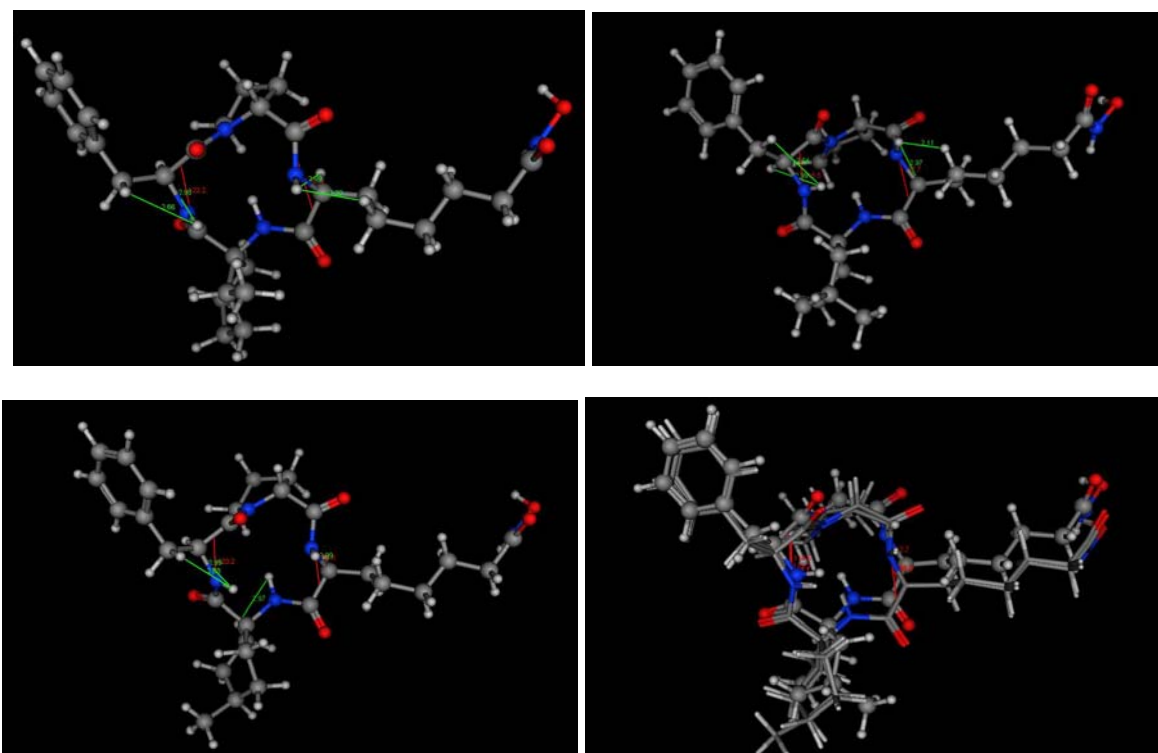


Fig. 4.3 CD spectra of cyclic tetrapeptides.

#### 4.2.5 Conformational studies by CD and NMR

We carried out circular dichroism (CD) spectrum study of compounds Ky-301, Ky-302 and Ky-303, in solvent of 0.1 mM methanol (**Fig. 4.3**). The CD spectrum of three compounds were similar to Chlamydocin and Ky-2's (*cyclo*(-L-Asu(NHOH)- Aib-L-Phe-D-Pro-) up to 260 nm.<sup>[19]</sup> Three compounds showed two negative ellipticity at 210 nm and 245 nm regions, a positive ellipticity at 230 nm regions with small but reproducible difference. This fact showed that three compounds have similar conformations with Ky-2's.

We have carried out NMR ( $\text{CDCl}_3$ ) studies for conformation of these inhibitors by MOE calculations (**Fig. 4.4**). Solution conformations of Ky-301, Ky-302 and Ky-303 were studied by using  $^1\text{H}$  NMR in  $\text{CDCl}_3$ . Complete assignments were made by using COSY and NOESY spectra. The  $J_{\text{NH-HC}\alpha}$  values were obtained from NMR charts and by that we estimated dihedral angle " $\theta$ ," using the Karplus graph. Dihedral angles  $\theta$  and  $\varphi$ , and NOE data are shown in **Table 4.3**. The energy-minimized structures of three compounds were calculated by MOE. The structure of Ky-302 is a little different from other two compounds at zinc binding group.



**Fig. 4.4** MOE of energy-minimized structures of compounds by NMR calculation. NOE ( $\text{\AA}$ ) (green line), Dihedral angle ( $\varphi$ ) (red line). Ky-301(top left), Ky-302(top right), Ky-303(below left) and Superimposition of three compounds (below right). Ky-301 and Ky-303(stick), Ky-302(ball and stick)

**Table 4.3** NOE, coupling constant and dihedral angles data of compounds from NMR.

AA	Ky-301				Ky-302				Ky-303			
	NOE	$J_{\text{NH-HC}\alpha}$ (Hz)	$\theta^\circ$	$\varphi^\circ$	NOE	$J_{\text{NH-HC}\alpha}$ (Hz)	$\theta^\circ$	$\varphi^\circ$	NOE	$J_{\text{NH-HC}\alpha}$ (Hz)	$\theta^\circ$	$\varphi^\circ$
L-Asu	L-Asu (NH-HC $\alpha$ ) (NH-HC $\beta$ )	7.2	148	-152	L-Asu (NH-HC $\alpha$ ) (NH-HC $\beta$ )	9.2	170	-130	L-Asu (NH-HC $\alpha$ )	6.8	142	-158
A4mc6c	--	--	--	--	--	--	--	--	A4mc6c (NH-HC $\beta$ )	--	--	--
L-Phe	L-Phe (NH-HC $\alpha$ ) (NH-HC $\beta$ )	10	180	-120	L-Phe (NH-HC $\alpha$ ) (NH-HC $\beta$ )	10	180	-120	L-Phe (NH-HC $\alpha$ ) (NH-HC $\beta$ )	10	180	-120
D-Pro	--	--	--	--	--	--	--	--	--	--	--	--

#### 4.2.6 Docking and molecular dynamics simulation for HDAC inhibitors towards HDACs

To understand the binding modes between these cyclic tetrapeptides and different HDACs, docking studies were conducted with AutoDock 4.0 program.<sup>[24,25]</sup> AutoDock docking protocol and scoring function have been successfully applied in the study of interpretation of the inhibitory activity of several HDAC ligands.<sup>[26,27]</sup> Three enzymes, a bacterial HDAC-like protein (HDLP) resembling a class I enzyme,<sup>[28]</sup> shows a 35.2% sequence identity to human HDAC1, a bacterial HDAC-like amidohydrolase (HDAH),<sup>[29]</sup> which has high sequential and functional homology to human class II HDACs and HDAC8<sup>[30]</sup> were used. The active site of HDAC protein was covered by a grid box size of 70×70×70 points with a spacing of 0.375 Å between the grid points. For cyclic tetrapeptides, all single bonds except the amide bonds and cyclic bonds were treated as active torsional bonds. For each inhibitor, one hundred and fifty independent dockings, i.e. 150 runs, were performed using genetic algorithm searches. A maximum number of 250 000 000 energy evaluations and a maximum number of 5000 generations were implemented during each genetic algorithm run. A mutation rate of 0.02 and a crossover rate of 0.8 were used. The crossover mode was arithmetic. Default nonbonded zinc parameters in AutoDock 4.0 were employed. Results differing by less than 2.0 Å in positional root-mean-square deviation (RMSD) were clustered together and represented by the result with the most favorable free energy of binding. The RMSD value is an all heavy atom

comparison between the docked structure and the initial structure. The LigPlot program<sup>[31]</sup> was also employed to analyze the docking results focusing on hydrogen bonds and hydrophobic interactions.

As expected, the results showed that three compounds (Ky-301, Ky-302 and Ky-303) bound to the active site of HDAC8 (**Fig. 4.5**), HDLP (**Fig. 4.6**) and HDAH (**Fig. 4.7**), the aliphatic chain was occupying the long, narrow channel, hydroxamic group was at the bottom of this channel, and the large cap domain interacted with external surface of these enzymes. And all compounds shared similar interaction mode with three enzymes. **Fig. 4.8** shows superimposition of three compounds in surfaces of the active site regions with HDAC8, HDLP and HDAH, respectively. In HDLP-inhibitors complexes, the aromatic ring of Phe and aliphatic ring of Anmc6c are bent to Try194 and Phe139, respectively. But, in HDAH-inhibitors complexes, the aromatic ring is vertical to Phe206. This study further supports the fact that, compared to class IIb HDAC, the inhibitors are favorable interactions with the surface binding to class I HDACs, hence showed high activity.

For each enzyme, one enzyme-inhibitor complex was chosen to analyze the hydrogen bonds and hydrophobic interactions between HDACs and cyclic tetrapeptides (**Fig. 4.9**, **Fig. 4.10** and **Fig. 4.11**). It showed that the hydroxy oxygen of tetrapeptide coordinated to zinc ion, it was the precondition of these HDAC inhibitors for their inhibitory activities. These compounds established hydrophobic interactions with some amino acid residues, such as Phe139, Lys222, Lys265, Phe196, Gln190, Ala195 of HDLP, Ile98, Phe150, Pro208, Asp98 of HDAH and Phe187, Gly186, Tyr80, Met254 of HDAC8, the hydrophobic effects were also crucial for stabilizing the complexes.

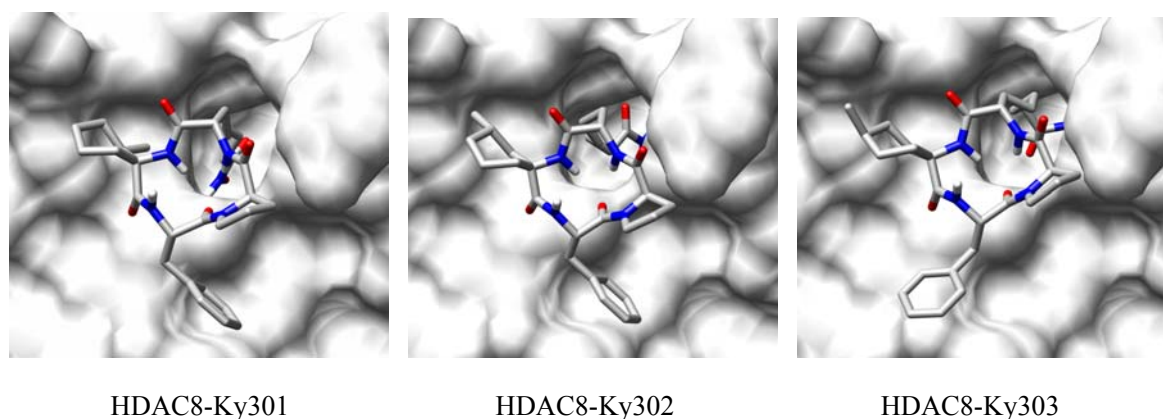
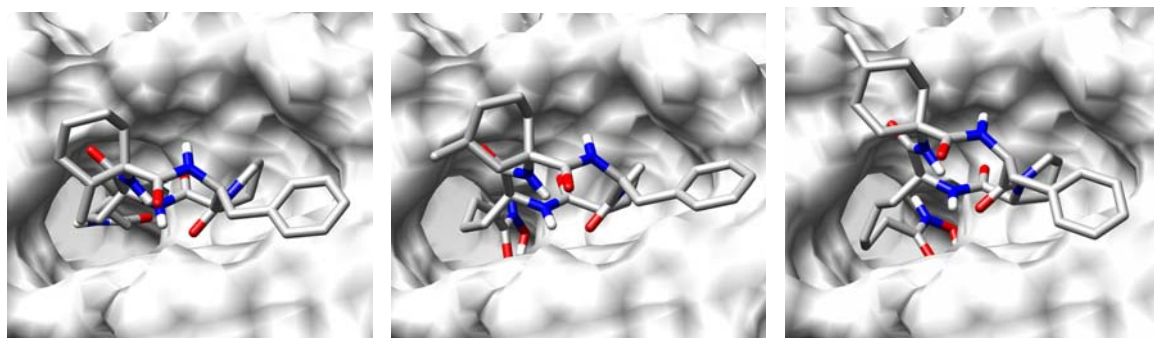


**Fig. 4.5** Top view of the surfaces of the active site regions of HDAC8-inhibitors complexes for docking.



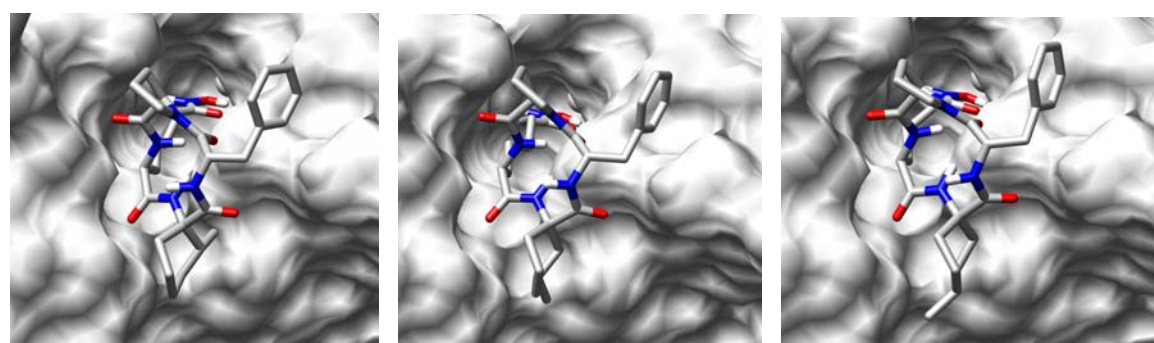


HDLP-Ky301

HDLP-Ky302

HDLP-Ky303

**Fig. 4.6** Top view of the surfaces of the active site regions of HDLP-inhibitors complexes for docking.

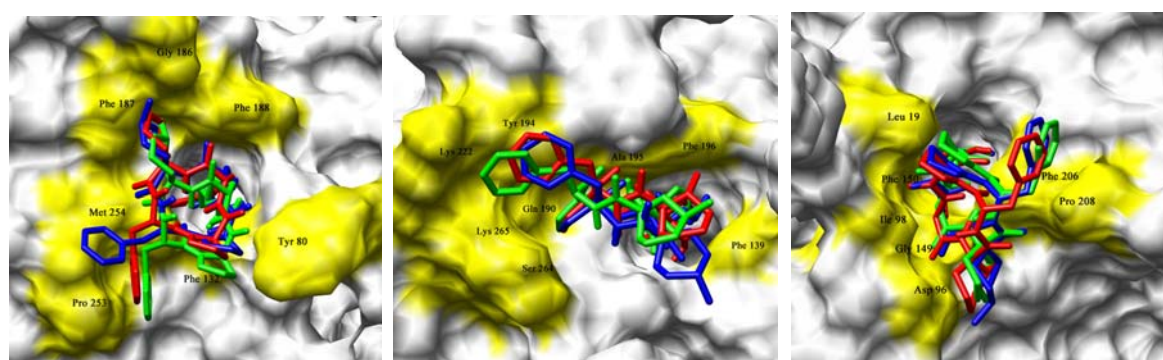


HDAH-Ky301

HDAH-Ky302

HDAH-Ky303

**Fig. 4.7** Top view of the surfaces of the active site regions of HDAH-inhibitors complexes for docking.



HDAC8-inhibitors complex

HDLP-inhibitors complex

HDAH-inhibitors complex

**Fig. 4.8** Superimposition in surfaces of the active site regions.

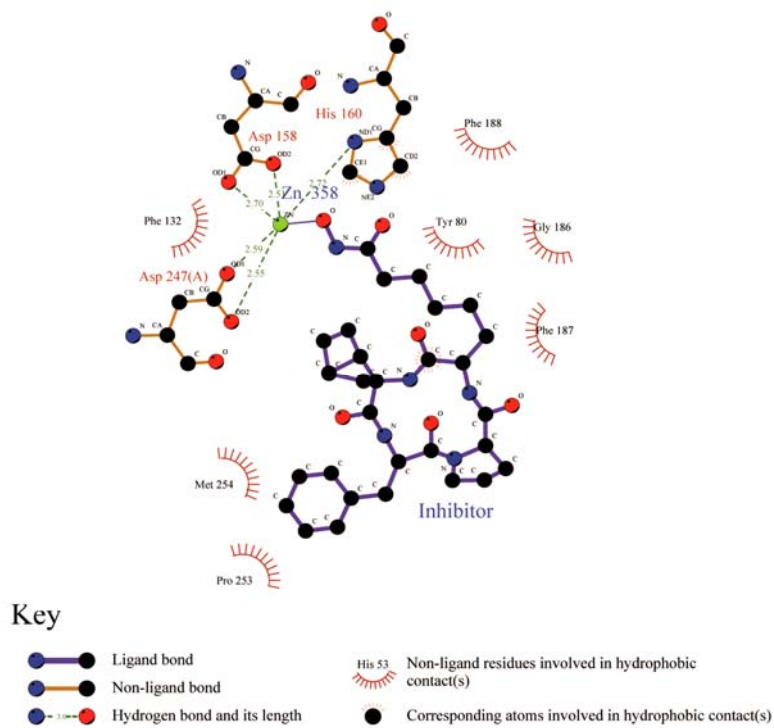


**Fig. 4.9** Hydrophobic interactions and hydrogen bonds at binding site of HDAC8-Ky301 complex.

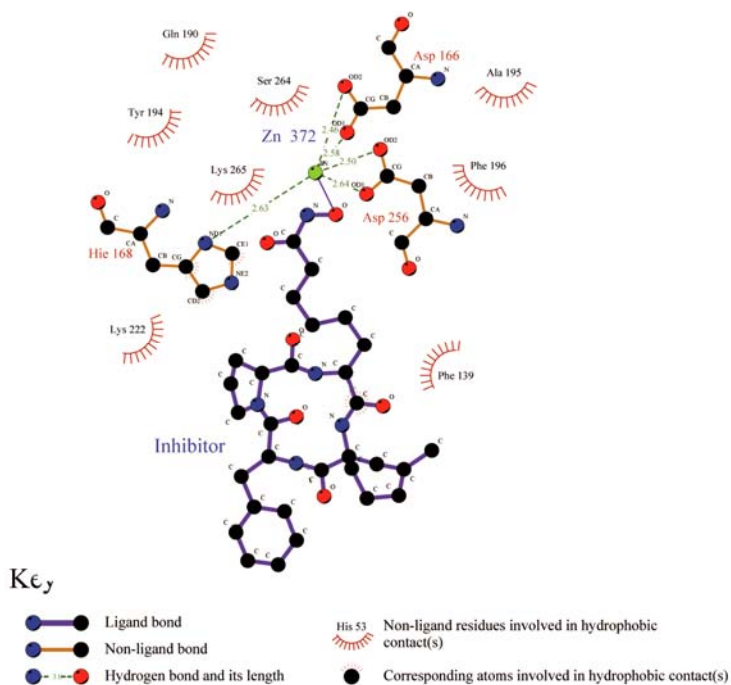


**Fig. 4.10** Hydrophobic interactions and hydrogen bonds at binding site HDLP-Ky302 complex.

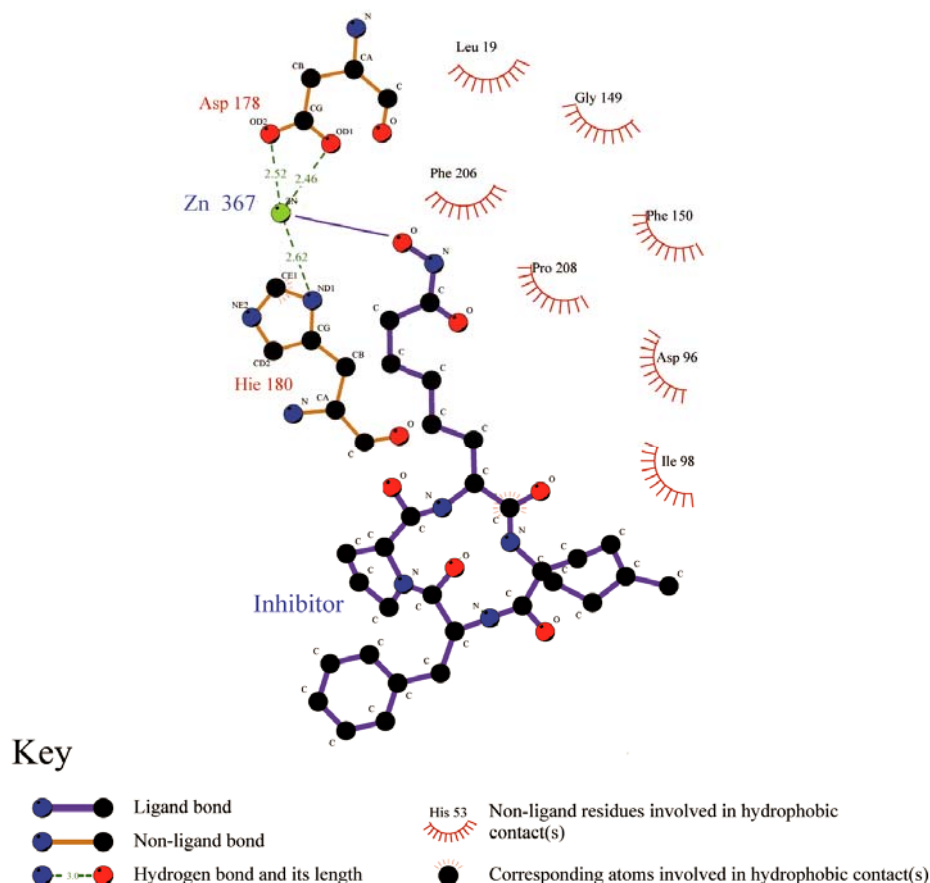


**Fig. 4.11** Hydrophobic interactions and hydrogen bonds at binding site HDAH-Ky303 complex.

In the HDAC8-Ky301 complex, the zinc ion that lay at the end of the hydrophobic tunnel was bound to two carboxylate oxygens of Asp158, Asp 247, respectively and the nitrogen atom of His160, the other two coordination sites were occupied by the carbonyl and hydroxyl oxygens of the hydroxamate of zinc binding group of Ky-301. The average distances between zinc and the nearby atoms during the last 500 ps in current MD simulations are shown in **Table 4.4**. The calculational result of HDLP-Ky302 complex showed that zinc coordinates with seven atoms, including two carboxylate oxygens of Asp166 and Asp256, respectively, a nitrogen atom of His168, and carbonyl and hydroxyl oxygens of the hydroxamate of zinc binding group of Ky-302. However, in HDAH–Ky303 complex, the zinc ion was bound to only two carboxylate oxygens of Asp178, a nitrogen atom of His180 and hydroxyl oxygens of zinc binding group of Ky-302. The results showed that the stability of HDAC8-Ky301 and HDLP-Ky302 complexes are stronger than HDAH–Ky303 complex. In the HDAC8-Ky301 complex and HDLP-Ky302 complex, the

inhibitor bound to zinc atom in heptahedron geometry. But, in HDAH –Ky303 complex, it is in pentahedron geometry. The results showed that the stability for inhibitors binding to classI HDACs are stronger than classIIb HDAC.

**Table 4.4** Average zinc coordination distances for compounds with enzymes in the MD simulations.

Complex	Atom1	Atom 2	Distance (Å)
HDAC8 – Ky301	Zn <sup>2+</sup>	Ky-301:OH	1.76
		Ky-301:CO	2.45
		Asp 158:OD1	2.70
		Asp 158:OD2	2.53
		Asp 247:OD1	2.59
		Asp 247:OD2	2.55
		His 160:ND1	2.72
HDLP – Ky302	Zn <sup>2+</sup>	Ky-302:OH	1.88
		Ky-302:CO	2.66
		Asp 166:OD1	2.58
		Asp 166:OD2	2.46
		Asp 256:OD1	2.64
		Asp 256:OD2	2.50
		His 168:ND1	2.63
HDAH –Ky303	Zn <sup>2+</sup>	Ky-303:OH	1.93
		Ky-303:CO	3.11
		Asp 178:OD1	2.46
		Asp 178:OD2	2.52
		His 180:ND1	2.62

### 4.3 Summary

We have successfully synthesized several Chlamydocin–hydroxamic acid analogues as HDAC inhibitors. We replaced Aib in 2-position of the Chlamydocin framework by several non-natural amino acid containing aliphatic rings with different methyl substitution position. HDAC inhibitory activity of inhibitors was evaluated *in vitro* and *in vivo* and it was found that the inhibitors were excellent potent toward HDAC enzymes within nanomolar range. The results indicated that append aliphatic ring of Chlamydocin can increase the inhibitory activity of HDACs.

### 4.4 Experimental

**General:** Unless otherwise noted, all solvents and reagents were reagent grade and used without purification. All compounds were routinely checked by thin layer chromatography (TLC) or high performance liquid chromatography (HPLC). Analytical HPLC were performed on a Hitachi instrument equipped with a chromolith performance RP-18e column (4.6 × 100 mm, Merck). The mobile phases used were A: H<sub>2</sub>O and 0.1% TFA, B: CH<sub>3</sub>CN with 0.1% TFA using a solvent gradient of A to B over 15 min with detection at 220 nm with a flow rate of 2 mL/min. TLC was performed on aluminium-backed silica gel plates (Merck DC-Alufohlen Kieselgel 60 F<sub>254</sub>) with spots visualized by UV light and heat. Flash chromatography was performed using silica gel 60 (230-400) eluting with solvents as indicated. Fast atom bombardment mass spectra (FAB-MS) and high resolution fast atom bombardment mass spectra (HR-FAB-MS) were measured on a JEOL JMS-SX 102A instrument. NMR spectra were recorded on a VarianINO VA400 MHz spectrometer. All NMR spectra were measured in CDCl<sub>3</sub> solutions with reference to TMS. All <sup>1</sup>H shifts are given in parts per millions (s = singlet; d = doublet; t = triplet; m = multiplet). Peptide were coupled using standard solution-phase chemistry with dicyclohexylcarbodiimide (DCC), N-Hydroxybenzotriazole (HOBt). Peptide cyclization was mediated by *N*-[(dimethylamino)-1*H*-1,2,3-triazolo[4,5-*b*]pyridin-1-yl-methylene]-*N*-methylmethanaminium hexafluorophosphate *N*-oxide (HATU). The cell lines for bioactive assay were all from Shanghai Institute of Biochemistry and Cell Biology, SIBS, CAS. The PRPMI 1640 for cell culture was purchased from Gibco, and MTT was from Hy-Clone.

#### 4.4.1 Synthesis of *cyclo*-(L-Asu(NHOH))-(±)A2mc6c-L-Phe-D-Pro-

##### 4.4.1.1 Synthesis of Z-(±)A2mc6c-OH (MW=291.34):

To a suspension of (±) 2-methyl-cyclohexanecarboxylic amino acid (1.57 g, 10.0 mmol) in acetone (10 mL) and water (10 mL) were added Z-Osu (2.7 g, 11.0 mmol) and Na<sub>2</sub>CO<sub>3</sub> (2.1 g, 20.0 mmol). After stirring for overnight, acetone was removed by evaporation; residue dissolved in ethyl acetate, and adjusted pH 2-3 with HCl, and then washed with brine. After drying over MgSO<sub>4</sub> and concentrating, product was purified by crystallization in ether and petroleum ether (1:9 v/v) to yield Z-(±)A2mc6c-OH (1.68 g, 5.8 mmol, 59%), HPLC: r.t. 5.94 min.

##### 4.4.1.2 Synthesis of Z-(±)A2mc6c-L-Phe-D-Pro-O<sup>t</sup>Bu (MW = 591.74):

The dipeptide was coupling in the same manner as 3.8.3 described to obtain H-L-Phe-D-Pro-O<sup>t</sup>Bu (1.05 g, 3.3 mmol). To a cooled solution of H- L-Phe-D-Pro-O<sup>t</sup>Bu (1.05 g, 3.3 mmol) and Z-(±)A2mc6c-OH (962 mg, 3.3 mmol) in DMF (6 mL) were successively added DCC (817 mg, 4.0 mmol), HOBt·H<sub>2</sub>O (506 mg, 5.0 mmol). After stirring for overnight, DMF was removed by evaporation; residue dissolved in ethyl acetate, and then successively washed with 10% citric acid solution, 4% sodium bicarbonate solution and brine. After drying over MgSO<sub>4</sub> and concentrating, the resulting oily substance was purified by silica gel chromatography using a mixture of chloroform and methanol (99:1 v/v) to obtain Z-(±) A2mc6c-L-Phe-D-Pro-O<sup>t</sup>Bu(1.24 g, 2.1 mmol, 63%). TLC: R<sub>f</sub>, 0.8 (CHCl<sub>3</sub>/MeOH=9/1). HPLC: double peaks 9.00 min, 42%; 9.34 min, 51%.

##### 4.4.1.3 Synthesis of Boc-L-Asu(OBzl))-(±)A2mc6c-L-Phe-D-Pro-O<sup>t</sup>Bu (MW =763.02 ):

The tripeptide Z-(±)A2mc6c-L-Phe-D-Pro-O<sup>t</sup>Bu(1.24 g, 2.1 mmol) was subjected to catalytic hydrogenation with Pd-C (105 mg) in acetic acid (4 mL). After overnight, the reaction was checked by TLC (CHCl<sub>3</sub>/MeOH/CH<sub>3</sub>COOH=90/10/2), the catalyst was filtered and reaction solution was removed by evaporation. The free amine was taken into ethyl acetate (30 mL) by the aid of 2M Na<sub>2</sub>CO<sub>3</sub> solution (10 mL). After dried over anhydrous Na<sub>2</sub>CO<sub>3</sub> ethyl acetate solution was evaporated to obtain H-(±)A2mc6c-L-Phe-D-Pro-O<sup>t</sup>Bu (868 mg, 1.9 mmol, 91%). To a cooled solution of H-(±)A2mc6c-L-Phe-D-Pro-O<sup>t</sup>Bu (868 mg, 1.9 mmol) and Boc-L-Asu(OBzl)-OH (721 mg, 1.9 mmol) in DMF (4 mL) were successively added DCC (470 mg, 2.3 mmol), HOBt·H<sub>2</sub>O (291 mg, 1.9 mmol). After stirring for overnight, DMF was

removed by evaporation; residue dissolved in ethyl acetate, and then successively washed with 10% citric acid solution, 4% sodium bicarbonate solution and brine. After drying over MgSO<sub>4</sub> and concentrating, the resulting oily substance was purified by silica gel chromatography using a mixture of chloroform and methanol (99:1 v/v) to obtain Boc-L-Asu(OBzl)-(±)A2mc6c-L-Phe-D-Pro-O<sup>t</sup>Bu (1.05 mg, 1.3 mmol, 69%). TLC: R<sub>f</sub>, 0.8 (CHCl<sub>3</sub>/MeOH=9/1). HPLC: double peaks r.t. 10.36 min, 28%; 10.74 min, 53%.

#### **4.4.1.4 *cyclo*(-L-Asu(OBzl)-(±)A2mc6c-L-Phe-D-Pro-) (MW = 644.80):**

The protected tetrapeptide Boc-L-Asu(OBzl)-(±)A2mc6c-L-Phe-D-Pro-O<sup>t</sup>Bu (1.05 mg, 1.3 mmol) was dissolved in TFA (4 mL) at 0 °C and kept for 3 hours. After evaporation of TFA, the residue was solidified using ether and petroleum ether to yield TFA salt of the linear tetrapeptide TFA·H-L-Asu(OBzl)-(±)A2mc6c-L-Phe-D-Pro-OH (800 mg, 1.2 mmol, 100%). To DMF (150 mL), TFA·H-L-Asu(OBzl)-A2mc6c-L-Phe-D-Pro-OH (800 mg, 1.2 mmol), HATU (685 mg, 1.8 mmol), and DIEA (0.53 mL, 3.0 mmol) were added in separate five portions in every 30 minutes with stirring at room temperature for the cyclization reaction. After completion of the reaction for 1 hour, DMF was evaporated under vacuum; the residue was dissolved in ethyl acetate and washed with 10% citric acid solution, 4% sodium bicarbonate solution and brine, respectively. It was then dried over anhydrous MgSO<sub>4</sub> and filtered. After evaporation of ethyl acetate, the residue was purified by silica gel chromatography using a mixture of chloroform and methanol (99:1v/v) to yield *cyclo*(-L-Asu(OBzl)-(±)A2mc6c-L-Phe-D-Pro-) (503 mg, 0.8 mmol, 65%). HPLC: double peaks r.t. 8.90 min, 29%; 9.22 min, 67%.

#### **4.4.1.5 *cyclo*(-L-Asu(NHOH)-(±)A2mc6c-L-Phe-D-Pro-) (MW=569.69):**

Compound *cyclo*(-L-Asu(OBzl)-(±)A2mc6c-L-Phe-D-Pro-) (503 mg, 0.8 mmol) was dissolved in methanol (3 mL) and Pd-C (40 mg) was added. The mixture was stirred under H<sub>2</sub> for 4 hours. After filtration of Pd-C, methanol was evaporated to yield *cyclo*(-L-Asu-A2mc6c-L-Phe-D-Pro-) (432 mg, 0.8 mmol, 100%). The product was dissolved in DMF (3 mL) at 0 °C, and O-Benzylhydroxylamine hydrochloride (HCl·NH<sub>2</sub>-OBzl)(187 mg, 1.2 mmol), HOBt·H<sub>2</sub>O (119 mg, 0.8 mmol), triethylamine (0.17 mL, 1.2 mmol) and DCC (241 mg, 1.2 mmol) were added. The mixture was stirred for overnight. After completion of the reaction, DMF was evaporated under vacuum; the residue was dissolved in ethyl acetate and washed with 10% citric acid solution, 4% sodium bicarbonate solution and brine, respectively. It was then dried over

anhydrous MgSO<sub>4</sub> and filtered. After evaporation of ethyl acetate, *cyclo(-L-Asu(NHOBzl)-(-±)A2mc6c-L-Phe-D-Pro-)* (403 mg, 0.6 mmol, 78% ) was obtained. The product *cyclo(-L-Asu(NHOBzl)-(-±)A2mc6c-L-Phe-D-Pro-)* (403 mg, 0.6 mmol) was dissolved in acetic acid (6 mL) and Pd-BaSO<sub>4</sub> (200 mg) was added. The mixture was stirred under H<sub>2</sub> for 24 hours. After filtration of Pd-BaSO<sub>4</sub>, acetic acid was evaporated and crystallized with ether to yield *cyclo(-L-Asu(NHOH)-(-±)A2mc6c-L-Phe-D-Pro-)* (259 mg, 0.4 mmol, 76%). TLC: R<sub>f</sub> 0.62 (CHCl<sub>3</sub>/ MeOH/CH<sub>3</sub>COOH=90/10/2). HPLC: double peaks r.t. 6.98 min, 42%; 7.36 min, 49%. HR-FAB-MS [M+H]<sup>+</sup> 570.3306 for C<sub>30</sub>H<sub>43</sub>N<sub>5</sub>O<sub>6</sub> (calcd 569.3213). <sup>1</sup>H NMR(400 MHz, CDCl<sub>3</sub>): δ<sub>H</sub> (ppm): 0.78(d, J=7.2 Hz, 3H), 1.05(d, J=6 Hz, 1H), 1.24-1.40(m, 8H), 1.60-1.86(m, 9H), 2.04(s, 1H), 2.14(s, 2H), 2.29(d, J=7.2 Hz, 1H), 3.19(m, 1H), 3.24(m, 1H), 3.47(s, 1H), 3.50(m, 1H), 3.84(m, 1H), 3.98(m, 1H), 4.32(m, 1H), 4.73(m, 1H), 5.20(t, J=9.2, 8.0 Hz, 1H), 6.41(s, 1H), 6.46(s, 1H), 7.18(d, J=7.2 Hz, 1H), 7.20-7.28(m, 5H), 7.53(d, J=10, 1H). <sup>13</sup>C NMR (400 MHz , CDCl<sub>3</sub>) δ<sub>C</sub> (ppm): 14.21, 18.68, 21.05, 24.57, 24.86, 25.07, 25.13, 27.28, 27.41, 28.77, 29.32, 32.76, 36.07, 46.98, 52.88, 53.22, 54.91, 57.97, 65.04, 65.83, 125.85, 128.74, 128.74, 129.23, 129.26, 137.09, 171.36, 173.26, 175.22, 175.86.

#### 4.4.2 Synthesis of *cyclo(-L-Asu(NHOH)-L-A3mc6c-L-Phe-D-Pro-)*

##### 4.4.2.1 Synthesis of Z-L-A3mc6c-OH (MW=291.34):

To a suspension of 3-methyl-cyclohexanecarboxylic amino acid (1.2 g, 7.7 mmol) in acetone (8 mL) and water (8 mL) were added Z-Osu (2.1 g, 8.5 mmol) and Na<sub>2</sub>CO<sub>3</sub> (1.6 g, 15.4 mmol). After stirring for overnight, acetone was removed by evaporation; residue dissolved in ethyl acetate, and adjusted pH 2-3 with citric acid solution, and then washed with saturated saline. After drying over MgSO<sub>4</sub> and concentrating, product was purified by crystallization in ether and petroleum ether (1:2 v/v) to yield (2.2 g, 6.0 mmol, 78%), HPLC: r.t. 5.83 min.

##### 4.4.2.2 Synthesis of Z-L-A3mc6c-L-Phe-D-Pro-O<sup>t</sup>Bu (MW = 591.74):

The dipeptide was coupling in the same manner as 3.8.3 described to obtain H-L-Phe-D-Pro-O<sup>t</sup>Bu(1.0 g, 3.0 mmol). To a cooled solution of H- L-Phe-D-Pro-O<sup>t</sup>Bu (1.0 g, 3.0 mmol) and Z-L-A3mc6c-OH (870 mg, 3.0 mmol) in DMF (6 mL) were successively added DCC (790 mg, 3.6 mmol), HOBt·H<sub>2</sub>O (460 mg, 3.0 mmol). After stirring for overnight, DMF was removed by evaporation; residue dissolved in ethyl acetate, and then successively washed with 10% citric acid solution, 4% sodium bicarbonate solution and brine. After drying over



MgSO<sub>4</sub> and concentrating, the resulting oily substance was purified by silica gel chromatography using a mixture of chloroform and methanol (99:1 v/v) to obtain Z-A3mc6c-L-Phe-D-Pro-O<sup>t</sup>Bu(1.32 g, 2.2 mmol, 74%). TLC: Rf 0.8 (CHCl<sub>3</sub>/MeOH=9/1). HPLC: r.t. 9.57 min, 90%.

#### 4.4.2.3 Synthesis of Boc-L-Asu(OBzl)-L-A3mc6c-L-Phe-D-Pro-O<sup>t</sup>Bu (MW =763.02):

The tripeptide Z-L-A3mc6c-L-Phe-D-Pro-O<sup>t</sup>Bu(1.32 g, 2.2 mmol) was subjected to catalytic hydrogenation with Pd-C (111 mg) in acetic acid (5 mL). After overnight, the reaction was checked by TLC (CHCl<sub>3</sub>/MeOH/CH<sub>3</sub>COOH=90/10/2), the catalyst was filtered and reaction solution was removed by evaporation. The free amine was taken into ethyl acetate (30 mL) by the aid of 2M Na<sub>2</sub>CO<sub>3</sub> solution (10 mL). After dried over anhydrous Na<sub>2</sub>CO<sub>3</sub> ethyl acetate solution was evaporated to obtain H-L-A3mc6c-L-Phe-D-Pro-O<sup>t</sup>Bu (917 mg, 2.0 mmol, 91%). To a cooled solution of H-L-A3mc6c-L-Phe-D-Pro-O<sup>t</sup>Bu (917 mg, 2.0 mmol) and Boc-L-Asu(OBzl)-OH (757 mg, 2.0 mmol) in DMF (4 mL) were successively added DCC (495 mg, 2.4 mmol), HOBt·H<sub>2</sub>O (306 mg, 2.0 mmol). After stirring for overnight, DMF was removed by evaporation; residue dissolved in ethyl acetate, and then successively washed with 10% citric acid solution, 4% sodium bicarbonate solution and brine. After drying over MgSO<sub>4</sub> and concentrating, the resulting oily substance was purified by silica gel chromatography using a mixture of chloroform and methanol (99:1 v/v) to obtain Boc-L-Asu(OBzl)-A3mc6c-L-Phe-D-Pro-O<sup>t</sup>Bu(1.1 g, 1.4 mmol, 72%). TLC: Rf 0.8 (CHCl<sub>3</sub>/MeOH=9/1). HPLC: r.t. 10.96 min, 95%.

#### 4.4.2.4 *cyclo*(-L-Asu(OBzl)-L-A3mc6c-L-Phe-D-Pro-) (MW = 644.80):

The protected tetrapeptide Boc-L-Asu(OBzl)-L-A3mc6c-L-Phe-D-Pro-O<sup>t</sup>Bu(1.1 mg, 1.4 mmol) was dissolved in TFA (5 mL) at 0 °C and kept for 3 hours. After evaporation of TFA, the residue was solidified using ether and petroleum ether to yield TFA salt of the linear tetrapeptide TFA·H-L-Asu(OBzl)-L-A3mc6c-L-Phe-D-Pro-OH (960 mg, 1.4 mmol, 100%). To DMF (150 mL), TFA·H-L-Asu(OBzl)-L-A3mc6c-L-Phe-D-Pro-OH (960 mg, 1.4 mmol), HATU (822 mg, 2.1 mmol), and DIEA (0.63 mL, 3.6 mmol) were added in separate five portions in every 30 minutes with stirring at room temperature for the cyclization reaction. After completion of the reaction for 1 hour, DMF was evaporated under vacuum; the residue was dissolved in ethyl acetate and washed with 10% citric acid solution, 4% sodium bicarbonate solution and brine, respectively. It was then dried over anhydrous MgSO<sub>4</sub> and filtered. After evaporation of ethyl

acetate, the residue was purified by silica gel chromatography using a mixture of chloroform and methanol (99:1v/v) to yield *cyclo(-L-Asu(OBzl)-L-A3mc6c-L-Phe-D-Pro-)* (659 mg, 1.0 mmol, 77%). HPLC: r.t. 10.04 min, 96%.

#### 4.4.2.5 *cyclo(-L-Asu(NHOH)-L-A3mc6c-L-Phe-D-Pro-)* (MW=569.69):

Compound *cyclo(-L-Asu(OBzl)-L-A3mc6c-L-Phe-D-Pro-)* (659 mg, 1.0 mmol) was dissolved in methanol (5 mL) and Pd-C (50 mg) was added. The mixture was stirred under H<sub>2</sub> for overnight. After filtration of Pd-C, methanol was evaporated to yield *cyclo(-L-Asu-L-A3mc6c-L-Phe-D-Pro-)* (560 mg, 1.0 mmol, 100%). The product was dissolved in DMF (3 mL) at 0 °C, and O-Benzylhydroxylamine hydrochloride (HCl NH<sub>2</sub>-OBzl) (239 mg, 1.5 mmol), HOBt·H<sub>2</sub>O (153 mg, 1.0 mmol), triethylamine (0.22 mL, 1.5 mmol) and DCC (310 mg, 1.5 mmol) were added. The mixture was stirred for overnight. After completion of the reaction, DMF was evaporated under vacuum; the residue was dissolved in ethyl acetate and washed with 10% citric acid solution, 4% sodium bicarbonate solution and brine, respectively. It was then dried over anhydrous MgSO<sub>4</sub> and filtered. After evaporation of ethyl acetate, *cyclo(-L-Asu(NHOBzl)-L-A3mc6c-L-Phe-D-Pro-)* (613 mg, 0.93 mmol, 93%) was obtained. The product *cyclo(-L-Asu(NHOBzl)-L-A3mc6c-L-Phe-D-Pro-)* (613 mg, 0.93 mmol) was dissolved in acetic acid (9 mL) and Pd-BaSO<sub>4</sub> (135 mg) was added. The mixture was stirred under H<sub>2</sub> for 24 hours. After filtration of Pd-BaSO<sub>4</sub>, acetic acid was evaporated and crystallized with ether to yield *cyclo(-Asu(NHOH)-L-A3mc6c-L-Phe-D-Pro-)* (406 mg, 0.7 mmol, 79%). TLC: R<sub>f</sub> 0.67 (CHCl<sub>3</sub>/ MeOH/CH<sub>3</sub>COOH=90/10/2). HPLC: r.t. 8.15 min. HR-FAB-MS [M+H]<sup>+</sup> 570.3257 for C<sub>30</sub>H<sub>43</sub>N<sub>5</sub>O<sub>6</sub> (calcd 569.3213). <sup>1</sup>H NMR(400 MHz, CDCl<sub>3</sub>): δ<sub>H</sub> (ppm): 0.88(dd, J=4.0, 6.0 Hz, 4H), 1.16(m, 3H), 1.19-1.30(m, 6H), 1.48-1.72(m, 10H), 2.04(s, 1H), 2.13(m, 2H), 2.30(d, J=8.4 Hz, 1H), 2.95(m, 1H), 3.21(m, 1H), 3.47(m, 1H), 3.98(m, 1H), 4.18(m, 1H), 4.68(t, J=6.0 Hz, 1H), 5.12(m, 1H), 6.38(s, 1H), 6.46(s, 1H), 7.18(d, J=9.2 Hz, 1H), 7.21-7.32(m, 5H), 7.49(d, J=10 Hz, 1H). <sup>13</sup>C NMR (400 MHz, CDCl<sub>3</sub>) δ<sub>C</sub> (ppm): 22.50, 24.78, 24.99, 25.15, 28.16, 29.04, 29.41, 29.60, 32.69, 33.17, 34.11, 36.07, 41.56, 42.83, 47.11, 53.22, 54.57, 57.85, 62.48, 62.63, 126.94, 128.72, 128.78, 129.25, 129.32, 137.09, 171.22, 172.48, 173.33, 174.36.

#### 4.4.3 Synthesis of *cyclo(-L-Asu(NHOH)-A4mc6c-L-Phe-D-Pro-)*

##### 4.4.3.1 Synthesis of *Z-A4mc6c-OH* (MW=291.34):

To a suspension of 4-methyl-cyclohexanecarboxylic amino acid (9.7 g, 61 mmol) in acetone (60 mL) and water (60 mL) were added Z-Osu (16.7 g, 67.1 mmol) and Na<sub>2</sub>CO<sub>3</sub> (12.9 g, 122 mmol). After stirring for overnight, acetone was removed by evaporation; residue dissolved in ethyl acetate, and adjusted pH 2-3 with citric acid solution, and then washed with saturated saline. After drying over MgSO<sub>4</sub> and concentrating, product was purified by crystallization in ether and petroleum ether (1:2 v/v) to yield (10.4 g, 35.7 mmol, 59%), HPLC: r.t. 3.94 min.

#### **4.4.3.2 Synthesis of Z-A4mc6c-L-Phe-D-Pro-O'Bu (MW = 591.74):**

The dipeptide was coupling in the same manner as 3.8.3 described to obtain H-L-Phe-D-Pro-O'Bu (1.05 g, 3.3 mmol). To a cooled solution of H-L-Phe-D-Pro-O'Bu (1.05 g, 3.3 mmol) and Z-A4mc6c-OH (971 mg, 3.0 mmol) in DMF (6 mL) were successively added DCC (743 mg, 3.3 mmol), HOBt·H<sub>2</sub>O (460 mg, 3.0 mmol). After stirring for overnight, DMF was removed by evaporation; residue dissolved in ethyl acetate, and then successively washed with 10% citric acid solution, 4% sodium bicarbonate solution and brine. After drying over MgSO<sub>4</sub> and concentrating, the resulting oily substance was purified by silica gel chromatography using a mixture of chloroform and methanol (99:1 v/v) to obtain Z-A4mc6c-L-Phe-D-Pro-O'Bu (480 mg, 0.8 mmol, 63%). TLC: R<sub>f</sub> 0.8 (CHCl<sub>3</sub>/MeOH=9/1). HPLC: r.t. 9.32 min, 58%.

#### **4.4.3.3 Synthesis of Boc-L-Asu(OBzl)-A4mc6c-L-Phe-D-Pro-O'Bu (MW =763.02 ):**

The tripeptide Z-A4mc6c-L-Phe-D-Pro-O'Bu (480 mg, 0.8 mmol) was subjected to catalytic hydrogenation with Pd-C (41 mg) in acetic acid (2 mL). After overnight, The reaction was checked by TLC (CHCl<sub>3</sub>/MeOH/CH<sub>3</sub>COOH=90/10/2), the catalyst was filtered and reaction solution was removed by evaporation. The free amine was taken into ethyl acetate (20 mL) by the aid of 2M Na<sub>2</sub>CO<sub>3</sub> solution (5 mL). After dried over anhydrous Na<sub>2</sub>CO<sub>3</sub> ethyl acetate solution was evaporated to obtain H-A4mc6c-L-Phe-D-Pro-O'Bu (244 mg, 0.5 mmol, 66%). To a cooled solution of H-A4mc6c-L-Phe-D-Pro-O'Bu (244 mg, 0.5 mmol) and Boc-L-Asu(OBzl)-OH (210 mg, 0.5 mmol) in DMF (3 mL) were successively added DCC (132 mg, 0.6 mmol), HOBt·H<sub>2</sub>O (82 mg, 0.5 mmol). After stirring for overnight, DMF was removed by evaporation; residue dissolved in ethyl acetate, and then successively washed with 10% citric acid solution, 4% sodium bicarbonate solution and brine. After drying over MgSO<sub>4</sub> and concentrating, the resulting oily substance was purified by silica gel chromatography using a mixture of chloroform and methanol (99:1 v/v) to obtain Boc-L-Asu(OBzl)-A4mc6c-L-Phe-D-

Pro-O<sup>t</sup>Bu(320 mg, 0.4 mmol, 76%). TLC: R<sub>f</sub> 0.8 (CHCl<sub>3</sub>/MeOH=9/1). HPLC: r.t. 10.77 min, 80%.

#### 4.4.3.4 *cyclo(-L-Asu(OBzl)-A4mc6c-L-Phe-D-Pro-)* (MW = 644.80):

The protected tetrapeptide Boc-L-Asu(OBzl)-A4mc6c-L-Phe-D-Pro-O<sup>t</sup>Bu (320 mg, 0.4 mmol) was dissolved in TFA (3 mL) at 0 °C and kept for 3 hours. After evaporation of TFA, the residue was solidified using ether and petroleum ether to yield TFA salt of the linear tetrapeptide TFA·H-L-Asu(OBzl)-A4mc6c-L-Phe-D-Pro-OH (260 mg, 0.4 mmol, 100%). To DMF (50 mL), TFA·H-L-Asu(OBzl)-A4mc6c-L-Phe-D-Pro-OH (260 mg, 0.4 mmol), HATU (228 mg, 0.6 mmol), and DIEA (0.18 mL, 1.0 mmol) were added in separate five portions in every 30 minutes with stirring at room temperature for the cyclization reaction. After completion of the reaction for 1 hour, DMF was evaporated under vacuum; the residue was dissolved in ethyl acetate and washed with 10% citric acid solution, 4% sodium bicarbonate solution and brine, respectively. It was then dried over anhydrous MgSO<sub>4</sub> and filtered. After evaporation of ethyl acetate, the residue was purified by silica gel chromatography using a mixture of chloroform and methanol (99:1v/v) to yield *cyclo(-L-Asu(OBzl)-A4mc6c-L-Phe-D-Pro-)* (145 mg, 0.2 mmol, 56%). HPLC: r.t. 10.09 min, 100%.

#### 4.4.3.5 *cyclo(-L-Asu(NHOH)-A4mc6c-L-Phe-D-Pro-)* (MW=569.69):

Compound *cyclo(-L-Asu(OBzl)-A4mc6c-L-Phe-D-Pro-)* (145 mg, 0.2 mmol) was dissolved in methanol (3 mL) and Pd-C (11 mg) was added. The mixture was stirred under H<sub>2</sub> for 4 hours. After filtration of Pd-C, methanol was evaporated to yield *cyclo(-L-Asu-A4mc6c-L-Phe-D-Pro-)* (122 mg, 0.2 mmol, 100%). The product was dissolved in DMF (3 mL) at 0 °C, and O-Benzylhydroxylamine hydrochloride (HCl·NH<sub>2</sub>-OBzl)(53 mg, 0.3 mmol), HOBT·H<sub>2</sub>O (34 mg, 0.2 mmol), triethylamine (48 μL, 0.3 mmol) and DCC (68 mg, 0.3 mmol) were added. The mixture was stirred for overnight. After completion of the reaction, DMF was evaporated under vacuum; the residue was dissolved in ethyl acetate and washed with 10% citric acid solution, 4% sodium bicarbonate solution and brine, respectively. It was then dried over anhydrous MgSO<sub>4</sub> and filtered. After evaporation of ethyl acetate, *cyclo(-L-Asu(NHOBzl)-A4mc6c-L-Phe-D-Pro-)* (133 mg, 0.2 mmol, 91% ) was obtained. The product *cyclo(-L-Asu(NHOBzl)-A4mc6c-L-Phe-D-Pro-)* (133 mg, 0.2 mmol) was dissolved in acetic acid (2 mL) and Pd-BaSO<sub>4</sub> (30 mg) was added. The mixture was stirred under H<sub>2</sub> for 24 hours. After filtration of Pd-BaSO<sub>4</sub>, acetic acid was evaporated and crystallized with ether to yield

*cyclo(-L-Asu(NHOH)-A4mc6c-L-Phe-D-Pro-)* (61 mg, 0.1 mmol, 54%). TLC: R<sub>f</sub> 0.65 (CHCl<sub>3</sub>/MeOH/CH<sub>3</sub>COOH=90/10/2). HPLC: r.t. 7.60 min, 47%. HR-FAB-MS [M+H]<sup>+</sup> 570.3262 for C<sub>30</sub>H<sub>43</sub>N<sub>5</sub>O<sub>6</sub> (calcd 569.3213). <sup>1</sup>H NMR (400 MHz, CDCl<sub>3</sub>): δ<sub>H</sub> (ppm): 0.77(d, J=12 Hz, 1H), 0.84(d, J=5.6 Hz, 3H), 1.25-1.30(m, 12H), 1.61-1.74(m, 6H), 2.05(s, 1H), 2.13-2.29(m, 4H), 2.94(d, J=5.2 Hz, 1H), 2.97(d, J=5.6 Hz, 1H), 3.29(m, 1H), 3.97(m, 1H), 4.23(m, 1H), 4.68(t, J=6.0 Hz, 1H), 5.15(dd, J=9.2, 6.4 Hz, 1H), 6.46(s, 1H), 6.67(s, 1H), 7.19(d, J=6.8 Hz, 1H), 7.21-7.28(m, 5H), 7.53(d, J=10 Hz, 1H). <sup>13</sup>C NMR (400 MHz, CDCl<sub>3</sub>) δ<sub>C</sub> (ppm): 21.63, 24.77, 24.94, 25.05, 25.26, 28.39, 28.70, 29.18, 31.25, 32.56, 32.75, 34.04, 36.26, 35.78, 36.04, 47.03, 53.16, 54.70, 57.82, 61.95, 126.89, 128.71, 128.71, 129.22, 129.22, 137.08, 173.21, 174.31, 174.39, 174.48.

#### 4.4.4 HDACs preparation and enzyme activity assay

In a 100-mm dish, 293T cells (1-2 × 10<sup>6</sup>) were grown for 24 hours and transiently transfected with 10 μg each of the vector pcDNA3-HDAC1 for human HDAC1, pcDNA3-HDAC4 for human HDAC4, or pcDNA3-mHDA2/HDAC6 for mouse HDAC6, using the Lipofect AMINE 2000 reagent (Invitrogen). After successive cultivation in DMEM for 24 hours, the cells were washed with PBS and lysed by sonication in lysis buffer containing 50 mM Tris-HCl (pH 7.5), 120 mM NaCl, 5 mM EDTA, and 0.5% NP40. The soluble fraction collected by micro

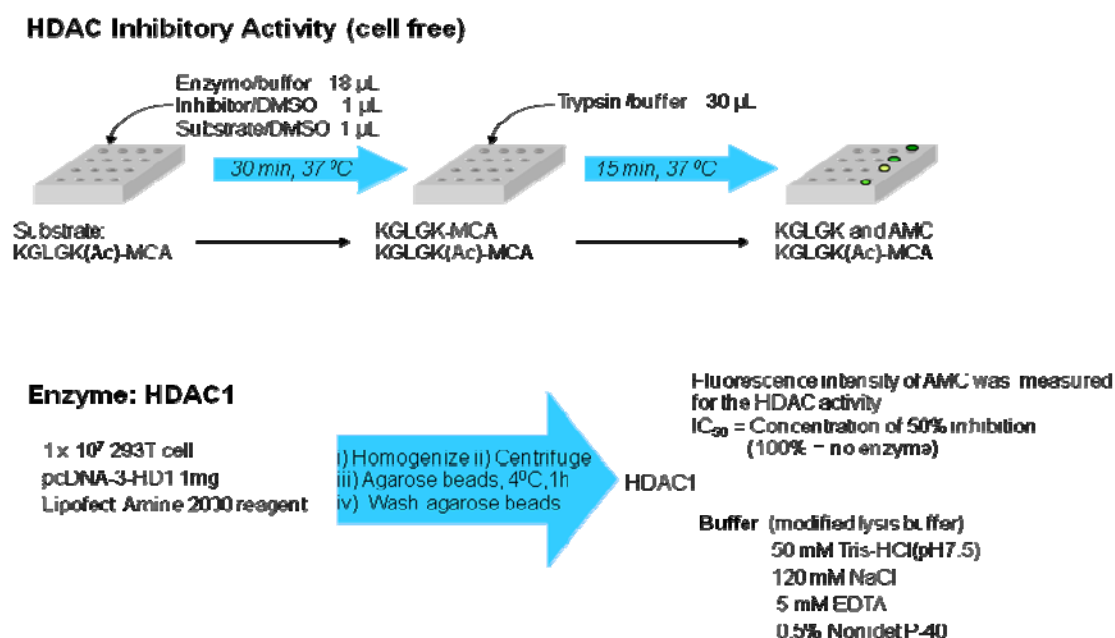


**Fig. 4.10** The method of enzyme activity assay

centrifugation was precleared by incubation with protein A/G plus agarose beads (Santa Cruz Biotechnologies, Inc.). After the cleared supernatant had been incubated for 1 hour at 4°C with 4 g of an anti-FLAG M2 antibody (Sigma-Aldrich Inc.) for HDAC1, HDAC4 and HDAC6, the agarose beads were washed three times with lysis buffer and once with histone deacetylase buffer consisting of 20 mM Tris-HCl (pH 8.0), 150 mM NaCl, and 10% glycerol. The bound proteins were released from the immune complex by incubation for 1 hour at 4°C with 40 g of the FLAG peptide (Sigma-Aldrich Inc.) in histone deacetylase buffer (200 mL). The supernatant was collected by centrifugation. For the enzyme assay, 10 µL of the enzyme fraction was added to 1 µL of fluorescent substrate (2 mM Ac-KGLGK(Ac)-MCA) and 9 µL of histone deacetylase buffer, and the mixture was incubated at 37°C for 30 minutes. The reaction was stopped by the addition of 30 µL of trypsin (20 mg/mL) and incubated at 37°C for 15 minutes. The released amino methyl coumarin (AMC) was measured using a fluorescence plate reader. The 50% inhibitory concentrations (IC<sub>50</sub>) were determined as the means with SD calculated from at least three independent dose response curves (**Fig. 4.10**).

#### 4.4.5 The p21 promoter assay

A luciferase reporter plasmid (pGW-FL) was constructed by cloning the 2.4 kb genomic fragment containing the transcription start site into *Hind*III and *Sma*I sites of the pGL3-Basic plasmid (Promega Co., Madison, WI). Mv1Lu (mink lung epithelial cell line) cells were transfected with the pGW-FL and a phagemid expressing neomycin/kanamycin resistance gene (pBK-CMV, Stratagene, La Jolla, CA) with the Lipofectamine reagent (Life Technology, Rockville, MD USA). After the transfected cells had been selected by 400 µg/mL Geneticin (G418, Life Technology), colonies formed were isolated. One of the clones was selected and named MFL-9. MFL-9 expressed a low level of luciferase, of which activity was enhanced

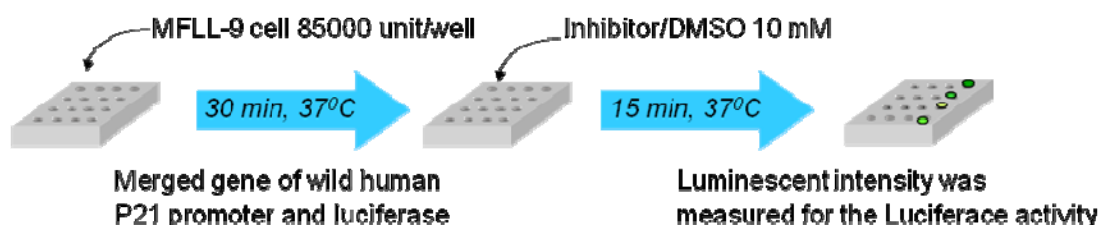


**Fig. 4.11** The p21 promoter assay

by TSA in a dose-dependent manner. MFLN-9 cells ( $1 \times 10^5$ ) cultured in a 96-well multi-well plate for 6 hours were incubated for 18 hours in the medium containing various concentrations of drugs. The luciferase activity of each cell lysate was measured with a LucLite luciferase Reporter Gene Assay Kit (Packard Instrument Co., Meriden, CT) and recorded with a Luminescencer-JNR luminometer (ATTO, Tokyo, Japan). Data were normalized to the protein concentration in cell lysates. Concentrations at which a drug induces the luciferase activity 10-fold higher than the basal level are presented as the 1000% effective concentration 1000% ( $EC_{1000}$ ). The human wild-type p21 promoter luciferase fusion plasmid, WWP-Luc, was a kind gift from Dr. B. Vogelstein (**Fig. 4.11**).

#### 4.4.6 Cell growth inhibition assay

The MTT colorimetric assay was used to determine growth inhibition (**Fig. 4.12**). HeLa, 7721, K-562 and MCF-7 were all cultured in a humidified atmosphere of 5%  $CO_2$  in air, with RPMI 1640 media, containing 10% fetal bovine serum. The cell lines were diluted to  $5\sim 9 \times 10^4$  cells/mL with the corresponding media and were plated in 96-well microplates. After adhere overnight, three HDACs inhibitors were added to culture medium at the concentrations of 20, 40, 60, 80, 100 nM and then the cells were incubated for 48 hours. Then 200  $\mu$ L MTT (0.5 mg/mL) reagent diluted in serum free media was added to each well and the cells were incubated for an additional 4 hours. Thereafter, the resulted dark blue crystal (formazan) was dissolved in 200  $\mu$ L DMSO, and an optical density was measured on a microplate spectrophotometer at 570 nm. All experiments were performed in triplicate and repeated at least three times. Data are presented as mean  $\pm$  standard deviation of three independent experiments. The  $IC_{50}$  values were calculated by nonlinear regression analysis using SPSS 17.0 software.

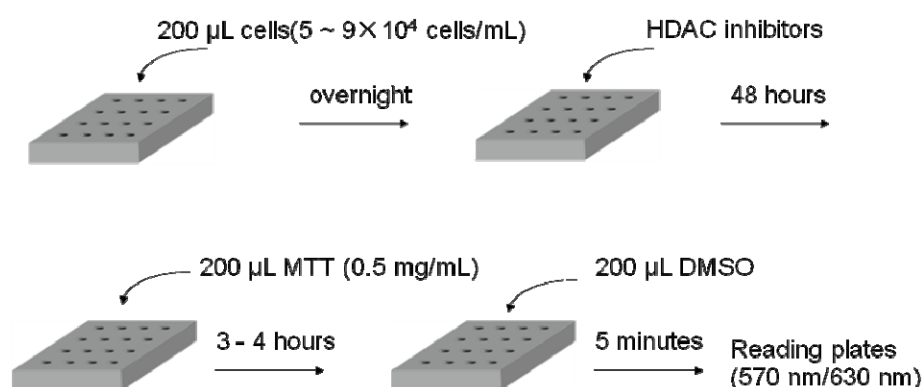


**Fig. 4.12** Cell growth inhibition assay (MCF-7, HeLa, K-562 and 7721 cell lines)

#### 4.4.7 Morphological reversion assay

Method crystal violet staining was used to observe the changes in cell morphology (**Fig. 4.13**).<sup>[20]</sup> MCF-7 cells and 7721 cells were plated into 96-well microplates at  $2 \times 10^4$  cells/mL and allowed to adhere overnight. Inhibitors were added to culture medium at the concentration of 100 nM (**Ky-301, Ky-302 and Ky-303**) and incubated for 24 hours. Cells were then washed once with PBS, and fixed in 4% buffered formalin for 1 hour at room temperature. The fixed cells were then washed once further with PBS and stained with 1% Crystal Violet in methanol for 5 minutes. Excess stain was removed by washing with tap water. After the microtiter plate was being air-dried at  $37^\circ\text{C}$ , MCF-7 cells and 7721 cells were taken Photographs using an inverted microscope.

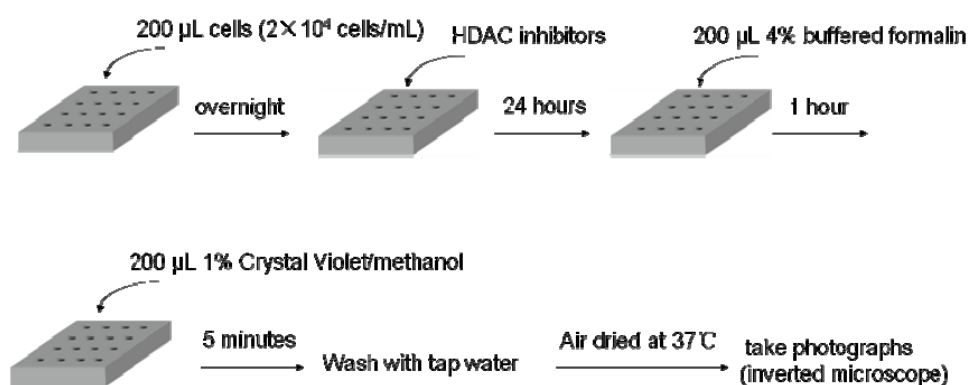


**Fig. 4.13** Morphological reversion assay

#### 4.4.8 Circular dichroism measurement

CD spectra were recorded on a JASCO J-820 spectropolarimeter (Tokyo, Japan) using a quartz cell of 1 cm light path length at room temperature. Peptide solutions (0.1 mM) were prepared in methanol and CD spectra were recorded in terms of molar ellipticity,  $[\theta]_M$  ( $\text{deg} \times \text{cm}^2 \times \text{dmol}^{-1}$ ).

#### 4.4.9 Molecular dynamics simulation

All the molecular mechanics and dynamics calculations were carried out with the AMBER9 package. The standard AMBER ff99 force field<sup>[44]</sup> was used as the parameters for the protein and water atoms, and the general AMBER force field (GAFF)<sup>[45]</sup> and AM1-BCC charges<sup>[46]</sup> were used for the ligands. Zinc was modeled using the Stote nonbonded model ( $q = +2e^-$ ,  $r = 1.7$



Å,  $\epsilon = 0.67$  kcal/mol).<sup>[47]</sup> Each initial structure for the simulation was prepared from the docked conformations of HDAC8-ligand complexes. The local hydrogen bonding network around the histidine residues was checked. Histidine residue 180 was assigned as HIE (histidine with hydrogen on its epsilon nitrogen), and other histidine residues as HID (histidine with hydrogen on its delta nitrogen). The force field parameters of cyclic tetrapeptides were prepared with the Antechamber module<sup>[48]</sup> of AMBER 9 package. Hydrogen atoms were added to the crystallographic protein with the AMBER LEaP module. Sodium counterions were added to neutralize the system. The system was then solvated with an octahedral box of TIP3P water molecules.<sup>[49]</sup> The minimum distance from the surface of the protein to the faces of the box was 10 Å. The particle mesh Ewald (PME) method<sup>[50]</sup> was used to treat long-range electrostatic interactions. The cutoff distance for the long-range electrostatic and the van der Waals energy terms were set at 12.0 Å. All covalent bonds to hydrogen atoms were constrained using the SHAKE algorithm.<sup>[51]</sup>

Energy minimization was achieved via three steps. At first, movement was allowed only for the water molecules and ions. Next, the ligand and the receptor residues were all allowed to move and the water molecules, together with ions, were constrained. Finally, all atoms were permitted to move freely. With each step, energy minimization was executed by the steepest descent method for the first 5000 steps and the conjugated gradient method for the subsequent 2500 steps.

Periodic boundary conditions were used. The time steps were 2 ps during the production dynamics. The temperature was maintained by rescaling the velocities using the Berendsen weak-coupling algorithm,<sup>[52]</sup> with a time constant of 2 ps for the heat bath.

After the system was heated to 300 K from the initial temperature of 0 K using the NVT ensemble in 120.0 ps, molecular dynamics were performed at a constant temperature of 300 K. After a 50 ps position-restrained dynamics, each simulation was proceeded 2 ns under periodic boundary conditions with NPT ensemble at 1 atm and at 300 K. The convergence of energy, temperatures, and pressures of the systems, and the atomic root-mean-square deviation of the enzyme and the inhibitor (RMSD), were used to verify the stability of the systems. Trajectories were analyzed using the PTRAJ modules.<sup>[53]</sup>

In the present MD simulations, the overall structure of all complexes appeared to be equilibrated after 1.5 ns. Hence, atom coordinates were collected at the interval of 5 ps for the last 500 ps to analyze the structure in detail. The series of snapshots between 1.5 and 2.0 ns of the equilibrium phase was used for free energy calculations and structure evaluation.

## 4.5 References

- [1] Yoshida, M.; Kijima, M.; Akita, M.; Beppu, T. *J. Biol. Chem.*, 1990, 265: 17174-17179.
- [2] Ueda, H.; Nakajima, H.; Hori, Y.; Fujita, T.; Nishimura, M.; Goto, T.; Okuhara, M. *J. Antibiot.* 1994, 47: 301-310.
- [3] Ueda, H.; Manda, T.; Matsumoto, S.; Mukumoto, S.; Nishigaki, F.; Kawamura, I.; Shimomura, K. *J. Antibiot.* 1994, 47: 315-323.
- [4] Furumai, R.; Matsuyama, A.; Kobashi, N.; Lee, K.-H.; Nishiyama, M.; Nakajima, H.; Tanaka, A.; Komatsu, Y.; Nishino, N.; Yoshida, M.; Horinouchi, S. *Cancer Res.* 2002, 62: 4916-4921.
- [5] Closse, A.; Hugenin, R. *Helv. Chim. Acta*, 1974, 57: 533-545.
- [6] Kijima, M.; Yoshida, M.; Suguta, K.; Horinouchi, S.; Beppu, T. *J. Biol. Chem.* 1993, 268: 22249-22435.
- [7] Hirota, A.; Suzuki, A.; Aizawa, K.; Tamura, S. *Biomed. Mass Spectrom.* 1974, 1, 15-19.
- [8] Hirota, A.; Suzuki, A.; Aizawa, K.; Tamura, S. *Agr. Biol. Chem.* 1973, 37: 955-959.
- [9] Shute, R. E.; Dunlap, B.; Rich, D. H. *J. Med. Chem.* 1987, 30: 71-78.
- [10] Darkin-Rattray, S. J.; Gurnett, A. M.; Myers, R. W.; Dulski, P. M.; Crumley, T. M.; Allocco, J. J.; Cannova, C.; Meinke, P. T.; Colletti, S. L.; Bednarek, M. A.; Singh, S. B.; Goetz, M. A.; Dombrowski, A. W.; Polishook, J. D.; Schmatz, D. M. *Proc. Natl. Acad. Sci. U.S.A.* 1996, 93: 13143-13147.
- [11] Meinke, P. T.; Liberator, P. *Curr. Med. Chem.* 2001, 8: 211-235.
- [12] Jung, M.; Brosch, G.; Ko"lle, D.; Scherf, H.; Gerha"user, C.; Loidi, P. *J. Med. Chem.* 1999, 42: 4669-4679.
- [13] Remiszewski, S. W.; Sambucetti, L. C.; Atadja, P.; Bair, K. W.; Cornell, W. D.; Green, M. A.; Howell, K. L.; Jung, M.; Known, P.; Trogani, N.; Walker, H. *J. Med. Chem.* 2002, 45: 753-757.
- [14] Woo, S. H.; Frechette, S.; Khalil, E. A.; Bouchain, G.; Vaisburg, A.; Bernstein, N.; Moradei, O.; Leit, S.; Allan, M.; Fournel, M.; Trachy-Bourget, M. C.; Li, Z.; Bestman, J. M.; Delorme, D. *J. Med. Chem.* 2002, 45: 2877-2885.
- [15] Furumai, R.; Komatsu, Y.; Nishino, N.; Kochbin, S.; Yoshida, Y.; Horinouchi, S. *Proc. Natl. Acad. Sci. U.S.A.* 2001, 98: 87-92.
- [16] Komatsu, Y.; Tomizaki, K.; Tsukamoto, M.; Kato, T.; Nishino, N.; Sato, S.; Yamori, T.; Tsuruo, T.; Furumai, R.; Yoshida, Y.; Horinouchi, S.; Hayashi, H. *Cancer Res.* 2001, 61: 4459-4466.
- [17] Nishino, N.; Jose, B.; Okamura, S.; Ebisusaki, S.; Kato, T.; Sumida, Y.; Yoshida, M. *Org. Lett.*, 2003, 5: 5079-5082.
- [18] Bhuiyan, M. P. I.; Kato, T.; Okauchi, T.; Nishino, N.; Maeda, S.; Nishino, T. G.; Yoshida, M. *Bioorg. Med. Chem.* 2006, 14: 3438-3446.
- [19] Norikazu Nishino, Binoy Jose, Ryuzo Shinta, Tamaki Kato, Yasuhiko Komatsub, Minoru Yoshida, *Bioorg. Med. Chem.* 2004, 12: 5777-5784.
- [20] Thomas A. Miller, David J. Witter, sandro Belvedere. *J. Med. Chem.*, 2003, 46: 5097-5116.
- [21] Nielsen, T. K.; Hildmann, C.; Dickmanns, A.; Schwienhorst, A.; Ficner, R. *J. Mol. Biol.* 2005, 354: 107-120.

- [22] Wang, D. F.; Wiest, O.; Helquist, P.; Lan-Hargest, H. Y.; Wiech, N. L. *J. Med. Chem.* 2004, 47: 3409-3417.
- [23] Nielsen, T. K.; Hildmann, C.; Dickmanns, A.; Schwienhorst, A.; Ficner, R., *J. Mol. Biol.* 2005, 354: 107-120.
- [24] R. Huey, G.M. Morris, A.J. Olson and D.S. Goodsell, *J. Comput. Chem.* 2007, 28: 1145-1152.
- [25] G.M. Morris, D.S. Goodsell, R.S. Halliday, R. Huey, W.E. Hart, R.K. Belew and A.J. Olson, *J. Comput. Chem.* 1998, 19: 1639-1662.
- [26] D.F. Wang, O.G. Wiest, P. Helquist, H.Y. Lan-Hargest and N.L. Wiech, *J. Med. Chem.* 2004, 47: 3409–3417.
- [27] N. Maulucci, M.G. Chini, S.D. Micco, I. Izzo, E. Cafaro, A. Russo, P. Gallinari, C. Paolini, M.C. Nardi, A. Casapullo, R. Riccio, G. Bifulco and F.D. Riccardis, *J. Am. Chem. Soc.* 2007, 129: 3007–3012.
- [28] Finnin M.S., Donigian J.R., Cohen A., Richon V.M., Rifkind R.A., Marks P.A., Breslow R., Pavletich N.P., *Nature* 1999, 401: 188-193.
- [29] Nielsen TK, Hildmann C, Dickmanns A, Schwienhorst A, Ficner R, *J Mol Biol*, 2005, 354: 107-120.
- [30] Somoza, J. R.; Skene, R. J.; Katz, B. A.; Mol, C.; Ho, J. D.; Jennings, A. J.; Luong, C.; Arvai, A.; Buggy, J. J.; Chi, E.; Tang, J.; Sang, B. C.; Verner, E.; Wynands, R.; Leahy, E. M.; Dougan, D. R.; Snell, G.; Navre, M.; Knuth, M. W.; Swanson, R. V.; McRee, D. E.; Tari, L. W. *Structure*, 2004, 12: 1325-1334.
- [31] A.C. Wallace, R.A. Laskowski and J.M. Thornton, *Protein. Eng.* 1995, 8: 127-134.

## Chapter 5

# Molecular Design of Cyclic Tetrapeptide HDAC Inhibitors by Replacement of L-Phe in Chlamydocin Framework

### 5.1 Introduction

High HDACs activity due to HAT mutation or abnormal recruitment of HDACs is associated with a number of malignant diseases, so HDAC inhibitors are a promising class of anticancer agents due to their efficacy against cancer cell line.<sup>[1,2]</sup> Therefore, design and synthesis of HDACs inhibitors represent exciting opportunity for the development of therapeutics for treatment of cancers. So far a number of natural and synthetic compounds have been reported as HDACs inhibitors, and several of them are already in clinical trials.<sup>[3]</sup> Among these the naturally occurring cyclic tetrapeptides, Chlamydocin which is isolated from fungus *Diheterosporia Chlamdosporia* containing Aib, L-Phe, D-Pro, and 2-amino-8-oxo-9,10-epoxydecanoic acid (Aoe) shows a highly HDAC inhibition with an IC<sub>50</sub> of 1.3 nM in vitro.<sup>[4]</sup> L-Aoe provides an epoxyketone moiety in the side chain which irreversible inhibits HDACs. To expect reversible and potent HDAC inhibitors, some Chlamydocin analogs with various functionalities have been reported.<sup>[5,6]</sup> Some potent HDAC inhibitors were reported with a benzyl cap group in surface recognition domain, such as TSA, SAHA and Trapoxin etc (**Fig. 5.1**). Therefore, it is importance that HDAC inhibitors of cyclic tetrapeptide contain L-Phe residue in scaffold.<sup>[7,8]</sup> To improve the hydrophobic interaction of the cap groups with HDACs, we focused on the benzene ring of L-Phe in Chlamydocin framework.

The discrepancy of inhibitory activity is 30-fold for TSA-HDLF comparing to SAHA-HDLF, though the catalytic mechanism for hydroxamic acid group of SAHA and TSA interacting with the zinc ion are the same manner.<sup>[9]</sup> To compare the structure to discover SAHA lack of methyl and double bond to TSA, the aromatic ring bears weak electron density and the saturated link of SAHA makes loose interactivity with around amino acid of tubular hydrophobic pocket.

FK228 is a natural product and shows potent *in vivo* antitumor activity.<sup>[10-13]</sup> There is no visible functional group in FK228 that interacts with the zinc ion in the HDAC binding pocket.

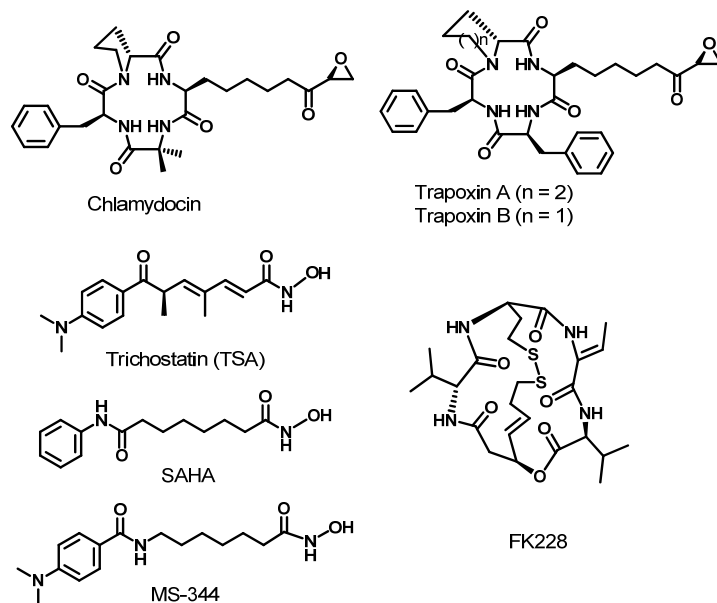


**Fig. 5.1** Several HDACs inhibitors.

Nishino and coworkers pointed out that the zinc-binding site is the sulfhydryl functional group and FK228 is converted to its active form (RedFK228) by cellular reducing activity.

To find out specific inhibitors, we designed and synthesized four novel cyclic tetrapeptides with methyl L-Phe in their macrocyclic frameworks, in which the thiol function was protected as disulfide hybrid (compound **1** *cyclo*(-L-Am7(S2Py)-Aib-L-Phe-D-Pro-), compound **2** *cyclo*(-L-Am7(S2Py)-Aib-L-Phe(2-Me)-D-Pro-), compound **3** *cyclo*(-L-Am7(S2Py)-Aib-L-Phe(4-Me)-D-Pro-), compound **4** *cyclo*(-L-Am7(S2Py)-Aib-L-Phe(3,5-2Me)-D-Pro-) as show in **Fig. 5.2**). We also synthesized cyclic tetrapeptide containing hydroxamic acid which has been reported as a comparison (*cyclo*(-L-Asu(NHOH)-Aib-L-Phe(4-Me)- D-Pro-), compound **5**).

Conformational analysis of HDAC inhibitors is very helpful for comprehending the structure-activity relationship (SAR) behavior and designing new drug candidates. Molecular dynamics (MD) simulation is a very useful technique for exploring the structure and the dynamic behavior of molecules of biochemical interest, a recent MD simulation study of HDLP-inhibitors has given us the details of binding mode of HDLP with hydroxamic acid inhibitors.<sup>[14]</sup> Free energy calculation methods can provide quantitative measurements of protein-ligand or protein-protein interactions.<sup>[15-17]</sup> A promising approach, molecular mechanics-Poisson Boltzmann surface area (MM-PBSA) has been used for evaluating the

binding free energy of macromolecules and their complexes.<sup>[18-22]</sup> To explore the interaction mechanisms of HDACs with cyclic tetrapeptide inhibitors containing sulfur, docking and MD simulations are conducted for HDAC8 with the compounds above. MM-PBSA method is also used to estimate the binding free energy of each HDAC8-ligand complex. Cyclic tetrapeptides are the most structurally complex HDAC inhibitors, but the details of interaction between cyclic tetrapeptides and HDACs are only partly known, up to now only two contributions analyzing the binding contacts between HDLP and the cyclic tetrapeptide were published.<sup>[23,24]</sup>

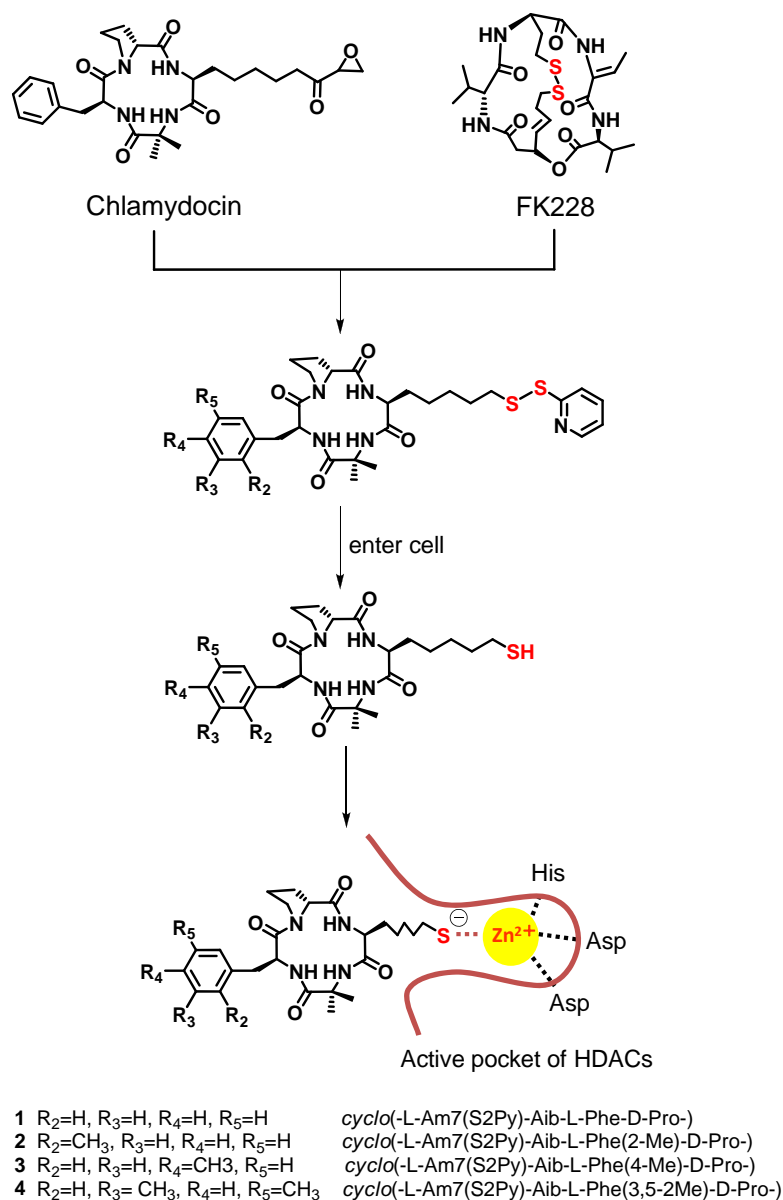


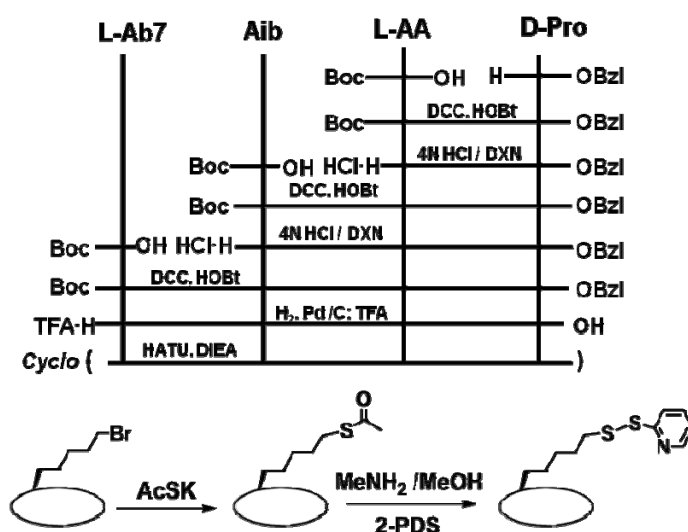
**Fig. 5.2** Design of HDAC inhibitors of cyclic tetrapeptides with L-Phe(*n*-Me).

## 5.2 Results and discussion

### 5.2.1 Chemistry

In order to synthesize potent HDAC inhibitors which have the similar cyclic framework as Chlamydocin, we prepared non-natural amino acids Boc-L-methyphenylalanines according to the literature.<sup>[25,26]</sup> The synthesis strategy was described in **scheme 3.1**.

The cyclic tetrapeptides were prepared according to general conventional solution phase method. Synthesis routes of target compounds **1**, **2** and **4** are shown in **Scheme 5.1**, and compound **3** and **5** is showed in **Scheme 5.2**.



**Scheme 5.1** Synthetic strategy of cyclic tetrapeptides.

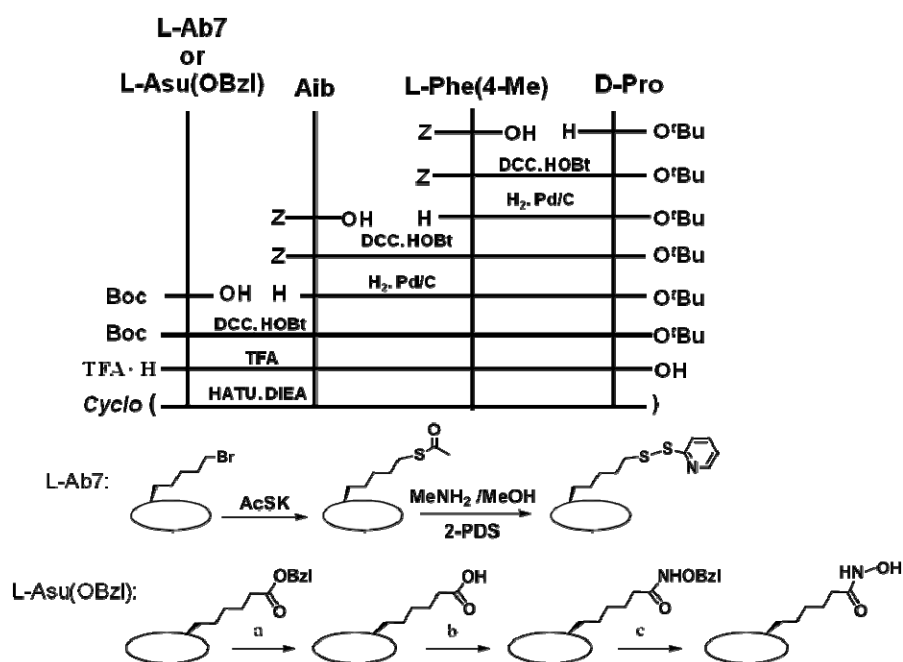
L-AA: L-Phe, L-Phe(2-Me), L-Phe(3,5-2Me)

Synthesis of compounds **1**, **2** and **4**: benzyl-protected D-Pro was reacted with Boc-protected Phe (or Phe(2-Me) or Phe(3,5-2Me)) to give protected dipeptide. Boc protection was then removed using 4N HCl/DXN and again coupled with Boc-Aib. The N-terminal of the tripeptide was deprotected by 4N HCl/DXN and coupled with Boc-L-Ab7 to yielded linear tetrapeptide. After the C-terminal benzyl protection was removed by catalytic hydrogenation, the N-terminal Boc protection was removed by treatment with trifluoroacetic acid (TFA). Cyclization reaction was carried out by the aid of HATU in DMF (2 mM) with minimum amount of DIEA (2.5 eq). The yield of cyclic tetrapeptides was 50%-60% after purification by silica gel chromatography. The cyclic tetrapeptide containing L-Ab7 was reacted with potassium thioacetate to convert the

bromide to thioacetate ester. Further treatment with methylamine in the presence of 2,2'-dipyridyl disulphide gave the targeted cyclic tetrapeptides.

The compounds **3** and **5** was prepared according to general **Scheme 5.2**, starting from *Z*-Pro *tert*-butyl ester. After the removal of *Z*-protection by catalytic hydrogenation, free amine was extracted and used for condensation with *Z*-L-Phe(4-Me) and *Z*-Aib using DCC/HOBt orderly. Boc-L-2-amino-7-bromoheptanoic acid (L-Ab7) was incorporated to prepare the linear tetrapeptide (Boc-L-Ab7-Aib-L-Phe(4-Me)-D-Pro-O*t*Bu). After removal of C-terminal and N-terminal protections by treating with TFA. Then liner tetrapeptide was cyclized and modified according to the same way as above.

All the synthesized compounds **1-4** were characterized by <sup>1</sup>H and <sup>13</sup>C NMR and HR-FAB-MS. The purity of the compounds were determined by HPLC analysis and showed purity above 97%.



**Scheme 5.2** Synthetic strategy of cyclic tetrapeptides.

Reagents: (a) H<sub>2</sub>, Pd/C, MeOH; (b) Cl·NH<sub>2</sub>-OBzl, DCC/HOBt, DMF; (c) Pd-BaSO<sub>4</sub>, CH<sub>3</sub>COOH.

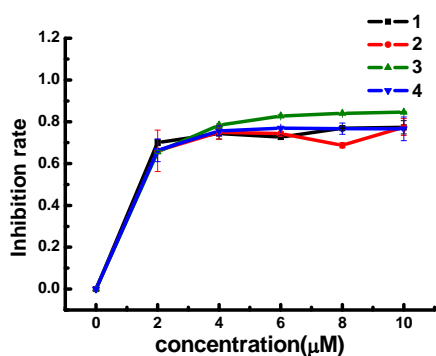
### 5.2.2 Cell growth inhibitory assay

The compounds were tested for antiproliferative *in vitro* by MTT assay against MCF-7 (human breast cancer), Hela (human cervix cancer) and 7721 (human liver cancer) cell lines. The IC<sub>50</sub>

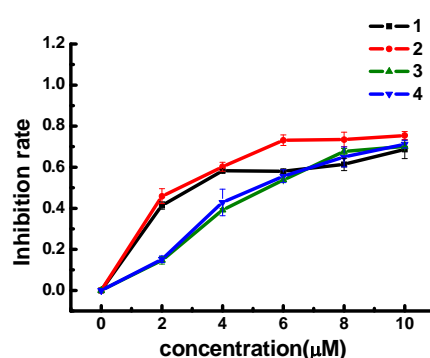


**Table 5.1** Cell growth inhibition for compounds **1-5**

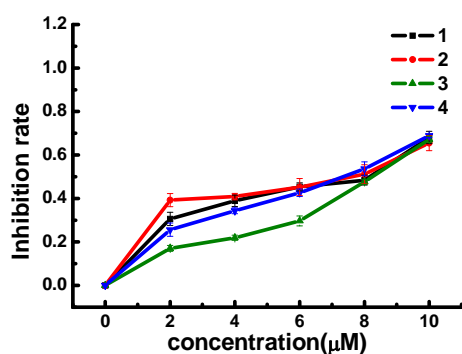
Compounds	IC <sub>50</sub> (μM)		
	Hela	MCF-7	7721
<b>1</b>	0.81	3.59	11.85
<b>2</b>	0.52	3.02	13.14
<b>3</b>	0.66	5.45	10.98
<b>4</b>	0.49	3.13	12.35
<b>5</b>	0.062	0.043	0.071



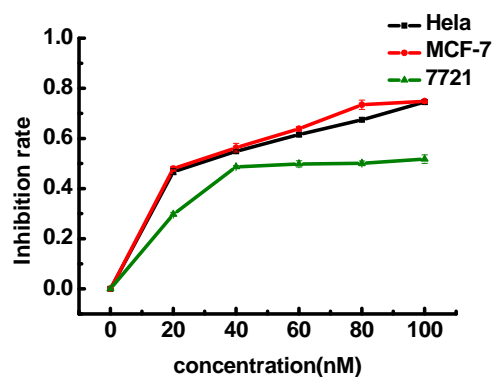
(a)



(b)



(c)



(d)

**Fig. 5.3** Effect of HDACs inhibitors on proliferation. (a) HeLa cell for compounds **1-4**, (b) MCF-7 cell for compounds **1-4**, (c) 7721 cell for compounds **1-4**, (d) HeLa, MCF-7 and 7721 cells for compound **5**.

value is shown in **Table 5.1**. All compounds showed good antitumor activities, which inhibited cell proliferation at a low concentration. The compounds **1-4** exhibited selectivity for the three human cancer cell lines, showing better sensitivity on HeLa than the other two cell lines with  $IC_{50}$ , but no obvious difference for one cell lines. The inhibition activity of compound **5** was stronger 10-100 fold than compounds **1-4** with  $IC_{50}$ , but there was no selectivity in three cell lines. The activity of Compounds 1-4 were almost the same.

### 5.2.3 Morphological reversion

Compounds were added to culture medium of MCF-7 cells at the concentration of 10  $\mu$ M (compounds **1-4**) and 100 nM (compound **5**) and MCF-7 cells were incubated. Cells were stained with 1% crystal violet. The inhibitors were found to induce dramatic changes in cellular shape under light microscopy. As the MCF-7 cells was treated by compounds **1-5** for 24 hours, cells progressively assumed flattened, rounded, and spindle shapes, with clear cellular borders and obvious gaps between cells (**Fig. 5.4**).

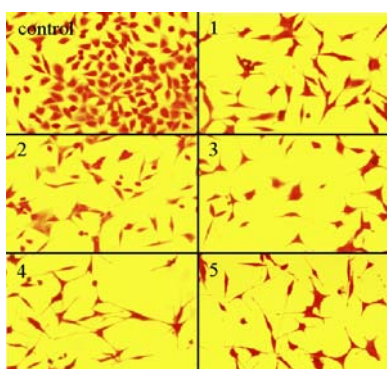


**Fig. 5.4** Morphological reversion of MCF-7 cells ( $\times 400$ ).

### 5.2.4 Enzyme inhibition and biological activity

Compound **1** was assayed for HDAC inhibitory activity using HDAC1, HDAC4 and HDAC6 prepared from 293T cells, and showed potent HDACs inhibitory activity, with the  $IC_{50}$  of 3.9 nM (HDAC1), 1.8 nM (HDAC4) and 40 nM (HDAC6), respectively (**Table 5.2**). The compound **1** was poorly inhibited by HDAC6 compared to HDAC1 and HDAC4 and the selectivity was better (HDAC6/HDAC4= 22.2). In the cellular activity, the cell permeability of compound **1** showed the better activity than TSA with 4-fold increased, which was reflected in their p21 promoter assay data.

**Table 5.2** HDAC inhibitory activity and p21 promoter activity data for TSA and compound **1**.

Compounds	IC <sub>50</sub> (nM)			HDAC1/	HDAC6/	p21 promoter assay
	HDAC1	HDAC4	HDAC6	HDAC4 <sup>a</sup>	HDAC4 <sup>a</sup>	EC <sub>1000</sub> (nM)
<b>TSA</b>	1.9	2.0	2.8	1.0	1.4	190
<b>1</b>	3.9	1.8	40.0	2.1	22.2	45

<sup>a</sup>Selectivity toward HDAC4

### 5.2.5 Conformation studies by CD and NMR

The interesting HDAC activity data of compounds **1-5** forced us to study their conformations. We have carried out circular dichroism (CD) spectral studies of compounds **1-5** (**Fig. 5.5**) and conformation by NMR (CDCl<sub>3</sub>) with MOE calculations for compound **2** (**Fig. 5.6**). CD spectra of compounds were carried out in methanol as solvent with peptide concentration of 0.1 mM. The CD spectrum of the synthesized compounds were similar to reference compound **1** at 190-260 nm. These compounds had two negative ellipticity at 210 nm and 245 nm, and a weak positive ellipticity at 230 nm. Compound **4** had a sharp ellipticity because of containing two methyl groups (L-Phe(3,5-2Me)). These similarities on CD spectra suggested that the peptide backbone of these compounds had also similar structures. This explained the fact that the change of methyl positions in L-Phe(*n*-Me) can not affect their conformations.

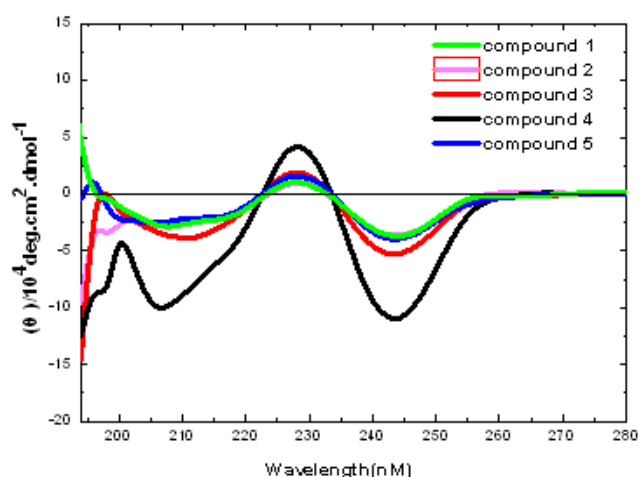


**Fig. 5.5** CD spectra of compounds **1-5**.

The solution conformation of compound **2** was studied using  $^1\text{H}$  NMR in  $\text{CDCl}_3$ . Complete assignments were made using COSY and NOESY spectra. The  $J_{\text{NH-HC}\alpha}$  values were obtained from NMR charts and by that we estimated dihedral angle “ $\theta$ ” ( $180^\circ$ ) using the Karplus graph. The structures of compound **2** having minimum energy configuration was generated by using MOE program and also using the  $\phi$  values ( $-120^\circ$ ) obtained from NMR (**Table 5.3**). The energy-minimized structures of compound **2** are shown in **Fig.5.6**. Compounds **1-5** have similar energy-minimized structures.

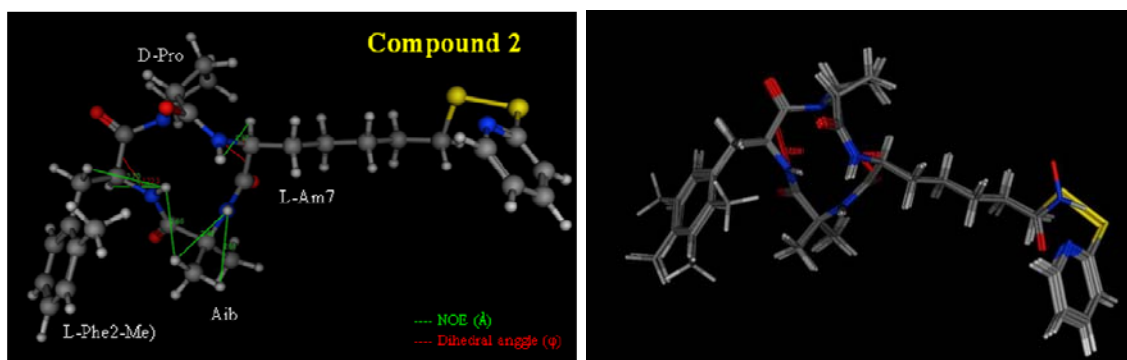


**Fig. 5.6** MOE of compound **2** by NMR calculation. Superimposition of compounds 1-5(right).

**Table 5.3** NOE, coupling constant and dihedral angles data from NMR charts of compound **2**.

residues	NOE	$J_{\text{NH-HC}\alpha}$	$\theta$	$\phi$
L-Am7	L-Am7(NH-HC $_{\alpha}$ )	10 Hz	$180^\circ$	$-120^\circ$
Aib	L-Aib(NH-HC $_{\beta}$ )	----	----	----
L-Phe(2-Me)	L-Phe(2-Me)(NH-HC $_{\alpha}$ )	10 Hz	$180^\circ$	$-120^\circ$
	L-Phe(2-Me)(NH-HC $_{\beta}$ )			
	L-Phe(2-Me)(NH)-Aib(HC $_{\beta}$ )			
D-Pro	----	----	----	----

## 5.2.6 Docking and molecular simulation for the HDAC inhibitors towards HDAC8

### 5.2.6.1 Docking studies

The results of dock modeling for compounds **1**, **2**, **3** and **4** into HDAC8 are shown in **Fig. 5.7**, all compounds bound in the active site of HDAC8 with a similar pattern to TSA, SAHA and MS344.<sup>[27]</sup> The aliphatic chain was occupying the long, narrow channel, the sulfhydryl group was at the bottom of this channel, and the large cap domain interacted with the external surface of the enzyme. The hydrogen bonds and hydrophobic interactions between HDAC8 and compound **1-4** are shown in **Fig. 5.8**. It showed that the sulfur atom of each compound established a hydrogen bond with the O(H) atom of Tyr306, this hydrogen bond was very important for keeping the binding of them to HDAC8. These compounds established hydrophobic interactions with some amino acid residues, such as Phe152, His180, Phe207 and Met274, etc., the hydrophobic effects were also crucial for stabilizing the complexes. In docking studies, the inhibitors bound to zinc atom of HDAC8 in pentahedron geometry.

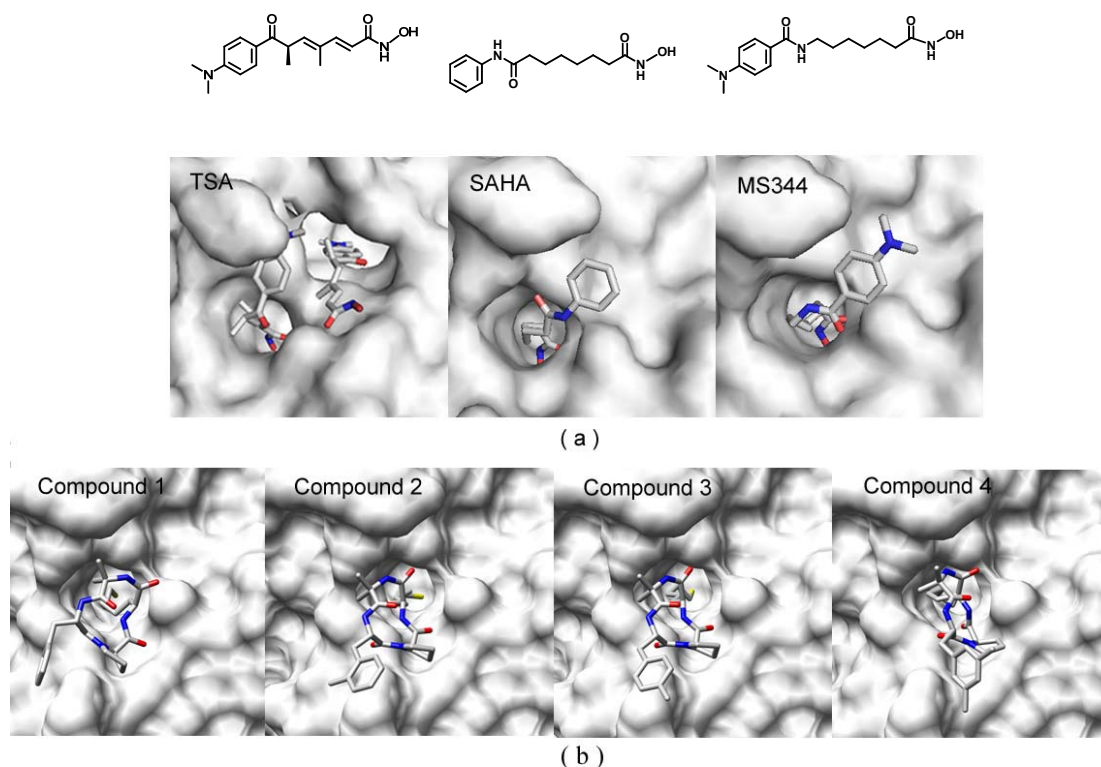


**Fig. 5.7** Top view of the surfaces of the active site of the (a) HDAC8-TSA, HDAC8-SAHA and HDAC8-MS344 from X-ray crystal structures; (b) HDAC8-Compound **1-4** for docking.

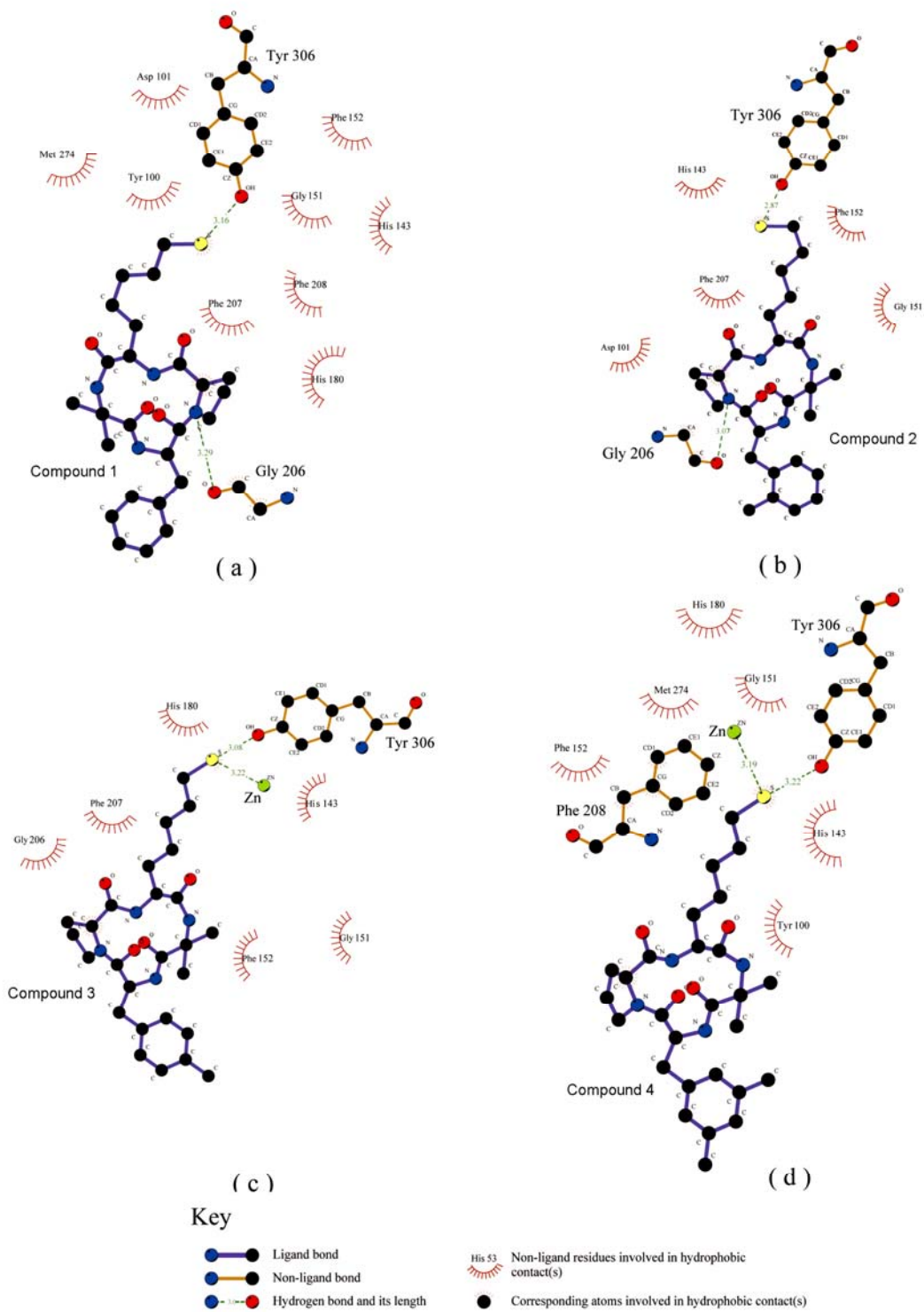


**Fig. 5.8** The hydrogen bonds and hydrophobic interactions between HDAC8 and compounds 1-4 for docking.

Molecular dynamics simulations were performed on four complexes of HDAC8 for 2 ns, respectively. All complexes converged and were stable as indicated by monitoring energetic and structural properties. The potential energy and root mean square deviations (RMSD) remained stable during the last 1000 ps of the simulation for the four systems. The RMSD between the C<sub>α</sub>, C, and N atoms of the structures obtained during the trajectories and the initial structures are shown in **Fig.5.9** for the four systems. Root-mean-squared-fluctuation (RMSF) of the C<sub>α</sub>, C, N atoms for these complexes were analyzed, it showed that the four structures shared similar RMSF distribution (**Fig.5.10**), and the conformational changes of the amino acid residues in the active site were all very small, especially in the bottom of the channel (His142, His143, Asp176, Asp178 and Asp267) (**Fig. 5.11**), indicated that the binding between HDAC8 and these compounds have lead directly to the rigidity of the complex. In the HDAC8-ligand X-ray structures, the zinc ion that lay at the end of the hydrophobic tunnel was bound to carboxylate oxygens of Asp178, Asp 267 and the nitrogen atom of His180, the other two

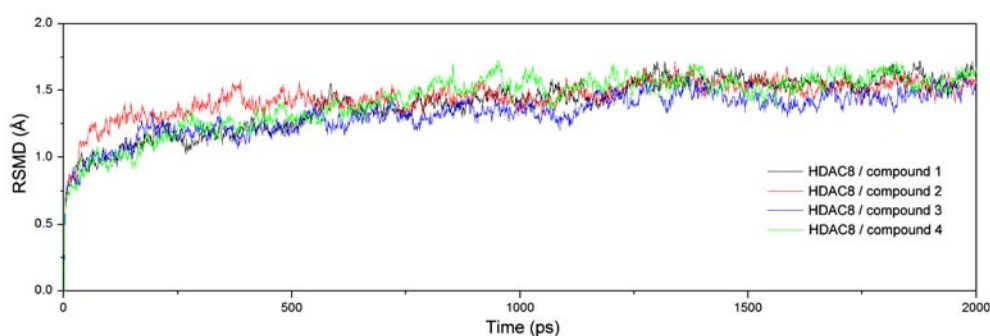


**Fig. 5.9** Root mean square deviation (RMSD) of the C<sub>α</sub>, C, and N atoms of the systems in the MD simulations with respect to the starting structure.

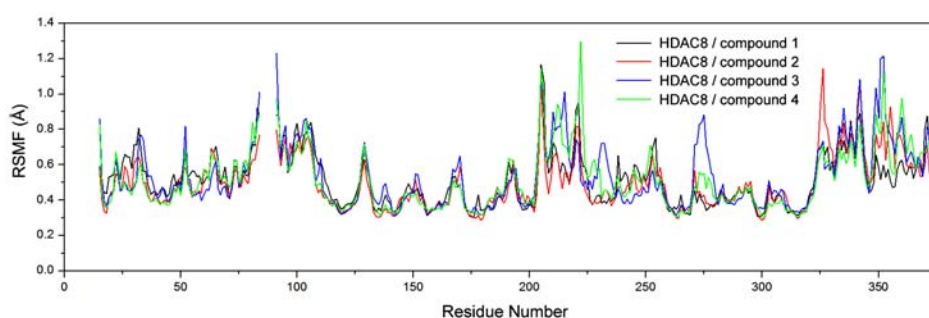


**Fig. 5.10** Root mean square fluctuation (RMSF) for all residues. RMSF averaged during the last 500 ps in the MD simulations.

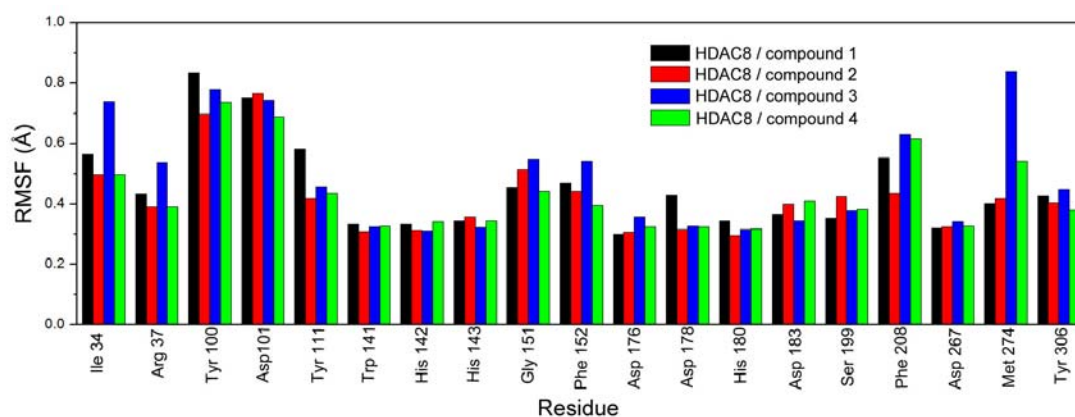


**Fig. 5.11** RMSF for the residues in the active site during the last 500 ps in the MD simulations.

coordination sites were occupied by the carbonyl and hydroxyl oxygens of the inhibitors' hydroxamate. The average distances between zinc and the nearby atoms during the last 500 ps in current MD simulations are shown in **Table 5.4**, it showed that zinc coordinates with five atoms, including one or two carboxylate oxygens of Asp178 and Asp267, a nitrogen atom of His180, and sulfur atom of the inhibitor, resulting in a pentahedral geometry. The coordination number of zinc in current MD simulations was equal to HDAC8-inhibitor crystal structures, but the atoms that coordinated to zinc were not the same, it revealed that all carboxylate oxygens of Asp178 and Asp267 and nitrogen atom of His180 can coordinate to the zinc ion. The sulfur atom occupied one coordination site, and this may be the precondition of these sulfur-containing HDAC inhibitors for their inhibitory activities.

**Table 5.4** Average zinc coordination distances for compound 1-4 with HDAC8 during the last 500 ps in the MD simulations

Complex	Atom1	Atom 2	Distance (Å)
HDAC8 - compound 1	Zn <sup>2+</sup>	His 142:NE2	5.16
		His 143:NE2	5.22
		Asp 178:OD1	3.60
		Asp 178:OD2	2.59
		His 180:ND1	2.84
		His 180:O	5.14



		Asp 267:OD1	2.73
		Asp 267:OD2	2.62
		Compound 1:S	2.84
HDAC8 - compound 2	Zn <sup>2+</sup>	His 142:NE2	3.36
		His 143:NE2	3.44
		Asp 178:OD1	2.67
		Asp 178:OD2	2.61
		His 180:ND1	2.75
		His 180:O	5.15
		Asp 267:OD1	3.98
		Asp 267:OD2	2.61
		Compound 2:S	2.85
HDAC8 - compound 3	Zn <sup>2+</sup>	His 142:NE2	3.92
		His 143:NE2	3.38
		Asp 178:OD1	2.72
		Asp 178:OD2	2.58
		His 180:ND1	2.83
		His 180:O	3.09
		Asp 267:OD1	4.33
		Asp 267:OD2	2.68
		Compound 3:S	2.81
HDAC8- compound 4	Zn <sup>2+</sup>	His 142:NE2	4.36
		His 143:NE2	3.51
		Asp 178:OD1	2.77
		Asp 178:OD2	2.60
		His 180:ND1	3.09
		His 180:O	5.37
		Asp 267:OD1	2.65

Asp 267:OD2	2.73
Compound 4:S	2.81

Hydrogen bonds between the ligand and protein played an essential role in stabilizing the complexes. These hydrogen bonds formed by the inhibitors in binding active pocket of HDAC8 were investigated. As shown in **Table 5.5**, the sulfur atoms of all compounds created strong hydrogen bond with the Tyr306 residue of HDAC8, it may be crucial for stabilizing the complex. Oxygen atoms in each compound also created hydrogen bonds with HDAC8, it can be seen that metal binding and surface recognition domain of cyclic tetrapeptides can create hydrogen bonds with HDAC8, and this may be the reason that cyclic tetrapeptides have high HDACs inhibitory activities. The carboxylate moieties of Asp176 and Asp183 formed hydrogen bonds with the ND1 atoms of His142 and His143, respectively. These two hydrogen bonds were also formed through corresponding amino acid residues in HDLP-inhibitor complexes, so they may be important in stabilizing the binding of HDAC8-inhibitor.

**Table 5.5** Hydrogen bonds between the compounds and HDAC8 active site of MD simulation

Inhibitor	Donor	Acceptor H	Acceptor	MD simulation		
				Occupied (%)	Distance (Å)	Angle (Degree)
Compound 1	Compound 1:S	Tyr306:HH	Tyr306:OH	99.60	2.969	13.95
	Compound 1:O2	His180:HE2	His180:NE2	99.80	2.895	18.90
	Asp176:OD2	His142:HD1	His142:ND1	98.80	2.804	27.18
	Asp183:OD2	His143:HD1	His143:ND1	95.81	2.917	21.03
Compound 2	Compound 2:S	Tyr306:HH	Tyr306:OH	100.00	2.942	14.76
	Compound 2:O2	His180:HE2	His180:NE2	63.24	3.012	23.04
	Compound 2:O3	Phe208:H	Phe208:N	3.59	3.131	46.78
	Asp176:OD2	His142:HD1	His142:ND1	99.80	2.747	30.46
	Asp183:OD2	His143:HD1	His143:ND1	88.71	2.856	22.05

Compound 3	Compound 3:S	Tyr306:HH	Tyr306:OH	98.20	2.922	11.99
	Compound 3:O2	His180:HE2	His180:NE2	65.47	2.995	38.38
	Compound 3:O3	Phe208:H	Phe208:N	65.07	3.027	38.74
	Asp176:OD2	His142:HD1	His142:ND1	92.02	2.911	32.69
	Asp183:OD2	His143:HD1	His143:ND1	99.00	2.922	16.59
Compound 4	Compound 4:S	Tyr306:HH	Tyr306:OH	100.00	2.945	11.08
	Compound 4:O2	His180:HE2	His180:NE2	99.60	2.889	22.17
	Asp176:OD2	His142:HD1	His142:ND1	99.60	2.737	30.63
	Asp183:OD2	His143:HD1	His143:ND1	29.34	2.978	45.24

### 5.2.6.3 Free energy calculation

Free energy of inhibitor binding in HDAC8 was analyzed by Molecular Mechanics-Poisson Boltzmann Surface Area (MM-PBSA) method<sup>[28-38]</sup> integrated in AMBER9. As shown in **Table 5.6**, to all complexes, intermolecular van der Waals ( $\Delta E_{\text{int}}^{\text{vdw}}$ ) and electrostatics ( $\Delta E_{\text{int}}^{\text{ele}}$ ) interactions provide major favorable contributions to the binding, nonpolar solvation terms

**Table 5.6** Binding free energies (kcal/mol) from MM-PBSA analysis of the HDAC8-ligand complexes

Contribution	HDAC8-1	HDAC8-2	HDAC8-3	HDAC8-4
$\Delta E_{\text{int}}^{\text{ele}}$	-87.32	-81.38	-84.27	-90.86
$\Delta E_{\text{int}}^{\text{vdw}}$	-24.03	-29.28	-27.56	-22.27
$\Delta E_{\text{int}}$	-111.35	-110.67	-111.83	-111.13
$\Delta G_{\text{sol}}^{\text{nonpol}}$	-4.80	-5.30	-5.98	-4.95
$\Delta G_{\text{sol}}^{\text{ele}}$	108.28	106.08	109.03	107.19
$\Delta G_{\text{sol}}$	103.48	100.78	103.05	102.24
$\Delta G_{\text{ele}}$	20.96	24.70	24.76	17.33
$\Delta G_{\text{b}}$	-7.87	-7.89	-8.78	-8.89

( $\Delta G_{\text{sol}}^{\text{nonpol}}$ ) contribute also favorably, whereas polar solvation terms ( $\Delta G_{\text{sol}}^{\text{ele}}$ ) oppose binding. The electrostatic interactions between water molecules and the inhibitors are stronger than that between HDAC8 and inhibitors, so the total electrostatic interactions ( $\Delta G_{\text{ele}}$ ) are unfavorable for binding. Hydrophobic interactions ( $\Delta G_{\text{sol}}^{\text{nonpol}}$ ) contribute almost half of the total binding energy ( $\Delta G_{\text{b}}$ ), this is expected since the surface recognition domains of the inhibitors are hydrophobic, and the surface of HDAC8 active site is constituted by some hydrophobic amino acid residues, such as Phe, Met and Leu, it can generate strong van der Waals and hydrophobic interactions with these inhibitors. The slightly change of hydrophobicity of surface recognition domain seems no obvious effect.

### 5.3 Summary

We have successfully synthesized several sulfur-containing cyclic tetrapeptides as HDAC inhibitors, and all of them showed potent anticancer activities toward cancer cell lines. The studies of MD simulation indicated that both surface recognition and metal binding domains of them were critical for their inhibitory activities. The hydrophobic interactions between HDAC8 and cyclic tetrapeptides were great important for stabilizing the complexes, but slightly change of hydrophobicity in surface recognition domain by introducing methylene group on the aromatic ring at L-Phe position seemed no obvious change for their anticancer activities. Based on the details of interaction between cyclic tetrapeptides and HDAC8, we can design some new cyclic tetrapeptides with different surface recognition and metal binding domains as potent HDAC inhibitors.

### 5.4 Experimental

**General:** Unless otherwise noted, all solvents and reagents were reagent grade and used without purification. All compounds were routinely checked by thin layer chromatography (TLC) or high performance liquid chromatography (HPLC). Analytical HPLC were performed on a Hitachi or Agilent 1100 instrument equipped with a chromolith performance RP-18e column (4.6 × 100 mm, Merck). The mobile phases used were A: H<sub>2</sub>O and 0.1% TFA, B: CH<sub>3</sub>CN with 0.1% TFA using a solvent gradient of 10% A to 100% B over 15 min with detection at 220 nm with a flow rate of 2 mL/min. TLC was performed on aluminium-backed silica gel plates (Merck DC-Alufolien Kieselgel 60 F<sub>254</sub>) with spots visualized by UV light and heat. Flash chromatography was performed using silica gel 60 (230-400) eluting with solvents as indicated. Fast atom bombardment mass spectra (FAB-MS) and high resolution fast atom

bombardment mass spectra (HR-FAB-MS) were measured on a JEOL JMS-SX 102A. NMR spectra were recorded on a VarianINO VA400 MHz spectrometer. All NMR spectra were measured in CDCl<sub>3</sub> solutions with reference to TMS. All <sup>1</sup>H shifts are given in parts per millions (s = singlet; d = doublet; t = triplet; m = multiplet). Peptide was coupled using standard solution-phase chemistry with dicyclohexylcarbodiimide (DCC), N-Hydroxybenzotriazole (HOBt). Peptide cyclization was mediated by *N*-[(dimethylamino)-1*H*-1,2,3-triazolo[4,5-*b*]pyridin-1-yl-methylene]-*N*-methyl-methanaminium hexafluorophosphate *N*-oxide (HATU). The cell lines for bioactive assay were all from Shanghai Institute of Biochemistry and Cell Biology, SIBS, CAS. The PRPMI 1640 for cell culture was purchased from Gibco, and MTT was from Hy-Clone.

#### **5.4.1 Synthesis of *cyclo*-(*L*-Am7(S2Py)-Aib-*L*-Phe-*D*-Pro-)**

##### **5.4.1.1 Synthesis of Boc-*D*-Pro-OBzl (MW = 305.35):**

Boc-*D*-Pro-OH (18.87 g, 87 mmol) was dissolved into DMF (450 mL). To the solution was added benzyl bromide (12.4 mL, 104.4 mmol) and triethyl amine (14.6 mL, 104.4 mmol). After stirring for overnight at room temperature, the solvent was removed by evaporation. Finally crude product was purified by silica gel chromatography using a mixture of chloroform and methanol (99/1 v/v) to yield pure Boc-*D*-Pro-OBzl (24.1 g, 79.1 mmol, 91%), HPLC: r.t. 8.68 min.

##### **5.4.1.2 Synthesis of Boc-*L*-Phe-*D*-Pro-OBzl (MW = 452.54):**

Boc-*D*-Pro-OBzl (24.1 g, 79.1 mmol) was dissolved in TFA (115 mL) and left standing on ice for 1 hour. After the reaction solution was concentrated by evaporation, ether was added to the residue and solidified to obtain white solid of TFA·*H*-*D*-Pro-OBzl (24.9 g, 78 mmol, 98.6%), HPLC: r.t. 4.3 min. While cooling on ice, HOBt·H<sub>2</sub>O (0.47 g, 3.48 mmol), DCC (0.72 g, 3.48 mmol) and triethyl amine (0.41 mL, 2.9 mmol) were added to DMF (7 mL) containing Boc-*L*-Phe-OH (0.79 g, 2.9 mmol) and TFA·*H*-*D*-Pro-OBzl (2.01 g, 2.9 mmol). After stirring for overnight, DMF was removed by evaporation; residue dissolved in ethyl acetate, and then successively washed with an aqueous 10% citric acid solution, an aqueous 4% sodium bicarbonate solution, and brine. After drying over MgSO<sub>4</sub> and concentrating, the resulting oily substance was purified by silica gel chromatography using a mixture of chloroform and

methanol (99:1 v/v) to obtain Boc-L-Phe-D-Pro-OBzl (1.27 g, 2.8 mmol, 97%) as oily compound. TLC: Rf 0.86 (CHCl<sub>3</sub>/MeOH=9/1), HPLC: r.t.8.9 min.

#### **5.4.1.3 Synthesis of Boc-Aib-L-Phe-D-Pro-OBzl (MW = 537.65):**

The dipeptide Boc-L-Phe-D-Pro-OBzl (1.27 g, 2.8 mmol) was dissolved in dioxane (7 mL) and added 4N HCl/dioxane (7mL). After 2 hours at room temperature, the reaction solution was removed by evaporation, ether was added to the residue and solidified to obtain white solid of HCl·H-L-Phe-D-Pro-OBzl (1.09 g, 2.8 mmol, 100%), HPLC: r.t. 5.73 min. To a cooled solution of HCl·H-Phe-D-Pro-OBzl (1.09 g, 2.8 mmol) and Boc-Aib-OH (680 mg, 3.36 mmol) in DMF (6 mL) were added HOBt·H<sub>2</sub>O (470 mg, 3.36 mmol), HBTU (1.49 g, 3.92 mmol), DIEA (0.97 mL, 5.6 mmol). After stirring for overnight, check with TLC (CHCl<sub>3</sub>/MeOH=9/1), DMF was removed by evaporation; residue dissolved in ethyl acetate, and then successively washed with an aqueous 10% citric acid solution, an aqueous 4% sodium bicarbonate solution and brine. After drying over MgSO<sub>4</sub> and concentrating, the resulting oily substance was purified by silica gel chromatography using a mixture of chloroform and methanol (99:1 v/v) to obtain Boc-Aib-L-Phe-D-Pro-OBzl (1.27 g, 2.37 mmol, 84%) as oily compound. TLC: Rf 0.84 (CHCl<sub>3</sub>/MeOH =9/1), HPLC: r.t. 8.82 min.

#### **5.4.1.4 Synthesis of Boc-L-Ab7-Aib-L-Phe-D-Pro-OBzl (MW = 543.73):**

The tripeptide Boc-Aib-L-Phe-D-Pro-OBzl (1.27 g, 2.37 mmol) was dissolved in dioxane (6 mL) and added 4N HCl/dioxane (6 mL). After 2 hours at room temperature, the reaction solution was removed by evaporation, ether was added to the residue and solidified to obtain white solid of HCl·H-Aib-L-Phe-D-Pro-OBzl (1.12 g, 2.37 mmol, 100%), HPLC: r.t. 6.10 min. While cooling on ice, HOBt·H<sub>2</sub>O (0.38 g, 4.6 mmol), DCC (0.59 g, 4.6 mmol) and triethyl amine (0.33 mL, 2.37 mmol) were added to DMF (6 mL) containing HCl·H-Aib-L-Phe-D-Pro-OBzl (1.12 g, 2.37 mmol) and Boc-L-Ab7-OH (1.38 g, 3.55 mmol) . After stirring for overnight, DMF was removed by evaporation; residue dissolved in ethyl acetate, and then successively washed with 10% citric acid solution, 4% sodium bicarbonate solution and brine. After drying over MgSO<sub>4</sub> and concentrating, the resulting oily substance was purified by silica gel chromatography using a mixture of chloroform and methanol (99:1 v/v) to obtain Boc-L-Ab7-Aib-L-Phe-D-Pro-OBzl (662 mg, 0.9 mmol, 38%) as oily compound. TLC: Rf 0.9 (CHCl<sub>3</sub>/MeOH=9/1), HPLC: r.t.10.17 min.

#### 5.4.1.5 Synthesis of *cyclo(-L-Ab7-Aib-L-Phe-D-Pro-)* (MW = 535.47):

Boc-L-Ab7-Aib-L-Phe-D-Pro-OBzl (662 mg, 0.9 mmol) was dissolved in methanol (5 mL) and subjected to catalytic hydrogenation in presence of the catalyst Pd-C (60 mg). After 8 hours, the catalyst was filtered and reaction solution was removed by evaporation. The residue Boc-L-Ab7-Aib-L-Phe-D-Pro-OH (574 mg, 0.89 mmol, 99%, HPLC: r.t. 7.85 min) was obtained. Boc-L-Ab7-Aib-L-Phe-D-Pro-OH (574 mg, 0.89 mmol) was dissolved in TFA (3 mL) and left standing on ice for 1 hour. After evaporation of TFA, the residue was solidified by trituration with ether and petroleum ether to yield TFA·H-L-Ab7-Aib-L-Phe-D-Pro-OH (608 mg, 0.89 mmol, 100%), HPLC: r.t. 5.40 min. To a volume of DMF (100 mL) TFA·H-L-Ab7-Aib-L-Phe-D-Pro-OH (608 mg, 0.89 mmol), HATU (500 mg, 1.32 mmol) and DIEA (0.38 mL, 2.19 mmol) were added in five aliquots with 30 min time interval, while the solution was stirred vigorously. After the final addition the reaction mixture was allowed to stir for an additional hour. Completion of the reaction was monitored by HPLC. DMF was removed by evaporation. The crude cyclic tetrapeptide was dissolved in ethyl acetate and was successively washed with 10% citric acid, 4% sodium bicarbonate and brine. Finally the ethyl acetate solution was dried over anhydrous MgSO<sub>4</sub> and filtered. After evaporation of ethyl acetate, the residue was purified by silica gel chromatography using a mixture of chloroform and methanol (99:1 v/v) to yield *cyclo(-L-Ab7-Aib-L-Phe-D-Pro-)* (220 mg, 0.4 mmol, 46%) as white foam. HPLC: r.t. 7.98 min.

#### 5.4.1.6 Synthesis of *cyclo(-L-Am7(S2Py)-Aib-L-Phe-D-Pro-)* (MW = 597.79):

Potassium thioacetate (80 mg, 0.62 mmol) was added to DMF (2 mL) containing cyclic tetrapeptide *cyclo(-L-Ab7-Aib-L-Phe-D-Pro-)* (220 mg, 0.4 mmol) and this was reacted for 4 hours. The reaction solution was concentrated, dissolved in ethyl acetate, and was successively washed with aqueous 10% citric acid solution and brine. After drying over MgSO<sub>4</sub> and concentrating the solvent yielded the thioester, *cyclo(-L-Am7(acetyl)-Aib-L-Phe-D-Pro-)* (184 mg, 0.35 mmol, 85%), TLC: R<sub>f</sub> 0.84, HPLC: r.t. 7.83 min. Subsequent treatment of thioester with MeNH<sub>2</sub>/ methanol (0.20 mL, 1.7 mmol) in the presence of 2,2'-dipyridyl disulfide (120 mg, 0.45 mmol) gave product *cyclo(-L-Am7(S2Py)-Aib-L-Phe-D-Pro-)*, which was purified by silica gel chromatography (99:1 v/v) and obtained as white foam (180 mg, 0.3 mmol, 87%). The yield: 10.4%, TLC: R<sub>f</sub> 0.83, HPLC: r.t. 8.33 min. HR-FAB-MS [M+H]<sup>+</sup> 598.2478 for C<sub>30</sub>H<sub>40</sub>O<sub>4</sub>N<sub>5</sub>S<sub>2</sub> (calcd 598.2522). <sup>1</sup>H NMR(400 MHz, CDCl<sub>3</sub>): δ 1.27(m, 2H), 1.34(s, 3H),

1.42(m, 2H), 1.61(m, 1H), 1.71(m, 1H), 1.77(s, 3H), 1.88(m, 1H), 2.168(m, 1H), 2.249(m, 1H), 2.775(t, 2H), 2.963(m,1H), 3.226(m, 2H), 4.19(m, 1H), 4.66(d,  $J=6\text{Hz}$ , 2H), 5.17(m, 1H), 6.06(s, 1H), 7.11(m, 1H), 7.21(d,  $J=4\text{Hz}$ , 1H), 7.25(m, 5H), 7.51(d,  $J=10\text{Hz}$ , 1H), 7.66(m, 1H), 7.73(d,  $J=8\text{ Hz}$ , 1H), 8.47(d,  $J=5\text{ Hz}$ , 1H).  $^{13}\text{C}$  NMR(400 MHz,  $\text{CDCl}_3$ ):  $\delta$  23.57, 24.75, 25.02, 25.09, 26.47, 28.06, 28.61, 28.83, 35.82, 38.66, 46.99, 53.43, 54.3, 57.78, 58.81, 119.62, 120.55, 126.72, 128.62, 128.62, 129.04, 129.04, 137.01, 137.04, 149.6, 160.54, 171.85, 172.84, 174.33, 175.63.

#### 5.4.2 Synthesis of *cyclo(-L-Am7(S2Py)-Aib-L-Phe(2-Me)-D-Pro-)*

##### 5.4.2.1 Synthesis of Boc-L-Phe(2-Me)-D-Pro-OBzl (MW = 466.57):

While cooling on ice, HOBt·H<sub>2</sub>O (1.84 g, 12 mmol), DCC (2.47 g, 12 mmol) and triethyl amine (1.4 mL, 10 mmol) were added to DMF (20 mL) containing Boc-L-Phe(2-Me)-OH (3.35 g, 12 mmol) and TFA·H-D-Pro-OBzl (3.19 g, 10 mmol). After stirring for overnight, DMF was removed by evaporation; residue dissolved in ethyl acetate, and then successively washed with an aqueous 10% citric acid solution, an aqueous 4% sodium bicarbonate solution, and brine. After drying over MgSO<sub>4</sub> and concentrating, the resulting oily substance was purified by silica gel chromatography using a mixture of chloroform and methanol (99:1 v/v) to obtain Boc-L-Phe(2-Me)-D-Pro-OBzl (3.45 g, 7.4 mmol, 73.9%) as oily compound. TLC: R<sub>f</sub> 0.85 ( $\text{CHCl}_3/\text{MeOH}=9/1$ ), HPLC: r.t. 11.1 min.

##### 5.4.2.2 Synthesis of Boc-Aib-L-Phe(2-Me)-D-Pro-OBzl (MW = 551.67):

The dipeptide Boc-L-Phe(2-Me)-D-Pro-OBzl (3.45 g, 7.4 mmol) was dissolved in TFA(15 mL). After 1 hour in ice bath, the reaction solution was removed by evaporation, ether was added to the residue and solidified to obtain white solid of TFA·H-L-Phe(2-Me)-D-Pro-OBzl (4.3 g, 7.4 mmol, 100%). To a cooled solution of TFA·H-Phe(2-Me)-D-Pro-OBzl (4.3 g, 7.4 mmol) and Boc-Aib-OH (1.8 g, 8.7 mmol) in DMF (30 mL) were added HOBt (1.36 g, 8.7 mmol), HBTU (4.2 g, 11.1 mmol), DIEA (3.6mL, 20.7 mmol). After stirring for overnight, check with TLC ( $\text{CHCl}_3/\text{MeOH}=9/1$ ), DMF was removed by evaporation; residue dissolved in ethyl acetate, and then successively washed with 10% citric acid solution, 4% sodium bicarbonate solution and brine. After drying over MgSO<sub>4</sub> and concentrating, the resulting oily substance was purified by silica gel chromatography using a mixture of chloroform and methanol (99:1 v/v) to obtain



Boc-Aib-L-Phe(2-Me)-D-Pro-OBzl (2.28 g, 4.1 mmol, 55.9%) as oily compound. TLC: Rf 0.85 (CHCl<sub>3</sub>/MeOH=9/1), HPLC: r.t. 10.8 min.

#### 5.4.2.3 Synthesis of Boc-L-Ab7-Aib-L-Phe(2-Me)-D-Pro-OBzl (MW = 757.75):

The tripeptide Boc-Aib-L-Phe(2-Me)-D-Pro-OBzl (2.28 g, 4.13 mmol) was dissolved in TFA (8 mL). After 1 hour in ice bath, the reaction solution was removed by evaporation, ether was added to the residue and solidified to obtain white solid of TFA·H-Aib-L-Phe(2-Me)-D-Pro-OBzl (2.4 g, 4.13 mmol, 100%). While cooling on ice, HOBt·H<sub>2</sub>O (632 mg, 4.13 mmol), DCC (1.0 g, 5.0 mmol) and triethyl amine (0.64 mL, 4.5 mmol) were added to DMF (5 mL) containing TFA·H-Aib-L-Phe(2-Me)-D-Pro-OBzl (2.4 g, 4.1 mmol) and Boc-L-Ab7-OH (1.5 g, 4.5 mmol). After stirring for overnight, DMF was removed by evaporation; residue dissolved in ethyl acetate, and then successively washed with 10% citric acid solution, 4% sodium bicarbonate solution, and brine. After drying over MgSO<sub>4</sub> and concentrating, the resulting oily substance was purified by silica gel chromatography using a mixture of chloroform and methanol (99:1 v/v) to obtain Boc-L-Ab7-Aib-L-Phe(2-Me)-D-Pro-OBzl (1.97 g, 2.6 mmol, 63%) as oily compound. TLC: Rf 0.8 (CHCl<sub>3</sub>/MeOH=9/1), HPLC: r.t. 10.9 min.

#### 5.4.2.4 Synthesis of *cyclo*-(L-Ab7-Aib-L-Phe(2-Me)-D-Pro-) (MW = 549.50):

Boc-L-Ab7-Aib-L-Phe(2-Me)-D-Pro-OBzl (1.97 g, 2.6 mmol) was dissolved in methanol (13 mL) and subjected to catalytic hydrogenation in presence of the catalyst Pd-C (130 mg). After 6 hours, the reaction was checked by TLC (CHCl<sub>3</sub>/MeOH/ CH<sub>3</sub>COOH=90/10/2), the catalyst was filtered and reaction solution was removed by evaporation. The residue Boc-L-Ab7-Aib-L-Phe(2-Me)-D-Pro-OH (1.53 g, 2.3 mmol, 88%) was obtained. Boc-L-Ab7-Aib-L-Phe(2-Me)-D-Pro-OH (1.53 g, 2.3 mmol) was dissolved in TFA (5 mL) and left standing on ice for 1 hour. After evaporation of TFA, the residue was solidified by trituration with ether and petroleum ether to yield TFA·H-L-Ab7-Aib-L-Phe(2-Me)-D-Pro-OH (1.6 g, 2.3 mmol, 100%). To a volume of DMF (230 mL) TFA·H-L-Ab7-Aib-L-Phe-D-Pro-OH (1.6 g, 2.3 mmol), HATU (1.31 mg, 3.4 mmol) and DIEA (1.0 mL, 5.7 mmol) were added in five aliquots with 30 min time interval, while the solution was stirred vigorously. After the final addition the reaction mixture was allowed to stir for an additional hour. Completion of the reaction was monitored by HPLC. DMF was removed by evaporation. The crude cyclic tetrapeptide was dissolved in ethyl acetate and was successively washed with 10% citric acid, 4% sodium bicarbonate and brine. Finally the ethyl acetate solution was dried over anhydrous MgSO<sub>4</sub> and filtered. After

evaporation of ethyl acetate, the residue was purified by silica gel chromatography using a mixture of chloroform and methanol (99:1 v/v) to yield *cyclo(-L-Ab7-Aib-L-Phe(2-Me)-D-Pro-)* (493 mg, 0.9 mmol, 39%) as white foam. HPLC: r.t. 8.08 min.

#### 5.4.2.5 Synthesis of *cyclo(-L-Am7(S2Py)-Aib-L-Phe(2-Me)-D-Pro-)* (MW=611.82)

Potassium thioacetate (145 mg, 1.28 mmol) was added to DMF (4 mL) containing cyclic tetrapeptide *cyclo(-L-Ab7-Aib-L-Phe(2-Me)-D-Pro-)* (493 mg, 0.9 mmol) and this was reacted for 4 hours. The reaction solution was concentrated, dissolved in ethyl acetate, and was successively washed with 10% citric acid solution, 4% sodium bicarbonate and brine. After drying over MgSO<sub>4</sub> and concentrating the solvent yielded the thioester, *cyclo(-L-Am7(acetyl)-Aib-L-Phe(2Me)-D-Pro-)* (451 mg, 0.8 mmol, 92%). Subsequent treatment of thioester with MeNH<sub>2</sub>/ methanol (0.45 mL, 4.1 mmol) in the presence of 2,2'-dipyridyl disulfide (364 mg, 1.7 mmol) gave product *cyclo(-L-Am7(S2Py)-Aib-L-Phe(2-Me)-D-Pro-)*, which was purified by silica gel chromatography (99:1 v/v) and obtained as white foam (449 mg, 0.7 mmol, 88%), The yield: 7.3%, HPLC: r.t. 8.42 min. HR-FAB-MS [M+H]<sup>+</sup> 612.2722 for C<sub>31</sub>H<sub>42</sub>O<sub>4</sub>N<sub>5</sub>S<sub>2</sub> (calcd 612.2679). <sup>1</sup>H NMR(400 MHz, CDCl<sub>3</sub>) : δ 1.08(m, 1H), 1.32(m, 1H), 1.34(s, 3H), 1.37(m, 3H), 1.60(m, 1H), 1.66(s, 3H), 1.70(m, 2H), 1.77(s, 2H), 1.93(m, 2H), 2.31(m, 1H), 2.39(s, 3H), 2.78(t, 1H), 2.962(m, 1H), 3.231(m, 1H), 3.439(m, 1H), 3.848(m, 1H), 4.176(m, 1H), 4.676(m, 1H), 5.19(m, 1H), 6.012(s, 1H), 7.113(m, 1H), 7.133(m, 1H), 7.263(s, 4H), 7.517(d, J=10Hz, 1H), 7.651(m, 1H), 7.71(m, 1H), 8.46(dd, J=4Hz, 1H). <sup>13</sup>C NMR (400 MHz, CDCl<sub>3</sub>): δ 19.72, 23.70, 24.86, 25.08, 26.46, 28.17, 28.72, 29.35, 33.02, 34.08, 38.72, 46.97, 52.35, 54.44, 57.87, 58.87, 119.69, 120.20, 126.20, 126.91, 129.43, 130.55, 135.35, 136.60, 137.15, 149.71, 160.62, 171.97, 173.03, 174.53, 175.80.

#### 5.4.3 Synthesis of *cyclo(-L-Am7(S2Py)-Aib-L-Phe(4-Me)-D-Pro-)*

##### 5.4.3.1 Synthesis of Z-D-Pro-O<sup>t</sup>Bu (MW = 305.37):

Z-D-Pro-OH (4.9 g, 20 mmol) was dissolved into *t*-butyl alcohol (50 mL). To the solution was added (Boc)<sub>2</sub>O (8.72 g, 40 mmol) and 4-methylaminopyridine (733 mg, 6 mmol). After 2 hours reaction at room temperature, the solution was concentrated. Finally crude product was purified by silica gel chromatography using a mixture of ethyl acetate and hexane (1/8 v/v) to yield pure Z-D-Pro-O<sup>t</sup>Bu (5.8 g, 19.2 mmol, 96%), HPLC: r.t. 8.08 min.

##### 5.4.3.2 Synthesis of Z-L-Phe(4-Me)-D-Pro-O<sup>t</sup>Bu (MW = 452.54):

Z- D-Pro-O<sup>t</sup>Bu (1.83 g, 6 mmol) was dissolved in acetic acid (12 mL) and subjected to catalytic hydrogenation in presence of the catalyst Pd-C (300 mg). After 18 hours, the reaction was checked by TLC (CHCl<sub>3</sub>/MeOH/CH<sub>3</sub>COOH=90/10/2), the catalyst was filtered and reaction solution was removed by evaporation. The residue was dissolved in ethyl acetate (30 mL), washed with 2 M Na<sub>2</sub>CO<sub>3</sub> solution (10 mL), ethyl acetate was evaporated to get H- D-Pro-O<sup>t</sup>Bu (2.13 g, 4.7 mmol, 78%), TLC: R<sub>f</sub> 0.6. While cooling on ice, DCC (1.17 g, 5.64 mmol) and HOBt·H<sub>2</sub>O (640 mg, 4.7 mmol) were added to DMF (10 mL) containing Z-L-Phe(4-Me)-OH (720 mg, 4.7 mmol) and H-D-Pro-O<sup>t</sup>Bu (2.13 g, 4.7 mmol). After stirring for 15 hours, DMF was removed by evaporation; residue dissolved in ethyl acetate, and then successively washed with 10% citric acid solution, 4% sodium bicarbonate solution and brine. After drying over MgSO<sub>4</sub> and concentrating, the resulting oily substance was purified by silica gel chromatography using a mixture of chloroform and methanol (99:1 v/v) to obtain Z-L-Phe(4-Me)-D-Pro-O<sup>t</sup>Bu (2.15 g, 4.6 mmol, 98%) as oily compound. TLC: R<sub>f</sub>, 0.9 (CHCl<sub>3</sub>/MeOH= 9/1), HPLC: r.t. 8.92 min.

#### **5.4.3.3 Synthesis of Z-Aib-L-Phe(4-Me)-D-Pro-O<sup>t</sup>Bu (MW = 551.67):**

Z-L-Phe(4-Me)-D-Pro-O<sup>t</sup>Bu (2.15 g, 4.6 mmol) was dissolved in acetic acid (10 mL) and subjected to catalytic hydrogenation in presence of the catalyst Pd-C (360 mg). After 18 hours, the reaction was checked by TLC (CHCl<sub>3</sub>/MeOH/CH<sub>3</sub>COOH= 90/10 /2), the catalyst was filtered and reaction solution was removed by evaporation. The residue was dissolved in ethyl acetate (30 mL), washed with 2 M Na<sub>2</sub>CO<sub>3</sub> solution (10 mL), ethyl acetate was evaporated to get H- L-Phe(4-Me)-D-Pro-O<sup>t</sup>Bu (2.04 g, 3.7 mmol, 82.5%). To a cooled solution of H- L-Phe(4-Me)-D-Pro-O<sup>t</sup>Bu (1.23 g, 3.7 mmol) and Z-Aib-OH (880 mg, 3.7 mmol) in DMF (8 mL) were successively added DCC (950 mg, 4.4 mmol), HOBt.H<sub>2</sub>O (500 mg, 3.7 mmol). After stirring for 15 hours, DMF was removed by evaporation; residue dissolved in ethyl acetate, and then successively washed with an aqueous 10% citric acid solution, an aqueous 4% sodium bicarbonate solution and brine. After drying over MgSO<sub>4</sub> and concentrating, the resulting oily substance was purified by silica gel chromatography using a mixture of chloroform and methanol (99:1 v/v) to obtain Z-Aib-L-Phe(4-Me)-D-Pro-O<sup>t</sup>Bu(2.04 g, 3.7 mmol, 100%). TLC: R<sub>f</sub> 0.86 (CHCl<sub>3</sub>/MeOH=9/1) , HPLC: r.t. 8.61 min.

#### **5.4.3.4 Synthesis of Boc-L-Ab7-Aib-L-Phe(4-Me)-D-Pro-O<sup>t</sup>Bu (MW = 723.74):**

The tripeptide Z-Aib-L-Phe(4-Me)-D-Pro-O<sup>t</sup>Bu(2.04 g, 3.7 mmol) was subjected to catalytic hydrogenation with Pd-C (300 mg) in acetic acid (8 mL). After 18 hours, the reaction was checked by TLC (CHCl<sub>3</sub>/MeOH/CH<sub>3</sub>COOH=90/10/2), the catalyst was filtered and reaction solution was removed by evaporation. The free amine was taken into ethyl acetate (30 mL) by the aid of 2M Na<sub>2</sub>CO<sub>3</sub> solution (10 mL). After dried over anhydrous Na<sub>2</sub>CO<sub>3</sub> ethyl acetate solution was evaporated to obtain H-Aib-L-Phe(4-Me)-D-Pro-O<sup>t</sup>Bu (690 mg, 1.8 mmol, 50%), HPLC: r.t. 5.54 min. To a cooled solution of H-Aib-L-Phe(4-Me)-D-Pro-O<sup>t</sup>Bu (690 mg, 1.8 mmol) and Boc-L-Ab7-OH (650 mg, 2.1 mmol) in DMF (4 mL) were successively added DCC (440 mg, 2.1 mmol), HOBt·H<sub>2</sub>O (240 mg, 1.8 mmol). After stirring for 15 hours, DMF was removed by evaporation; residue dissolved in ethyl acetate, and then successively washed with 10% citric acid solution, 4% sodium bicarbonate solution and brine. After drying over MgSO<sub>4</sub> and concentrating, the resulting oily substance was purified by silica gel chromatography using a mixture of chloroform and methanol (99:1 v/v) to obtain Boc-L-Ab7-Aib-L-Phe(4-Me)-D-Pro-O<sup>t</sup>Bu(941 mg, 1.3 mmol, 75%). TLC: R<sub>f</sub> 0.84 (CHCl<sub>3</sub>/MeOH=9/1), HPLC: r.t. 9.48 min.

#### 5.4.3.5 Synthesis of *cyclo*(-L-Ab7-Aib-L-Phe(4-Me)-D-Pro-) (MW = 549.50):

Boc-L-Ab7-Aib-L-Phe(4-Me)-D-Pro-O<sup>t</sup>Bu (941 mg, 1.3 mmol) was dissolved in TFA (4 mL) and left standing on ice for 3 hours. After evaporation of TFA, the residue was solidified by trituration with ether to yield TFA·H-L-Ab7-Aib-L-Phe(4-Me)-D-Pro-OH (800 mg, 1.1 mmol, 85%), HPLC: r.t. 5.63 min. To a volume of DMF (110 mL) TFA·H-L-Ab7-Aib-L-Phe(4-Me)-D-Pro-OH (800 mg, 1.1 mmol), HATU (630 mg, 1.65 mmol) and DIEA (0.46 mL, 2.64 mmol) were added in five aliquots with 30 min time interval, while the solution was stirred vigorously. After the final addition the reaction mixture was allowed to stir for an additional hour. Completion of the reaction was monitored by HPLC. DMF was removed by evaporation. The crude cyclic tetrapeptide was dissolved in ethyl acetate and was successively washed with 10% citric acid, 4% sodium bicarbonate and brine. Finally the ethyl acetate solution was dried over anhydrous MgSO<sub>4</sub> and filtered. After evaporation of ethyl acetate, the residue was purified by silica gel chromatography using a mixture of chloroform and methanol (99:1 v/v) to yield *cyclo*(-L-Ab7-Aib-L-Phe(4-Me)-D-Pro-) (385 mg, 0.7 mmol, 65%) as white foam. TLC: R<sub>f</sub> 0.75 (CHCl<sub>3</sub>/MeOH=9/1), HPLC: r.t. 7.90 min.

#### 5.4.3.6 Synthesis of *cyclo*(-L-Am7(S2Py)-Aib-L-Phe(4-Me)-D-Pro-)(MW = 611.82)

Potassium thioacetate (120 mg, 1.05 mmol) was added to DMF (2 mL) containing cyclic tetrapeptide *cyclo(-L-Ab7-Aib-L-Phe(4-Me)-D-Pro-)* (385 mg, 0.7 mmol) and this was reacted for 4 hours. The reaction solution was concentrated, dissolved in ethyl acetate, and was successively washed with 10% citric acid solution, 4% sodium bicarbonate and brine. After drying over MgSO<sub>4</sub> and concentrating the solvent yielded the thioester, *cyclo(-L-Am7(acetyl)-Aib-L-Phe(4-Me)-D-Pro-)* (324 mg, 0.6 mmol, 85%), HPLC: r.t. 7.74 min. Subsequent treatment of thioester with MeNH<sub>2</sub>/methanol (0.32 mL, 3 mmol) in the presence of 2,2'-dipyridyl disulfide (200 mg, 0.9 mmol) gave product, which was purified by silica gel chromatography and obtained as white foam *cyclo(-L-Am7(S2Py)-Aib-L-Phe(4-Me)-D-Pro-)* (281 mg, 0.46 mmol, 76%). The yield: 9.2%, TLC: R<sub>f</sub> 0.77, HPLC: r.t. 8.86 min. HR-FAB-MS [M+H]<sup>+</sup> 612.2680 for C<sub>31</sub>H<sub>42</sub>O<sub>4</sub>N<sub>5</sub>S<sub>2</sub> (calcd 612.2679). <sup>1</sup>H NMR (400 MHz; CDCl<sub>3</sub>): δ 0.86(m, 1H), 1.28(m, 3H), 1.34(s, 3H), 1.42(m, 2H), 1.70(m, 3H), 1.78(s, 3H), 1.80(m, 2H), 2.17(m, 1H), 2.26(s, 3H), 2.33(m, 1H), 2.78(t, 1H), 2.88(m, 1H), 3.17(m, 1H), 3.27(m, 2H), 4.17(m, 1H), 4.66(d, *J*=6Hz, 1H), 5.15(m, 1H), 5.96(s, 1H), 6.84(s, 3H), 7.09(m, 2H), 7.27(s, 1H), 7.49(d, *J*=10Hz, 1H), 7.66(t, 1H), 7.72(d, *J*=8Hz, 1H), 8.46(d, *J*=4Hz, 1H). <sup>13</sup>C NMR (400 MHz, CDCl<sub>3</sub>): δ 21.05, 23.57, 24.76, 25.04, 25.1, 26.53, 28.08, 28.62, 28.79, 35.37, 38.67, 47.00, 53.49, 54.26, 57.78, 58.84, 119.61, 120.54, 128.88, 128.88, 129.30, 129.30, 133.89, 136.21, 136.99, 149.62, 160.56, 171.85, 172.90, 174.29, 175.63.

#### 5.4.4 Synthesis of *cyclo(-L-Am7(S2Py)-Aib-L-Phe(3,5-2Me)-D-Pro-)*

##### 5.4.4.1 Synthesis of Boc-L-Phe(3,5-2Me)-D-Pro-OBzl (MW = 480.60):

While cooling on ice, HOBt·H<sub>2</sub>O (1.23 g, 8.0 mmol), DCC (1.98 g, 9.6 mmol) and triethyl amine (1.23 mL, 8.8 mmol) were added to DMF (16 mL) containing Boc-L-Phe(3,5-2Me)-OH (2.45 g, 8.3 mmol) and TFA·H-D-Pro-OBzl (1.93 g, 8.0 mmol). After stirring for overnight, DMF was removed by evaporation; residue dissolved in ethyl acetate, and then successively washed with an aqueous 10% citric acid solution, an aqueous 4% sodium bicarbonate solution, and brine. After drying over MgSO<sub>4</sub> and concentrating, the resulting oily substance was purified by silica gel chromatography using a mixture of chloroform and methanol (99:1 v/v) to obtain Boc-L-Phe(3,5-2Me)-D-Pro-OBzl (3.83 g, 8.0 mmol, 99%) as oily compound. TLC: R<sub>f</sub> 0.85 (CHCl<sub>3</sub>/MeOH =9/1), HPLC: r.t. 9.27 min, 98%.

##### 5.4.4.2 Synthesis of Boc-Aib-L-Phe(3,5-2Me)-D-Pro-O<sup>t</sup>Bu (MW = 565.70):

The dipeptide Boc-L-Phe(3,5-2Me)-D-Pro-OBzl (3.83 g, 8.0 mmol) was dissolved in dioxane (15 mL) and added 4N HCl/dioxane (15mL). After 2 hours at room temperature, the reaction solution was removed by evaporation, ether was added to the residue and solidified to obtain white solid of HCl·H-L-Phe(3,5-2Me)-D-Pro-OBzl (3.33 g, 8.0 mmol, 100%, HPLC: r.t. 5.91 min, 96%). To a cooled solution of HCl·H-L-Phe(3,5-2Me)-D-Pro-OBzl (3.33 g, 8.0 mmol) and Boc-Aib-OH (1.90 g, 8.0 mmol) in DMF (16 mL) were added HOBt·H<sub>2</sub>O (1.23 g, 8.0 mmol), HBTU(3.03 g, 8.0 mmol), DIEA (1.73 mL, 12.0 mmol). After stirring for overnight, check with TLC (CHCl<sub>3</sub>/ MeOH=9/1), DMF was removed by evaporation; residue dissolved in ethyl acetate, and then successively washed with 10% citric acid solution, 4% sodium bicarbonate solution and brine. After drying over MgSO<sub>4</sub> and concentrating, the resulting oily substance was purified by silica gel chromatography using a mixture of chloroform and methanol (99:1 v/v) to obtain Boc-Aib-L-Phe(3,5-2Me)-D-Pro-OBzl (1.93 g, 3.4 mmol, 43%) as oily compound. TLC: Rf 0.85 (CHCl<sub>3</sub>/MeOH=9/1), HPLC: r.t. 8.86 min, 89%.

#### 5.4.4.3 Synthesis of Boc-L-Ab7-Aib-L-Phe(3,5-2Me)-D-Pro-O<sup>t</sup>Bu (MW =771.78):

The tripeptide Boc-Aib-L-Phe(3,5-2Me)-D-Pro-OBzl (1.93 g, 3.4 mmol) was dissolved in dioxane (7 mL) and added 4N HCl/dioxane (7 mL). After 2 hours at room temperature, the reaction solution was removed by evaporation, ether was added to the residue and solidified to obtain white solid of HCl·H-Aib-L-Phe(3,5-2Me)-D-Pro-OBzl (1.71 g, 3.4 mmol, 100%, HPLC: r.t. 6.05 min, 95%). While cooling on ice, HOBt·H<sub>2</sub>O (521 mg, 3.4 mmol), DCC (1.03 g, 5.0 mmol) and triethyl amine (0.74 mL, 5.1 mmol) were added to DMF (7 mL) containing HCl·H-Aib-L-Phe(3,5-2Me)-D-Pro-OBzl (1.93 g, 3.4 mmol) and Boc-L-Ab7-OH (1.13 g, 3.4 mmol). After stirring for overnight, DMF was removed by evaporation; residue dissolved in ethyl acetate, and then successively washed with 10% citric acid solution, 4% sodium bicarbonate solution, and brine. After drying over MgSO<sub>4</sub> and concentrating, the resulting oily substance was purified by silica gel chromatography using a mixture of chloroform and methanol (99:1 v/v) to obtain Boc-L-Ab7-Aib-L-Phe(3,5-2Me)-D-Pro-OBzl (1.48 g, 1.9 mmol, 58%) as oily compound. TLC: Rf 0.8 (CHCl<sub>3</sub>/MeOH=9/1), HPLC: r.t. 9.56 min, 93%.

#### 5.4.4.4 Synthesis of *cyclo*-(L-Ab7-Aib-L-Phe(3,5-2Me)-D-Pro-) (MW = 563.53):

Boc-L-Ab7-Aib-L-Phe(3,5-2Me)-D-Pro-OBzl (1.48 g, 1.9 mmol) was dissolved in methanol (4 mL) and subjected to catalytic hydrogenation in presence of the catalyst Pd-C (100 mg). After 10 hours, the reaction was checked by TLC (CHCl<sub>3</sub>/MeOH/ CH<sub>3</sub>COOH=90/10/2), the catalyst

was filtered and reaction solution was removed by evaporation. The residue Boc-L-Ab7-Aib-L-Phe(3,5-2Me)-D-Pro-OH (1.30 g, 1.9 mmol, 100%) was obtained. Boc-L-Ab7-Aib-L-Phe(3,5-2Me)-D-Pro-OH (1.30 g, 1.9 mmol) was dissolved in TFA (4 mL) and left standing on ice for 1 hour. After evaporation of TFA, the residue was solidified by trituration with ether and petroleum ether to yield TFA·H-L-Ab7-Aib-L-Phe(3,5-2Me)-D-Pro-OH (1.22 g, 1.9 mmol, 100%). To a volume of DMF (200 mL) TFA·H-L-Ab7-Aib-L-Phe(3,5-2Me)-D-Pro-OH (1.22 g, 1.9 mmol), HATU (1.08 mg, 2.9 mmol) and DIEA (0.83 mL, 4.75 mmol) were added in five aliquots with 30 min time interval, while the solution was stirred vigorously. After the final addition the reaction mixture was allowed to stir for an additional hour. Completion of the reaction was monitored by HPLC. DMF was removed by evaporation. The crude cyclic tetrapeptide was dissolved in ethyl acetate and was successively washed with 10% citric acid, 4% sodium bicarbonate and brine. Finally the ethyl acetate solution was dried over anhydrous MgSO<sub>4</sub> and filtered. After evaporation of ethyl acetate, the residue was purified by silica gel chromatography using a mixture of chloroform and methanol (99:1 v/v) to yield *cyclo(-L-Ab7-Aib-L-Phe(3,5-2Me)-D-Pro-)* (533 mg, 1.0 mmol, 53%) as white foam. TLC: R<sub>f</sub> 0.9 (CHCl<sub>3</sub>/MeOH=9/1), HPLC: r.t. 8.23 min, 97%.

#### 5.4.4.5 Synthesis of *cyclo(-L-Am7(S2Py)-Aib-L-Phe(3,5-2Me)-D-Pro-)*(MW= 611.82):

Potassium thioacetate (145 mg, 1.28 mmol) was added to DMF (4 mL) containing cyclic tetrapeptide *cyclo(-L-Ab7-Aib-L-Phe(2-Me)-D-Pro-)* (493 mg, 0.9 mmol) and this was reacted for 4 hours. The reaction solution was concentrated, dissolved in ethyl acetate, and was successively washed with 10% citric acid solution, 4% sodium bicarbonate and brine. After drying over MgSO<sub>4</sub> and concentrating the solvent yielded the thioester, *cyclo(-L-Am7(acetyl)-Aib-L-Phe(3,5-2Me)-D-Pro-)* (481 mg, 0.9 mmol, 94%, HPLC: r.t. 8.10 min, 98%). Subsequent treatment of thioester with 9N MeNH<sub>2</sub> in 40% methanol (0.50 mL, 4.5 mmol) in the presence of 2,2'-dipyridyl disulfide (311 mg, 1.4 mmol) gave product *cyclo(-L-Am7(S2Py)-Aib-L-Phe(3,5-2Me)-D-Pro-)*, which was purified by silica gel chromatography (99:1 v/v) and obtained as white foam (204 mg, 0.3 mmol, 38%). The yield: 6.9%. TLC: R<sub>f</sub> 0.8, HPLC: r.t. 8.11 min, 98%. HR-FAB-MS: [M+H]<sup>+</sup> 626.2814 for C<sub>32</sub>H<sub>44</sub>O<sub>4</sub>N<sub>5</sub>S<sub>2</sub> (calcd 626.2835). <sup>1</sup>H NMR(400 MHz, CDCl<sub>3</sub>) δ: 0.80(m, 1H), 1.28(m, 2H), 1.34(s, 3H), 1.42(m, 2H), 1.60(m, 1H), 1.69(m, 3H), 1.77(s, 3H), 2.17(m, 1H), 2.30(s, 6H), 2.33(m, 1H), 2.78(t, 2H), 2.90(m, 1H), 3.22(m, 2H), 3.87(m, 1H), 4.17(m, 1H), 4.65(s, 1H), 5.14(m, 1H), 5.92(s, 1H), 6.84(s, 3H), 7.09(m, 1H), 7.27(s, 2H), 7.49(d, J=10.4Hz, 1H), 7.66(t, 1H), 7.72(d, J=8Hz, 1H), 8.46(d,

$J=4\text{Hz}$ , 1H).  $^{13}\text{C}$  NMR (400 MHz,  $\text{CDCl}_3$ )  $\delta$ : 21.26, 21.26, 23.57, 24.76, 25.05, 25.09, 26.53, 28.07, 28.62, 28.79, 35.64, 38.68, 47.01, 53.40, 54.25, 57.79, 58.84, 119.62, 120.53, 126.82, 128.82, 128.33, 136.9, 136.97, 137.99, 137.99, 149.61, 160.57, 171.84, 172.91, 174.29, 175.57.

#### 5.4.5 Synthesis of *cyclo*(-L-Asu(NHOH)-Aib-L-Phe(4-Me)-D-Pro-)

##### 5.4.5.1 Synthesis of Boc-Asu(OBzl)-Aib-L-Phe(4-Me)-D-Pro-O<sup>t</sup>Bu (MW = 750.96):

The tripeptide was coupling in the same manner as 4.4.3 described to obtain H-Aib-L-Phe(4-Me)-D-Pro-O<sup>t</sup>Bu (610 mg, 1.4 mmol), To a cooled solution of the free amine (610 mg, 1.4 mmol), Boc-L-Asu(OBzl)-OH (660 mg, 1.7 mmol) and HOBt·H<sub>2</sub>O (200 mg, 1.4 mmol) in DMF (3 mL), DCC (370 mg, 1.7 mmol) was added and stirred for overnight at room temperature. DMF was removed by evaporation; residue dissolved in ethyl acetate, and then successively washed with an aqueous 10% citric acid solution, an aqueous 4% sodium bicarbonate solution and brine. After drying over  $\text{MgSO}_4$  and concentrating, the resulting oily substance was purified by silica gel chromatography using a mixture of chloroform and methanol (99:1 v/v) to obtain Boc-Asu(OBzl)-Aib-L-Phe(4-Me)-D-Pro-O<sup>t</sup>Bu (940 mg, 1.2 mmol, 83%). TLC: Rf 0.75 ( $\text{CHCl}_3/\text{MeOH}=9/1$ ), HPLC: r.t. 10.05 min.

##### 5.4.5.2 Synthesis of *cyclo*(-Asu(NHOH)-Aib-L-Phe(4-Me)-D-Pro-) (MW = 604.74):

The protected tetrapeptide (901 mg, 1.2 mmol) was dissolved in TFA (3 mL) at 0 °C and kept for 3 hours. After evaporation of TFA, the residue was solidified using ether and petroleum ether to yield TFA salt of the linear tetrapeptide TFA·H-Asu(OBzl)-Aib-L-Phe(4-Me)-D-Pro-OH (796 mg, 1.1 mmol, 90%), TLC: Rf 0.5, HPLC: r.t. 6.50 min. To DMF (100 mL), TFA·H-Asu(OBzl)-Aib-L-Phe(4-Me)-D-Pro-OH (796 mg, 1.1 mmol), HATU (630 mg, 1.7 mmol), and DIEA (0.45 mL, 2.7 mmol) were added in separate five portions in every 30 min with stirring at room temperature for the cyclization reaction. After completion of the reaction, DMF was evaporated under vacuum; the residue was dissolved in ethyl acetate and washed with 10% citric acid solution, 4% sodium bicarbonate solution and brine, respectively. It was then dried over anhydrous  $\text{MgSO}_4$  and filtered. After evaporation of ethyl acetate, the residue was purified by silica gel chromatography using a mixture of chloroform and methanol (99:1v/v) to yield *cyclo*(-Asu(OBzl)-Aib-L-Phe(4-Me)-D-Pro-) (540 mg, 0.9 mmol, 81%). HPLC, r.t. 8.70 min. Compound *cyclo*(-Asu(OBzl)-Aib-L-Phe(4-Me)-D-Pro-) (540 mg, 0.9 mmol) was dissolved in methanol (4 mL) and Pd-C (50 mg) was added. The mixture was stirred



under H<sub>2</sub> for 5 hours. After filtration of Pd-C, methanol was evaporated to yield *cyclo(-Asu-Aib- L-Phe(4-Me)-D-Pro-)* (421 mg, 0.8 mmol, 92%) TLC: Rf 0.72, HPLC: r.t. 5.91 min. The product was dissolved in DMF (2 mL) at 0 °C, and O-Benzylhydroxylamine hydrochloride (HCl NH<sub>2</sub>-OBzl) (196 mg, 1.2 mmol), HOBt (111 mg, 0.8 mmol), triethylamine (0.18 mL, 1.2 mmol) and DCC (260 mg, 1.2 mmol) were added. The mixture was stirred for 24 hours. After completion of the reaction, DMF was evaporated under vacuum; the residue was dissolved in ethyl acetate and washed with 10% citric acid solution, 4% sodium bicarbonate solution and brine, respectively. It was then dried over anhydrous MgSO<sub>4</sub> and filtered. After evaporation of ethyl acetate, *cyclo(-Asu(NHOBzl)-Aib-L-Phe(4-Me)-D-Pro-)* (400 mg, 0.6 mmol, 78%, TLC: Rf 0.82, HPLC: r.t. 6.90 min ) was obtained. The product (400 mg, 0.6 mmol) was dissolved in acetic acid (6 mL) and Pd-BaSO<sub>4</sub> (200 mg) was added. The mixture was stirred under H<sub>2</sub> for 24 hours. After filtration of Pd-BaSO<sub>4</sub>, acetic acid was evaporated and crystallized with ether to yield *cyclo(-L-Asu(NHOH)-Aib-L-Phe(4-Me)-D-Pro-)* (255 mg, 0.4 mmol, 65%), TLC: Rf 0.7(CHCl<sub>3</sub>/MeOH=9/1), HPLC: 5.07 min, 98%. The yield: 19.2%. ESI-MS: [M+H]<sup>+</sup>530.3012 for C<sub>27</sub>H<sub>40</sub>O<sub>6</sub>N<sub>5</sub>(calcd 530.2979). <sup>1</sup>H NMR(400 MHz, CDCl<sub>3</sub> ) δ: 1.21(m, 2H), 1.33(m, 8H), 1.61(s, 3H), 1.77(m, 6H), 2.15(m, 2H), 2.29(s, 4H), 2.89(m, 1H), 3.20(m, 2H), 3.85(m, 1H), 4.31(m, 1H), 4.70(d, J=6.4Hz, 1H), 5.13(d, J=5.4, 1H), 7.10(m, 5H), 7.29(s, 1H), 7.66(d, J=10, 1H). <sup>13</sup>C NMR (400 MHz , CDCl<sub>3</sub>) δ: 19.20, 23.68, 24.74, 24.82, 24.93, 25.06, 25.97, 28.34, 28.86, 32.64, 35.54, 46.76, 53.34, 54.48, 57.74, 58.56, 128.86, 128.86, 129.30, 129.30, 133.77, 136.21, 171.21, 172.21, 173.10, 174.63, 175.53.

#### 5.4.6 Circular dichroism measurement

CD spectra were recorded on a JASCO J-810 spectropolarimeter (Tokyo, Japan) using a quartz cell of 1 cm light path length at room temperature. Peptide solutions (0.1 mM) were prepared in methanol and CD spectra were recorded in terms of molar ellipticity, [θ]<sub>M</sub> (deg × cm<sup>2</sup> × dmol<sup>-1</sup>).

#### 5.4.7 Cell growth inhibition assay

The MTT colorimetric assay was used to determine growth inhibition. HeLa, 7721 and MCF-7 were all cultured in a humidified atmosphere of 5% CO<sub>2</sub> in air, with RPMI 1640 media, containing 10% fetal bovine serum. The cell lines were diluted to 5~9×10<sup>4</sup> cells/mL with the corresponding media and were plated in 96-well microplates. After adhere overnight, HDACs inhibitors **1-4** were added to culture medium at the concentrations of 2, 4, 6, 8, 10 μM and then the cells were incubated for 48 hours. The concentrations of compound **5** were 20, 40, 60, 80,

100 nM. Then 200  $\mu$ L MTT (0.5 mg/mL) reagent diluted in serum free media was added to each well and the cells were incubated for an additional 4 hours. Thereafter, the resulted dark blue crystal (formazan) was dissolved in 200  $\mu$ L DMSO, and a optical density was measured on a microplate spectrophotometer at 570 nm. All experiments were performed in triplicate and repeated at least three times. Data are presented as mean  $\pm$  standard deviation of three independent experiments. The IC<sub>50</sub> values were caculated by nonlinear regression analysis using SPSS 17.0 software.

#### **5.4.8 Morphological reversion assay**

Method crystal violet staining was used to observe the changes in cell morphology. MCF-7 cells were plated into 96-well microplates at  $2 \times 10^4$  cells/mL and allowed to adhere overnight. Inhibitors were added to culture medium at the concentration of 10  $\mu$ M (compounds **1-4**) and 100 nM (compounds **5**) and incubated for 24 hours. Cells were then washed once with PBS, and fixed in 4% buffered formalin for 1 hour at room temperature. The fixed cells were then washed once further with PBS and stained with 1% crystal violet in methanol for 5 minutes. Excess stain was removed by washing with tap water. After the microtiter plate was being air-dried at 37<sup>0</sup>C, MCF-7 cells were taken photographs using an inverted microscope.

#### **5.4.9 Computational methodology for the HDAC inhibitors towards HDAC8**

##### **5.4.9.1 Docking calculation**

Docking studies were conducted with AutoDock 4.0 program<sup>[39,40]</sup> using a Lamarckian genetic algorithm. AutoDock docking protocol and scoring function have been successful applied in the interpretation of the inhibitory activity of several HDAC inhibitors.<sup>[41]</sup> Initial structure for the HDAC8 modeled from the atom coordinates of the X-ray crystal structure (PDB code: 1T69). The active site of HDAC8 was covered by a grid box size of 70 $\times$ 70 $\times$ 70 points with a spacing of 0.375 Å between the grid points. For the cyclic tetrapeptides, all single bonds except the amide bonds and cyclic bonds were treated as active torsional bonds. For each inhibitor, two hundred independent dockings, i.e. 200 runs, were performed using genetic algorithm searches. A maximum number of 250 000 000 energy evaluations and a maximum number of 10 000 generations were implemented during each genetic algorithm run. The default nonbonded zinc parameters in Autodock 4.0 were employed. The LigPlot program<sup>[42]</sup> was also employed to analyze the docking results focusing on hydrogen bonds and hydrophobic interactions.

### 5.4.9.2 Molecular dynamics simulation

All the molecular mechanics and dynamics calculations were carried out with the AMBER9<sup>[43]</sup> package. The standard AMBER ff99 force field<sup>[44]</sup> was used as the parameters for the protein and water atoms, and the general AMBER force field (GAFF)<sup>[45]</sup> and AM1-BCC charges<sup>[46]</sup> were used for the ligands. Zinc was modeled using the Stote nonbonded model ( $q = +2e^-$ ,  $r = 1.7 \text{ \AA}$ ,  $\epsilon = 0.67 \text{ kcal/mol}$ ).<sup>[47]</sup> Each initial structure for the simulation was prepared from the docked conformations of HDAC8-ligand complexes. The local hydrogen bonding network around the histidine residues was checked. Histidine residue 180 was assigned as HIE (histidine with hydrogen on its epsilon nitrogen), and other histidine residues as HID (histidine with hydrogen on its delta nitrogen). The force field parameters of cyclic tetrapeptides were prepared with the Antechamber module<sup>[48]</sup> of AMBER 9 package. Hydrogen atoms were added to the crystallographic protein with the AMBER LEaP module. Sodium counterions were added to neutralize the system. The system was then solvated with an octahedral box of TIP3P water molecules.<sup>[49]</sup> The minimum distance from the surface of the protein to the faces of the box was  $10 \text{ \AA}$ . The particle mesh Ewald (PME) method<sup>[50]</sup> was used to treat long-range electrostatic interactions. The cutoff distance for the long-range electrostatic and the van der Waals energy terms were set at  $12.0 \text{ \AA}$ . All covalent bonds to hydrogen atoms were constrained using the SHAKE algorithm.<sup>[51]</sup>

Energy minimization was achieved in three steps. At first, movement was allowed only for the water molecules and ions. Next, the ligand and the receptor residues were all allowed to move and the water molecules, together with ions, were constrained. Finally, all atoms were permitted to move freely. In each step, energy minimization was executed by the steepest descent method for the first 5000 steps and the conjugated gradient method for the subsequent 2500 steps.

Periodic boundary conditions were used. The time steps were 2 ps during the production dynamics. The temperature was maintained by rescaling the velocities using the Berendsen weak-coupling algorithm,<sup>[52]</sup> with a time constant of 2 ps for the heat bath.

After the system was heated to 300 K from the initial temperature of 0 K using the NVT ensemble in 120.0 ps, molecular dynamics were performed at a constant temperature of 300 K. After a 50 ps position-restrained dynamics, each simulation was proceeded 2 ns under periodic boundary conditions with NPT ensemble at 1 atm and at 300 K. The convergence of energy, temperatures, and pressures of the systems, and the atomic root-mean-square deviation of the enzyme and the inhibitor (RMSD), were used to verify the stability of the systems. Trajectories were analyzed using the PTRAJ modules.<sup>[53]</sup>

In the present MD simulations, the overall structure of all complexes appeared to be equilibrated after 1.5 ns. Hence, atom coordinates were collected at the interval of 5 ps for the last 500 ps to analyze the structure in detail. The series of snapshots between 1.5 and 2.0 ns of the equilibrium phase was used for free energy calculations and structure evaluation.

### 5.4.9.3 Free energy calculations

For MM-PBSA methodology, snapshots were taken at 5 ps time intervals from the corresponding 500 ps MD trajectories. The explicit water molecules were removed from the snapshots. The energy components were calculated using very large cut off (999 Å). The binding free energy,  $\Delta G_{\text{bind}}$ , was estimated as follows:

$$\Delta G_b = \Delta E_{\text{MM}} + \Delta G_{\text{sol}} - T\Delta S \quad (1)$$

where  $\Delta E_{\text{MM}}$  is the molecular mechanics energy and is given by  $\Delta E_{\text{MM}} = \Delta E_{\text{int}}^{\text{ele}} + \Delta E_{\text{int}}^{\text{vdw}}$  (2)

where  $\Delta E_{\text{int}}^{\text{ele}}$  and  $\Delta E_{\text{int}}^{\text{vdw}}$  represent the HDAC8-ligand electrostatic and van der Waals interactions, respectively.

The solvation free energy ( $\Delta G_{\text{sol}}$ ) was estimated as the sum of electrostatic solvation free energy ( $\Delta G_{\text{sol}}^{\text{ele}}$ ) and nonpolar solvation free energy ( $\Delta G_{\text{sol}}^{\text{nonpol}}$ ):

$$\Delta G_{\text{sol}} = \Delta G_{\text{sol}}^{\text{ele}} + \Delta G_{\text{sol}}^{\text{nonpol}} \quad (3)$$

where  $\Delta G_{\text{sol}}^{\text{ele}}$  was calculated using the generalized Born (GB) model of Onufriev et al.<sup>[54]</sup> and the  $\Delta G_{\text{sol}}^{\text{nonpol}}$  was determined with a function of the solvent-accessible surface- area:<sup>[55]</sup>

$$\Delta G_{\text{sol}}^{\text{nonpol}} = \gamma \cdot A + b$$

where A is the solvent-accessible surface area estimated with the LCPO method<sup>[56]</sup> and the parameters  $\gamma = 0.0072 \text{ kcal}/(\text{mol } \text{Å}^2)$  and  $b = 0.0 \text{ kcal/mol}$ .

The change of solute entropy upon complexation,  $T\Delta S_{\text{conf}}$ , was not estimated in this work. It seems that entropy does not contribute much to the relative binding free energy of the ligands with similar to the same protein, and in some studies there were good agreements between the experimental and calculated relative binding energy.

## 5.5 References

- [1] Ailsa J. Frew, Ricky W. Johnstone, Jessica E. Bolden, *Cancer Letters*. 2009, 280: 125–133.
- [2] Oronza Antonietta Botrugno, Fabio Santoro, Saverio Minucci, *Cancer Lett*. 2009, 280: 134-144.
- [3] Jessica EB, Melissa JP, Ricky WJ. *Nature Reviews Drug Discovery*, 2006, 5: 769-784.
- [4] Closse, A.; Huguenin, R. *Helv. Chim. Acta*. 1974, 57: 553-545.
- [5] Norikazu Nishino, Binoy Jose, Ryuzo Shinta, Tamaki Kato, Yasuhiko Komatsub, and Minoru Yoshida, *Bioorg. Med. Chem*. 2004, 12: 5777–5784.

- [6] Mohammed P. I. Bhuiyan, Tamaki Kato, Tatsuo Okauchi, Norikazu Nishino, Satoko Maeda, Tomonori G. Nishino and Minoru Yoshida, *Bioorg. Med. Chem.* 2006,14: 3438–3446.
- [7] Norikazu Nishino, Gururaj M. Shivashimpi, Preeti B. Soni, Mohammed P. I. Bhuiyan, Tamaki Kato, Satoko Maeda, Tomonori G. Nishino and Minoru Yoshida, *Bioorg. Med. Chem.* 2008,16: 437–445.
- [8] Gururaj M. Shivashimpi, Satoshi Amagai, Tamaki Kato, Norikazu Nishino, Satoko Maeda, Tomonori G. Nishino and Minoru Yoshida, *Bioorg. Med. Chem.* 2007,15: 7830–7839.
- [9] Finnin, M. S.; Donigian, J. R.; Cohen, A.; Richon, V. M.; Rifkind, R. A.; Marks, P. A.; Breslow, R.; Pavletich, N. P. *Nature* 1999, 401: 188-193.
- [10] Ueda, H.; Nakajima, H.; Hori, Y.; Fujita, T.; Nishimura, M.; Goto, T.; Okuhara, M. *J. Antibiot. (Tokyo)* 1994, 47: 301–10.
- [11] Shigematsu, N.; Ueda, H.; Takase, S.; Tanaka, H.; Yamamoto, K.; Tada, T. *J. Antibiot. (Tokyo)* 1994, 47: 311–314.
- [12] Ueda, H.; Manda, T.; Matsumoto, S.; Mukumoto, S.; Nishigaki, F.; Kawamura, I.; Shimomura, K. *J. Antibiot. (Tokyo)* 1994, 47: 315–323.
- [13] Furumai, R.; Matsuyama, A.; Kobashi, M.; Lee, K-H.; Nishiyama, M.; Nakajima, H.; Tanaka, A.; Komatsu, Y.; Nishino, N.; Yoshida, M.; Horinouchi S. *Cancer Res.* 2002, 62: 4916-4921.
- [14] C.L. Yan, Z.L. Xiu, X.H. Li, S.M. Li, C. Hao and H. Teng, *Proteins*, 2008, 73: 134-149.
- [15] Michel J, Verdonk ML, Essex JW. *J Med Chem*, 2006, 49: 7427-7439.
- [16] Wu C, Wang ZX, Lei HX, Zhang W, Duan Y. *J Am Chem Soc*, 2007, 129: 1225-1232.
- [17] Lafont V, Schaefer M, Stote RH, Altschuh D, Dejaegere A. *Proteins*, 2007, 67: 418-434.
- [18] Zhou ZG, Madrid M, Evanseck JD, Madura JD. *J Am Chem Soc*, 2005, 127: 17253-17260.
- [19] Huo S, Wang J, Cieplak P, Kollman PA, Kuntz ID. *J Med Chem*, 2002, 45: 1412–1419.
- [20] Wang W, Lim WA, Jakalian A, Wang J, Wang JM, Luo R, Bayly CT, Kollman PA. *J Am Chem Soc*, 2001, 123: 3986-3994.
- [21] Donini OAT, Kollman PA. *J Med Chem*, 2000, 43: 4180-4188.
- [22] Hou TJ, Guo SL, Xu XJ. *J Phys Chem B*, 2002, 106: 5527-5535.
- [23] M. Rodriguez, S. Terracciano, E. Cini, G. Settembrini, I. Bruno, G. Bifulco, M. Taddei and L. Gomez-Paloma, *Angew. Chem. Int. Ed.* 2006, 118: 437-441.
- [24] N. Maulucci, M.G. Chini, S.D. Micco, I. Izzo, E. Cafaro, A. Russo, P. Gallinari, C. Paolini, M.C. Nardi, A. Casapullo, R. Riccio, G. Bifulco and F.D. Riccardis, *J. Am. Chem. Soc.* 2007, 129: 3007-3012.
- [25] Li Xiaohui, Wang Guan, Li Jianxun, Xiu zhilong, Nishino Norikazu. *Chem.J.Chinese Universities [JJ]*, 2008, 29: 1363-1366.
- [26] Louis A. Watanabe, Binoy Jose, Tamaki Kato, Norikazu Nishino, Minoru Yoshida, *Tetrahedron Letters*, 2004, 45: 491–494.
- [27] Somoza, J. R.; Skene, R. J.; Katz, B. A.; Mol, C.; Ho, J. D.; Jennings, A. J.; Luong, C.; Arvai, A.; Buggy, J. J.; Chi, E.; Tang, J.; Sang, B. C.; Verner, E.; Wynands, R.; Leahy, E. M.; Dougan, D. R.; Snell, G.; Navre, M.; Knuth, M. W.; Swanson, R. V.; McRee, D. E.; Tari, L. W. *Structure*, 2004, 12: 1325-1334.
- [28] Zhou ZG, Madrid M, Evanseck JD, Madura JD. *J Am Chem Soc*, 2005, 127: 17253-17260.

- [29] Huo S, Wang J, Cieplak P, Kollman PA, Kuntz ID. *J Med Chem*, 2002, 45: 1412–1419.
- [30] Wang W, Lim WA, Jakalian A, Wang J, Wang JM, Luo R, Bayly CT, Kollman PA. *J Am Chem Soc*, 2001, 123: 3986-3994.
- [31] Donini Oreola A. T, Kollman Peter A. *J Med Chem*, 2000, 43: 4180-4188.
- [32] Hou TJ, Guo SL, Xu XJ. *J Phys Chem B*, 2002, 106: 5527-5535.
- [33] Srinivasan J, Cheatham TE, Cieplak P, Kollman PA, Case DA. *J Am Chem Soc*, 1998, 120: 9401-9409.
- [34] Gohlke H, Kiel C, Case DA. *J Mol Biol*, 2003, 330: 891-913.
- [35] Massova I, Kollman PA. *Perspect Drug Discov Des*, 2000, 18: 113-135.
- [36] Kollman PA, Massova I, Reyes C, Kuhn B, Huo S, Chong L, Lee M, Lee T, Duan Y, Wang W, Donini O, Cieplak P, Srinivasan J, Case DA, Cheatham TE. *Acc Chem Res*, 2000, 33: 889-897.
- [37] Kuhn B, Kollman PA. *J Am Chem Soc*, 2000, 122: 3909-3916.
- [38] Masukawa KM, Kollman PA, Kuntz ID. *J Med Chem*, 2003, 46: 5628-5637.
- [39] R. Huey, G.M. Morris, A.J. Olson and D.S. Goodsell, *J. Comput. Chem.* 2007, 28: 1145-1152.
- [40] G.M. Morris, D.S. Goodsell, R.S. Halliday, R. Huey, W.E. Hart, R.K. Belew and A.J. Olson, *J. Comput. Chem.* 1998, 19: 1639-1662.
- [41] D.F. Wang, O.G. Wiest, P. Helquist, H.Y. Lan-Hargest and N.L. Wiech, *J. Med. Chem.* 2004, 47: 3409-3417.
- [42] A.C. Wallace, R.A. Laskowski and J.M. Thornton, *Protein. Eng.* 1995, 8: 127-134.
- [43] Case, D. A.; Darden, T. A.; Cheatham, T. E.; Simmerling, C. L.; Wang, J.; Duke, R. E.; Luo, R.; Merz, K. M.; Pearlman, D. A.; Crowley, M.; Walker, R. C.; Zhang, W.; Wang, B.; Hayik, S.; Roitberg, A.; Seabra, G.; Wong, K. F.; Paesani, F.; Wu, X.; Brozell, S.; Tsui, V.; Gohlke, H.; Yang, L.; Tan, C.; Mongan, J.; Hornak, V.; Cui, G.; Beroza, P.; Mathews, D. H.; Schafmeister, C.; Ross, W. S.; Kollman, P. A. AMBER version 9; *University of California: San Francisco, CA*, 2006.
- [44] Wang, J. M.; Cieplak, P.; Kollman, P. A. *J. Comput. Chem.* 2000, 21: 1049-1074.
- [45] Wang, J.; Wolf, R. M.; Caldwell, J. W.; Kollman, P. A.; Case, D. A. *J. Comput. Chem.* 2004, 25: 1157-1174.
- [46] Jakalian, A.; Bush, B. L.; Jack, D. B.; Bayly, C. I. *J. Comput. Chem.* 2000, 21: 132-146.
- [47] Stote RH, Karplus M. *Proteins*, 1995, 23: 12-31.
- [48] Wang JM, Wang W, Kollman PA. *Abstr Pap Am Chem Soc*, 2001, 222, U403.
- [49] Jorgensen WL, Chandrasekhar J, Madura JD, Impey RW, Klein ML. *J Chem Phys*, 1983, 79: 926-935.
- [50] Darden T, York D, Pedersen L. *J Chem Phys*, 1993, 98: 10089-10092.
- [51] Ryckaert JP, Ciccotti G, Berendsen HJC. *J Comput Phys*, 1977, 23: 327-341.
- [52] Berendsen H.J.C., Postma J.P.M., Vangunsteren W.F., Dinola A., Haak J.R. *J Chem Phys*, 1984, 81: 3684-3690.
- [53] Honig B, Nicholls A. *Science*, 1995, 268: 1144-1149.
- [54] Onufriev A, Bashford D, Case DA. *Proteins*, 2004, 55: 383-394.
- [55] Sitkoff D, Sharp KA, Honig B. *J Phys Chem*, 1994, 98: 1978-1988.
- [56] Weiser J, Shenkin PS, Still WC. *J Comput Chem*, 1999, 20: 217-230.

## Chapter 6

# Molecular Design of Cyclic Tetrapeptide HDAC Inhibitors by Replacement of L-Phe in Chlamydocin Framework

### 6.1 Introduction

Reversible acetylation and deacetylation of the  $\epsilon$ -amino groups of lysines by histone acetyl transferase (HAT) and histone deacetylase (HDAC) enzymes play a crucial role in the regulation of gene expression by altering the chromatin architecture and controlling DNA to transcriptional regulators.<sup>[1-5]</sup> HAT and HDAC inhibitors have been studied as potential therapeutics for treatment of cancers.<sup>[6-8]</sup> In histone deacetylase inhibitors, a wide variety of structurally unrelated natural and synthetic cyclopeptides play an important role with reversible or irreversible zinc bind group as effective anticancer activities agents. for example, Chlamydocin,<sup>[9]</sup> Trapoxin,<sup>[10]</sup> Cyl-1,<sup>[11]</sup> Cyl-2,<sup>[12]</sup> HC-toxins,<sup>[13]</sup> Apicidin<sup>[14,15]</sup>, depsipeptide FK228,<sup>[16-18]</sup> and their analogues CHAPs, SCOPs and so on.<sup>[19-28]</sup> The conformational features of compounds have been established by X-ray and NMR spectroscopic studies and by comparison of their biological activity with that of simplified synthetic analogues.

Chlamydocin is a cyclic tetrapeptide containing an epoxyketone moiety in the zinc bind group which makes it irreversible inhibit HDACs and an aromatic ring moiety (L-Phe) in cyclic framework which provides specific hydrophobic interaction with the rim of HDAC enzymes. Chlamydocin inhibits HDAC activity *in vitro* with an IC<sub>50</sub> value of 1.3 nM. Though the activity is major due to the epoxyketone moiety, there are evidences which support that the cyclic tetrapeptide framework also has a significant structural role.<sup>[28]</sup> Whereas, HC-Toxins are also cyclic tetrapeptide that do not contain aromatic ring in macrocyclic framework which yet are potent inhibitors of HDACs (**Fig.6.1**).

Recently, current HDAC inhibitors in clinical trials are regarded as broad spectrum HDACs inhibitors with moderate anticancer effect. Therefore, it is desirable clinically to develop specific anticancer drugs that are effective for a particular HDAC over expressed in cancer.<sup>[29]</sup> It is less homologous that the amino acid residues of HDAC isoforms bind to inhibitor at rim of active site. So, the modification of the cap group allows to have a significant impact upon isoform selectivity.<sup>[30]</sup> Therefore, one of various approaches is to modify the cap group of

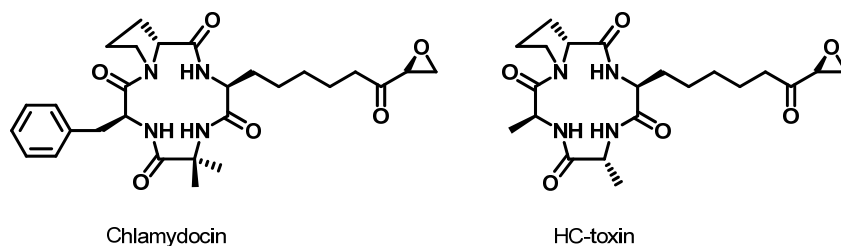


**Fig. 6.1** HDACs inhibitors.

the HDAC inhibitors. To investigate the interaction of aliphatic cap group with the surface of HDAC enzymes, we designed and synthesized cyclic tetrapeptide that replaced L-Phe by chlorine-contain aliphatic amino acid (Ac5 or Ac6) in their capping group, and replaced the epoxyketone moiety of Chlamydocin with hydroxamic acid group to synthesize potent reversible and selective HDAC inhibitors (**Ky-335** *cyclo(-L-Asu(NHOH)-Aib-L-Ac5-D-Pro-)* and **Ky-336** *cyclo(-L-Asu(NHOH)-Aib-L-Ac6-D-Pro-)*) (**Fig.6.2**). On the other hand, we designed the side chain of chlorine-contain cyclic tetrapeptide *Acn* in framework to be modified by oxygen or sulfur with chelating zinc ion of HDAC active pocket bottom. *cyclo(-L-Ac5-Aib-L-Phe-L-Pro-)* was synthesized as a intermediate prodrug (**Fig.6.3**). However, this cyclic tetrapeptide was reacted with potassium thioacetate to convert the chlorine to thioacetate ester, the reaction was failed. In synthesis process, we lighted on the L-Ac5 change into L-Pro obtaining **Ky-337** *cyclo(-L-Asu(NHOH)-Aib-L-Pro-D-Pro-)*. The inhibitory activity of the cyclic tetrapeptides against histone deacetylase enzymes were evaluated and the result showed potent inhibitors.

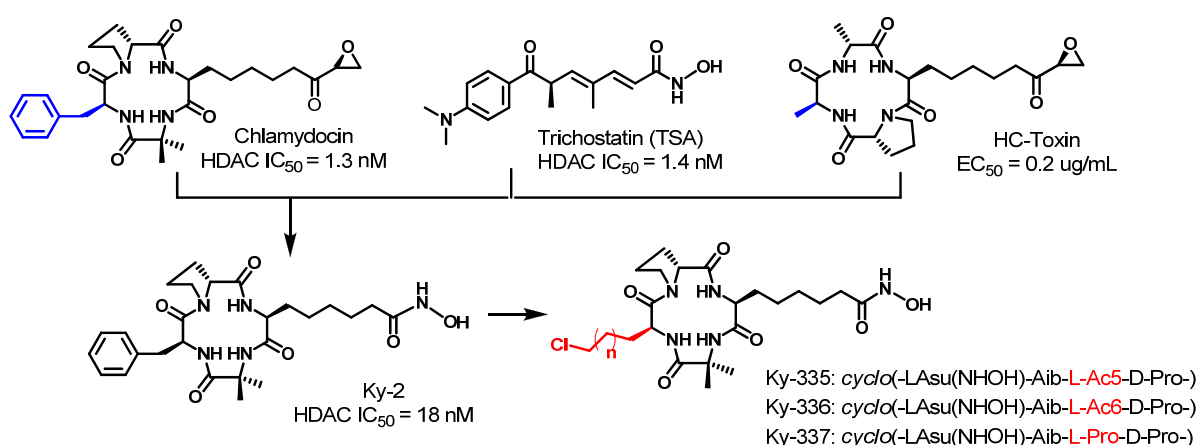


**Fig.6.2** Design chlorine-contain HDAC inhibitors



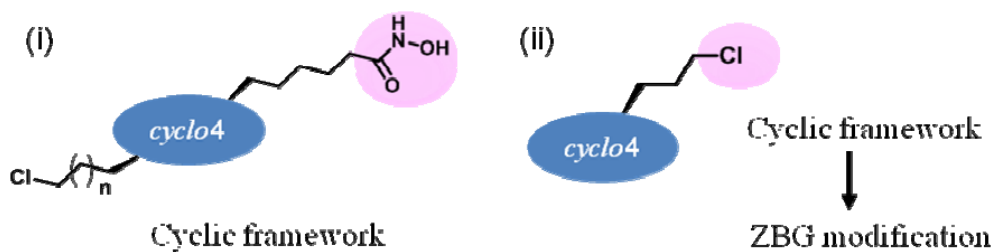
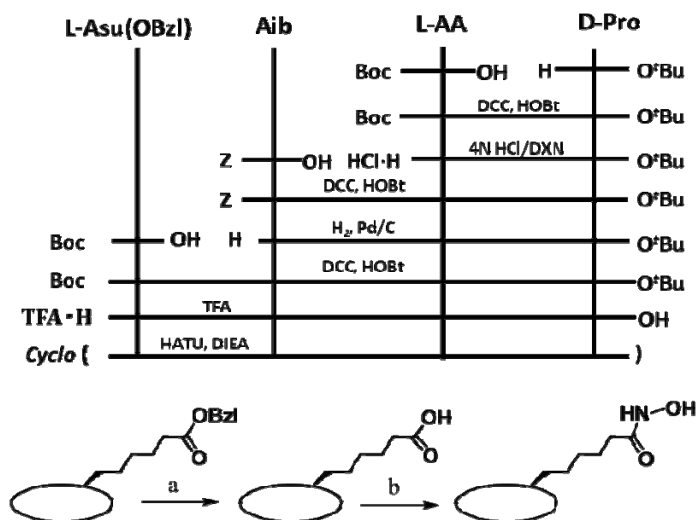


**Fig. 6.3** Design chloro-containing HDAC inhibitors.

## 6.2 Results and discussion

### 6.2.1 Chemistry

Our aim is to synthesize potent HDACs inhibitors. Initially we synthesized Chlamydocin analogues by replacing the phenylalanine at 3-position of the cyclic framework by 2-amino-5-chloro-pentanoic acid (L-Ac5-OH) and 2-amino-6-chloro-hexanoic acid (L-Ac6-OH). Cyclic tetrapeptides were prepared according to general **Scheme 6.1** by the conventional solution phase method. *tert*-Butyl protected D-Pro was coupled with Boc-L-Ac5 (or Ac6) to give the dipeptide Boc-L-Ac5-D-Pro-O<sup>t</sup>Bu. The Boc group of dipeptide was deprotected by 4 N HCl/ dioxane and coupled with Z-Aib using DCC/HOBt-H<sub>2</sub>O orderly. The Z group of the resulted tripeptide Z-Aib-L-Ac5-D-Pro-O<sup>t</sup>Bu was deprotected by catalytic hydrogenation. It was then coupled with Boc protected amino suberic acid benzyl ester (Boc-L-Asu(OBzl)) to give linear tetrapeptide Boc-L-Asu(OBzl)-Aib-L-Ac5-D-Pro-O<sup>t</sup>Bu. The C-terminal and N-terminal protections of the tetrapeptide were removed by treatment with trifluoroacetic acid (TFA) and the resulted linear peptide was cyclized in DMF (2 mM) with minimum amount of DIEA (2.5 equiv) under high dilution condition using HATU as a coupling reagent to give *cyclo*(-L-Asu(OBzl)-Aib-L-Ac5-D-Pro-) in 50-60% yield. The OBzl of side chain of cyclic peptide was deprotected by catalytic hydrogenation and then coupled with hydroxylamine hydrochloride and the resulted product was deprotected by catalytic hydrogenation to yield the desired compounds and finally purified using gel filtration. We replaced L-Phe residue with non-natural amino acids (Ac5 and Ac6) to study the effect on the HDACs inhibitory activity. All the synthesized compounds were characterized by <sup>1</sup>H NMR and HR-FAB-MS. The purity of the compounds was determined by HPLC analysis and all the synthesized cyclic tetrapeptides showed purity above 97%.



**Scheme 6.1** Structure of cyclo(-L-Asu(NHOH)-Aib-L-AA-D-Pro-).

Reagents: (a) H<sub>2</sub>, Pd/C, MeOH; (b) HCl·NH<sub>2</sub>OH, BOP, DIEA, DMF. L-AA: L-Ac5; L-Ac6; L-Pro.

## 6.2.2 Enzyme inhibition and biological activity

We assayed three synthesized compounds (Ky-335, Ky-336 and Ky-337) for HDACs inhibitory activity using HDAC1, HDAC4 and HDAC6 enzymes prepared by 293T cells. In addition, to know the inhibitory activity of these compounds in cell based condition, we carried out p21 promoter assay. The results of HDAC inhibitory activity and the p21 promoter assay of compounds are shown in **Table 6.1**.

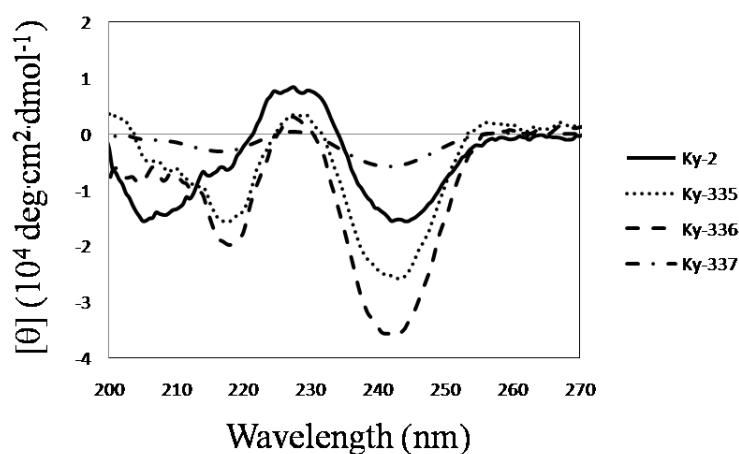
Inhibitory activity of TSA and Ky-2 are also shown in **Table 6.1** for comparison with synthesized compounds. Three compounds all showed good activity against HDAC1 and HDAC4 in nanomolar range, but these compounds were poorly inhibited by HDAC6 and their selectivity was better (HDAC6/HDAC1 = 10). The compound Ky-336 showed the best activity in both cell free and cell based conditions than the other two compounds Ky-335 and Ky-337 and the activity of Ky-336 was similar to TSA and Ky-2 data. The activity toward HDAC1 slightly changed with the difference of the length of the side chain of aliphatic amino acid. However, the changes in activity toward HDAC4 and HDAC6 were not so remarkable. The result suggested that hydrophobicity of aliphatic amino acid can also increase interaction with rim of HDACs active pocket and aromatic ring is no need in cyclic framework. Also cell permeability was enhanced in this case, which was reflected in their p21 activity data.

**Table 6.1** HDAC inhibitory activity and p21 promoter assay

No.	Compounds	HDAC inhibitory activities IC <sub>50</sub> (nM)			EC <sub>1000</sub> (nM)
		HDAC1	HDAC4	HDAC6	p <sup>21</sup> promoter activity
	Trichostatin A	23	34	65	20
Ky-2	<i>cyclo</i> (-L-Asu(NHOH)-Aib-L-Phe-D-Pro-)	18	17	230	18
Ky-335	<i>cyclo</i> (-L-Asu(NHOH)-Aib-L-Ac5-D-Pro-)	14	19	110	210
Ky-336	<i>cyclo</i> (-L-Asu(NHOH)-Aib-L-Ac6-D-Pro-)	7.9	15	96	36
Ky-337	<i>cyclo</i> (-L-Asu(NHOH)-Aib-L-Pro-D-Pro-)	53	60	310	210

### 6.2.3 Conformational study

We carried out circular dichroism (CD) spectrum study of compounds Ky-335, Ky-336 and Ky-337, in methanol as solvent with peptide concentration of 0.1 mM (**Fig. 6.4**). The CD spectrum of three compounds were similar to reference Ky-2 (*cyclo*(-L-Asu(NHOH)-Aib-L-Phe-D-Pro-) at 215 nm to 260 nm. Three compounds showed a negative ellipticity at 220 nm and 240 nm regions, a positive ellipticity at 230 nm regions and different ellipticity at 200 nm ~ 215 nm. Ky-336 of CD spectrum with more negative ellipticity showed good biological activity. This fact showed that chlorine-contain cyclic tetrapeptide (Ky-335 and Ky-336) compounds have similar conformations.

**Fig.6.4** CD spectra of cyclic tetrapeptides.

We have carried out NMR ( $\text{CDCl}_3$ ) studies for conformation of Ky-335 and Ky-336 by with MOE calculations (Ky-337 no dissolves in  $\text{CDCl}_3$ ). Solution conformation of Ky-335 and Ky-336 were studied using  $^1\text{H}$  NMR in  $\text{CDCl}_3$  (**Fig. 6.5**). Complete assignments were made using COSY and NOESY spectra. The  $J_{\text{NH-HC}\alpha}$  values of Ky-335 and Ky-336 were obtained from NMR charts and by that we estimated dihedral angle “ $\theta$ ,” using the Karplus graph. Dihedral angles  $\theta$  and  $\phi$ , and NOE data are shown in **Table 6.2**. Two compounds have similar energy-minimized structures.

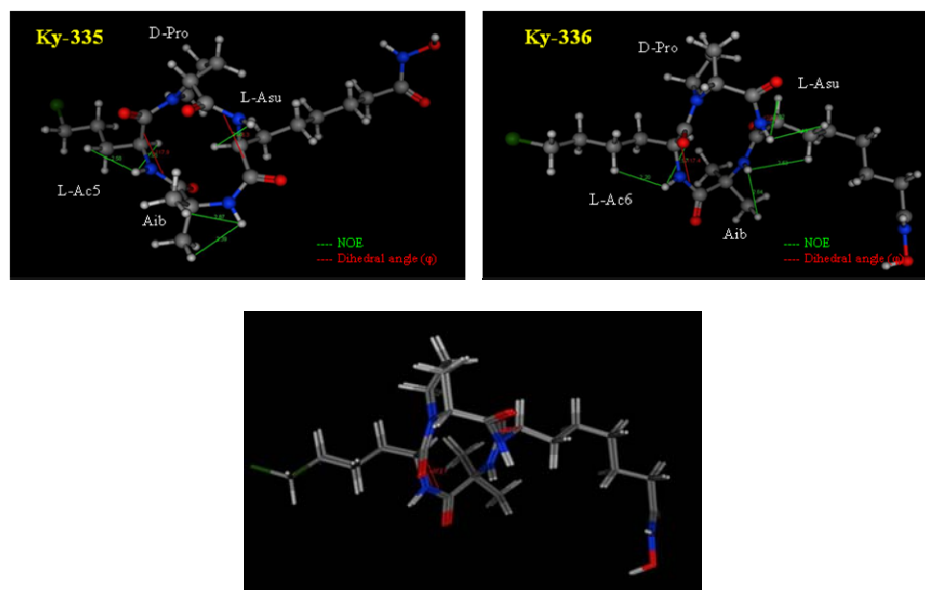


**Fig. 6.5** MOE of Ky-335 and Ky-336 by NMR calculation. Superimposition of compounds (below).

**Table 6.2** NOE, coupling constant and dihedral angles data from NMR.

residues	NOE		$J_{\text{NH-HC}\alpha}$	$\theta$	$\phi$
	Ky-335	Ky-336			
L-Asu	L-Asu(NH-HC $\alpha$ )	L-Asu(NH-HC $\alpha$ )	10 Hz	180°	-120°
		L-Asu(NH-HC $\beta$ )			
Aib	Aib(NH-HC $\beta$ )	Aib(NH-HC $\beta$ )	----	----	----
		Aib(NH)-L-Asu(HC $\beta$ )			
L-Ac6 or L-Ac5	L-Ac5(NH-HC $\alpha$ )	L-Ac6(NH-HC $\alpha$ )	10 Hz	180°	-120°
		L-Ac5(NH-HC $\beta$ )			
D-Pro			----	----	----

#### 6.2.4 Docking for HDAC inhibitors towards HDAC8

To understand the binding modes between HDACs and this series of HDAC inhibitors, docking studies for HDAC8 and HDLP with these inhibitors were conducted with AutoDock 4.0 program. The active sites of HDAC8 and HDLP were covered by a grid box of 70×70×70 points with a spacing of 0.375 Å between the grid points. For all inhibitors, all the single bonds except the amide bonds and cyclic bonds were treated as active torsional bonds. For each inhibitor, 150 independent dockings were performed using genetic algorithm searches. A maximum number of 250 000 000 energy evaluations and a maximum number of 5 000 generations were implemented during each genetic algorithm run. A mutation rate of 0.02 and a crossover rate of 0.8 were used. The default nonbonded zinc parameters in Autodock 4.0 were employed. Results differing by less than 2.0 Å in positional root-mean-square deviation (RMSD) were clustered together. The RMSD value is an all heavy atom comparison between the docked structure and the initial structure. The LigPlot program was also employed to analyze the docking results focusing on hydrogen bonds and hydrophobic interactions.

The docking results are shown in **Fig.6.6** and **Fig.6.7**. It indicated that all inhibitors bound to the active site of HDAC8 and HDLP with a similar pattern, the surface recognition domain interacted with the external surface of the enzyme, and the hydroxamic acid group as metal binding domain was at the bottom of active pocket. In the active sites of HDAC8, zinc ion coordinated with the oxygen atom of carbonyl group, while in the active site of HDLP, zinc ion coordinated with the oxygen atom of oxhydroxyl group. The average distances between zinc ion and the nearby atoms were tested during the last 500 ps in current MD simulations. The average distances of zinc ion to oxygen atom of carbonyl group of HDAC8 were 1.84, 1.75 and 1.86 Å, respectively, while the distances with the oxygen atom of oxhydroxyl group of HDLP were 1.73, 1.96 and 1.76 Å respectively. Chelating with zinc was essential for inhibitors in the HDAC inhibitory activities. In the results of docking for HDAC8-inhibitors, the hydrogen bond was built between Lys19 of HDAC8 and Ky-337. For HDLP-inhibitors, the chlorine atom of Ky-335 created a hydrogen bond with Tyr194 of HDLP. The hydrophobic interaction between inhibitors and HDACs were also crucial for stabilizing the binding. As shown, some amino acids, including Tyr80, His122, His 123, Gly131, Phe132, His160, Phe187, Phe188, Pro253 and Met254 of HDAC8, Phe139, His168, Gln190, Ala195, Phe196, Phe198, Leu263, Ser264 and Lys265 of HDLP, contact inhibitors via hydrophobic interactions. For each inhibitor, six or

seven of these amino acids of HDAC8 or HDLP were involved in establishing hydrophobic interactions (**Fig. 6.8**).

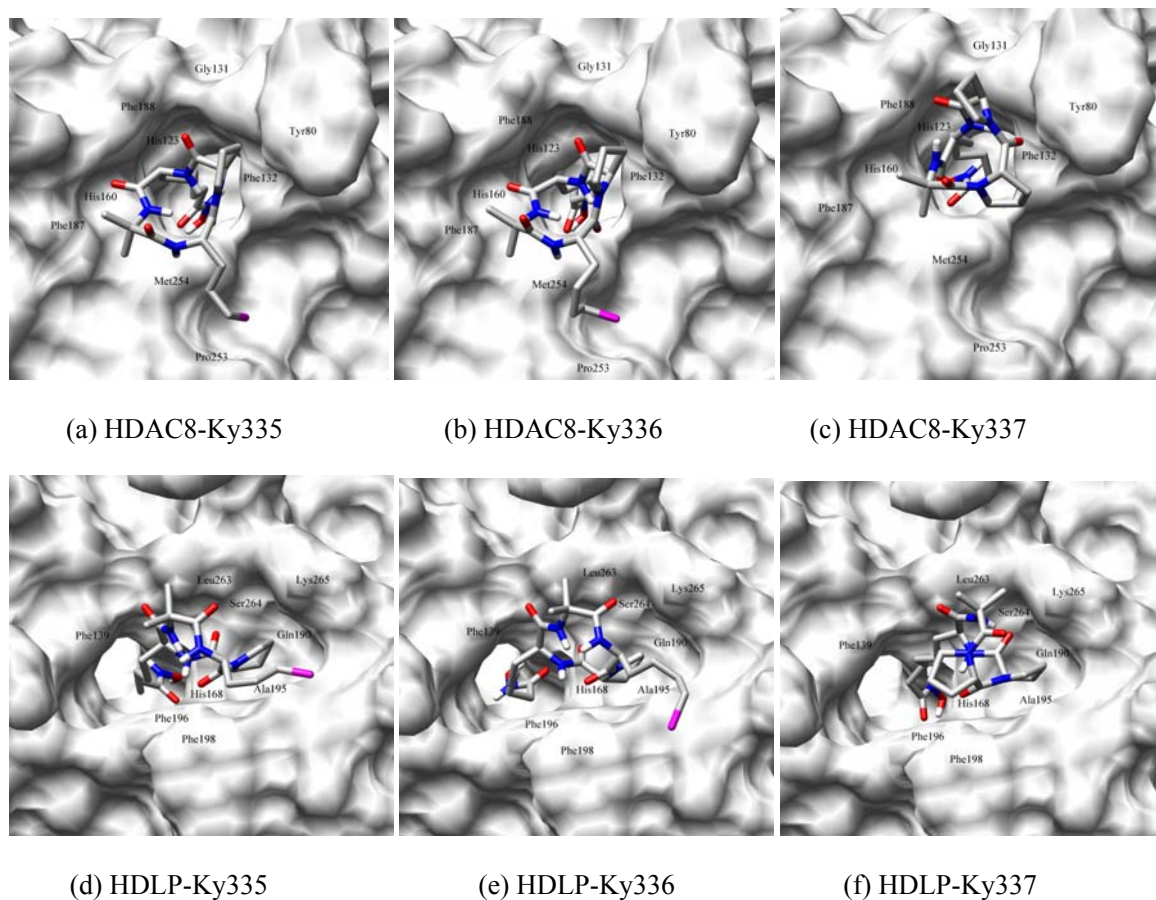


**Fig. 6.6** Top view of the surfaces of the active site for docking.

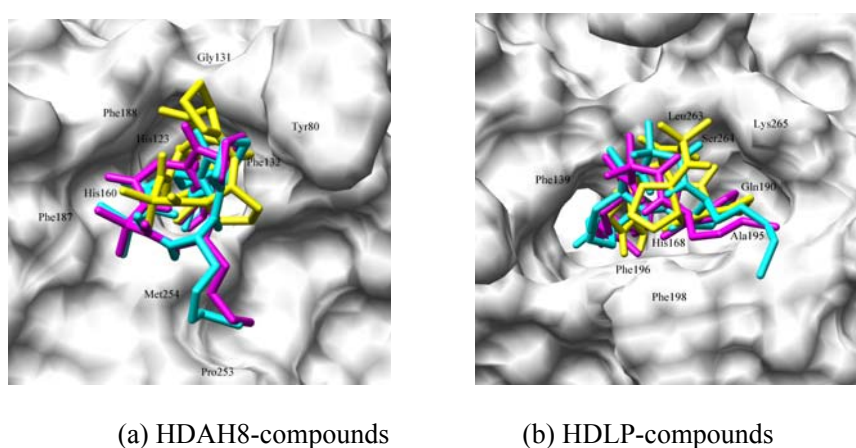


**Fig. 6.7** Superimposition in surfaces of the active site regions for docking. Ky-335 (magenta), Ky-336 (cyan), Ky-337 (yellow).

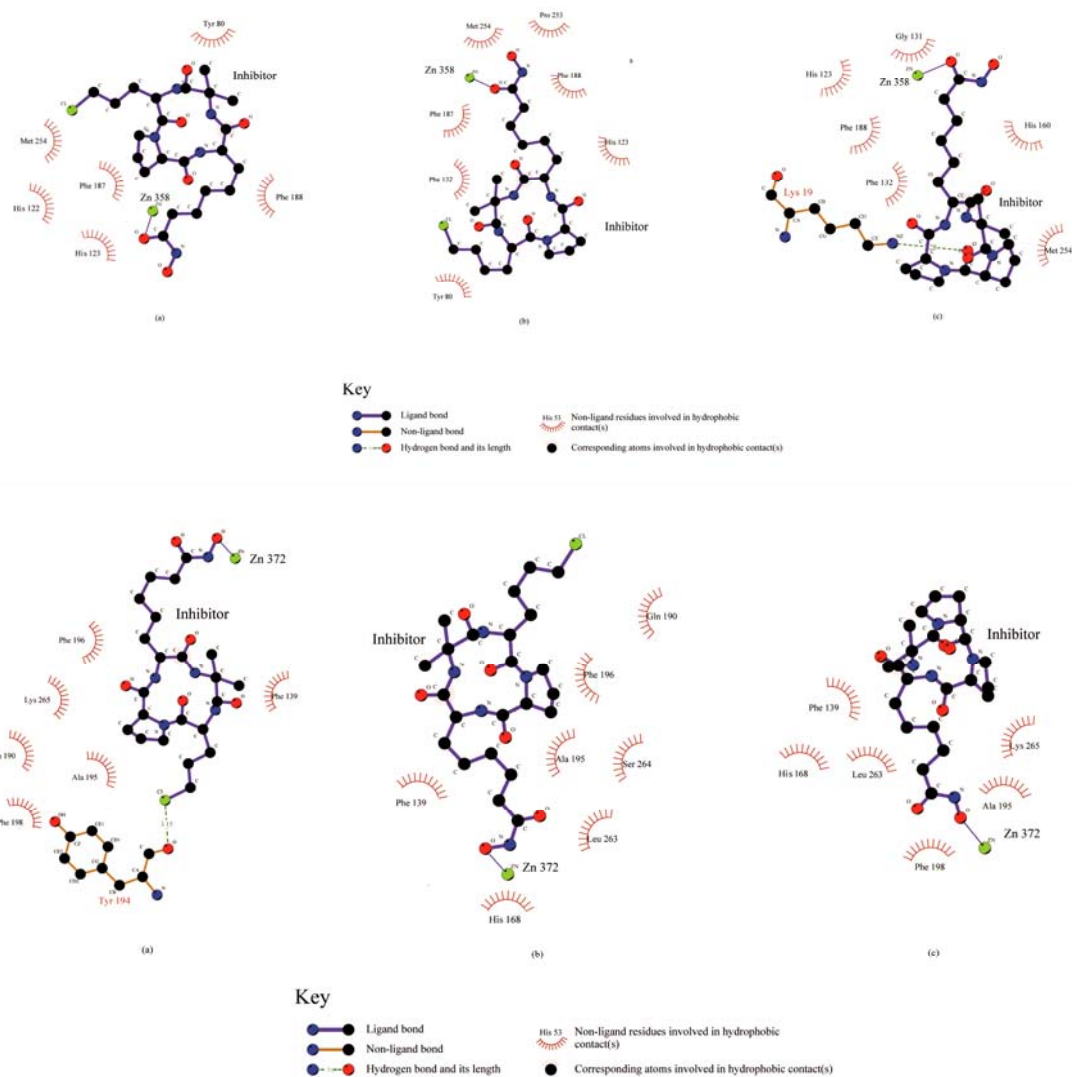


**Fig. 6.8** The hydrogen bonds and hydrophobic interactions (above) HDAC8 and (below) HDLP for docking. (a) Ky-335, (b) Ky-336, (c) Ky-337.

### 6.3 Summary

In summary, in order to find novel and potent non-aromatic HDAC inhibitors, we designed and synthesized three cyclic tetrapeptide hydroxamic acids by changing chlorine-contain aliphatic amino acid at 3-position of cyclic framework. These inhibitors showed potent HDAC inhibitory activity in vivo and in vitro. They also showed some selectivity among the HDAC isoforms. The length of aliphatic chain was important, and four CH<sub>2</sub> length was the optimum for in vivo activity. The Ky-335 and Ky-336 showed better HDAC inhibitory activities than Ky-337 and

the same as Ky-2 and TSA. In the cellular activity, the Ky-336 showed the best than other two compounds, and similar to Ky-2. These results further confirmed that modification of the cap group of HDAC inhibitors can lead to potent HDAC inhibitors, which may have potential as anticancer agents. We also carried out conformational analysis of these inhibitors by CD and NMR calculation methods, and conducted docking studies for HDAC8 and HDLP with these inhibitors with AutoDock 4.0 program. Ky-336 of CD spectrum with more negative ellipticity showed good biological activity. The presence of an aliphatic chain can also increase its interactions with the rim of HDACs active pocket.

## 6.4 Experimental

**General:** Unless otherwise noted, all solvents and reagents were reagent grade and used without purification. All compounds were routinely checked by thin layer chromatography (TLC) or high performance liquid chromatography (HPLC). Analytical HPLC were performed on a Hitachi equipped with a chromolith performance RP-18e column (4.6 × 100 mm, Merck). The mobile phases used were A: H<sub>2</sub>O and 0.1% TFA, B: CH<sub>3</sub>CN with 0.1% TFA using a solvent gradient of A to B over 15 min with detection at 220 nm with a flow rate of 2 mL/min. TLC was performed on aluminium-backed silica gel plates (Merck DC-Alufolien Kieselgel 60 F<sub>254</sub>) with spots visualized by UV light and heat. Flash chromatography was performed using silica gel 60 (230-400) eluting with solvents as indicated. Fast atom bombardment mass spectra (FAB-MS) and high resolution fast atom bombardment mass spectra (HR-FAB-MS) were measured on a JEOL JMS-SX 102A instrument. NMR spectra were recorded on a Bruker 500 MHz spectrometer. All NMR spectra were measured in CDCl<sub>3</sub> solutions with reference to TMS. All <sup>1</sup>H shifts are given in parts per millions (s = singlet; d = doublet; t = triplet; m = multiplet). Peptide were coupled using standard solution-phase chemistry with dicyclohexylcarbodiimide (DCC), N-Hydroxybenzotriazole (HOBt). Peptide cyclization was mediated by *N*-[(dimethylamino)-1*H*-1,2,3-triazolo[4,5-*b*]pyridin-1-yl-methylene]-*N*-methylmethanaminium hexafluorophosphate *N*-oxide (HATU).

### 6.4.1 Synthesis of *cyclo(-L-Asu(NHOH)-Aib-L-Ac5-D-Pro-)*

#### 6.4.1.1 Synthesis of Boc-L-Ac5-D-Pro-O<sup>t</sup>Bu (MW = 404.20):

While cooling on ice, DCC (1.2 g, 6.0 mmol) and HOBt·H<sub>2</sub>O (800 mg, 5.0 mmol) were added to DMF (10 mL) containing Boc-L-Ac5-OH (1.3 g, 5.0 mmol) and H-D-Pro-O<sup>t</sup>Bu (855 mg, 5.0



mmol). After stirring for overnight, DMF was removed by evaporation; residue dissolved in ethyl acetate, and then successively washed with 10% citric acid solution, 4% sodium bicarbonate solution and brine. After drying over MgSO<sub>4</sub> and concentrating, the resulting oily substance was purified by silica gel chromatography (3.4 x 20 cm) using a mixture of chloroform and methanol (99:1 v/v) to obtain Boc-L-Ac5-D-Pro-O<sup>t</sup>Bu (1.6 g, 3.9 mmol, 79%) as oily compound. TLC: R<sub>f</sub> 0.9 (CHCl<sub>3</sub>/MeOH= 9/1) , HPLC: r.t. 7.87 min.

#### **6.4.1.2 Synthesis of Z-Aib-L-Ac5-D-Pro-O<sup>t</sup>Bu (MW = 523.24):**

The dipeptide Boc-L-Ac5-D-Pro-O<sup>t</sup>Bu (1.6 g, 3.9 mmol) was dissolved in 4N HCl/dioxane (10 mL). After 30 minutes at 0 °C, the reaction solution was removed by evaporation, ether was added to the residue and solidified to obtain white solid of HCl·H-L-Ac5-D-Pro- O<sup>t</sup>Bu (1.2 g, 3.9 mmol, 100%). To a cooled solution of HCl·H-L-Ac5-D-Pro-O<sup>t</sup>Bu (1.2 g, 3.9 mmol) and Z-Aib-OH (950 mg, 5.0 mmol) in DMF (10 mL) were added HOBt·H<sub>2</sub>O (770 mg, 5.0 mmol), DCC(1.2 g, 6.0 mmol), Et<sub>3</sub>N (0.7 mL, 5.0 mmol). After stirring for overnight, check with TLC (R<sub>f</sub> 0.75, CHCl<sub>3</sub>/MeOH=9/1), DMF was removed by evaporation; residue dissolved in ethyl acetate, and then successively washed with 10% citric acid, 4% sodium bicarbonate and brine. After drying over MgSO<sub>4</sub> and concentrating, the resulting oily substance was purified by silica gel chromatography(1.6 x 20 cm) using a mixture of chloroform and methanol (99:1 v/v) to obtain Z-Aib-L-Ac5-D-Pro-O<sup>t</sup>Bu (0.7 g, 1.3 mmol, 34%) as oily compound. TLC: R<sub>f</sub> 0.9 (CHCl<sub>3</sub>/MeOH =9/1), HPLC: r.t. 7.29 min.

#### **6.4.1.3 Synthesis of Boc-L-Asu(OBzl)-Aib-L-Ac5-D-Pro-O<sup>t</sup>Bu (MW = 722.40):**

The tripeptide Z-Aib-L-Ac5-D-Pro-O<sup>t</sup>Bu (0.7 g, 1.3 mmol) was subjected to catalytic hydrogenation with Pd-C (80 mg) in acetic acid (10 mL). After overnight, The reaction was checked by TLC (CHCl<sub>3</sub>/MeOH/CH<sub>3</sub>COOH=90/10/2), the catalyst was filtered and reaction solution was removed by evaporation. The free amine was taken into ethyl acetate (30 mL) by the aid of 2M Na<sub>2</sub>CO<sub>3</sub> solution (10 mL). After dried over anhydrous Na<sub>2</sub>CO<sub>3</sub> ethyl acetate solution was evaporated to obtain H-Aib-L-Ac5-D-Pro-O<sup>t</sup>Bu(330 mg, 0.85 mmol, 65%). To a cooled solution of H-Aib-L-Ac5-D-Pro-O<sup>t</sup>Bu(300 mg, 0.7 mmol) and Boc-L-Asu(OBzl)-OH (400 mg, 1.0 mmol) in DMF (3 mL) were successively added DCC (200 mg, 1.2 mmol), HOBt·H<sub>2</sub>O (200 mg, 1.0 mmol). After stirring for overnight, DMF was removed by evaporation; residue dissolved in ethyl acetate, and then successively washed with 10% citric acid solution, 4% sodium bicarbonate solution and brine. After drying over MgSO<sub>4</sub> and

concentrating, the resulting oily substance was purified by silica gel chromatography using a mixture of chloroform and methanol (99:1 v/v) to obtain Boc-L-Asu(OBzl)-Aib-L-Ac5-D-Pro-O<sup>t</sup>Bu (330 g, 0.45 mmol, 63%). TLC: R<sub>f</sub> 0.8 (CHCl<sub>3</sub>/MeOH=9/1). HPLC: r.t. 9.64 min.

#### **6.4.1.4 *cyclo(-L-Asu(OBzl)-Aib-L-Ac5-D-Pro-)* (MW = 576.27):**

The protected tetrapeptide Boc-L-Asu(OBzl)-Aib-L-Ac5-D-Pro-O<sup>t</sup>Bu (330 g, 0.45 mmol) was dissolved in TFA (5 mL) at 0<sup>o</sup>C and kept for 3 hours, and checked by TLC (R<sub>f</sub> 0.2, CHCl<sub>3</sub>/MeOH=9/1). After evaporation of TFA, the residue was solidified using ether and petroleum ether to yield TFA salt of the linear tetrapeptide TFA·H-Asu(OBzl)-Aib-L-Ac5-D-Pro-OH (267 mg, 0.4 mmol, 96%). To DMF (50 mL), TFA·H-Asu(OBzl)-Aib-L-Ac5-D-Pro-OH (267 mg, 0.4 mmol), HATU (183 mg, 0.4 mmol), and DIEA (0.2 mL, 1.4 mmol) were added in separate five portions in every 30 minutes with stirring at room temperature for the cyclization reaction. After completion of the reaction for 1 hour, DMF was evaporated under vacuum; the residue was dissolved in ethyl acetate and washed with 10% citric acid solution, 4% sodium bicarbonate solution and brine, respectively. It was then dried over anhydrous MgSO<sub>4</sub> and filtered. After evaporation of ethyl acetate, the residue was purified by silica gel chromatography (1.6 x 20 cm) using a mixture of chloroform and methanol (99:1 v/v) to yield *cyclo(-L-Asu(OBzl)-Aib-L-Ac5-D-Pro-)* (130 mg, 0.2 mmol, 57%). HPLC: r.t. 8.05 min.

#### **6.4.1.5 *cyclo(-L-Asu(NHOH)-Aib-L-Ac5-D-Pro-)* (MW=501.23):**

Compound *cyclo(-L-Asu(OBzl)-Aib-L-Ac5-D-Pro-)* (0.13 g, 0.2 mmol) was dissolved in methanol (5 mL) and Pd-C (50 mg) was added. The mixture was stirred under H<sub>2</sub> for 6 hours. After filtration of Pd-C, methanol was evaporated to yield *cyclo(-L-Asu-Aib-L-Ac5-D-Pro-)* (110 mg, 2.0 mmol, 98%, HPLC: r.t. 5.40 min). The product was dissolved in DMF (3 mL) at 0<sup>o</sup>C, and NH<sub>2</sub>OH·HCl (33 mg, 0.48 mmol), benzotriazole-1-yloxy-tris(dimethylamino) phosphonium-hexafluorophosphate (BOP, 159 mg, 0.36 mmol) and DIEA (0.19 mL, 1.08 mmol) were added. The mixture was stirred for 30 minutes and then checked by TLC (R<sub>f</sub> 0.13, CHCl<sub>3</sub>/MeOH=9/1, FeCl<sub>3</sub> spray). After completion of the reaction, DMF was evaporated under vacuum; the residue was purified by LH-20 to yield *cyclo(-L-Asu(NHOH)-Aib-L-Ac5-D-Pro-)* (52 mg, 0.1 mmol, 50%). HPLC: r.t. 4.95 min. HR-FAB MS: [M+H]<sup>+</sup> 502.2417 Calcd. 501.2534, C<sub>22</sub>H<sub>36</sub>ClN<sub>5</sub>O<sub>6</sub>. <sup>1</sup>H NMR (500 MHz, CDCl<sub>3</sub>) δ<sub>H</sub>: 1.20(t, 2H), 1.24(t, 2H), 1.36(s, 3H), 1.62-1.67(m, 1H), 1.77(s, 3H), 1.80-1.96(m, 2H), 2.15(m, 1H), 2.88(s, 1H), 2.95(s, 1H), 3.55(m,

3H), 3.72(m, 1H), 4.26(ddd,  $J=7.1, 10.3, 3.3$  Hz, 1H), 4.78(t,  $J=7.9$  Hz, 1H), 4.88(ddd,  $J=7.5, 10, 2.9$  Hz, 1H), 6.48(s, 1H), 7.16(d,  $J=10$  Hz, 1H), 7.45(d,  $J=10$  Hz, 1H).

#### 6.4.2 Synthesis of cyclo(-L-Asu(NHOH)-Aib-L-Pro-D-Pro-)

##### 6.4.2.1 Z-Aib-L-Pro-D-Pro-O<sup>t</sup>Bu (MW = 487.27):

To a cooled solution of HCl-H-L-Pro-D-Pro-O<sup>t</sup>Bu (1.3 g, 4.8 mmol) and Z-Aib-OH (950 mg, 5.0 mmol) in DMF (10 mL) were added HOBt·H<sub>2</sub>O (770 mg, 5.0 mmol), DCC (1.2 g, 6.0 mmol), Et<sub>3</sub>N (0.7 mL, 5.0 mmol). After stirring for overnight, check with TLC (R<sub>f</sub> 0.75, CHCl<sub>3</sub>/MeOH=9/1), DMF was removed by evaporation; residue dissolved in ethyl acetate, and then successively washed with 10% citric acid, 4% sodium bicarbonate and brine. After drying over MgSO<sub>4</sub> and concentrating, the resulting oily substance was purified by silica gel chromatography (1.6 x 20 cm) using a mixture of chloroform and methanol (99:1 v/v) to obtain Z-Aib-L-Pro-D-Pro-O<sup>t</sup>Bu (0.68 g, 1.4 mmol, 36%) as oily compound. TLC: R<sub>f</sub> 0.9 (CHCl<sub>3</sub>/MeOH =9/1), HPLC: r.t. 7.09 min.

##### 6.4.2.2 Synthesis of Boc-L-Asu(OBzl)-Aib-L-Pro-D-Pro-O<sup>t</sup>Bu (MW = 686.43):

The tripeptide Z-Aib-L-Pro-D-Pro-O<sup>t</sup>Bu (0.68 g, 1.4 mmol) was subjected to catalytic hydrogenation with Pd-C (80 mg) in acetic acid (10 mL). After overnight, the reaction was checked by TLC (CHCl<sub>3</sub>/MeOH/CH<sub>3</sub>COOH=90/10/2), the catalyst was filtered and reaction solution was removed by evaporation. The free amine was taken into ethyl acetate (30 mL) by the aid of 2M Na<sub>2</sub>CO<sub>3</sub> solution (10 mL). After dried over anhydrous Na<sub>2</sub>CO<sub>3</sub> ethyl acetate solution was evaporated to obtain H-Aib-L-Pro-D-Pro-O<sup>t</sup>Bu (460 mg, 1.3 mmol, 93%). To a cooled solution of H-Aib-L-Pro-D-Pro-O<sup>t</sup>Bu (0.46 g, 1.3 mmol) and Boc-L-Asu(OBzl)-OH (570 mg, 1.5 mmol) in DMF (3 mL) were successively added DCC (370 mg, 1.8 mmol), HOBt·H<sub>2</sub>O (230 mg, 1.5 mmol). After stirring for overnight, DMF was removed by evaporation; residue dissolved in ethyl acetate, and then successively washed with 10% citric acid solution, 4% sodium bicarbonate solution and brine. After drying over MgSO<sub>4</sub> and concentrating, the resulting oily substance was purified by silica gel chromatography (1.6 x 20 cm) using a mixture of chloroform and methanol (99:1 v/v) to obtain Boc-L-Asu(OBzl)-Aib-L-Pro-D-Pro-O<sup>t</sup>Bu (710 g, 1.0 mmol, 78%). TLC: R<sub>f</sub> 0.8 (CHCl<sub>3</sub>/MeOH=9/1). HPLC: r.t. 9.39 min.

##### 6.4.2.3 cyclo(-L-Asu(OBzl)-Aib-L-Pro-D-Pro-) (MW = 540.29):

The protected tetrapeptide Boc-L-Asu(OBzl)-Aib-L-Pro-D-Pro-O<sup>t</sup>Bu (710 mg, 1.0 mmol) was dissolved in TFA (5 mL) at 0°C and kept for 3 hours, and checked by TLC (R<sub>f</sub> 0.2, CHCl<sub>3</sub>/MeOH=9/1). After evaporation of TFA, the residue was solidified using ether and petroleum ether to yield TFA salt of the linear tetrapeptide TFA·H-Asu(OBzl)-Aib-L-Pro-D-Pro-OH (640 mg, 1.0 mmol, 98%). To DMF (100 mL), TFA·H-Asu(OBzl)-Aib-L-Pro-D-Pro-OH (640 mg, 1.0 mmol), HATU (460 mg, 1.2 mmol), DIEA (0.59 mL, 3.4 mmol) were added in separate five portions in every 30 minutes with stirring at room temperature for the cyclization reaction. After completion of the reaction for 1 hour, DMF was evaporated under vacuum; the residue was dissolved in ethyl acetate and washed with 10% citric acid solution, 4% sodium bicarbonate solution and brine, respectively. It was then dried over anhydrous MgSO<sub>4</sub> and filtered. After evaporation of ethyl acetate, the residue was purified by silica gel chromatography (1.6 x 20 cm) using a mixture of chloroform and methanol (99:1v/v) to yield *cyclo*(-L-Asu(OBzl)-Aib-L-Pro-D-Pro-) (270 mg, 0.5 mmol, 49%). HPLC: r.t. 8.05 min.

#### 6.4.2.4 *cyclo*(-L-Asu(NHOH)-Aib-L-Pro-D-Pro-) (MW= 465.26):

Compound *cyclo*(-L-Asu(OBzl)-Aib-L-Pro-D-Pro-) (270 mg, 0.5 mmol) was dissolved in methanol (5 mL) and Pd-C (25 mg) was added. The mixture was stirred under H<sub>2</sub> for 6 hours. After filtration of Pd-C, methanol was evaporated to yield *cyclo*(-L-Asu-Aib-L-Pro-D-Pro-) (230 mg, 0.5 mmol, 96%, HPLC: r.t. 5.53 min). The product was dissolved in DMF (4 mL) at 0°C, and NH<sub>2</sub>OH·HCl (470 mg, 0.7 mmol), BOP (230 mg, 0.5 mmol) and DIEA (0.27 mL, 1.5 mmol) were added. The mixture was stirred for 30 minutes and then checked by TLC (R<sub>f</sub> 0.13, CHCl<sub>3</sub>/MeOH=9/1, spray FeCl<sub>3</sub>). After completion of the reaction, DMF was evaporated under vacuum; the residue was purified by LH-20 to yield *cyclo*(-L-Asu(NHOH)-Aib-L-Pro-D-Pro-) (100 mg, mmol, %). HPLC: r.t. 4.80 min. HR-FAB MS: [M+H]<sup>+</sup> 465.2664 Calcd. 465.2587, C<sub>22</sub>H<sub>35</sub>N<sub>5</sub>O<sub>6</sub>. <sup>1</sup>H NMR: The compound do not dissolve in CDCl<sub>3</sub>.

#### 6.4.3 Synthesis of *cyclo*(-L-Asu(NHOH)-Aib-L-Ac6-D-Pro-)

##### 6.4.3.1 Synthesis of Boc-L-Ac6-D-Pro-O<sup>t</sup>Bu (MW = 418.22):

While cooling on ice, DCC (1.22 g, 5.0 mmol) and HOBt·H<sub>2</sub>O (770 mg, 5.0 mmol) were added to DMF (10 mL) containing Boc-L-Ac6-OH (1.33 g, 5.0 mmol) and H-D-Pro-O<sup>t</sup>Bu (787 mg, 4.6 mmol). After stirring for overnight, DMF was removed by evaporation; residue dissolved in ethyl acetate, and then successively washed with 10% citric acid solution, 4% sodium

bicarbonate solution and brine. After drying over MgSO<sub>4</sub> and concentrating, the resulting oily substance was purified by silica gel chromatography (3.4 x 15 cm) using a mixture of chloroform and methanol (99:1 v/v) to obtain Boc-L-Ac6-D-Pro-O<sup>t</sup>Bu (1.51 g, 3.6 mmol, 78%) as oily compound. TLC: R<sub>f</sub> 0.9 (CHCl<sub>3</sub>/MeOH= 9/1), HPLC: r.t. 8.18 min.

#### **6.4.3.2 Synthesis of Boc-Aib-L-Ac6-D-Pro-O<sup>t</sup>Bu (MW = 503.28):**

The dipeptide Boc-L-Ac6-D-Pro-O<sup>t</sup>Bu (1.21 g, 2.9 mmol) was dissolved in 4N HCl/dioxane (10 mL). After 30 minutes at 0 °C, the reaction solution was removed by evaporation, ether was added to the residue and solidified to obtain white solid of HCl·H-L-Ac6-D-Pro-O<sup>t</sup>Bu (880 mg, 2.4 mmol, 87%). To a cooled solution of HCl·H-L-Ac6-D-Pro-O<sup>t</sup>Bu (880 mg, 2.4 mmol) and Boc-Aib-OH (560 mg, 2.8 mmol) in DMF (5 mL) were added HOBt·H<sub>2</sub>O (420 mg, 2.8 mmol), DCC (610 mg, 3.0 mmol), Et<sub>3</sub>N (0.4 mL, 2.8 mmol). After stirring for overnight, check with TLC (R<sub>f</sub> 0.85, CHCl<sub>3</sub>/MeOH=9/1), DMF was removed by evaporation; residue dissolved in ethyl acetate, and then successively washed with 10% citric acid, 4% sodium bicarbonate and brine. After drying over MgSO<sub>4</sub> and concentrating, the resulting oily substance was purified by silica gel chromatography (1.6 x 15 cm) using a mixture of chloroform and methanol (99:1 v/v) to obtain Boc-Aib-L-Ac6-D-Pro-O<sup>t</sup>Bu (880 mg, 1.7 mmol, 71%) as oily compound. TLC: R<sub>f</sub> 0.9 (CHCl<sub>3</sub>/MeOH =9/1), HPLC: r.t. 7.98 min.

#### **6.4.3.3 Synthesis of Boc-L-Asu(OBzl)-Aib-L-Ac6-D-Pro-O<sup>t</sup>Bu (MW = 736.42):**

The tripeptide Boc-Aib-L-Ac6-D-Pro-O<sup>t</sup>Bu (880 mg, 1.7 mmol) was dissolved in 4N HCl/dioxane (15 mL). After 30 minutes at 0 °C, the reaction solution was removed by evaporation, ether was added to the residue and solidified to obtain white solid of HCl·H-Aib-L-Ac6-D-Pro-O<sup>t</sup>Bu (710 mg, 1.6 mmol, 95%). To a cooled solution of HCl·H-Aib-L-Ac6-D-Pro-O<sup>t</sup>Bu (710 mg, 1.6 mmol) and Boc-L-Asu(OBzl)-OH (680 mg, 1.8 mmol) in DMF (4 mL) were added HOBt·H<sub>2</sub>O (280 mg, 1.8 mmol), DCC (440 mg, 2.2 mmol), Et<sub>3</sub>N (0.25 mL, 1.8 mmol). After stirring for overnight, check with TLC (R<sub>f</sub> 0.90, CHCl<sub>3</sub>/MeOH=9/1), DMF was removed by evaporation; residue dissolved in ethyl acetate, and then successively washed with 10% citric acid, 4% sodium bicarbonate and brine. After drying over MgSO<sub>4</sub> and concentrating, the resulting oily substance was purified by silica gel chromatography (1.6 x 20 cm) using a mixture of chloroform and methanol (99:1 v/v) to obtain Boc-L-Asu(OBzl)-Aib-L-Ac6-D-Pro-O<sup>t</sup>Bu (960 mg, 1.3 mmol, 76%) as oily compound. TLC: R<sub>f</sub> 0.9 (CHCl<sub>3</sub>/MeOH =9/1), HPLC: r.t. 9.42 min.

#### 6.4.3.4 *cyclo(-L-Asu(OBzl)-Aib-L-Ac6-D-Pro-)* (MW = 590.29):

The protected tetrapeptide Boc-L-Asu(OBzl)-Aib-L-Ac6-D-Pro-O<sup>t</sup>Bu (960 mg, 1.3 mmol) was dissolved in TFA (8 mL) at 0<sup>o</sup>C and kept for 3 hours, and checked by TLC (R<sub>f</sub> 0.2, CHCl<sub>3</sub>/MeOH=9/1). After evaporation of TFA, the residue was solidified using ether and petroleum ether to yield TFA salt of the linear tetrapeptide TFA.H-L-Asu(OBzl)-Aib-L-Ac6-D-Pro-OH (850 mg, 1.2 mmol, 93%). To DMF (50 mL), TFA.H-L-Asu(OBzl)-Aib-L-Ac6-D-Pro-OH (850 mg, 1.2 mmol), HATU (550 mg, 1.4 mmol), and DIEA (0.7 mL, 4.1 mmol) were added in separate five portions in every 30 minutes with stirring at room temperature for the cyclization reaction. After completion of the reaction for 1 hour, DMF was evaporated under vacuum; the residue was dissolved in ethyl acetate and washed with 10% citric acid solution, 4% sodium bicarbonate solution and brine, respectively. It was then dried over anhydrous MgSO<sub>4</sub> and filtered. After evaporation of ethyl acetate, the residue was purified by silica gel chromatography (1.6 x 20 cm) using a mixture of chloroform and methanol (99:1v/v) to yield *cyclo(-L-Asu(OBzl)-Aib-L-Ac6-D-Pro-)* (290 mg, 0.5 mmol, 42%). HPLC: r.t. 8.32 min.

#### 6.4.3.5 *cyclo(-L-Asu(NHOH)-Aib-L-Ac6-D-Pro-)* (MW= 515.25):

Compound *cyclo(-L-Asu(OBzl)-Aib-L-Ac6-D-Pro-)* (290 mg, 0.5 mmol) was dissolved in methanol (10 mL) and Pd-C (25 mg) was added. The mixture was stirred under H<sub>2</sub> for 6 hours. After filtration of Pd-C, methanol was evaporated to yield *cyclo(-L-Asu-Aib-L-Ac6-D-Pro-)* (230 mg, 0.5 mmol, 96%, HPLC: r.t. 5.72 min). The product was dissolved in DMF (4 mL) at 0<sup>o</sup>C, and NH<sub>2</sub>OH·HCl (60 mg, 0.92 mmol), BOP (310 mg, 0.69 mmol) and DIEA (0.36 mL, 2.1 mmol) were added. The mixture was stirred for 30 minutes and then checked by TLC (R<sub>f</sub> 0.13, CHCl<sub>3</sub>/MeOH=9/1, FeCl<sub>3</sub> spray). After completion of the reaction, DMF was evaporated under vacuum; the residue was purified by LH-20 to yield *cyclo(-L-Asu(NHOH)-Aib-L-Ac6-D-Pro-)* (200 mg, 0.39 mmol, 78%). HPLC: r.t. 5.24 min. HR-FAB MS: [M+H]<sup>+</sup> 516.2620, Calcd. 515.2511, C<sub>23</sub>H<sub>38</sub>ClN<sub>5</sub>O<sub>6</sub>. <sup>1</sup>H NMR (500 MHz, CDCl<sub>3</sub>) δ<sub>H</sub>: 1.24(t, 2H), 1.36(s, 3H), 1.43(d, *J*= 6.7 Hz, 1H), 1.47(d, *J*= 6.7 Hz, 1H), 1.49(t, 2H), 1.16-1.74(m, 6H), 1.76(s, 3H), 1.78-1.88(m, 4H), 2.16-2.40(m, 4H), 2.88(s, 1H), 2.96(s, 1H), 3.53(m, 3H), 3.72(m, 1H), 4.24(ddd, *J*= 8, 9.9, 2.4 Hz, 1H), 4.77(t, *J*= 7.9 Hz, 1H), 4.85(ddd, *J*= 7.1, 10, 2.9 Hz, 1H), 6.40(s, 1H), 7.18(d, *J*=10 Hz, 1H), 7.40(d, *J*= 10 Hz, 1H).

#### **6.4.4 HDACs preparation and enzyme activity assay**

In a 100-mm dish, 293T cells ( $1-2 \times 10^6$ ) were grown for 24 hours and transiently transfected with 10  $\mu$ g each of the vector pcDNA3-HDAC1 for human HDAC1, pcDNA3-HDAC4 for human HDAC4, or pcDNA3-mHDA2/HDAC6 for mouse HDAC6, using the Lipofect AMINE 2000 reagent (Invitrogen). After successive cultivation in DMEM for 24 hours, the cells were washed with PBS and lysed by sonication in lysis buffer containing 50 mM Tris-HCl (pH 7.5), 120 mM NaCl, 5 mM EDTA, and 0.5% NP40. The soluble fraction collected by micro centrifugation was precleared by incubation with protein A/G plus agarose beads (Santa Cruz Biotechnologies, Inc.). After the cleared supernatant had been incubated for 1 hour at 4°C with 4  $\mu$ g of an anti-FLAG M2 antibody (Sigma-Aldrich Inc.) for HDAC1, HDAC4 and HDAC6, the agarose beads were washed three times with lysis buffer and once with histone deacetylase buffer consisting of 20 mM Tris-HCl (pH 8.0), 150 mM NaCl, and 10% glycerol. The bound proteins were released from the immune complex by incubation for 1 hour at 4°C with 40  $\mu$ g of the FLAG peptide (Sigma-Aldrich Inc.) in histone deacetylase buffer (200  $\mu$ L). The supernatant was collected by centrifugation. For the enzyme assay, 10  $\mu$ L of the enzyme fraction was added to 1  $\mu$ L of fluorescent substrate (2 mM Ac-KGLGK(Ac)-MCA) and 9  $\mu$ L of histone deacetylase buffer, and the mixture was incubated at 37°C for 30 minutes. The reaction was stopped by the addition of 30  $\mu$ L of trypsin (20 mg/mL) and incubated at 37°C for 15 minutes. The released amino methyl coumarin (AMC) was measured using a fluorescence plate reader. The 50% inhibitory concentrations (IC<sub>50</sub>) were determined as the means with SD calculated from at least three independent dose response curves.

#### **6.4.5 The p21 promoter assay**

A luciferase reporter plasmid (pGW-FL) was constructed by cloning the 2.4 kb genomic fragment containing the transcription start site into *Hind*III and *Sma*I sites of the pGL3-Basic plasmid (Promega Co., Madison, WI). Mv1Lu (mink lung epithelial cell line) cells were transfected with the pGW-FL and a phagemid expressing neomycin/kanamycin resistance gene (pBK-CMV, Stratagene, La Jolla, CA) with the Lipofectamine reagent (Life Technology, Rockville, MD USA). After the transfected cells had been selected by 400  $\mu$ g/mL Geneticin (G418, Life Technology), colonies formed were isolated. One of the clones was selected and named MFL-9. MFL-9 expressed a low level of luciferase, of which activity was enhanced by TSA in a dose-dependent manner. MFL-9 cells ( $1 \times 10^5$ ) cultured in a 96-well multi-well

plate for 6 hours were incubated for 18 hours in the medium containing various concentrations of drugs. The luciferase activity of each cell lysate was measured with a LucLite luciferase Reporter Gene Assay Kit (Packard Instrument Co., Meriden, CT) and recorded with a Luminescencer-JNR luminometer (ATTO, Tokyo, Japan). Data were normalized to the protein concentration in cell lysates. Concentrations at which a drug induces the luciferase activity 10-fold higher than the basal level are presented as the 1000% effective concentration 1000% ( $EC_{1000}$ ). The human wild-type p21 promoter luciferase fusion plasmid, WWP-Luc, was a kind gift from Dr. B. Vogelstein.

#### 6.4.6 Circular dichroism measurement

CD spectra were recorded on a JASCO J-820 spectropolarimeter (Tokyo, Japan) using a quartz cell of 1 cm light path length at room temperature. Peptide solutions (0.1 mM) were prepared in methanol and CD spectra were recorded in terms of molar ellipticity,  $[\theta]_M$  ( $\text{deg} \times \text{cm}^2 \times \text{dmol}^{-1}$ ).

#### 6.5 References

- [1] Hassig, C. A.; Schrieber, S. L. *Curr. Opin. Chem. Biol.* 1997, 1: 300–308.
- [2] Kouzarides, T. *Curr. Opin. Gen. Dev.* 1999, 9: 40–48.
- [3] Grozinger, C. M.; Schrieber, S. L. *Chem. Biol.* 2002, 9: 3–16.
- [4] Yoshida, M.; Matsuayama, A.; Komatsu, Y.; Nishino, N. *Curr. Med. Chem.* 2003, 10: 2351–2358.
- [5] Fiona McLaughlin; Nicholas B. La Thsngue, *Biochemical pharmacology*, 2004, 68: 1139-1144.
- [6] M. Biel, A. Krestovali, E. Karatzali, J. Papamatheakis, A. Giannis, *Angew. Chem.* 2004, 116: 4065–4067.
- [7] P. A. Marks, T. Miller, V. M. Richon, *Curr. Opin. Pharmacol.* 2003, 3: 344 – 351.
- [8] Manuela Rodriguez, Stefania Terracciano, Elena Cini, Giulia Settembrini, Ines Bruno, Giuseppe Bifulco, Maurizio Taddei, Luigi Gomez-Paloma, *Angew. Chem.* 2006, 118: 437 –441.
- [9] Closse, A.; Hugenin, R. *Helv. Chim. Acta*, 1974, 57: 533-545.
- [10] Kijima, M.; Yoshida, M.; Suguta, K.; Horinouchi, S.; Beppu, T. *J. Biol. Chem.* 1993, 268: 22249-22435.
- [11] Hirota, A.; Suzuki, A.; Aizawa, K.; Tamura, S. *Biomed. Mass Spectrom.* 1974, 1, 15-19.
- [12] Hirota, A.; Suzuki, A.; Aizawa, K.; Tamura, S. *Agr. Biol. Chem.* 1973, 37: 955-959.
- [13] Shute, R. E.; Dunlap, B.; Rich, D. H. *J. Med. Chem.* 1987, 30: 71-78.
- [14] Darkin-Rattray, S. J.; Gurnett, A. M.; Myers, R. W.; Dulski, P. M.; Crumley, T. M.; Allocco, J. J.; Cannova, C.; Meinke, P. T.; Colletti, S. L.; Bednarek, M. A.; Singh, S. B.; Goetz, M. A.; Dombrowski, A. W.; Polishook, J. D.; Schmatz, D. M. *Proc. Natl. Acad. Sci. U.S.A.* 1996, 93: 13143-13147.
- [15] Meinke, P. T.; Liberator, P. *Curr. Med. Chem.* 2001, 8: 211-235.
- [16] Ueda, H.; Nakajima, H.; Hori, Y.; Fujita, T.; Nishimura, M.; Goto, T.; Okuhara, M. *J. Antibiot.* 1994, 47: 301-310.



- [17] Ueda, H.; Manda, T.; Matsumoto, S.; Mukumoto, S.; Nishigaki, F.; Kawamura, I.; Shimomura, K. *J. Antibiot.* 1994, 47: 315-323.
- [18] Furumai, R.; Matsuyama, A.; Kobashi, N.; Lee, K.-H.; Nishiyama, M.; Nakajima, H.; Tanaka, A.; Komatsu, Y.; Nishino, N.; Yoshida, M.; Horinouchi, S. *Cancer Res.* 2002, 62: 4916-4921.
- [19] Mohammed P. I. Bhuiyan, Tamaki Kato, Tatsuo Okauchi, Norikazu Nishino, Satoko Maeda, Tomonori G. Nishino, Minoru Yoshida, *Bioorganic & Medicinal Chemistry*, 2006,14: 3438–3446.
- [20] Norikazu Nishino, Gururaj M. Shivashimpi, a Preeti B. Soni, Mohammed P. I. Bhuiyan, Tamaki Kato, Satoko Maeda, Tomonori G. Nishino, Minoru Yoshida, *Bioorganic & Medicinal Chemistry*, 2008, 16: 437–445.
- [21] Gururaj M. Shivashimpi, Satoshi Amagai, Tamaki Kato, Norikazu Nishino, Satoko Maeda, Tomonori G. Nishino, Minoru Yoshida, *Bioorganic & Medicinal Chemistry*, 2007, 15: 7830–7839.
- [22] Norikazu Nishino, Binoy Jose, Ryuzo Shinta, Tamaki Kato, Yasuhiko Komatsub, Minoru Yoshida, *Bioorganic & Medicinal Chemistry*, 2004, 12: 5777–5784.
- [23] Binoy Jose, Yusuke Oniki, Tamaki Kato, Norikazu Nishino, Yuko Sumida, Minoru Yoshida, *Bioorganic & Medicinal Chemistry Letters*, 2004: 14: 5343–5346.
- [24] Norikazu Nishino, Daisuke Yoshikawa, Louis A. Watanabe, Tamaki Kato, Binoy Jose, Yasuhiko Komatsu, Yuko Sumidab, Minoru Yoshida, *Bioorganic & Medicinal Chemistry Letters*, 2004, 14: 2427–2431.
- [25] Norikazu Nishino, Binoy Jose, Shinji Okamura, Shutoku Ebisusaki, Tamaki Kato, Yuko Sumida, Minoru Yoshida, *Org. Lett.*, 2003, 5(26): 5079-5028.
- [26] Nurul M. Islam, Tamaki Kato, Norikazu Nishino, Hyun-Jung Kim, Akihiro Ito, Minoru Yoshida, *Bioorganic & Medicinal Chemistry Letters*, 2010, 20: 997–999.
- [27] Komatsu, Y.; Tomizaki, K.; Tsukamoto, M.; Kato, T.; Nishino, N.; Sato, S.; Yamori, T.; Tsuruo, T.; Furumai, R.; Yoshida, M.; Horinouchi, S.; Hayashi, H. *Cancer Res.* 2001, 61: 4459–4466.
- [28] Kim, S.D. *J. Biochem. Mol. Biol.* 1995, 28: 227–231.
- [29] Kahnberg, P.; Lucke, A. J.; Glenn, M. P.; Boyle, G. M.; Tyndall, J. D. A.; Parsons, P.G.; Fairlie, D. P. *J. Med. Chem.* 2006, 49: 7611–7622.
- [30] Nielsen, T. K.; Hildmann, C.; Dickmanns, A.; Schwienhorst, A.; Ficner, R. *J. Mol. Biol.* 2005, 354: 107–120.

## Chapter 7

### Cyclic Tetrapeptide HDAC Inhibitors: a Potent Anticancer

#### Prodrug

Currently, histone deacetylase (HDACs) have been considered as a promising target in anticancer drug development, and many studies suggest that HDAC inhibitors can reactivate gene expression and inhibit the growth and survival of tumor cells, and HDAC inhibitors are emerging as a new class of anticancer agents. A number of structurally diverse classes of HDAC inhibitors (natural and synthetic) are known to interact with a zinc atom of HDACs and to induce the acetylation of histone and non-histone protein. Among them, SAHA, depsipeptide (FK228), sodium phenyl-butyrate, alproic acid, PXD101, LAQ824, MS-275, CI-994 and pyroxamide are already in phase I or II clinical trials in cancer patients. Suberoylanilide hydroxamic acid (SAHA, Zolinza) which contains a hydroxamic acid functional group for bind to the active site  $Zn^{2+}$  of HDACs, recently approved by the U.S. Food and Drug Administration (FDA) for the treatment of cutaneous T cell lymphoma (CTCL) in patients with progressive, persistent, or recurrent disease On October 6, 2006. On November 5, 2009, Romidepsin (FK228, Istodax) was also approved by the FDA for the treatment of CTCL. Romidepsin was isolated in a culture of *Chromobacterium violaceum* from a soil sample and found to have little to no antibacterial activity, but was potently cytotoxic against several human cancer cell lines, with no effect on normal cells; studies on mice later found it to have antitumor activity *in vivo* as well. Romidepsin acts as a prodrug with the disulfide bond undergoing reduction within the cell to release a zinc-binding thiol. The thiol reversibly interacts with a zinc atom in the binding pocket of  $Zn^{2+}$ -dependent HDACs. HDAC inhibitors are potential treatments for cancer through the ability to restore normal expression of genes, which may result in cell cycle arrest, differentiation, and apoptosis.

In this dissertation, the primary objective was to design and synthesize of cyclic tetrapeptide based HDAC inhibitors. The strategy was to modify the cap group of cyclic tetrapeptide by changing non-natural amino acids in different residue positions of cyclic tetrapeptide scaffold. As the area surrounding the opening to the binding pocket has less homology between HDAC isoforms compared to the active site, the modification of the cap group allows to have a

significant impact upon isoform selectivity.

In Chapter 2 of this thesis, to explore the molecular details of interactions between HDACs and cyclic tetrapeptides, and analyzed selective inhibition, we constructed 3D model of human HDAC1 structure using human HDAC8 as template and performed docking and molecule dynamics simulation studies between HDAC1, HDAC8 and Apicidin comparing the binding modes of Apicidin-HDAC1 and Apicidin-HDAC8 complexes. The zinc-chelated conformation of HDAC1 model and Apicidin was rightly the lowest binding energy conformation ( $\Delta G_{\text{binding}} = -9.67$  kcal/mol), and the ethyl ketone moiety was primary foundation in coordinating with  $\text{Zn}^{2+}$  in a distance of 1.78 Å and establishing hydrogen bond with the O(H) of Tyr303. This hydrogen bond was very important for stabilizing the binding of ligands to HDAC1. The tetrapeptide core extended its hydrophobic interactions thanks to the N-O-methyl-Trp side chain. Apicidin is known as isoform-selective inhibitor for class I HDACs, with  $\text{IC}_{50}$  value of 1 nM for HDAC1 while  $> \text{IC}_{50}$  1000 nM for HDAC8. In molecule dynamics simulations of complexes of Apicidin binding to HDAC1 and HDAC8, the hydrogen bond existence maps showed that, Apicidin mainly created two hydrogen bonds with Tyr303 while none in Apicidin-HDAC8. Comparing with Apicidin-HDAC1, there were few residues forming hydrophobic interactions and less hydrogen bonds in Apicidin-HDAC8, which mean less stabilities and lower inhibitory activity. In Chapter 3 of this thesis, a variety of non-natural amino acids for the use of synthesis potent HDACs inhibitors of cyclic tetrapeptide were synthesized.

In Chapter 4 of this thesis, a series of Chlamydocin analogues based cyclic tetrapeptide hydroxamic acid HDAC inhibitors were designed by changing Aib using containing aliphatic ring non-natural amino acids. The three methyl substitutional positions of aliphatic ring were accomplished, and found that 3-methyl position was the optimum for cyclic tetrapeptide with *n*-methyl-amino-cyclohexane-carboxylic acid (*Anmc6c*) at 2-position. These inhibitors showed potent HDAC inhibitory activity *in vivo* and *in vitro*. They also showed some selectivity among the HDAC isoforms (HDAC6/HDAC1 = 10). Compound Ky-302 showed the best activity than Ky-301 and Ky-303 in the cellular activity, which 6-fold increased than Ky-2 and Trichostatin A. We carried out molecular docking studies on Chlamydocin–hydroxamic acid analogues and HDLP, HDAC8 and HDAH, respectively. HDAC8-Ky301 and HDLP-Ky302 complexes had chelate zinc coordinates with seven atoms, but the zinc ion of HDAH –Ky303 complex was bound to five atoms. The results showed that the stability and activity of HDAC8-Ky301 and HDLP-Ky302 complexes were stronger than HDAH –Ky303 complex. This study further

supports the fact that, compared to class IIb HDAC, the inhibitors are favorable interactions with the surface binding to class I HDACs, hence showed high activity.

In Chapter 5 of this thesis, author designed and synthesized HDACs inhibitors of replacing L-Phe by L-Phe(*n*-Me) and bearing L-2-amino-7-(2-pyridyl)-disulphidyl heptanoyl (L-Am7 (S2Py)) in Chlamydocin scaffold, which equipped thiol function protected by disulfide hybrid. The aim is to change exiguous hydrophobicity to know that it plays an important role in cap group interaction with rim of active pocket. All compounds showed better sensitivity on Hela than MCF-7 and 7721 cell lines, but no obvious difference for the same one cell lines. The activity of Compounds 1-4 were almost the same. We performed docking and molecular dynamics simulation towards HDAC8. The results showed that the sulfur atom of each compound established a hydrogen bond with the O(H) atom of Tyr306, and this hydrogen bond was very important for keeping the binding of them to HDAC8. These compounds established hydrophobic interactions with some amino acid residues, such as Phe152, His180, Phe207 and Met274, etc., the hydrophobic effects were also crucial for stabilizing the complexes.

In Chapter 6 of this thesis, HDAC inhibitors of cyclic tetrapeptide of phenylalanine residue replaced by two aliphatic amino acids containing chlorine (Ac5 and Ac6) in Chlamydocin framework were designed and synthesized. All compounds showed good activity against HDAC1 and HDAC4 in nanomolar range, but were poorly inhibited to HDAC6 and their selectivity was better (HDAC6/HDAC1=10). The compound Ky-336 showed the best activity in both cell free and cell based conditions than the other two compounds Ky-335 and Ky-337 and the activity of Ky-336 was similar to TSA and Ky-2 data. The result suggested that hydrophobicity of aliphatic amino acid can also increase interaction with rim of HDACs active pocket and aromatic ring was no need in cyclic framework. Also cell permeability was enhanced in this case, which was reflected in their p21 activity data.

In conclusion, in order to find novel and potent HDAC inhibitors, we designed and synthesized a series of Chlamydocin-based cyclic tetrapeptide. These inhibitors showed potent HDAC inhibitory activity *in vivo* and *in vitro*. They also showed some selectivity among the HDAC isoforms. These results further confirmed the hypothesis that modification of the cap group of HDAC inhibitors can lead to potent HDAC inhibitors, which may become potential as anticancer agents. We carried out conformational analysis of these inhibitors by NMR and CD studies. We also performed docking and molecular dynamics simulation for these inhibitors and analyzed the binding interactions between HDACs and these inhibitors at active pocket.

## Acknowledgements

I am highly grateful to my supervisor Professor Norikazu Nishino (Kyushu Institute of Technology) for giving me the rare opportunity to engage in this study and for his gratis supervision throughout the work.

Cordial thanks to the Japan Society for the Promotion of Science (JSPS) for providing the rare opportunity and financial support to me.

I express my sincere gratitude to Prof. Tamaki Kato (Kyushu Institute of Technology) for his all time cooperation, invaluable suggestions and guidance.

I am very much thankful to Mrs. Sachiko Yamamoto for enthusiastic help.

Many thanks to the present and past members of the Nishino Laboratory for their kind support, discussion and collaboration.

Many thanks to the present and past members of the Xiu Laboratory for their kind support, discussion and collaboration.

Finally, I would like to thank my family for their providing support. Thanks to my husband, Wang Qing for his ceaseless support and encouraging.

Li Xiao Hui

Department of Biological Functions and Engineering  
Graduate School of Life Science and Systems Engineering  
Kyushu Institute of Technology  
Kitakyushu, 808-0196  
Japan

## List of Publications

1. **Li Xiaohui**, Li Jianxun, Li Shirong, Xiu Zhilong, Nishino Norikazu, “Cyclic Peptide Histone Deacetylase Inhibitors”, *Progress in Chemistry*. 19 (5): 762-768, (2007).
2. XIAOQING LIU, ZHILONG XIU, **XIAOHUI LI**, “Numerical Characterization of the Conformation of Cyclic Peptides and its Application”, *Journal of Computational Chemistry*. 28( 16): 2545-2557, (2007).
3. **LI Xiao-Hui**, WANG Guan, LI Jian-Xun, XIU Zhi-Long, NISHINO Norikazu, “The Synthesis and Resolution of Boc-L-Methylphenylalanines”, *Chemical Journal of Chinese Universities*. 29(3): 542-545, (2008).
4. Chunli Yan, Zhilong Xiu, **Xiaohui Li**, Shenmin Li, Ce Hao, Hu Teng, “Comparative molecular dynamics simulations of histone deacetylase-like protein: Binding modes and free energy analysis to hydroxamic acid inhibitors”, *PROTEINS: Structure, Function, and Bioinformatics*. 73(1): 134-149, (2008).
5. LIU Xiao-qing, **LI Xiao-hui**, TENG Hu and XIU Zhi-long, “Solvent Effect on Conformation of a Cycloheptapeptide, Stylopeptide 1, Evaluated by Molecular Dynamics in Methonal and Aqueous Environments”, *Chem. Res. Chinese Universities*. 25(4): 560—563, (2009).
6. **LI Xiaohui**, ZHAO Junwei, TENG Hu, NISHINO Norikazu, XIU Zhilong, “Selective Inhibition Study of Apicidin towards Class I HDACs by Molecular Dynamics Simulation”, *Chemical Journal of Chinese Universities*. 31(2): 374-378, (2010).
7. **Li Xiaohui**, Huang dawei, Sun Lei, Xiu Zhilong, Nishino Norikazu, “Design, Synthesis, and Antitumor Activity of Cyclic Tetrapeptide HDACi based on Chlamydocin Framework” *Chinese Journal of Organic chemistry*. in press. (2010).
8. **Xiaohui Li**, Dawei Huang, Lei Sun, Zhilong Xiu, Norikazu Nishino, “Synthesis, evaluation and molecular modeling studies of cyclic tetrapeptides as HDAC inhibitors”. To be submitted in *Bioorganic & Medicinal Chemistry*.

## Presentations at Conferences

1. Poster Presentation: **Xiaohui Li**, Takahide Kanyama, Yasuhiko Otsuka, Tamaki Kato, Norikazu Nishino, Nobuyuki Kobashi, Akihiro Ito, and Minoru Yoshida. “Role of Prolyl Residue in Cyclic Tetrapeptides designed as Histone Deacetylase Inhibitors”, 11<sup>th</sup> *Chinese Peptide Symposium*, Lanzhou, China, **2010**.
2. Poster Presentation: Jiani Li, **Xiaohui Li**, Yasuhiko Otsuka, Tamaki Kato, Norikazu Nishino, Nobuyuki Kobashi, Akihiro Ito, and Minoru Yoshida. “Remodeling of Cyclic Tetrapeptides Framework of Chlamydocin as Histone Deacetylase Inhibitors”, 11<sup>th</sup> *Chinese Peptide Symposium*, Lanzhou, China, **2010**.
3. Poster Presentation: Shimiao Wang, **Xiaohui Li**, Zhilong Xiu, Norikazu Nishino. “Preliminary study of anticancer mechanism of cyclic tetrapeptide HDACis”, 11<sup>th</sup> *Chinese Peptide Symposium*, Lanzhou, China, **2010**.
4. Poster Presentation: Dawei Huang, **Xiaohui Li**, Zhilong Xiu, Norikazu Nishino. “Synthesis, evaluation and molecular modeling studies of L-2-amino- n-bromooctanoic acid derivatives as Histone Deacetylase Inhibitors”, 11<sup>th</sup> *Chinese Peptide Symposium*, Lanzhou, China, **2010**.
5. Poster Presentation: Jiani Li, Hiroyuki Ishii, **Xiaohui Li**, Tamaki Kato, Norikazu Nishino. “Design and Synthesis of Histone Deacetylase Inhibitors by Replacement of Aib in Chlamydocin Hydroxamic Acid Analogues”, 8<sup>th</sup> *Australian Peptide conference*, Couran cove, Australia, **2009**.
6. Poster Presentation: Nsiama Tienabe Kipassa, Shutoku Ebisuzaki, **Xiaohui Li**, Tamaki Kato, Norikazu Nishino. “Design and Synthesis of Chlamydocin Analogues as Histone Deacetylase Inhibitors by Introduction of Various Imino acids”, 8<sup>th</sup> *Australian Peptide conference*, Couran cove, Australia, **2009**.
7. Poster Presentation: **Li Xiao-Hui**, Huang Da-Wei, Sun Lei, Xiu Zhi-Long, Nishino Norikazu. “Design and Synthesis of Histone Deacetylase Inhibitors with Cyclic Tetrapeptides”, 10<sup>th</sup> *Chinese Peptide Symposium*, Xi’an, China, **2008**.
8. Poster Presentation: **Xiao-Hui Li**, Satoru Takahashi, Gururaj Mahadev Shivashimpi, Tamaki kato, Norikazu Nishino. “Separation of diastereomers cyclic dipeptides containing alpha-alkyl amino acid for optical resolution”, *Japanese Peptide Symposium*, Japan, **2007**.